

Limestone Addition in Cement

THÈSE N° 5335 (2012)

PRÉSENTÉE LE 3 AVRIL 2012

À LA FACULTÉ DES SCIENCES ET TECHNIQUES DE L'INGÉNIEUR
LABORATOIRE DES MATÉRIAUX DE CONSTRUCTION
PROGRAMME DOCTORAL EN SCIENCE ET GÉNIE DES MATÉRIAUX

ÉCOLE POLYTECHNIQUE FÉDÉRALE DE LAUSANNE

POUR L'OBTENTION DU GRADE DE DOCTEUR ÈS SCIENCES

PAR

Olga CHOWANIEC

acceptée sur proposition du jury:

Prof. P. Murali, président du jury
Prof. K. Scrivener, directrice de thèse
Dr P. Bowen, rapporteur
Prof. D. E. Macphee, rapporteur
Dr T. Matschei, rapporteur



ÉCOLE POLYTECHNIQUE
FÉDÉRALE DE LAUSANNE

Suisse
2012

*Principium cuius hinc nobis exordia sumet,
nullam rem e nihilo gigni divinitus umquam.*

*But only Nature's aspect and her law
Which, teaching us, hath his exordium
Nothing from nothing ever yet was born.*

Lucretius "De Rerum Natura"

Acknowledgements

My adventure which lead to this dissertation I totally due Prof. Karen Scrivener, who I would like to thank for giving me the opportunity to explore the world of cement science under her supervision, for all time spent discussing, correcting, reading and believing that it is possible.

The present work was possible thanks to financial support of Swiss Cement Industry – HOLCIM, for what I'm very thankful. Especially I would like to thank Dr. Silvia Vieira and Dr. Thomas Matschei from HOLCIM Group Support for their presence and collaboration.

I would like to thanks to all my LMC colleagues, who number was growing during the four years spent at EPFL, for all the good time spent with you during, coffee brakes, sport classes, hiking, traveling and working.

Je remercie tout particulièrement Emmanuel pour son aide pendant la première année de ma thèse, pour toutes les discussions que nous avons eues ainsi que ton soutien qui m'a beaucoup aidé. Merci de m'avoir permis d'apprendre de toi.

Merci Lionel, pour ton précieux temps passé à préparer mes expériences et à faire du béton, ainsi que ta bonne humeur et la patience dont tu as fais preuve pour m'aider à améliorer mon Français.

Merci Kyle, Gewnn et Steve pour vos critiques constructives, votre soutien et votre collaboration. Merci Rouben pour sauver mes resulta de DRX. C'était un plaisir de travailler avec vous.

Merci à tous mes collègues de bureau, plus particulièrement à Rodrigo qui a pris la responsabilité de me présenter tous les endroits importants du monde du laboratoire LMC, pour sa bonne humeur de tous les jours et sa diplomatie. Merci Patrick pour les nombreuses discussions que nous avons partagées en train, et devant le MEB. Merci Arnaud, John et Mathieu qui avez éclairé mes journées.

Merci à mes étudiants, et tout particulièrement Gaëtan pour ton excellent travail, les discussions partagées et pour m'avoir motivé à apprendre le Français.

Merci à tous les gens que j'ai pu rencontrer pendant tout ce temps, et pour toutes ces discussions sur mon travail partagées lors des meetings, séminaires ou autres conférences.

Je remercie de tout mon coeur Tristan pour sa présence à mes côtés, pour son soutien inconditionnel, en particulier la dernière année. Je te dédie ce travail.

Abstract

Addition of fine limestone provides an excellent means to reduce the amount of clinker in cement. It is now well accepted that limestone partially reacts in cementitious systems with C_3A to produce hemi- and monocarboaluminate phases and as a consequence more sulfate is available to form ettringite and the total volume of hydrates increases. The mechanism by which limestone affects the hydration is crucial in understanding its influence on the properties of cementitious materials.

Laboratory and Commercial Cements with two different types of clinker, low and high C_3A with different gypsum and limestone addition, were investigated. Hydrated pastes and mortars were investigated in terms of kinetics, phases assemblage, microstructure development, porosity, mechanical properties and durability (sulfate attack and sorptivity).

An improvement in sample preparation for XRD measurement was made, which allows preferential orientation to be avoided and improves Rietveld Analysis quantification. The elastic modulus was found to correlate well with compressive strength and could be used as a nondestructive method to measure compressive strength.

Monocarboaluminate formation was found to increase with increasing C_3A . For high C_3A cement it is visible at 2 days of hydration and at 720 days 4.5% of monocarboaluminate is measured in the system. For Low C_3A cement it is visible at 7 days of hydration and at 720 days 1.6% of monocarboaluminate is measured in the system. Mc is formed only after all gypsum, which is more reactive than limestone is consumed to produce ettringite. No monosulfate is observed in the limestone systems.

The optimum gypsum, was found to have as much effect at early ages on the hydration as 10% of limestone addition. Consequently variations in the gypsum level were investigated but it was difficult to quantify differences between samples with increasing gypsum addition.

Studies of behavior in sulfate solution indicated that C_3A is the dominant factor. Limestone addition produces slight changes in the form of degradation but do not fundamentally change whether deterioration takes place or not.

Keywords : limestone; C_3A ; gypsum; hydration; porosity; compressive strength; sulfate attack

Résumé

L'ajout de calcaire fin est un excellent moyen pour permettre de réduire la quantité de clinker dans le ciment. Il est maintenant reconnu que le calcaire réagit en partie dans les systèmes cimentaires avec le C_3A pour produire des phases hemi- et monocarboaluminates, ce qui a pour conséquence de laisser plus de sulfates à disposition pour la formation d'ettringite et d'augmenter le volume total des hydrates. Le mécanisme selon lequel le calcaire affecte l'hydratation est primordial pour comprendre l'influence sur les propriétés de matériaux cimentaires.

Des ciments commerciaux et de laboratoire avec deux sortes de clinker, à haute ou faible teneur en C_3A , avec des additions différentes de gypse et de calcaire, ont été étudiés. L'étude de pâtes et de mortiers hydratés a été menée en termes de cinétique, d'assemblages des phases, de développement de la microstructure, de porosité, de propriétés mécaniques et de durabilité (attaque sulfatique et sorptivité). La méthode de préparation pour diffraction par rayons X a été améliorée, permettant d'éviter les problèmes liés à l'orientation préférentielle et d'améliorer la quantification par analyse Rietveld. Le module d'élasticité a montré une bonne corrélation avec la résistance en compression et constituerait donc une méthode non-destructrice pour mesurer la résistance en compression.

Il a été observé que la formation de Mc augmente avec la quantité de C_3A . Pour le ciment à haute teneur en C_3A il est visible à deux jours d'hydratation et 4.5% de monocarboaluminate sont mesurés dans le système à 720 jours. Pour le ciment à basse teneur en C_3A il apparaît à 7 jours et 1.6% sont mesurés dans le système à 720 jours. Le Mc ne forme qu'après la réaction complète du gypse - plus réactif que le calcaire - pour former de l'ettringite. Aucune trace de monosulfate n'est détectée dans les systèmes contenant du calcaire.

La quantité optimale de gypse a un effet observable sur l'hydratation à jeune âge comparable à l'ajout de 10% de calcaire. Une étude a été menée mais il a été difficile de quantifier les différences entre les échantillons à différents teneurs de gypse. Des études sur le comportement en solution sulfatique ont indiqué que le C_3A est le facteur dominant. L'ajout de calcaire produit de légers changements dans la forme de dégradation mais ne change pas fondamentalement s'il y a présence de dégradation ou pas.

Mots-clés : calcaire; C_3A ; gypse; hydratation; porosité; résistance à la compression; attaque sulfatique

Contents

Acknowledgements	I
Abstract	III
Résumé	V
Contents	VII
List of figures	XIII
List of tables	XXIII
Glossary	XXV
1 Introduction	1
2 Literature review	3
2.1 Early hydration kinetics and phase assemblage	3
2.1.1 Early hydration kinetics	3
2.1.2 Phase assemblage	5
2.2 Physical properties with limestone addition	5
2.2.1 Particle size distribution	5
2.2.2 Workability	6
2.3 Mechanical properties	7
2.3.1 Strength	7
2.3.2 Volume changes	8
2.4 Durability	8
2.4.1 Porosimetry	8
2.4.2 Permeability	9
2.4.3 Carbonation	9
2.4.4 Freeze/thaw resistance	9
2.4.5 Sulfate resistance	10

2.4.6	Thaumasite formation	10
2.4.7	Chlorides	10
2.5	Summary	11
3	Materials and Methods	13
3.1	Objective of the study	13
3.2	Primary Materials Characterization	14
3.2.1	Raw materials characterization	15
3.2.2	Cement blend characterization	15
3.2.2.1	XRD and TGA analysis comparison	17
3.2.2.2	Particle Size Distribution, Specific Surface and Specific Gravity	18
3.3	Preparation of samples	20
3.4	Methods	20
3.4.1	X-Ray Diffraction – XRD	20
3.4.1.1	XRD analysis in the limestone cement systems – crystals susceptible to preferred orientation	21
3.4.2	Thermo Gravimetric Analysis – TGA	25
3.4.2.1	TGA possibilities	26
3.4.3	X-Ray Fluorescence (XRF)	28
3.4.4	Particle Size distribution	29
3.4.5	Specific Surface and Density	29
3.4.6	Scanning Electron Microscopy (SEM)	29
3.4.7	Mercury Intrusion Porosimetry (MIP)	29
3.4.8	Isothermal Calorimetry	30
3.4.9	Chemical Shrinkage	31
3.4.10	Compressive and Flexural Strength	31
3.4.11	Elastic Modulus	32
3.4.11.1	Elastic Modulus to determine compressive strength	32
3.4.12	Sulfate Attack	33
4	Limestone addition in the low and high C₃A clinker cements	35
4.1	Influence of C ₃ A amount on the hemi- and monocarboaluminate formation	36
4.1.1	Compressive Strength	37
4.1.2	Calorimetry	38
4.1.3	Hydration products with limestone and different clinker composition	41
4.1.3.1	GEMS predictions	43
4.1.4	Porosity	46
4.1.5	Microstructural development	48
4.1.6	Summary – Hc and Mc formation with different C ₃ A content cements	49

4.2	Increasing limestone addition with high C ₃ A clinker cements	51
4.2.1	Compressive Strength	52
4.2.2	Kinetics of the hydration	53
4.2.3	Phase assemblage	55
4.2.3.1	Influence on the AFm phase formation	59
4.2.3.2	GEMS prediction of phase formation	62
4.2.4	Porosimetry	64
4.3	Summary	64
5	Influence of gypsum on hydration of PC and limestone cements	67
5.1	Influence of gypsum on the hydration of alite in the alite – gypsum – limestone system	68
5.1.1	Alite – gypsum – limestone systems – kinetics	69
5.1.2	Phase assemblage of alite – gypsum – limestone mixes	72
5.2	Influence of gypsum on cement hydration	78
5.2.1	Compressive strength	79
5.2.2	Hydration kinetics	82
5.2.3	Development of phases (XRD, TGA)	84
5.2.4	Porosimetry	90
5.2.5	Microstructure	94
5.2.6	Summary - Influence of gypsum	96
5.3	Influence of limestone on gypsum optimum	97
5.3.1	Influence of limestone on the compressive strength	97
5.3.2	Influence of Limestone on the kinetics	100
5.3.3	Influence of limestone on the phase assemblage	104
5.3.4	Influence of limestone on the porosity and microstructure development	107
5.4	GEMS vs XRD, aluminium gypsum and calcium uptake into C-S-H	112
5.5	Summary	115
6	Influence of the temperature on hydration and properties of PC and limestone cement	119
6.1	Influence of the temperature on the kinetics	120
6.2	Influence of the temperature on the compressive strength	127
6.3	Activation Energy	135
6.3.1	Activation Energy for different cement systems	136
6.4	Summary	139

7	Influence of limestone and gypsum on the durability of cementitious materials	141
7.1	Sulfate attack	141
7.1.1	State of the art	141
7.1.2	Influence of limestone on the sulfate attack	143
7.1.2.1	Methods	143
7.1.2.2	Microstructure investigation	144
7.2	Sorptivity	155
7.3	Summary	157
8	Main findings and future perspective	159
8.1	Main findings	159
8.1.1	Methods	159
8.1.2	Hc and Mc formation	159
8.1.3	Ettringite formation	160
8.1.4	C–S–H composition	160
8.1.5	Kinetics	161
8.1.6	Porosity	162
8.1.7	Compressive strength	162
8.1.8	Alite–gypsum–limestone system	163
8.1.9	Temperature influence	163
8.1.10	Durability	163
8.2	Perspective	163
	Appendices	165
	Appendix A Materials	167
	Appendix B Methods	175
	Appendix C SEM EDS analysis	177
	Appendix D Influence of limestone on cement hydration	181
D.0.1	Influence of C ₃ A content on hemi- and monocarboaluminate formation	181
D.0.2	Commercial cements	184
D.0.2.1	Kinetics	184
D.0.2.2	Phase assemblage	185
D.0.2.3	Porosity	185

Appendix E Comparison of Laboratory and commercial cements	191
E.1 Cement composition and particle size distribution	191
E.2 Kinetics of hydration	193
E.3 Compressive strength	195
Appendix F Gypsum influence on hdyration	197
Bibliography	203
Curriculum Vitae	211

List of Figures

2.1	Isothermal Calorimetry data for: C_3S and $C_3S+CaCO_3$ [59].	4
2.2	Degree of Hydration for paste with increasing limestone addition and different w/c ratio[8].	4
2.3	Rosin-Rammler-Sperling-Bennet diagram of clinker and limestone and limestone cement [76].	6
2.4	Compressive Strength of blended cements vs. percentage of the substituted Portland Cement [85].	8
3.1	XRD, TGA, XRF method comparison. Quantification of SO_3 in cement.	17
3.2	Particle size distribution. Batch comparison. Cements with low C_3A content. .	19
3.3	Particle size distribution. Batch comparison. Cements with high C_3A content. .	19
3.4	X-ray diffraction results. Comparison of the two methods for limestone cement samples preparation, ground and sliced. Calcite quantification.	22
3.5	X-ray diffraction results. Comparison of the two methods for limestone cement samples preparation, ground and sliced. Ettringite quantification.	22
3.6	X-ray diffraction results. Comparison of the two methods for limestone cement samples preparation, ground and sliced. Monocarboaluminate quantification. .	23
3.7	XRD patterns for techniques of sample preparation, grounded – powders and slices. Sample with low and high C_3A clinker with (dark line) and without (light line) 10% of limestone.	24
3.8	TGA analysis. Heating mode – linear $10^\circ C/min$	27
3.9	TGA analysis. Heating mode – step method.	27
3.10	TGA analysis. Heating mode – linear $10^\circ C/min$ – hemicarboaluminate (Hc), monocarboaluminate (Mc) and calcite.	27
3.11	TGA analysis. Hemicarboaluminate decomposition at different heating mode. .	28
3.12	Isothermal Calorimetry curve typical for Portland cement hydration.	30
3.13	Young's Modulus vs. Compressive Strength	33
4.1	Compressive Strength at different ages. Samples with low (L=3%) and high (H=8%) C_3A content, with and without 10% of limestone addition. Gypsum content at optimum.	37

4.2	Isothermal Calorimetry data. Samples with low (L=3%) C ₃ A content, with 0 and 10% of limestone addition. Batch I.	39
4.3	Isothermal Calorimetry data. Samples with low (L=3%) C ₃ A content, with 0 and 10% of limestone addition. Batch II.	39
4.4	Isothermal Calorimetry data. Samples with high (H=8%) C ₃ A content, with 0 and 10% of limestone addition. Batch I.	40
4.5	Isothermal Calorimetry data. Samples with high (H=8%) C ₃ A content, with 0 and 10% of limestone addition. Batch II.	40
4.6	XRD Rietveld Analysis, monocarboaluminate and monosulfate quantification. Samples with low and high C ₃ A, 0 and 10% of limestone addition.	41
4.7	XRD Rietveld Analysis – calcite quantification and calculated calcite content.	42
4.8	SEM EDS analysis – C-S-H composition at 24 hours of hydration for sample LOCg5.5.	44
4.9	Portlandite formation by XRD Rietveld analysis, GEMS default settings, GEMS with fixed Ca/Si ratio obtained by SEM EDS analysis.	45
4.10	Monocarboaluminate formation by XRD Rietveld analysis and GEMS calculation with default C-S-H composition and with fixed Al/Si ratio.	46
4.11	MIP data for cement with low C ₃ A (3%) clinker content and with 0 and 10% of limestone addition.	47
4.12	MIP data for cement with high C ₃ A (8%) clinker content and with 0 and 10% of limestone addition.	47
4.13	Scanning Electron Microscopy at 10 and 24 hours of hydration for samples with low (3%) and high (8%) C ₃ A clinker with 0 and 10% of limestone addition. Magnification=6000x, HV=15kV, WD=12.5mm.	48
4.14	Indication of the optimum gypsum for each limestone addition	51
4.15	Compressive Strength of mortars with increasing limestone addition at different times of hydration.	52
4.16	Isothermal Calorimetry with increasing limestone addition. Cement with high (8%) C ₃ A clinker, gypsum amount is in optimum for each sample.	53
4.17	Isothermal Calorimetry with increasing limestone addition – cumulative curve. Cement with high (8%) C ₃ A clinker and increasing limestone addition gypsum amount is in optimum for each sample.	54
4.18	Slope of the acceleration period with limestone addition.	54
4.19	Time of the aluminate reaction with limestone addition.	55
4.20	Thermal Gravimetry data for high C ₃ A clinker with increasing limestone addition, at 24 hours of hydration.	56
4.21	XRD Rietveld Analysis data for high C ₃ A clinker with increasing limestone addition. C ₃ S quantification.	56

4.22	XRD Rietveld Analysis and TGA data for high C ₃ A clinker with increasing limestone addition. Portlandite (CH) quantification.	57
4.23	XRD Rietveld Analysis data for high C ₃ A clinker with increasing limestone addition. C ₃ A quantification.	57
4.24	XRD Rietveld Analysis data for high C ₃ A clinker with increasing limestone addition. C ₄ AF quantification.	58
4.25	XRD Rietveld Analysis. Low and high C ₃ A clinker with increasing limestone addition. Monocarboaluminate and monosulfate formation up to 90 days of hydration.	59
4.26	XRD Rietveld Analysis. Low and high C ₃ A clinker with increasing limestone addition. Ettringite formation up to 90 days of hydration.	60
4.27	XRD patterns at 2 days of hydration. High C ₃ A clinker with increasing limestone addition. Ettringite, hemicarboaluminate and monocarboaluminate peak.	61
4.28	GEMS calculations data. Monocarboaluminate prediction formation for samples with increasing limestone addition.	62
4.29	Monocarboaluminate formation by XRD Rietveld analysis and GEMS calculations. Samples with increasing limestone addition and gypsum at optimum content.	63
4.30	Mercury Intrusion Porosimetry (MIP) data at 10, 24 hours and 28 days of hydration. For samples with increasing limestone addition.	64
5.1	Isothermal Calorimetry Data for alite and gypsum mixes.	70
5.2	Isothermal Calorimetry Data for alite and gypsum mixes – cumulative curve.	70
5.3	Isothermal Calorimetry Data for alite, gypsum and 10% of limestone mixes.	71
5.4	Isothermal Calorimetry Data for alite, gypsum and 10% of limestone mixes – cumulative curve.	71
5.5	XRD Rietveld Analysis. C ₃ S and portlandite quantification in the system of alite-gypsum-limestone. 7 days of hydration.	73
5.6	XRD Rietveld Analysis. Amorphous phase quantification in the system of alite-gypsum-limestone. 7 days of hydration.	73
5.7	Mercury Intrusion Porosimetry. Alite, different amount of gypsum with 0 and 10% of limestone addition.	74
5.8	Thermogravimetric Analysis. Alite with different gypsum content and with 0% of limestone addition.	75
5.9	Thermogravimetric Analysis. Alite with different gypsum content and with 10% of limestone addition.	75
5.10	Thermogravimetric Analysis. Alite with different gypsum content and with 0 and 10% of limestone addition. Water loss up to 550°C.	76

5.11 Thermogravimetric Analysis. Alite with different gypsum content and with 0 and 10% of limestone addition. Portlandite content.	76
5.12 Scanning Electron Microscopy for samples alite – gypsum – limestone mixes. Magnification=1600x, HV=15kV, WD=12.5mm.	77
5.13 Compressive Strength of mortars at 28 days of hydration. Clinker with low (3%) C ₃ A content and increasing gypsum addition.	80
5.14 Compressive Strength of mortars at 10 and 24 hours of hydration. Clinker with low (3%) C ₃ A content and increasing gypsum addition.	80
5.15 Compressive Strength of mortars at 28 days of hydration. Clinker with high (8%) C ₃ A content and increasing gypsum addition.	81
5.16 Compressive Strength of mortars at 10 and 24 hours of hydration. Clinker with high (8%) C ₃ A content and with increasing gypsum addition.	81
5.17 Isothermal Calorimetry data for low C ₃ A clinker with increasing gypsum content.	82
5.18 Isothermal Calorimetry data for low C ₃ A clinker with increasing gypsum content – Cumulative.	83
5.19 Isothermal Calorimetry data for high C ₃ A clinker with increasing gypsum content.	83
5.20 Isothermal Calorimetry data for high C ₃ A clinker with increasing gypsum content – Cumulative.	84
5.21 XRD Rietveld Analysis, ettringite formation and C ₃ A consumption up to 24 hours of hydration in low C ₃ A cement with increasing gypsum content.	85
5.22 XRD Rietveld Analysis, ettringite formation and C ₃ A consumption up to 24 hours of hydration in high C ₃ A cement with increasing gypsum content.	85
5.23 XRD Rietveld Analysis, monosulfate phase formation, low C ₃ A clinker with increasing gypsum addition.	86
5.24 XRD Rietveld Analysis, monosulfate phase formation, high C ₃ A clinker with increasing gypsum addition.	86
5.25 XRD Rietveld Analysis, C ₃ S phase consumption up to 24 hours of hydration, low C ₃ A clinker with increasing gypsum addition.	87
5.26 XRD Rietveld Analysis, C ₃ S phase consumption up to 24 hours of hydration, high C ₃ A clinker with increasing gypsum addition.	87
5.27 TGA at 10 hours of hydration of low C ₃ A clinker cement with increasing gypsum addition.	88
5.28 TGA at 24 hours of hydration of low C ₃ A clinker cement with increasing gypsum addition.	88
5.29 TGA at 10 hours of hydration of high C ₃ A clinker cement with increasing gypsum addition.	89
5.30 TGA at 24 hours of hydration of high C ₃ A clinker cement with increasing gypsum addition.	89

5.31	Mercury Intrusion Porosimetry at 10 hours of hydration. Low C ₃ A clinker with increasing gypsum addition.	91
5.32	Mercury Intrusion Porosimetry at 24 hours of hydration. Low C ₃ A clinker with increasing gypsum addition.	91
5.33	Mercury Intrusion Porosimetry at 10 hours of hydration. High C ₃ A clinker with increasing gypsum addition.	92
5.34	Mercury Intrusion Porosimetry at 24 hours of hydration. Low C ₃ A clinker with increasing gypsum addition.	92
5.35	Total porosity vs. Compressive strength at 10 and 24 hours of hydration. Low and high C ₃ A clinker with increasing gypsum addition.	93
5.36	Scanning Electron Microscopy at 10 and 24 hours of hydration for samples with low C ₃ A clinker and increasing gypsum addition. Magnification=6000x, HV=15kV, WD=12.5mm.	94
5.37	Scanning Electron Microscopy at 10 and 24 hours of hydration for samples with high C ₃ A clinker and increasing gypsum addition. Magnification=6000x, HV=15kV, WD=12.5mm.	95
5.38	Compressive Strength of mortars at 28 days of hydration. Clinker with low (3%) C ₃ A content with 0 and 10% limestone addition.	98
5.39	Compressive Strength of mortars at 10 and 24 hours of hydration. Clinker with low (3%) C ₃ A content, with 0 and 10% limestone addition.	98
5.40	Compressive Strength of mortars at 28 days of hydration. Clinker with high (8%) C ₃ A content with 0 and 10% of limestone addition.	99
5.41	Compressive Strength of mortars at 10 and 24 hours of hydration. Clinker with high (8%) C ₃ A content with 0 and 10% of limestone addition.	99
5.42	Isothermal Calorimetry data – Heat Evolution Rate. Clinker with low (3%) C ₃ A content and with 10% of limestone addition.	101
5.43	Isothermal Calorimetry data – Heat Evolution Rate. Clinker with high (8%) C ₃ A content and with 10% of limestone addition.	101
5.44	Isothermal Calorimetry data for samples with low and high C ₃ A clinker, 0 and 10% of limestone addition and increasing gypsum content.	102
5.45	Isothermal Calorimetry data – Cumulative Curve. Clinker with low (3%) C ₃ A content with increasing gypsum content and with 0 and 10% of limestone addition.	103
5.46	Isothermal Calorimetry data – Cumulative. Clinker with high (8%) C ₃ A content with increasing gypsum content and with 0 and 10% of limestone addition.	103
5.47	XRD Rietveld Analysis, monosulfate (Ms) and monocarboaluminate (Mc) quantification. Sample with low C ₃ A clinker cement, increasing gypsum addition, 0 and 10% of limestone addition.	105

5.48	XRD Rietveld Analysis, monosulfate (Ms) and monocarboaluminate (Mc) quantification. Sample with high C ₃ A clinker cement, increasing gypsum addition, 0 and 10% of limestone addition.	105
5.49	% of C ₃ S hydrated in function of gypsum addition. Low C ₃ A clinker cements with 0 and 10% of limestone.	106
5.50	% of C ₃ S hydrated in function of gypsum addition. High C ₃ A clinker cements with 0 and 10% of limestone.	106
5.51	MIP data at 10 hours of hydration. Sample with low C ₃ A clinker cement, increasing gypsum addition, 0 and 10% of limestone addition.	108
5.52	MIP data at 24 hours of hydration. Sample with low C ₃ A clinker cement, increasing gypsum addition, 0 and 10% of limestone addition.	108
5.53	MIP data at 10 hours of hydration. Sample with high C ₃ A clinker cement, increasing gypsum addition, 0 and 10% of limestone addition.	109
5.54	MIP data at 24 hours of hydration. Sample with high C ₃ A clinker cement, increasing gypsum addition, 0 and 10% of limestone addition.	109
5.55	Scanning Electron Microscopy at 10 and 24 hours of hydration for samples with low C ₃ A clinker, increasing gypsum addition, 0 and 10% of limestone addition. Magnification=6000x, HV=15kV, WD=12.5mm.	110
5.56	Scanning Electron Microscopy at 10 and 24 hours of hydration for samples with high C ₃ A clinker, increasing gypsum addition, 0 and 10% of limestone addition. Magnification=6000x, HV=15kV, WD=12.5mm.	111
5.57	Comparison of XRD Rietveld analysis and GEMS calculation of ettringite and monosulfate. Systems with high C ₃ A clinker, 0% of limestone and increasing gypsum content.	113
5.58	Comparison of XRD Rietveld analysis and GEMS calculation of ettringite and monocarboaluminate. Systems with high C ₃ A clinker, 10% of limestone and increasing gypsum content.	114
6.1	Isothermal Calorimetry Data at different temperatures. Sample with low C ₃ A content, 3.8% of gypsum 0, 10% of limestone addition.	121
6.2	Isothermal Calorimetry Data at different temperatures. Cumulative curve. Sample with low C ₃ A content, 3.8% of gypsum, 0, 10% of limestone addition. .	121
6.3	Isothermal Calorimetry Data at different temperatures. Sample with low C ₃ A content, 5.5% of gypsum, 0, 10% of limestone addition.	122
6.4	Isothermal Calorimetry Data at different temperatures. Cumulative curve. Sample with low C ₃ A content, 5.5% of gypsum, 0, 10% of limestone addition. .	122
6.5	Isothermal Calorimetry Data at different temperatures. Sample with low C ₃ A content, 6.0% of gypsum, 0, 10% of limestone addition.	123

6.6	Isothermal Calorimetry Data at different temperatures. Cumulative curve. Sample with low C ₃ A content, 6.0% of gypsum, 0, 10% of limestone addition. .	123
6.7	Isothermal Calorimetry Data at different temperatures. Sample with high C ₃ A content, 3.8% of gypsum, 0, 10% of limestone addition.	124
6.8	Isothermal Calorimetry Data at different temperatures. Sample with high C ₃ A content, 3.8% of gypsum, 0, 10% of limestone addition.	124
6.9	Isothermal Calorimetry Data at different temperatures. Sample with high C ₃ A content, 6.0% of gypsum, 0, 10% of limestone addition	125
6.10	Isothermal Calorimetry Data at different temperatures. Sample with high C ₃ A content, 6.0% of gypsum, 0, 10% of limestone addition.	125
6.11	Isothermal Calorimetry Data at different temperatures. Sample with high C ₃ A content, 9.0% of gypsum, 0, 10% of limestone addition.	126
6.12	Isothermal Calorimetry Data at different temperatures. Sample with high C ₃ A content, 9.0% of gypsum, 0, 10% of limestone addition.	126
6.13	Compressive Strength at 10h of hydration and different temperatures. Samples with high C ₃ A clinker, different gypsum content and with 0 and 10% of limestone addition.	128
6.14	Compressive Strength at 24h of hydration and different temperatures. Samples with high C ₃ A clinker, different gypsum content and with 0 and 10% of limestone addition.	128
6.15	Compressive Strength at 28d of hydration and different temperatures. Samples with high C ₃ A clinker, different gypsum content and with 0 and 10% of limestone addition.	129
6.16	Isothermal Calorimetry Data – Maturity of the system at different temperatures.	130
6.17	Isothermal Calorimetry Data, and X–ray Diffraction, Rietveld Analysis Data – Maturity of the system at different temperatures by degree of hydration. . . .	131
6.18	Compressive Strength – corresponding maturity at different temperatures to 10h maturity at 20°C, by calorimetry and XRD.	132
6.19	Compressive Strength – corresponding maturity at different temperatures to 24h maturity at 20°C, by calorimetry and XRD.	133
6.20	Mercury Intrusion Porosimetry – Sample with 3.8% of gypsum and high C ₃ A content, SO ₃ /Al ₂ O ₃ = 0.62. Corresponding maturity at 10 and 30 °C to 10h maturity at 20°C.	133
6.21	Mercury Intrusion Porosimetry – Sample with 5.5% of gypsum and high C ₃ A content, SO ₃ /Al ₂ O ₃ = 0.90. Corresponding maturity at 10 and 30 °C to 10h maturity at 20°C.	134

6.22	Mercury Intrusion Porosimetry – Sample with 6.0% of gypsum and high C ₃ A content, SO ₃ /Al ₂ O ₃ = 0.99. Corresponding maturity at 10 and 30 °C to 10h maturity at 20°C.	134
6.23	Total Porosimetry vs. Compressive Strength at different temperatures.	135
6.24	Examples of superposition of calorimetry curves for calculating activation energy.	136
6.25	Activation Energies results for low C ₃ A clinker.	138
6.26	Activation Energies results for high C ₃ A clinker.	138
7.1	Sulfate attack experiment - sampling.	143
7.2	Expansion – Laboratory Cement. Samples with low C ₃ A content (3%), 0 and 10% of limestone addition and different gypsum content.	145
7.3	Expansion – Laboratory Cement. Samples with high C ₃ A content (8%), 0 and 10% of limestone addition and different gypsum content.	145
7.4	Expansion – Commercial Cement. Samples with low and high C ₃ A content, different limestone addition and 6.5% of gypsum content.	146
7.5	The same value of expansion and different level of destruction– Commercial Cement. Samples with low and high C ₃ A content, different limestone addition and gypsum content.	147
7.6	XRD Pattern for samples with the same level of expansion and different time of exposure, 180 and 360 days. High C ₃ A clinker.	148
7.7	XRD Pattern for samples at the same time (480 days) but different expansion level. High C ₃ A clinker.	148
7.8	XRD Patterns for samples at 360 days in sulfate solution. Low C ₃ A clinker.	149
7.9	XRD Patterns for samples at 360 days in sulfate solution. High C ₃ A clinker.	149
7.10	TGA, derivative curves for samples with the same level of expansion and different time of exposure, 180 and 360 days. High C ₃ A clinker.	150
7.11	TGA, derivative curves for samples at the same time (480 days) but different expansion level. High C ₃ A clinker.	150
7.12	TGA, derivative curves for samples at 360 days in sulfate solution. Low C ₃ A clinker.	151
7.13	TGA, derivative curves for samples at 480 days in sulfate solution. High C ₃ A clinker.	151
7.14	SEM, sulfate concentration in the samples.	153
7.15	SEM pictures (gray pictures) and sulfate profile (colored pictures). Mag:100x, HV:15kV, WD:12.5mm.	154
7.16	Sorptivity data at 28 and 90 days of hydration. Low C ₃ A clinker with 0 and 10% of limestone.	155
7.17	Sorptivity data at 28 days of hydration. High C ₃ A clinker with 0 and 10% of limestone.	156

7.18 Sorptivity data at 28 and 90 days of hydration. Commercial Cements.	156
A.1 Particle size distribution. Cements with low C_3A content.	167
A.2 Particle size distribution. Cements with high C_3A content.	168
A.3 Particle size distribution. Commercial Cements.	168
C.1 Inner C–S–H composition by SEM EDS analysis. High C_3A clinker, 3.8 and 9.0 % of gypsum at 10 and 24 hours of hydration.	177
C.2 Inner C–S–H composition by SEM EDS analysis. High C_3A clinker, 10% of limestone addition and different gypsum content at 10 and 24 hours of hydration.	178
C.3 Inner and outer C–S–H composition by SEM EDS analysis. High C_3A clinker, 10% of limestone addition and different gypsum content at 28 days of hydration.	179
C.4 Inner and outer C–S–H composition by SEM EDS analysis. Low C_3A clinker, 0 and 10% of limestone addition and different gypsum content at 24 hours of hydration.	180
D.1 XRD Rietveld analysis – C_3S quantification.	181
D.2 XRD Rietveld analysis – C_2S quantification.	182
D.3 XRD Rietveld analysis – C_3A quantification.	182
D.4 XRD Rietveld analysis – C_4AF quantification.	183
D.5 XRD Rietveld analysis – ettringite quantification.	183
D.6 XRD Rietveld analysis – portlandite quantification.	184
D.7 Heat Evolution Rated for samples with low C_3A content and increasing limestone content.	184
D.8 Heat Evolved for samples with low C_3A clinker and increasing limestone content.	185
D.9 Thermal Gravimetry data at 24 hours of hydration. Commercial cements with low C_3A content and increasing limestone addition.	185
D.10 Portlandite quantification by XRD Rietveld Analysis and TGA analysis. Commercial cements with low C_3A content and increasing limestone addition. . . .	186
D.11 XRD Rietveld Analysis. C_3S quantification. Commercial cements with low C_3A content and increasing limestone addition.	186
D.12 XRD Rietveld Analysis. C_3A quantification. Commercial cements with low C_3A content and increasing limestone addition.	187
D.13 XRD Rietveld Analysis. C_4AF quantification. Commercial cements with low C_3A content and increasing limestone addition.	187
D.14 XRD Rietveld Analysis. Degree of hydration. Commercial cements with Low C_3A content and increasing limestone addition.	188
D.15 XRD Rietveld Analysis. Ettringite (Ett) and monocarboaluminate (Mc) quantification. Commercial cements with low C_3A content and increasing limestone addition.	188

D.16 XRD Rietveld Analysis. Calcite quantification. Commercial cements with low C ₃ A content and increasing limestone addition.	189
D.17 MIP at 24 hours and 28 days of hydration.	189
E.1 Particle size distribution of laboratory and commercial cements. Cements with low C ₃ A content.	192
E.2 Particle size distribution of laboratory and commercial cements. Cements with high C ₃ A content.	192
E.3 Heat Evolution Rate up to 60 hours of hydration. Cements with low C ₃ A content. Comparison between laboratory and commercial cements.	193
E.4 Total Heat Evolved up to 60 hours of hydration. Cements with low C ₃ A content. Comparison between laboratory and commercial cements	193
E.5 Heat Evolution Rate up to 60 hours of hydration. Cements with high C ₃ A content. Comparison between laboratory and commercial cements	194
E.6 Total Heat Evolved up to 60 hours of hydration. Cements with high C ₃ A content. Comparison between laboratory and commercial cements	194
E.7 Compressive strength. Clinker with low (3%) C ₃ A content with different gypsum addition and with 0 and 10% of limestone addition.	195
F.1 XRD Rietveld Analysis, C ₃ A and ettringite quantification. Sample with low C ₃ A clinker cement, 3.8% of gypsum addition, 0 and 10% of limestone addition.	197
F.2 XRD Rietveld Analysis, C ₃ A and ettringite quantification. Sample with low C ₃ A clinker cement, 5.5% of gypsum addition, 0 and 10% of limestone addition.	198
F.3 XRD Rietveld Analysis, C ₃ A and ettringite quantification. Sample with low C ₃ A clinker cement, 9.0% of gypsum addition, 0 and 10% of limestone addition.	198
F.4 XRD Rietveld Analysis, C ₃ A and ettringite quantification. Sample with high C ₃ A clinker cement, 3.8% of gypsum addition, 0 and 10% of limestone addition.	199
F.5 XRD Rietveld Analysis, C ₃ A and ettringite quantification. Sample with high C ₃ A clinker cement, 6.0% of gypsum addition, 0 and 10% of limestone addition.	199
F.6 XRD Rietveld Analysis, C ₃ A and ettringite quantification. Sample with high C ₃ A clinker cement, 9.0% of gypsum addition, 0 and 10% of limestone addition.	200
F.7 Thermo Gravimetric Analysis, water loss up to 550°C. Sample with low C ₃ A clinker cement, increasing gypsum addition, 0 and 10% of limestone addition. .	200
F.8 Thermo Gravimetric Analysis, water loss up to 550°C. Sample with high C ₃ A clinker cement, increasing gypsum addition, 0 and 10% of limestone addition. .	201
F.9 XRD Rietveld Analysis, C ₃ S quantification. Sample with low C ₃ A clinker cement, increasing gypsum addition, 0 and 10% of limestone addition.	201
F.10 XRD Rietveld Analysis, C ₃ S quantification. Sample with high C ₃ A clinker cement, increasing gypsum addition, 0 and 10% of limestone addition.	202

List of Tables

3.1	Schema of cement mixes used	14
3.2	Chemical Composition of raw materials, XRF analysis	16
3.3	XRD analysis of laboratory and commercial raw materials	16
3.4	Specific Surface and Specific Gravity	18
3.5	Standard deviation for cement phases quantified by XRD Rietveld Analysis. Experimental data	25
3.6	Heating mode results comparison	26
4.1	Composition of samples with limestone addition	36
4.2	C-S-H composition at 24 hours of hydration by SEM EDS analysis	43
4.3	Gypsum content by dilution and added gypsum content and $\text{SO}_3/\text{Al}_2\text{O}_3$ ratio .	51
5.1	Alite, gypsum, limestone systems composition	69
5.2	Composition of mixes with different gypsum content	78
6.1	Maturity of the system at different temperatures indicated by Isothermal Calorime- try and Degree of Hydration from XRD Rietveld Analysis	129
6.2	Calculated Activation Energy	137
A.1	Laboratory Cements Composition. Cements without limestone	169
A.2	Laboratory Cements Composition. Cements with limestone	170
A.3	Laboratory Cements Composition. Cements with increasing limestone addition.	171
A.4	Commercial Cements Composition	171
A.5	XRD analysis of laboratory cement – Low C_3A clinker	172
A.6	XRD analysis of laboratory cement – High C_3A clinker	173
A.7	XRD analysis – laboratory cement High (8%) C_3A clinker and increasing lime- stone content and commercial cement	174
B.1	Phases structures used in the XRD Rietveld Refinement	176
E.1	Laboratory vs. Commercial Cements. Compared samples	191
E.2	Laboratory vs. Commercial Cements. Clinkers composition	191

Glossary

Abbreviations

BET:	Brunauer, Emmett and Teller
BSE:	Back-Scattered Electrons
EDS:	Energy Dispersive Spectroscopy
MIP:	Mercury Intrusion Porosimetry
PC:	Portland Cement
PSD:	Particle Size Distribution
SE:	Secondary Electrons
SEM:	Scanning Electron Microscopy
TGA:	Thermo Gravimetric Analysis
w/c:	water/cement ratio
XRD:	X-Ray Diffraction

Cement chemistry notation

C:	CaO
S:	SiO ₂
H:	H ₂ O
A:	Al ₂ O ₃
F:	Fe ₂ O ₃
\bar{S} :	SO ₃
C ₃ S:	Tricalcium Silicate
C ₂ S:	Dicalcium Silicate
C ₃ A:	Tricalcium Aluminate
C ₄ AF:	Tetracalcium Aluminoferrite
C–S–H:	Calcium Silicate Hydrate
CH:	Calcium Hydroxide
AFt or Ett:	Ettringite – C ₆ A \bar{S} H ₃₂
AFm or Ms:	C ₃ A·CaSO ₄ ·12H ₂ O
	where X may be OH [–] (Hydroxy–AFm),
	SO ₄ ^{2–} (monosulfoaluminate),
Mc:	C ₃ A·CaCO ₃ ·11H ₂ O (monocarboaluminate)
Hc:	C ₃ A·0.5CaCO ₃ ·11.5H ₂ O (hemicarboaluminate)

Chapter 1

Introduction

Limestone is a main raw material to produce clinker, which is a main constituent of cement. Additionally limestone can be use as a secondary cementitious material usually as a substitute of clinker. The main reason for substitution clinker with limestone or other secondary cementitious material is economical and ecological.

Among all supplementary cementitious materials such as slag, fly ash, natural pozzolan, clays, limestone is the most widely available natural material, which can be directly used in cement production. After grinding and blending with cement it can directly influence the properties of cementitious materials. The hydration reactions are complex and still not well understood. They are the subject of many research projects.

The aim of this thesis is to study hydration of limestone cement whit different clinker compositions and different gypsum additions.

Limestone reacts with C_3A to produce hemi- and monocarboaluminate phases. As a consequence no monosulfate is formed and stabilization of ettringite occurs. Because cement hydration is the sum of the multiple interactions of the hydrating cement phases the reaction of C_3A with limestone has a direct influence on the later properties of cementitious materials. C_3A , in the cement system reacts rapidly after mixing with water which can have an influence on the rheology and setting time of the cement. To regulate the C_3A reaction calcium sulfate is added to the system. The addition of limestone to the cement influences the C_3A reaction. Hence the interest in studying how limestone additions changes the properties of cement with different C_3A and gypsum contents.

In this study laboratory and commercial cements with low and high C_3A contents, different gypsum addition and different limestone additions were investigated in terms of kinetics, phase assemblage, microstructural development and durability. The properties of laboratory prepared cements were compared to commercial cements.

The layout of the thesis is as follow:

Chapter 2 contains a literature review on limestone cement, the main findings in the literature on limestone on the hydration and properties of cementitious materials.

Chapter 3 presents the materials and methods used in this study. It explains the composition and nature of the samples tested and the techniques used. Improvements of XRD and Rietveld Analysis are shown. Is demonstrated the possibility of using elastic modulus as a nondestructive method of measuring compressive strength.

Chapter 4 consists of two parts. The first part focuses on monocarboaluminate (Mc) and hemicarboaluminate (Hc) formation by comparison of cement with 0 and 10% of limestone addition and low and high C_3A clinker. The time of formation of Mc and Hc is investigated and the effect of their amount as a function of the cement composition especially C_3A content. In this part gypsum addition is at the optimum (the highest strength at 24 hours of hydration). The second part presents the influence of increasing limestone addition on the properties of the laboratory prepared cements with high C_3A clinker and gypsum at optimum.

Chapter 5 presents the influence of different amounts of gypsum on the hydration and properties of cement with low and high C_3A clinker. The dependency of the optimum gypsum on the cement composition is studied. The influence of gypsum in the pure alite–gypsum–limestone system also is presented in this chapter.

Chapter 6 presents the influence of temperature on the cement with different C_3A , gypsum and limestone content and activation energies for each cement.

Chapter 7 shows influence of limestone and gypsum on the durability, sulfate attack and sorptivity.

Chapter 8 contains the main findings and perspective for the future research.

Chapter 2

Literature review

The influence of limestone on the durability and properties of cementitious materials depends on many aspects, such as the method of cement preparation (intergrinding or blending), amount of limestone which is added and its physical properties (fineness, particle size distribution), fineness of cement, amount of main phases in the cement system, amount of water used in the cement mixing. However regardless of the cement composition up to certain level of clinker substitution limestone additions improve the properties of cementitious materials and above this level the properties are deteriorated. The limit can vary as a function of cement composition and fineness. In this chapter the main literature findings are presented.

2.1 Early hydration kinetics and phase assemblage

2.1.1 Early hydration kinetics

The presence of limestone in the cement system changes the hydration process from the beginning of hydration. First of all limestone provides nucleation sites for hydration products, which may increase the rate of hydration of the clinker. Pastes of pure C_3S with limestone give higher heat evolution by Isothermal Calorimetry, normalized to cement content than paste composed only of C_3S and water (Fig. 2.1) [59].

Limestone is also reported to increase reaction, as measured by bound water [38]; and increases CH content [81]. Sharma and Pandey [81] reported that 5% limestone affects the calcium hydroxide as the presence of limestone enhances the formation of CH at early ages until 1 day [81]. Even 5% of limestone addition results in an acceleration of the early hydraulic activity of the clinker [71] [85]. If the w/binder ratio is the same as plain cement, the water/clinker ratio increases, and more water is available for hydration reaction. Bonavetti [8] reported that limestone addition increase the degree of hydration at all times of hydration and for different water/cement ratios [8] (Fig. 2.2).

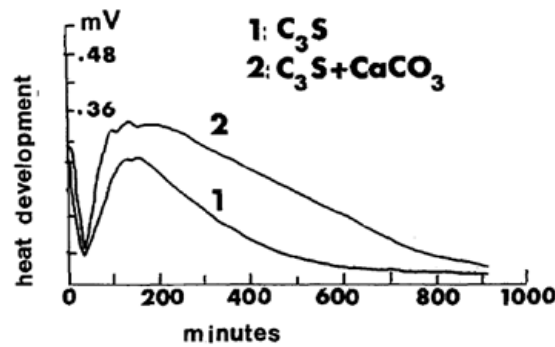


Figure 2.1: Isothermal Calorimetry data for: C_3S and $C_3S+CaCO_3$ [59].

Bouasker et al [10] studied hydration degree and chemical shrinkage of paste with different limestone contents and w/c ratios and also found that limestone increases the degree of hydration when 20 and 40% of limestone is incorporated in comparison to sample without limestone. However the increase in limestone addition from 20 to 40% did not lead to any additional increase in the degree of hydration. They also reported that limestone addition increases chemical shrinkage up to 24 hours of hydration [10].

Setting time is affected by the presence of the limestone. Kenai [41] reported that increasing the limestone addition to 35% leads to a decrease in setting time of 40 min (initial setting time for samples without limestone is 3 hours and with 35% of limestone it is 2 hours 20 min). Others suggested that this is due to acceleration of hydration of C_3A by $CaCO_3$ to form carboaluminates and of C_3S to form C-S-H and CH in cement [71].

All the findings show that limestone has an influence on hydration by incorporating additional nucleation sites and space for hydration. However limestone additions may also modify the hydrated phases formed during hydration.

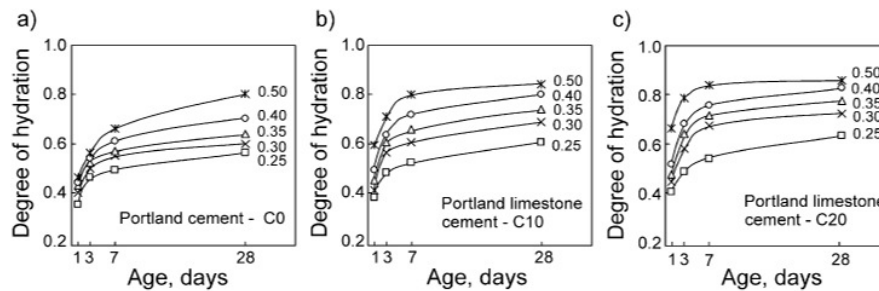


Figure 2.2: Degree of Hydration for paste with increasing limestone addition and different w/c ratio[8].

2.1.2 Phase assemblage

It is now well understood that limestone is partly reactive in cement systems, it reacts with C_3A to produce mono- and hemicarboaluminate phases [38] [51]. The formation of carboaluminate phases leaves more sulfate available to form ettringite therefore increases are observed in the amount of ettringite formed [9] [38] [49] [51]. The additional ettringite formed increases the total volume of hydration products and this can contribute to the reduction of porosity and permeability of cement paste [51]. However there are many disagreements about the time when the Hc and Mc phase are formed and in which order. There are indications that the first phase formed is Hc and after some time its amount decreases and Mc is formed [49], but also a suggestion that first Mc and later Hc is formed [38]. According to different authors the formation of Mc can start at the beginning of the hydration [38], or at 1,2 [3], 3 days [9] or just at 7 days of hydration [49]. Almost all researchers, however, show that amount of Mc increases up to 28 days of hydration [3] [38] [49]. Although the reactivity of limestone in the cement system is established, the amount of limestone which is able to react is still not clear. Matschei et al [51] claims that from thermodynamic for a typical portland cement composition up to 5% of calcite reacts. However others have found that in cement with 5% and 15% of limestone after 129 days of hydration only 1%, 1.5% of the calcium carbonate respectively is reacted [44]. It is claimed that the reaction of limestone with C_3A allows limestone to regulate early aluminate reactions. However limestone has lower solubility than gypsum thus the sulfate ions enter more quickly into solution than carbonate ions. Therefore calcium carbonate is not as effective as gypsum in controlling setting.

2.2 Physical properties with limestone addition

2.2.1 Particle size distribution

It is well recognized that limestone can improve the physical properties of cementitious materials such as particle size distribution, water demand and workability [8] [22] [23].

Limestone additions can improve the particle size distribution by incorporating additional size of grains, different to clinker. Clinker has narrower size distribution compared to the limestone which can be seen in Fig. 2.3 [76].

The particle size distribution of limestone depends on the method of preparation. Inter-grinding or blending give totally different particle size distributions. By blending the particle size distribution can be suitably adjusted to the application. When the cement is made by intergrinding of the constituents, the differences in their grindabilities strongly influences each other and so the particle size distribution [76]. There is a concentration of clinker in the coarser fraction material which is harder and concentration of limestone in the finer fraction

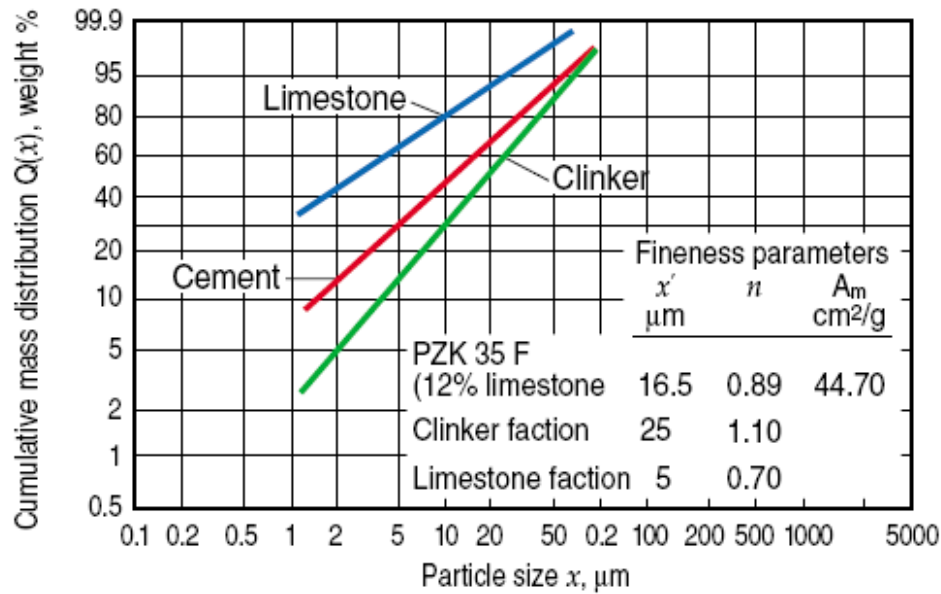


Figure 2.3: Rosin-Rammler-Sperling-Bennet diagram of clinker and limestone and limestone cement [76].

material which is in general softer. A Rosin–Rammler–Sperling–Bennet diagram (Fig. 2.3) shows the particle size distribution for clinker, limestone and a mix of this two. It can be observed that the particle size distribution is narrower for clinker and the position parameter (x') (*the equivalent spherical diameter which 38.6% by mass of the material is coarser than*) is $25\mu\text{m}$, while for the limestone it is $5\mu\text{m}$. The production of 50MPa strength cement without any additives requires the position parameter at the level of $30\mu\text{m}$, for cement with 10% of limestone it is $26\mu\text{m}$ and for 20% $14\mu\text{m}$ [32].

2.2.2 Workability

The water demand decrease when the particle size distribution is wider and increase when particle size distribution is narrower. However Shiller and Ellerbrock [76] reported that in Portland limestone cement which contains 10% of limestone, regardless of a narrow or wide particle size distribution, had a decreased water demand. Moreover even when the cement with limestone is ground to a finer fraction to get the same strength as the pure cement, the water demand is lower than pure cement because of the improved particle size distribution[76].

Limestone which has wider particle size distribution than ground clinker and less particles in the range $5\text{--}20\mu\text{m}$, therefore limestone grains fills the voids between clinker grains; and densifying the structure of hardened cement paste. The fineness of the limestone is not

reported to have a significant influence on setting [41].

Tezuka [89] reported that the workability of mortars with limestone is improved when 5% of limestone replaced clinker, the water demand reduce from 0.49 to 0.48 for the same consistency. This dependency is constant for different amount of cement in mortars. To compare, when the ground quartz was added in the same proportion the water demand increased. All these results show the possibility of the optimizing the particle size distribution in Portland limestone cements for special applications.

Kenai [41] reported that the water demand depends on the purity of limestone. When the purity of limestone is below 65% calcium carbonate, then the inclusion from 5-20% of limestone increases water demand for normal consistency by about 0.3% [41].

2.3 Mechanical properties

2.3.1 Strength

Soroka [85] reported that limestone additions in cement influences the strength of cement pastes. They reported that limestone improves significantly compressive strength and this is more pronounced at earlier ages(Fig. 2.4). They found levels of limestone which can be substituted without adverse effect. Up to 3 day 29% could be substituted and up to 7 and 28 day 24% and 13% respectively. They concluded that limestone affects compressive strength mainly due to the increasing rate of the cement hydration, based on the theory of filler effect, also that if monocarboaluminate is formed it did not adversely affect strength.

The density of cement and mortars increase when filler is presented and the permeability is lower [85]. The air-content in mortars containing filler is lower than mortars without filler, and this can contribute to the improvement in mortar strength.

Substitution up to 10% of limestone addition doesn't reduce the strength of cement and concrete [48][77][85]. At the higher additions the strength is generally decreased. The loss in strength can be reduced by finer grinding of the cement, however it depends on the cement and limestone fineness [41]. Up to certain limestone additions, lower than 35% an optimum of limestone fineness can be found to get the same level of strength for cements with limestone addition as for Portland cements [41]. However, high replacement levels above 35% of limestone, decrease strength regardless to the fineness of clinker or limestone.

The flexural strength also showed decrease with increasing limestone addition, but the rate of reduction is proportionally smaller than for compressive strength [41].

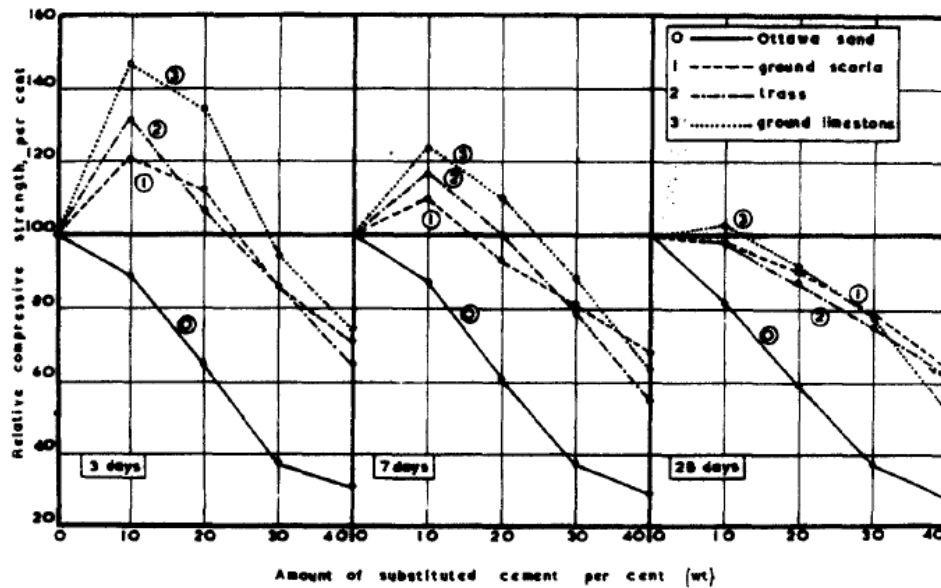


Figure 2.4: Compressive Strength of blended cements vs. percentage of the substituted Portland Cement [85].

2.3.2 Volume changes

Kenai [41] reported that the 28 day shrinkage increased for cement containing 15% of limestone and around 9% of C_3A [41], but the shrinkage is still less than the EN 12617- 4 standard requirement. There is a little knowledge about how bigger additions of limestone influence shrinkage. Maybe bigger amounts and lower quality of limestone can lead to higher shrinkage. Also the amount of C_3A in clinker is significant, it is reported that with low amount of C_3A (4% to 6%) the shrinkage can be higher [41].

2.4 Durability

2.4.1 Porosimetry

The durability of the cementitious materials depends on the pore structure. Most important is the connectivity of the pores and their ability to transport the deleterious ions into the material. The incorporation of the limestone to cement significantly changes the porosimetry and the pore connectivity in the material. The structure with limestone is denser [84]. Matschei reported that the presence of $CaCO_3$ in small amounts should reduce the total pore volume [51]. Kenai [41] reported that the total porosity measure by Archimedes method for cement pastes 5-35% of limestone ranged from 15-22% for all compositions. The porosity

decreased with age and increase with percent of limestone addition [41]. It was also reported that the proportion of small pores to larger pores ($>500\text{\AA}$) with age was higher for limestone cement compared to OPC [41].

Pipilikaki [65] using MIP reported that the paste of limestone cement with 35% of limestone addition has a lack of pores from 50nm to $10\mu\text{m}$ (large capillaries), but it has a great amount of pores in size from 10nm to 50nm (medium capillaries) which is an effect of addition of mineral admixtures in the cement pastes. Therefore he concluded Limestone Cement paste has narrower distribution of pores which indicates better homogeneity of the material [65].

2.4.2 Permeability

Permeability is a most important factor in the durability of concrete expose in various environments. Schmidt [77] reported that the materials based on cement with limestone displayed lower permeability than materials without limestone. This effect is not well understood whether it is caused by finer grinding or more efficient particle packing or both [77].

Also Kenai [41] reported that water permeability is lower for concretes with limestone filler when the 15% of limestone were incorporated to the cement [41].

2.4.3 Carbonation

Sprung [86] reported that, regardless of the strength of concrete, carbonation is increased by presence of limestone (they were working up to 20% of limestone substitution). The carbonation depth for concretes made from Portland Limestone Cement was deeper than for concretes made from Ordinary Portland Cement. However, after 3 years the increase in carbonation depth was minimal for concrete made of Portland Limestone Cement [77].

2.4.4 Freeze/thaw resistance

It is possible to make concrete with cement containing limestone with good freez/thaw resistance. Sprung [86] reported that the concrete from Portland Limestone Cement with 20% of limestone substitution, with the same strength as that from plain cement, had increased resistance to frost damage. Concrete cubes exposed for 100 freeze/thaw cycles had a mass loss less than 10% and were considered frost resistant. Up to 20% of limestone could be incorporated into the cement and the freeze/thaw resistance maintained [86].

Sprung [86] also found that the freeze/thaw resistance depends on the quality of limestone; the most important factor is the clay content in limestone, because clay can absorb the moisture which expands on freezing [86]. Sometimes substitutions in the medium range resulted in the worst performance. In this case 11% of substitutions in the medium range had the worst resistance.

A very important factor is water/cement ratio. Sprung [86] showed that for a w/c smaller than 0.6, concrete is frost resistance [86].

Schmidt [77] also reported that the freeze/thaw resistance for concrete made from Portland Limestone Cement was slightly better than concrete made from Portland Cement, even when concrete cubes were stored in the salt solution and subjected to 70 freeze/thaw cycles [77].

2.4.5 Sulfate resistance

Gonzalez [31] found that limestone cement pastes with 10% of limestone addition show no significant changes in the sulfate performance but if the limestone filler content is 20% by mass clinker than sulfate resistance is lower than for samples made by pure cement [31].

Pipilikaki [65] reported that limestone addition decrease the sulfate resistance of the mortars due to the fact the Portland Limestone Cement (35% of limestone addition by mass of cement) has a greater critical pore diameter than Portland Cement.

Schmidt [78] related the changes in sulfate resistance to the changes in porosity. 5% addition lowered porosity and slowed down sulfate ingress, while 25% addition increased porosity and the rate of sulfate ingress [78].

2.4.6 Thaumasite formation

Another deterioration mechanism is thaumasite formation. Although thaumasite is stable at 20°C [78] its formation is very slow at this temperature and is favored by temperatures below 15°C, preferably below 8°C.

Many authors claim that cement with limestone addition are more vulnerable to thaumasite formation. However the work of Schmidt [78] clearly demonstrates that this is mainly due to the physical effect at high limestone additions, which results in a more porous matrix. Furthermore it was shown from a thermodynamic basis that ingress of sulfate first reacted with all available aluminate to produce ettringite before thaumasite could form. That leads to conclusion that thaumasite formation is a final step in a degradation process which starts with ettringite formation.

2.4.7 Chlorides

Chloride ingress causes damage in reinforces concrete. The water/cement ratio is important. When the water/cement ratio for mortars containing 15% of limestone in cement was 0.60 the chloride penetration was deeper than for samples without limestone. When the water/cement ratio was 0.40 the samples with limestone filler had the same chloride penetration as sample without limestone [70].

2.5 Summary

Limestone cements have been subject of several studies for many years. However, the mechanism by which limestone addition affects the properties of cementitious materials is still not well understood. It is known that limestone is reactive in the cement system and it reacts with C_3A during hydration reaction to form Mc and Hc, this directly influences hydration and properties of cementitious materials. Furthermore, the limestone influence on durability especially sulfate attack which is attributed to the limestone presence in the cement, is not well understood until now.

Literature review leave many questions on limestone influence on the hydration and properties of cementitious materials based on the limestone cement. In this work following questions were investigated:

- What are the factors influencing the kinetics of Mc and Hc formation?
- How the limestone influences the hydration and properties when different amounts of C_3A are in the clinker?
- What is the role of gypsum in cements with and without limestone?
- How the temperature influences the hydration of cement with different gypsum and limestone additions?
- Can limestone cement be resistant to sulfate attack?

Chapter 3

Materials and Methods

The properties of cementitious materials are influenced by many different aspects. The compounds of cement, particle size distribution, and fineness have direct or indirect influence on later properties of hydrated systems; therefore the materials which are used are characterized below.

This chapter outlines the experiments strategies and the techniques used in the study, to understand the mechanisms of limestone addition in cement with different amount of cement components. Multiple techniques were used on selected specimens to investigate the hydration kinetics, hydration products and phase assemblage. Durability studies were also made on some samples.

3.1 Objective of the study

In the present study cement systems were studied in terms of hydration kinetics, phase formation, porosity, compressive strength and sulfate attack. Limestone and gypsum additions in the systems were varied according to the objective of investigation.

The main focus was on the reaction of limestone with C_3A and how this is influenced by the amount of C_3A . The addition of gypsum was found to have a major influence on the properties of cement especially compressive strength. Therefore the optimum gypsum, indicated by the highest compressive strength at 24 hours, was determined for the cements studied and samples at optimum gypsum were major objective of the study.

Four samples, two with low and two with high C_3A clinker and with 0 and 10% of limestone were used to investigate the hemicarboaluminate and monocarboaluminate formation and how C_3A content in the clinker influences the limestone reaction. The influence of limestone on hydration with different C_3A content clinker was further investigated in terms of porosity and compressive strength and sulfate attack.

Second objective was to investigate how increasing limestone addition can influence hydration and properties of cementitious materials. Clinker with high C_3A content was chosen for

this study with 0, 5, 10, 15, 20% of limestone addition. The literature shows that increasing limestone addition decreases compressive strength. The optimum gypsum for these systems was extrapolated from the values for the 0 and 10% blends.

Finally the variations of gypsum around optimum content were investigated and the explanation for the significant differences in compressive strength with different gypsum content studied in terms of hydration kinetics, phase consumption, hydration products and porosity. Samples were composed with low and high C₃A content with different gypsum content from 2.2 – 9.0%. The effect of limestone addition on gypsum optimum was investigated.

During the study laboratory cements were prepared by Holcim Group Support. In order to study the relevance of laboratory cements they were compared with commercial cement. Four different cements, 3 with low C_3A clinker and 1 with high C_3A clinker were received from a commercial cement plant.

3.2 Primary Materials Characterization

The laboratory cements consisted of two types of clinker with low and high C_3A content, with various levels of gypsum addition. Each mix of clinker with gypsum was substituted by 10% of limestone addition to keep the same Gypsum/Clinker ratio for each pair of samples. Samples with increasing limestone content were also used and here the gypsum content was kept at the supposed optimum level extrapolated from 0 and 10% blends. The second stage was comparison between cements made in laboratory and at the cement plant. The commercial cements came from Holcim Group Support, however their composition shows differences from those made in the laboratory which makes comparison difficult.

The scheme of the samples and additions is presented in the [Table 3.1](#)

Table 3.1: Schema of cement mixes used

Cement	Laboratory Cement								Commercial Cement		
Clinker	Low C ₃ A				High C ₃ A				Low C ₃ A	High C ₃ A	
Gypsum [%]	2.2	3.9	5.5	6.0	9.0	3.8	5.5	6.0	9.0	6.5	5.5
Limestone [%]	0	0	0	0	0	0	0	0	0	4	
	10	10	10	10	10	10	10	10	10	13	10
							5			22	
							15				
							20				

Abbreviation The following abbreviation is used in the text:

H10Cg3.5 where:

H – high C₃A clinker

10 – limestone content [%]

C – calcite

g – gypsum

3.5 – gypsum content [%]

3.2.1 Raw materials characterization

The raw materials were blended by Holcim Group Support. In the [Table 3.2](#) the chemical composition and in the [Table 3.3](#) phase composition of raw materials are presented.

3.2.2 Cement blend characterization

The composition of the cement blends is presented in the Annex: [Tables A.1](#), [A.2](#), [A.3](#) and [A.4](#).

Anhydrated samples were characterized by:

1. XRF – Chemical Characterization – [Table A.1](#), [Tables A.2](#), [A.3](#), [A.4](#)
2. XRD – Crystalline Phases Characterization – [Tables A.5](#), [A.6](#), [A.7](#)
3. TGA – Thermo Gravimetric Analysis – [Fig. 3.1](#) comparison with XRD
4. Malvern – Particle Size Distribution – [Tables A.1](#), [A.2](#), [A.3](#)
5. Helium Picnometer – Specific Gravity – BET, Blain – Specific Surface – [Table 3.4](#)

Table 3.2: Chemical Composition of raw materials, XRF analysis

	CaO	SiO ₂	Al ₂ O ₃	Fe ₂ O ₃	SO ₃	MgO	Na ₂ O	K ₂ O	Cl	LOI
Laboratory Cements										
Low C ₃ A	63.04	22.63	3.92	4.69	1.00	1.88	0.30	0.98	0.04	0.69
High C ₃ A	63.84	20.93	5.86	2.40	1.53	2.83	0.23	1.15	<0.01	0.23
Limestone	50.44	6.11	0.71	0.43	0.47	1.02	0.05	0.22	0.03	40.26
Gypsum	31.80	2.25	0.33	0.18	45.11	0.38	0.20	0.10	0.00	19.73

Commercial Cements – lack of detailed data

Table 3.3: XRD analysis of laboratory and commercial raw materials

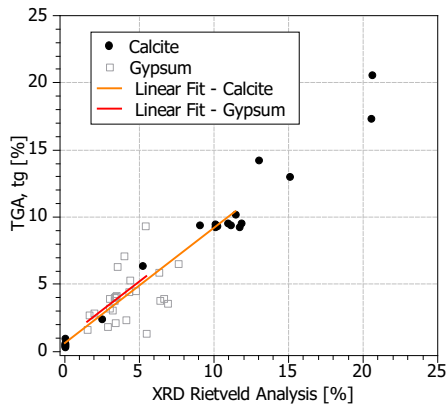
	Laboratory				Commercial		
	Low C ₃ A	High C ₃ A	Limestone	Low C ₃ A	High C ₃ A	Limestone	
Alite	56.4	68.3	–	69.57	63.39	no data	
Belite	22.3	11.5	–	11.58	14.70		
Aluminate cub.	1.6	7.3	–	2.86	6.98		
Aluminate orth.	1.0	0.2	–	1.84	2.33		
Ferrite	17.0	9.0	–	9.98	6.71		
Arcanite	0.2	1.8	–	2.42	3.47		
Free Lime	0.0	0.0	–	0.0	0.0		
Portlandite	0.3	0.3	–	0.0	0.0		
Periclase	1.2	1.6	–	1.13	1.24		
Calcite	–	–	96.34	–	–		
Dolomite	–	–	1.05	–	–		
Quartz	–	–	2.61	0.61	1.15		

3.2.2.1 XRD and TGA analysis comparison

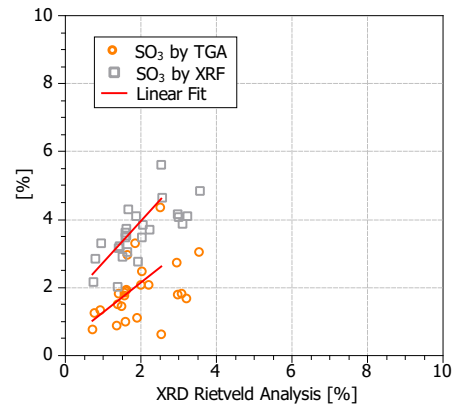
Calcite and gypsum content can be quantified by both XRD and TGA. The comparison of the results are shown in Fig. 3.1 a.

The amount of calcite is in good agreement by both quantification methods. However there are some discrepancies between what should be in the samples and what was obtained by XRD and TGA analysis. The error of measurement has to be taken into account. The error in XRD Rietveld analysis for 1 wt.-% of calcite is ± 0.3 wt.-% for 2wt. -% amount of gypsum is ± 0.4 wt.-%. The quantification for calcite is good. The gypsum quantification contains bigger errors due to the smaller amount of gypsum in the sample and also three different phases which are separately quantified by XRD analysis.

TGA and XRF are in good linear agreement (Fig. 3.1 b), however XRF shows systematically 1% more SO_3 than TGA due to certain amount of sulfate which is present in the raw clinker.



(a) XRD vs. TGA quantification method. Comparison of the results of both techniques. Quantification of calcite and gypsum.



(b) XRD vs. TGA vs. XRF quantification method. Comparison of the results of both techniques. Quantification of SO_3 content.

Figure 3.1: XRD, TGA, XRF method comparison. Quantification of SO_3 in cement.

3.2.2.2 Particle Size Distribution, Specific Surface and Specific Gravity

Cements were prepared by blending. During the study two different batches were used. Their particle size distribution varied slightly and is presented in the Figs 3.2 and 3.3. These variations sometimes made comparisons difficult. The particles size distributions for other mixes are compiled in the appendix Figs A.1, A.2 and A.3.

Limestone shows a bimodal distribution with about 60% centered around $2\mu\text{m}$ and a coarse fraction centered around $35\mu\text{m}$. The PSD of cement is dominated by clinker, the high C_3A clinker has more particles below $10\mu\text{m}$ than low C_3A clinker. The commercial cements are coarser with particles mainly above $10\mu\text{m}$ in comparison to laboratory cements.

The specific surface of the cements powders showed that the cement which is used has fine particles (Table 3.4) and there are only slight differences in their specific surface and specific gravity.

Table 3.4: Specific Surface and Specific Gravity

Sample name	Specific Surface Blain [cm^2]	Specific Gravity [g/cm^3]
L0Cg2.2	4764	3.24
L0Cg3.8	4936	3.22
L0Cg5.5	5107	3.22
L0Cg6.0	4868	3.17
L10Cg2.0	5229	3.18
L10Cg3.5	5406	3.18
L10Cg5.0	5398	3.17
L10Cg5.5	5278	3.14
H0Cg6.0	4645	3.14
H5Cg5.5	4883	3.12
H10Cg3.5	5423	3.17
H10Cg5.0	5647	3.16
H10Cg5.5	5115	3.10
H10Cg8.2	5719	3.12

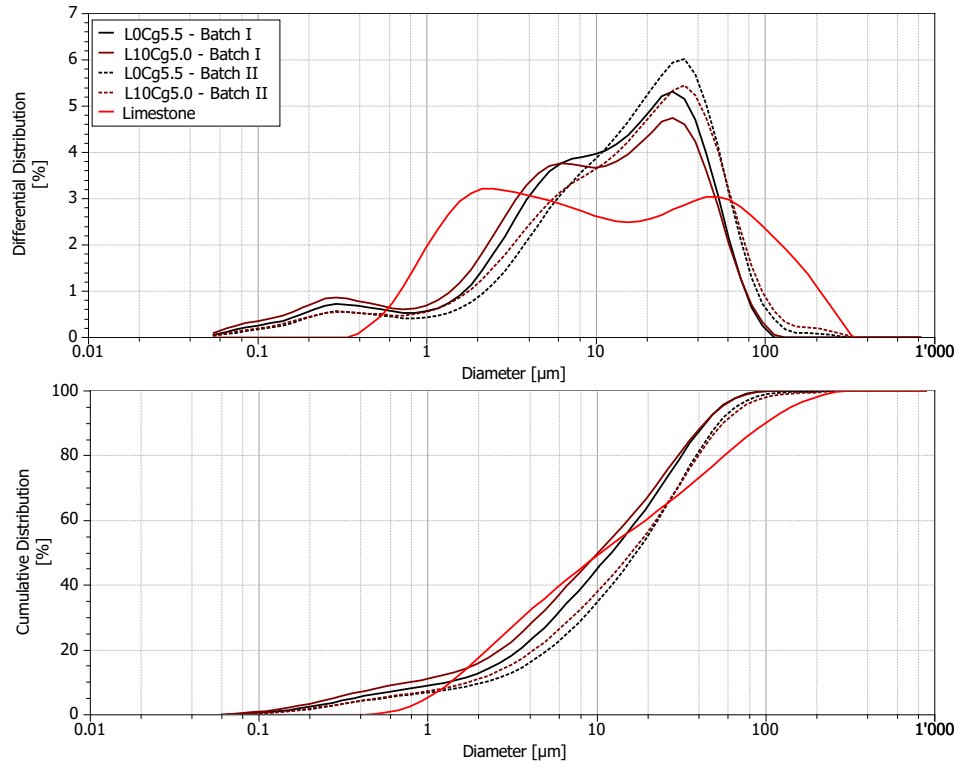


Figure 3.2: Particle size distribution. Batch comparison. Cements with low C_3A content.

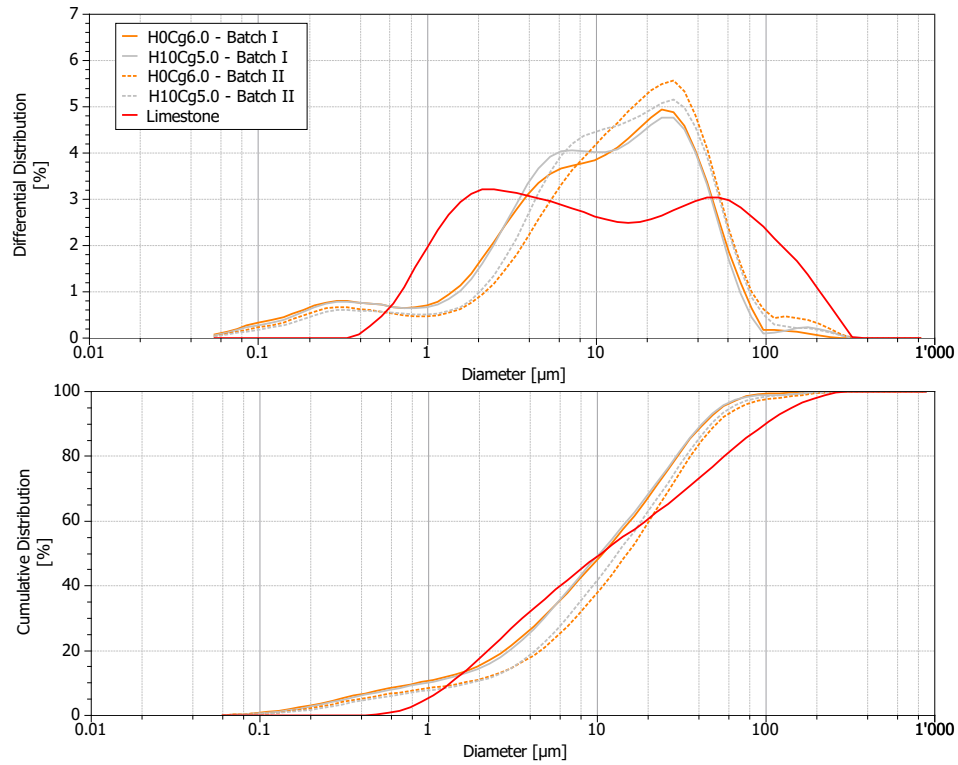


Figure 3.3: Particle size distribution. Batch comparison. Cements with high C_3A content.

3.3 Preparation of samples

Cement pastes The cement pastes were prepared by mechanical mixing (500rpm) of cement with water at $w/c=0.40$. The samples were cast in cylinders, and stored in a room at constant temperature 20°C . On the bottom and top of each cylinder a small amount of water was kept to provide saturated conditions. At certain times three slices were cut from the samples and immersed in isopropanol for five days to stop the hydration reaction. Afterwards the samples were dried in a desiccator for next five days then measured.

The solid cement pastes were studied by XRD, TGA, MIP and SEM. For the XRD experiment, powders were obtained by grinding of the piece of solid paste in the mortar. For SEM, TGA and MIP pieces of solid cement paste of appropriate dimensions were tested.

Isothermal Calorimetry, Continuous XRD, Chemical Shrinkage, Autogenous Shrinkage and Vicat test were performed on the fresh cement pastes.

To study the effect of the temperature cement pastes were stored in the different temperature baths at 10°C , 20°C and 30°C for a total duration of the experiment.

For the Continuous XRD the cement paste was directly cast in the XRD steel mould, covered with thin capton film and directly exposed in the XRD apparatus. The temperature in the XRD chamber was 23.5° .

Mortars were mixed with $w/c=0.50$ and cast in $40\times40\times160\text{mm}$ steel moulds. Samples were demoulded after 24 hours, or earlier if the experiment demanded it. The prisms were kept above the level of water in a closed box up to certain age, and after that tested.

Compressive Strength tests were done on the prisms $40\times40\times160\text{mm}$ at 10 hours, 1, 7, 28 and 90 days of hydration. For each time three prisms were tested.

For compressive strength tests at different temperatures prisms were stored in different temperature chambers until the required age and then tested.

3.4 Methods

3.4.1 X-Ray Diffraction – XRD

X-Ray Diffraction is a powerful technique which allows crystalline phases to be studied in cement systems. Each crystalline phase has a unique X-ray diffraction pattern determined by the spacing of the crystallographic planes described by Bragg's law [Eq. 3.1](#). So it is possible to distinguish the particular phases from the XRD pattern.

$$n\lambda = 2d\sin\theta \quad (3.1)$$

With development of the Rietveld Analysis (1969) there is a possibility to quantify the amount of phases in the cement mixture [20] [61] [66] [74] [79] [95].

Rietveld Analysis entails comparison of the experimental pattern with a simulated pattern of a mixture consisting of known phases. All patterns for known crystalline phases are combined in Inorganic Crystal Structure Database (ICSD). The comparison is based on multiple parameters such as the presumed amounts, crystal parameters, and equipment parameters. The simulated pattern is fitted using least squares fitting.

Samples type used in the XRD depends on the cement system and required result and can either be powders, solid or paste. To analyze the composition of anhydrous cement powder samples are used. With hydrated samples powder or solid paste can be used. Solid samples are a slice of cylinder which fits the holder diameter. This can be freshly cut or measured after stopping hydration. Powder samples are usually ground solid samples fresh or after stopping hydration.

XRD measurement parameters All data in the presented study were collected using a PANalytical X'Pert Pro MPD diffractometer in a Θ – Θ configuration employing CuK_α radiation ($\lambda=1.54\text{\AA}$). The divergence slit size was fixed and equal to 0.5° . The samples were scanned in a rotating stage between 7 and 70° with a step size of 0.0167° acquired for 77.470s, with a scan speed of 0.027396. The total scan time was 40 minutes.

3.4.1.1 XRD analysis in the limestone cement systems – crystals susceptible to preferred orientation

The compaction of powder into the sample holder may cause some crystallographic planes to orient to one of the compacting direction. This phenomenon can create a systematic variation in diffraction peak intensities, and significantly influence the quantitative results of sample composition. The phases in the cement system most susceptible to preferred orientation are gypsum, anhydrite, hemihydrate and calcite. In Rietveld Analysis a certain degree of preferred orientation can be corrected by the March model [21].

The initial analysis of slices of the limestone cement systems, calcite (Fig. 3.4) and ettringite (Fig. 3.5) were found to show a high degree of preferred orientation which caused many problems of phase quantification. The preferred orientation of calcite is probably due to the very small size of the limestone grains which means that they can be aligned during cutting. Traditional methods of preparing powder samples such as frontloading with frosted glass side compaction or vertical loading and also backloading

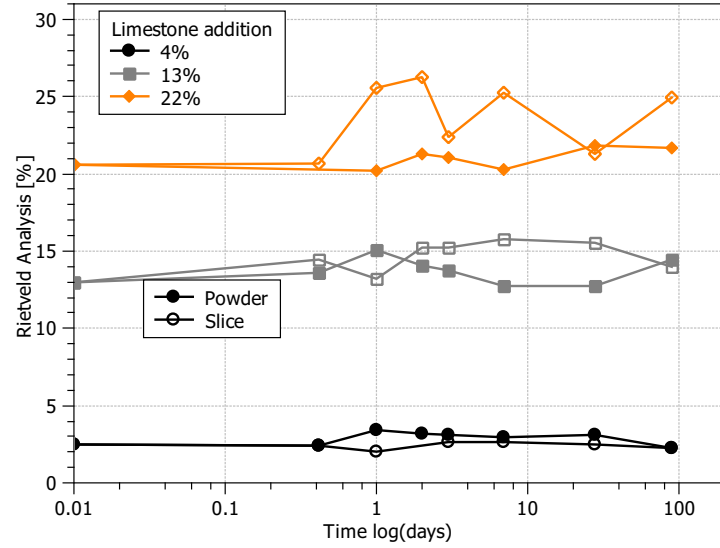


Figure 3.4: X-ray diffraction results. Comparison of the two methods for limestone cement samples preparation, ground and sliced. Calcite quantification.

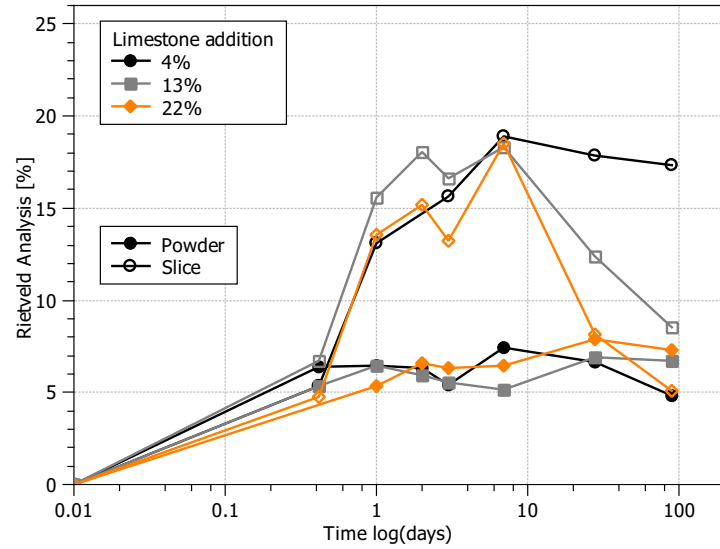


Figure 3.5: X-ray diffraction results. Comparison of the two methods for limestone cement samples preparation, ground and sliced. Ettringite quantification.

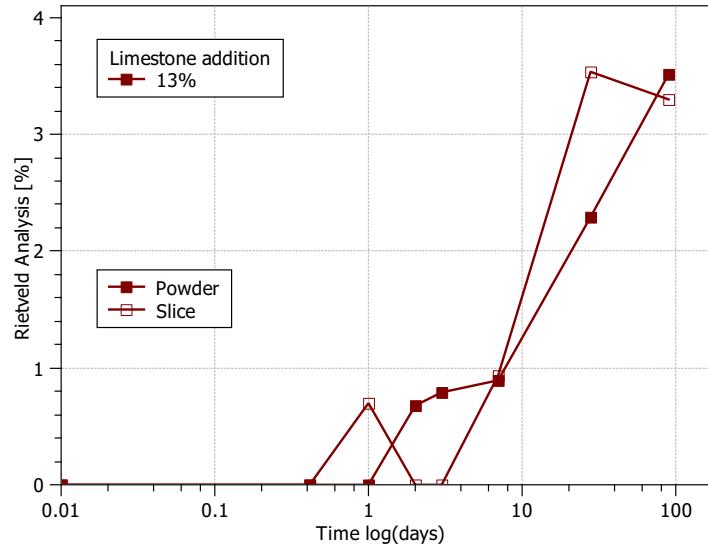


Figure 3.6: X-ray diffraction results. Comparison of the two methods for limestone cement samples preparation, ground and sliced. Monocarboaluminate quantification.

did not give good results either. Therefore a new way of treating samples was developed. First the samples were ground before XRD measurement. The powder was placed in the steel mould (3.5cm) and compacted using a long spatula. The powder compaction consisted of the continuous displacement on the sample surface with up and down movements. All the moves were made in a short time and are repeated several times, each time the angle of the spatula is rotated relative to its previous position around 15 degrees. This process avoids additional pressing on the sample, which could produce preferred orientation for calcite. The only disadvantage of presented method was drying of the samples in isopropanol and later in desiccator before measurement. This was found to have negative influence on ettringite crystals, which loses its crystallinity in isopropanol. However method could be easily used for fresh cement pastes.

In Fig. 3.7 diffraction traces for the same sample by the two techniques are compared. For powders the patterns shows more background noise probably due to a greater roughness of the compacted powder samples in comparison to solid slices. A consequence of this increased roughness is that small peaks, for example the hemicarboaluminate (Hc) peak are less visible in the powder samples patterns. Monocarboaluminate is more apparent maybe due to carbonation of the hemicarboaluminate in the powder sample. The other difference is in the intensity and visibility of certain peaks. The biggest difference is between patterns of sliced samples and powdered samples for monosulfoaluminate. In the patterns of sliced samples monosulfate is almost not visible. This is due to preferential oriented ettringite which influences the identification

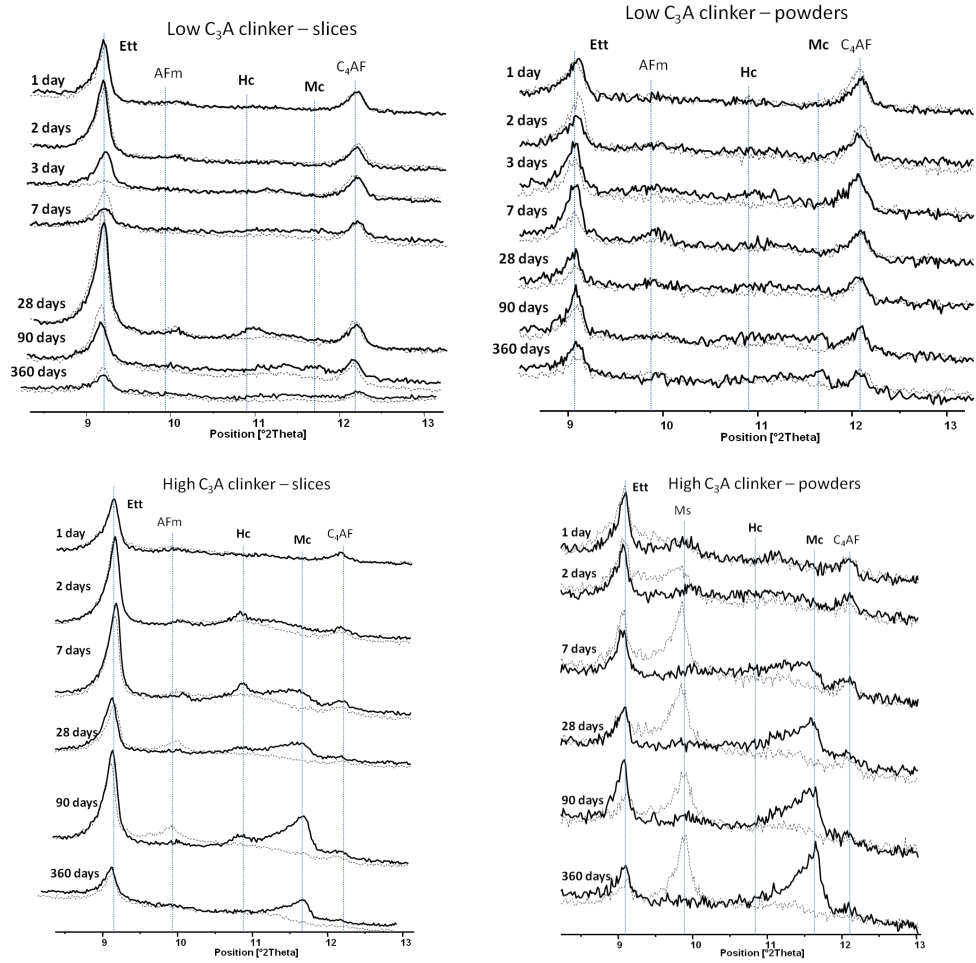


Figure 3.7: XRD patterns for techniques of sample preparation, grounded – powders and slices. Sample with low and high C_3A clinker with (dark line) and without (light line) 10% of limestone.

of monosulfate. On the other hand the quantity of ettringite may be lower in these powdered samples due to the loss of crystallinity due to immersion in isopropanol.

With the new way of treating samples we were able to eliminate the preferential orientation factor and more precisely quantify the phases. Moreover phases such as monocarboaluminate, are visible earlier (Fig. 3.6). Additionally to avoid use of isopropanol, which has negative influence on ettringite this technique could be used to analyze fresh cement pastes.

The development of the compacting technique allows the hydration reaction to be followed quantitatively, reproducibly and with minimum error. Additionally the powder samples allow better identification and quantification of AFm phases.

Error of the measurement The error of the measurement was calculated by repetition of experiment on the sample. Three samples of the same specimen were tested and analyzed using Rietveld Analysis. The standard deviation of the measurements are presented in the Table 3.5.

Table 3.5: Standard deviation for cement phases quantified by XRD Rietveld Analysis. Experimental data

Phase	σ
Alite	1.5
Belite	1.2
Aluminate cub.	0.293
Aluminate orth.	0.293
Ferrite	1.0
Calcite	2.4
Ettringite	2.7
Monosulfate	0.203
Portlandite	1.2
Monocarboaluminate	1.02

3.4.2 Thermo Gravimetric Analysis – TGA

TGA it is a method of determining the sample composition by detecting the sample mass loss with increasing temperature and comparison with the thermal data for pure phases possible present in the sample. The mass loss curve obtained is later transformed into derivative form where weight loss effects are more visible.

In the cement field TGA is mostly used for following hydration reaction [27] [69] and phase identification [14] [45] [72] and studying the effect of pozzolanic additives

[26] [40].

In this project a Mettler–Toledo TGA/SDTG 851 instrument was used for thermogravimetric measurements. Mostly 10°C/min was used in the range of temperature 30°C up to 900°C. A 30ml/min nitrogen flux was used in the chamber during the heating in order to avoid carbonation of the samples during the experiment. Water loss from dehydroxylation of the cement phases was measured using both tangent and horizontal method, and it was dependent on the phase.

3.4.2.1 TGA possibilities

The limitation of linear heating of the treating sample is the overlap of phases decomposition ranges and difficulties with the exact phases identification and quantification. In Fig. 3.8 three region of phase decomposition are visible.

The first region corresponds to the C–S–H and AFm AFt decomposition. The mass loss for these phases overlap, which makes quantification difficult.

Therefore other ways of heating samples were studied to try to better distinguish which phases are present.

A second method is to heat the sample up to temperature of the maximum of the peak, previously indicated by standard method, with the speed of 10°C/min and keep the sample at this temperature for another 15 min (plateau). The two methods are compared in the Figs 3.8, 3.9.

Table 3.6: Heating mode results comparison

TGA heating methods		
	Linear	Step
Total mass loss [%]	18.35	19.37
Loss up to 450°C [%]	13.26	12.86
Portlandite amount [%]	11.01	10.76

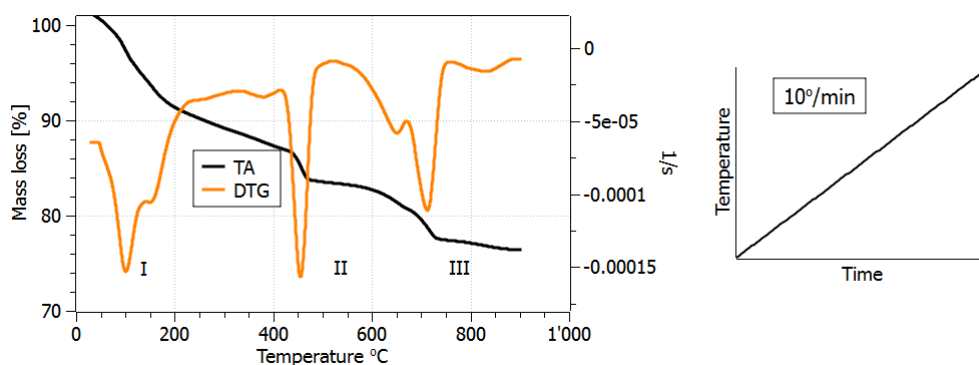


Figure 3.8: TGA analysis. Heating mode – linear 10°C/min.

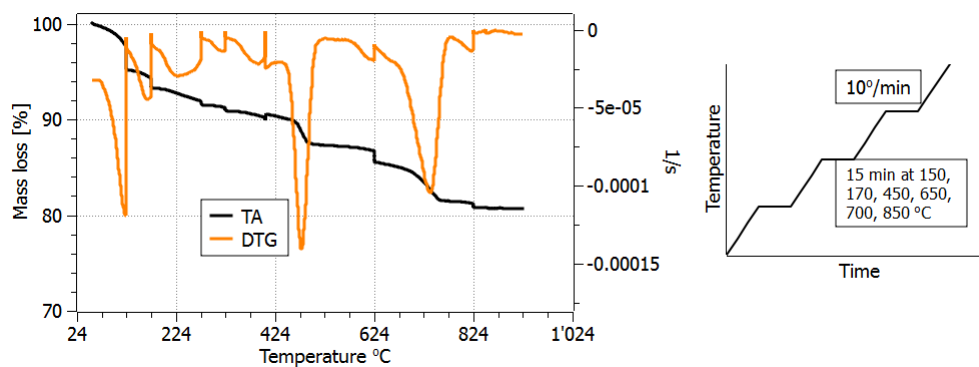


Figure 3.9: TGA analysis. Heating mode – step method.

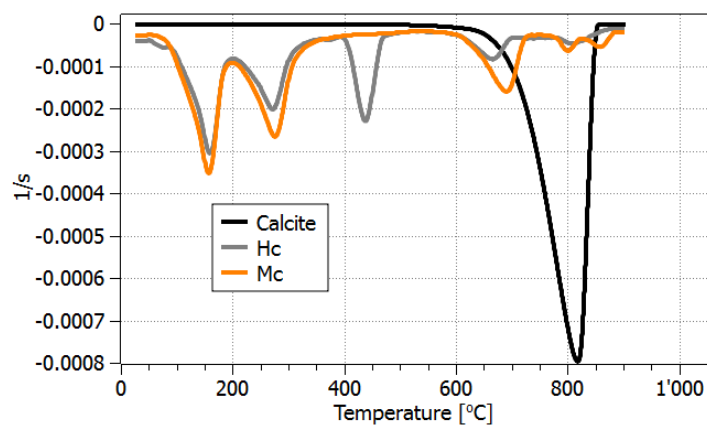


Figure 3.10: TGA analysis. Heating mode – linear 10°C/min – hemicarboaluminate (Hc), monocarboaluminate (Mc) and calcite.

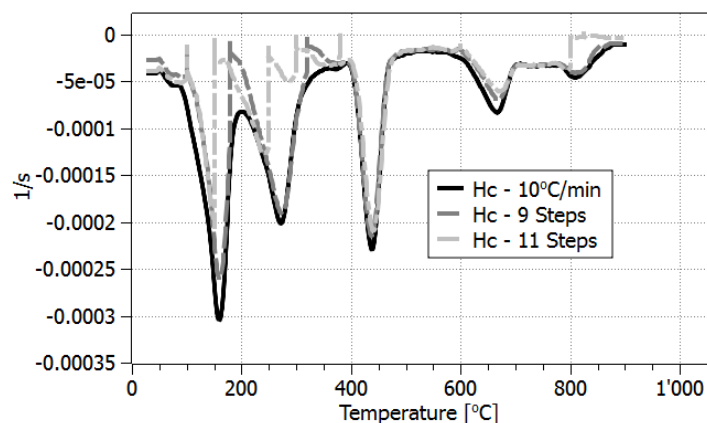


Figure 3.11: TGA analysis. Hemicarboaluminate decomposition at different heating mode.

The step method allows to separate peaks which can be distinguish in all three regions however the number of peaks multiplied. The comparison of results in the Table 3.6 show agreement in phases quantification for both methods. However there are some additional peaks visible on the step method result curve. Those small peaks before main peaks could be an artefact. Consequently this method was not used further.

The pure phases were prepared to see the influence of the different method on the one phase decomposition pattern. First the Hc, Mc and limestone were tested under linear method conditions all the results are on the Fig. 3.10. The decomposition pattern for limestone shows only one main peak with its maximum at 820°C. The pattern of Hc and Mc are very similar there is only one peak at 450°C which is present for Hc and not present for Mc. In Fig. 3.11 the patterns of Hc decomposition in different modes is presented. The results show that with increasing amounts of steps the number of decomposition peaks increases. For a pure phase those effects are mostly artifacts created during analysis of the sample.

The method used in future experiments was linear method for all tested samples by Thermal Gravimetry Analysis.

3.4.3 X-Ray Fluorescence (XRF)

X-Ray Fluorescence measurement was performed by external laboratory APC Solutions SA, CH-1021 Degens. The equipment used was a Bruker AXS S4 Explorer spectrophotometer operating at a power of 1 kW and equipped with Rh X-ray source. Used crystals are OVO55FC for Na, F, Cl with 0.46° divergence collimator, PET for Al, Si, P and Mn with 0.23° divergence collimator and LiF220, with 0.23° divergence collimator for all other elements.

3.4.4 Particle Size distribution

Particle Size Distribution was measured using a Malvern Mastersizer type S laser beam granulometer. The particle size range for this measurement is 0.05 to 900 μm in dispersion. Cement powders were dispersed in isopropanol.

3.4.5 Specific Surface and Density

Density measurements were done using a Micromeritics Accupyc 1330 V2 instrument. Specific surface (BET) was measured using a Micromeritics Gemini 2375 V4 instrument.

3.4.6 Scanning Electron Microscopy (SEM)

Scanning Electron Microscopy is a very powerful technique and in the last 25 years this method of cementitious materials study has been developed and widely used. The study of microstructures by SEM and BSE of polished surface gives a lot of advantages: representative cross-section; wide range of magnification; contrast dependent atomic number; reproducible for a given sample, etc.

Backscattered electron (BSE) images were taken using FEI quanta 200 with tungsten filament. The accelerating voltage was set to 15keV. For this measurement all samples were previously impregnated with epoxy resin and polished using a Struers Rotopol machine, with increasing diamond powder particles from 9 μm to 1/4 μm . The protocol for polishing of the samples depended on the age of the sample. The regular procedure was 90min at 9 μm , 45min at 3 μm , 45min at 1 μm , and if necessary 15min at 1/4 μm . The lubricant used was laboratory petrol. Force acquired on the samples was 20kN.

3.4.7 Mercury Intrusion Porosimetry (MIP)

The principle of MIP is the measurement of the volume of mercury which was able to penetrate the pore structure of the sample under pressure. The pressure with which mercury is introduced into sample is controlled which allows the pore size distribution to be obtained based on the inverse relationship between the pore radius (r) and the pressure (P), given by the Washburn equation (Eq. 3.2).

$$r = -2g\cos\Theta/P \quad (3.2)$$

where:

g – surface tension of mercury (480 Dyne/cm)

Θ – contact angle of mercury on the solid material (145°)

Measurements were done using Porotec Pascal 140 and Pascal 440. A few small pieces of solid cement paste previously immersed for 5 days in isopropanol and dried in a desiccator to stop hydration, were put into empty and dry dilatometer. The total weight of the sample was around 1g. The dilatometer with the sample was placed in the apparatus Pascal 140, where mercury was introduced into the dilatometer and pressure up to 140MPa. The pressure increment is monitored. After dilatometer with sample is put into Pascal 440 where the pressure can reach 440MPa.

There are few assumption in the MIP techniques:

- Surface tension of mercury and contact angle do not change during the analysis
- So called pore size distribution is really the volume accessible through pores of entry
- The pore structure skeleton is not deformed during applied pressure

3.4.8 Isothermal Calorimetry

Isothermal Calorimetry is a technique which allows the kinetics of the hydration reaction of cement to be followed. The hydration reaction can be divided in several stages (Fig. 3.12).

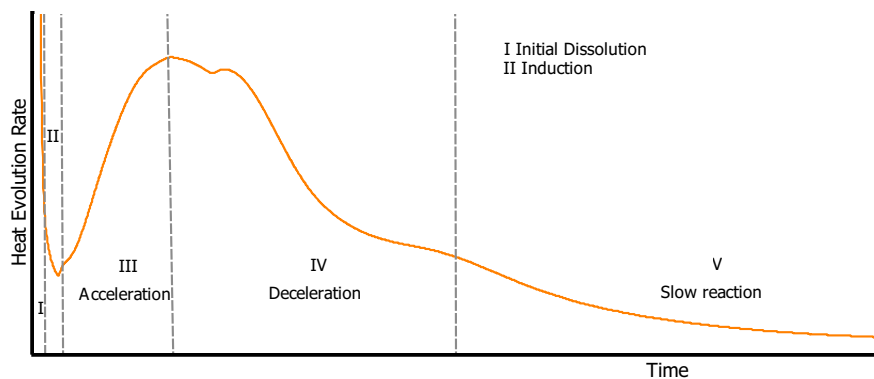


Figure 3.12: Isothermal Calorimetry curve typical for Portland cement hydration.

I stage – Initial Dissolution – occurs immediately after the contact of cement with water and corresponds to a rapid release of heat . Some precipitation of C–S–

H, and AFt and hydration of hemihydrate can also occur. The length of Initial Dissolution is around 10 minutes.

II stage – Induction – it is a slow reaction period whose duration is up to about 3 hours and can change with temperature, composition of cement, w/c ratio, chemical admixtures etc.

III stage – Acceleration – silicate reaction proceeds rapidly up to maximum of heat evolution to give C-S-H and CH as main products.

IV stage – formation of C-S-H and CH decelerates, the aluminate reaction is in its maximum.

V stage – controlled by diffusion, the hydration reaction is slow.

Isothermal Calorimeter from TA, TAM Air was used in the study. It has 8 twin-type sample channels, one dedicated to the sample and one to the reference. The reference material was distilled water. Sample of cement paste and water were placed in a glass ampoules of 20ml, followed with immediate placement of the ampoules in the calorimeter. The mass of cement paste used was 10 grams.

3.4.9 Chemical Shrinkage

The volumetric approach was used to measure chemical shrinkage. The set up used was assembled in our laboratory for this purpose. The procedure consists of placing about 3.5 grams of cement paste into a plastic container which was then filled with water to the top and covered with rubber stopper through the center of which passed an 1-ml water filled capillary tube. The water used is deionized water and on the top a drop of colored oil is added as an indicator to follow the reaction and to avoid evaporation. The plastic container with the glass tube is then immersed in a thermostatic water bath kept at constant temperature, in this project it was 20°C and 30°C.

During the hydration reaction, the chemical shrinkage changes are indicated by the diminishing water level in the glass tube. A webcam connected to a computer, every 5 min is recording a photo of the glass tube with a colored oil indicator that allows automatic acquisition and processing of the data. Each cement paste had 3 replicas to get better statistical result.

3.4.10 Compressive and Flexural Strength

Compressive and flexural strengths were measured using a hydraulic press. The samples were mortar prism of 40x40x160mm dimension. The strength was measured at different times 10, 24 hours, 7, 28, 90 days. Up to the age of the test, samples were kept in a humidity box, above the water level and at 20°C.

3.4.11 Elastic Modulus

Elastic materials possess resonance frequencies that are determined by the elastic modulus, mass and geometry of the specimen. The dynamic properties of material can be computed (if geometry, mass and mechanical resonant frequencies are measured). Dynamic Young's Modulus is determined using resonant frequency in their flexural or longitudinal mode of vibration. Dynamic Shear Modulus is found using torsional resonant vibrations. Dynamic Young's Modulus and dynamic shear modulus are used to compute Poisson's ratio.

Young's Modulus and shear modulus were determined and calculated according to ASTM E1876–01, on the mortar prism of 40X40x160mm dimension. A wave is initiated in three possible modes. It may be difficult to obtain a stable value of the longitudinal mode. There is a possibility to determine shear modulus directly from torsional mode, afterwards by iteration with the knowledge of the shear modulus the Young's modulus can be computed.

3.4.11.1 Elastic Modulus to determine compressive strength

The elastic modulus can be used to estimate compressive strength (Fig. 3.13). Every compressive strength measurement was preceded by an elastic modulus measurement and all the results were combined in Fig. 3.13. The results show that there is a good agreement between Elastic Modulus and Compressive Strength. Elastic modulus is a nondestructive method therefore the same sample can be used to determine compressive strength at all ages and additionally an error coming from sample preparation, while during standard compressive strength test is diminished while using Elastic Modulus. Moreover at young ages the modulus increases more rapidly than compressive strength, so it is more sensitive to differences between samples.

The function for the fit line was found and is presented in Eq. 3.3.

$$f(x) = -0.30 + 0.12x + 0.033x^2 \quad (3.3)$$

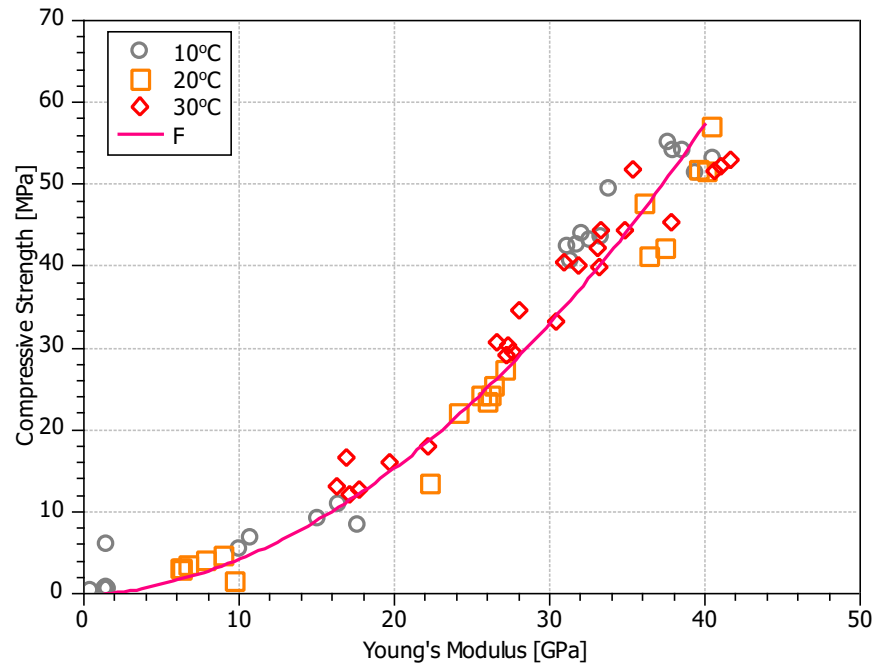


Figure 3.13: Young's Modulus vs. Compressive Strength

3.4.12 Sulfate Attack

For this test, mortar prisms of 40x40x160mm, with a metal pins of 50mm in the middle of both ends were cast. These were kept for 28 days in a humidity box, above the water level. After that their surfaces were cut to obtain prism of 20x20x160mm and placed in the Na_2SO_4 , 3g/l solution. 6 prism per cement were immersed in the sulfate solution. The volume of the solution was 9l, and the volume to solid ratio was 23.4. After certain period of time the expansion of the mortar prism was measured. During the first month of measurement the prism were measured each week. Later up to one year each 2 weeks. Later each three four weeks. The solution was exchanged each two weeks to keep the pH at the same level, around 8.

Chapter 4

Limestone addition in the low and high C_3A clinker cements

In this chapter the influence of increasing amounts of limestone on the hydration and properties of cement with different C_3A clinker contents and gypsum contents will be presented.

In the first section the influence of C_3A content on limestone reaction and hemi- and monocarboaluminate formation is presented, by investigating four samples. Two samples with low C_3A clinker with 0 and 10% of limestone and two with high C_3A clinker with 0 and 10% of limestone.

The second section concentrates on investigation of influence of increasing limestone addition on the properties of cement with high C_3A clinker content. High C_3A clinker cements are laboratory prepared cements.

Influence of limestone addition was investigated by calorimetry, phase assemblage (XRD, TGA), porosimetry and compressive strength.

Composition of all cements used in this chapter is presented in the [Table 4.1](#). The full chemical analysis is given in Annex [Section A](#).

Table 4.1: Composition of samples with limestone addition

Laboratory cement				Commercial cements			
Sample	Composition	[%]	SO_3 / Al_2O_3	Sample	Composition	[%]	SO_3 / Al_2O_3
L0Cg5.5	clinker	94.5	2.60	CAL2.5Cg6.5	clinker	91	1.55
	gypsum	5.5			gypsum	6.5	
	limestone	0			limestone	2.5	
L10Cg5.0	clinker	85.0	2.60	CAL13Cg6.5	clinker	80.5	1.37
	gypsum	5.0			gypsum	6.5	
	limestone	10			limestone	13	
				CAL22Cg6.5	clinker	71.5	1.22
					gypsum	6.5	
					limestone	22	
H0Cg6.0	clinker	94	0.98				
	gypsum	6.0					
	limestone	0					
H5Cg5.5	clinker	89.5	0.95				
	gypsum	5.5					
	limestone	5					
H10Cg5.0	clinker	85.	0.90				
	gypsum	5.0					
	limestone	10					
H15Cg4.5	clinker	80.5	0.87				
	gypsum	4.5					
	limestone	15					
H20Cg4.0	clinker	76.0	0.82				
	gypsum	4.0					
	limestone	20					

4.1 Influence of C₃A amount on the hemi- and monocarboaluminate formation

The influence of limestone addition on cements with different clinker compositions were investigated to determine the time of formation of carboaluminates and their influence on the properties of cementitious materials.

The present study looks into hemicarboaluminate (Hc) and monocarboaluminate (Mc) formation with respect to C₃A content. Optimum gypsum content indicated by the highest compressive strength at 24 hours was kept for each sample.

4.1.1 Compressive Strength

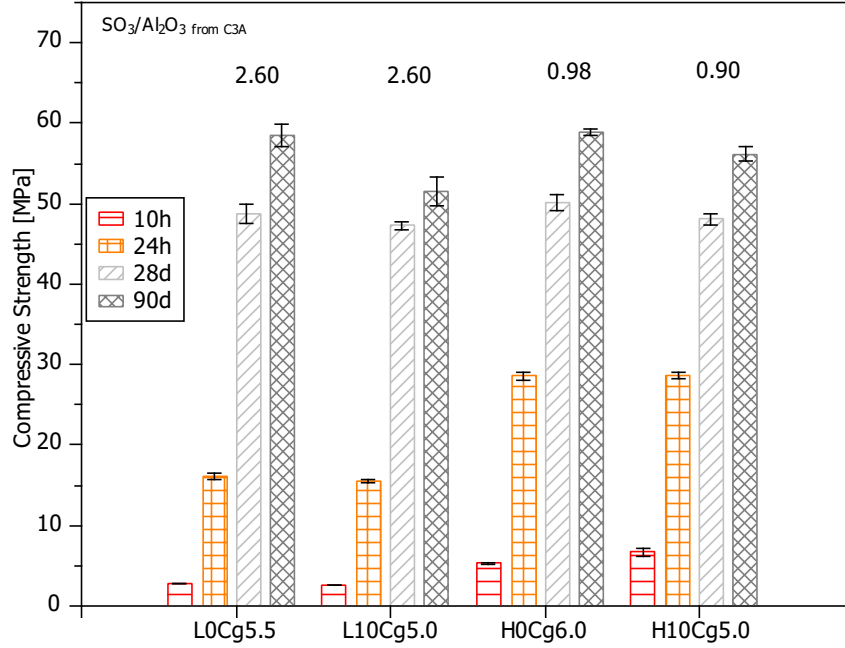


Figure 4.1: Compressive Strength at different ages. Samples with low (L=3%) and high (H=8%) C₃A content, with and without 10% of limestone addition. Gypsum content at optimum.

Fig. 4.1 shows the compressive strength of the 4 cements composed of two different clinkers with low (3%) and high (8%) C₃A content and with 0 and 10% of limestone addition. At 10 and 24 hours the strength of the cement with 10% of limestone is virtually identical to the reference cements with no addition. At 28 days, the cements with limestone have slightly lower compressive strength than their references (sample without limestone), but by 90 days the compressive strength for cement with the low C₃A clinker and 10% of limestone is significantly lower than its reference sample. On the other hand for the cements made with the high C₃A clinker the strength of the cement with 10% of limestone is only slightly less than the reference sample without limestone.

The shortfall in strength development at longer ages can be attributed to the exhaustion of anhydrous clinker phases, which are presented in lower amounts due to substitution by limestone addition. On the other hand with limestone addition clinker phases can hydrate more completely due to extra space available in limestone blends, however increase in hydration does not compensate for low compressive strength of limestone. The comparatively better performance of the high C₃A clinker suggests that the

formation of carboaluminate phases partially compensates for the lack of hydratable clinker phases.

4.1.2 Calorimetry

In the [Figs 4.2 – 4.5](#) the calorimetry results for the different cements, normalized per gram of clinker are presented. In each case two different batches were used. In the case of the cement with low C_3A clinker all the curves show a main hydration peak, from alite, with a slight shoulder about one third of the way down the deceleration part due to aluminate reaction on exhaustion of the sulphates [\[29\]](#) [\[68\]](#).

In both batches the addition of limestone, shifts the acceleration period about 1–2 hours earlier. However the slopes in the acceleration period are practically the same. The height of the alite peak increases for one batch and decreases for the other. These differences might be attributed to differences in Particle Size Distribution for different batches.

In the cements with the high C_3A clinker the shoulder peak from the reaction of aluminate phase is much more pronounced, in fact two subsidiary peaks can be seen in the deceleration period. Also the main alite peak is higher corresponding to the higher alite content of this clinker. There is little effect of limestone on the time of onset of the acceleration period, which even in the cement without limestone is much shorter than for low C_3A clinker cement.

Again the effect of limestone on the height of the main alite peak seems to vary with the different batches as presented in the [Section 3.2.2.2](#). In one pair of curves the slopes in the acceleration period are the same, while in the other the slope is steeper with limestone.

It seems that the influence of limestone on hydration kinetics can be obscured by other parameters such as particle size distribution of cement, variations in mixing, etc. On the other hand tendency of limestone to increase the hydration of clinker is confirmed in [Section 5.3.2](#).

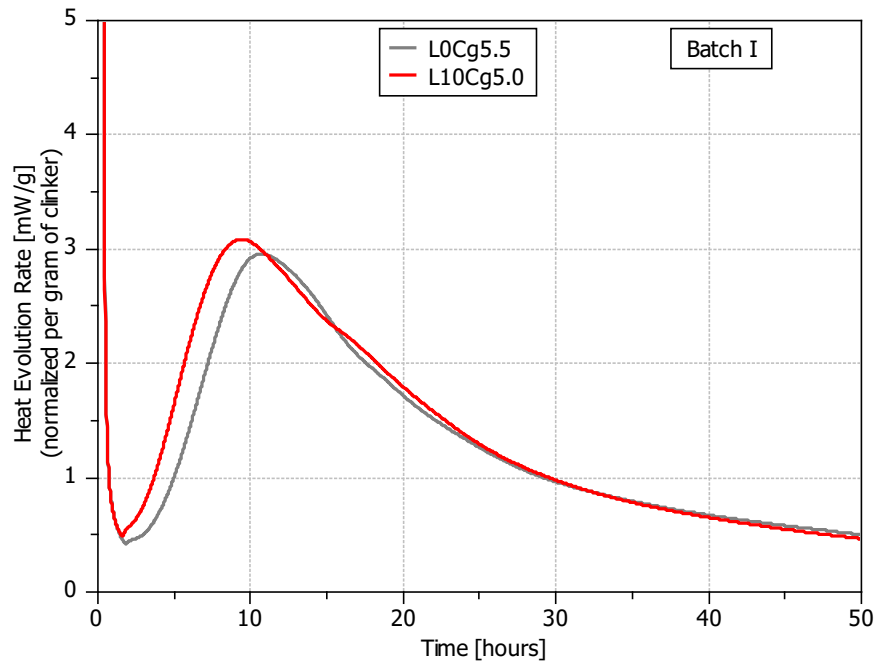


Figure 4.2: Isothermal Calorimetry data. Samples with low ($L=3\%$) C_3A content, with 0 and 10% of limestone addition. Batch I.

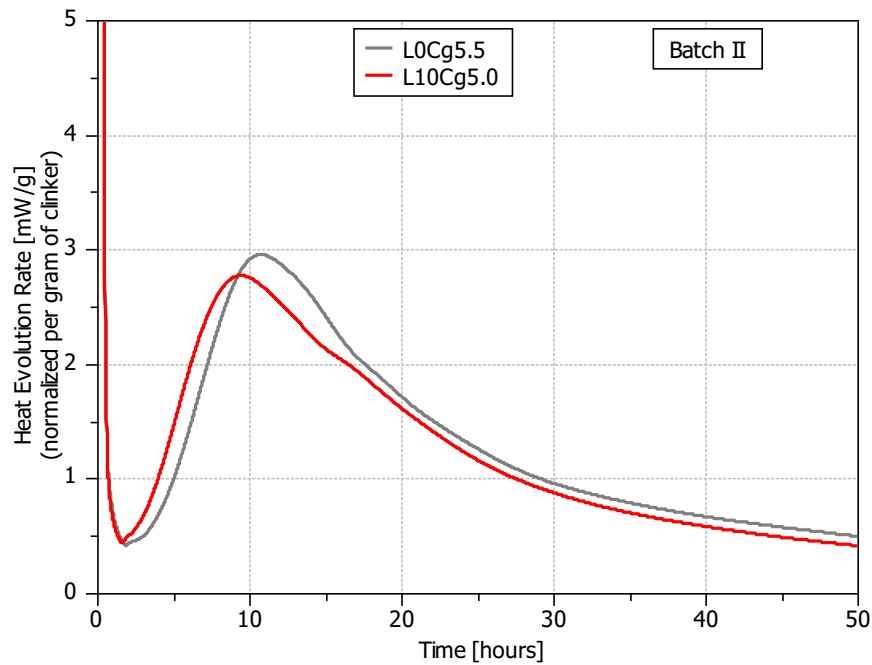


Figure 4.3: Isothermal Calorimetry data. Samples with low ($L=3\%$) C_3A content, with 0 and 10% of limestone addition. Batch II.

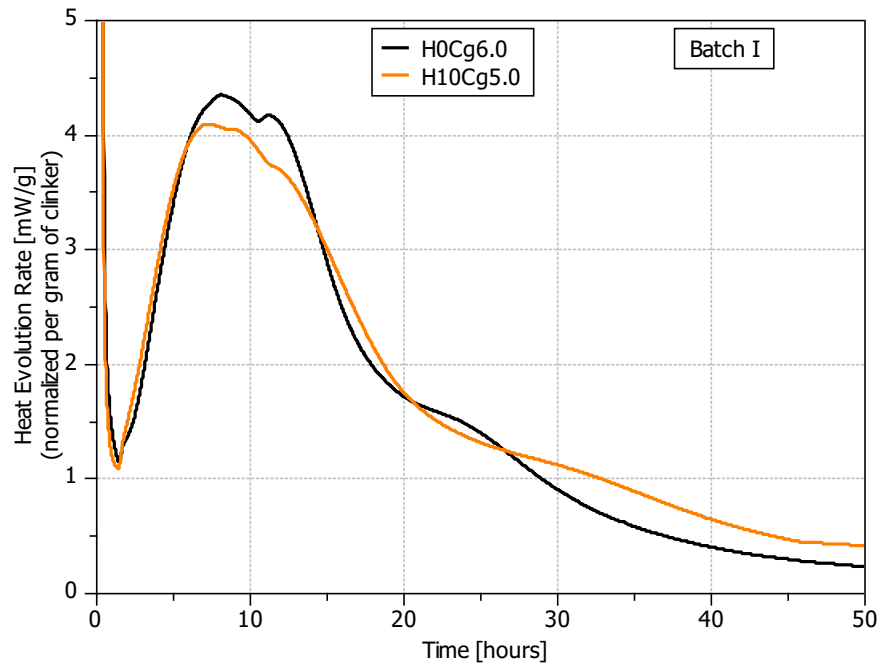


Figure 4.4: Isothermal Calorimetry data. Samples with high ($H=8\%$) C_3A content, with 0 and 10% of limestone addition. Batch I.

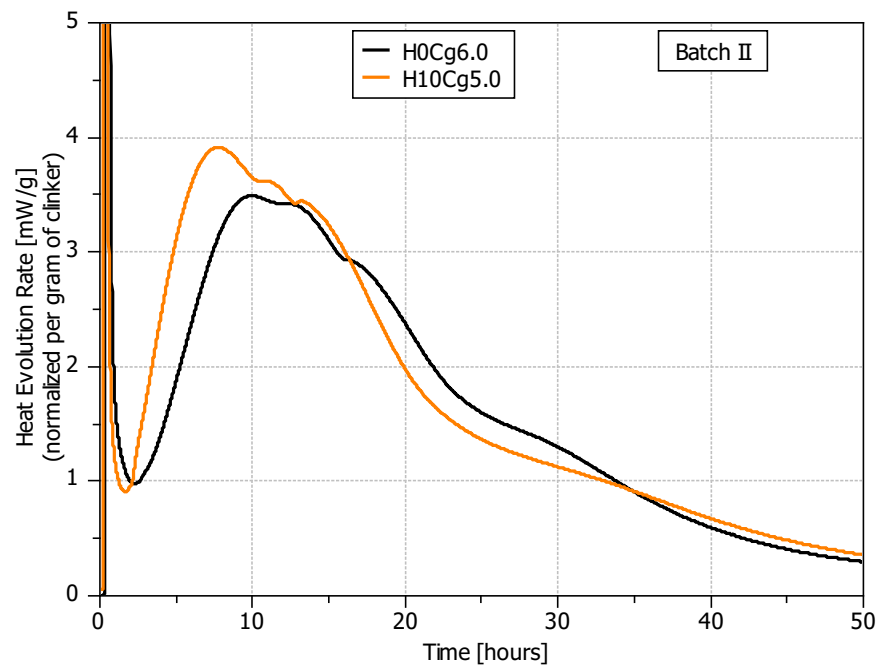


Figure 4.5: Isothermal Calorimetry data. Samples with high ($H=8\%$) C_3A content, with 0 and 10% of limestone addition. Batch II.

4.1.3 Hydration products with limestone and different clinker composition

As described in the previous chapter, sample preparation is crucial to avoid preferred orientation of limestone and other phases.

Qualitatively the XRD patterns confirm previous findings that calcium monosulfoaluminate does not form in cements containing limestone. Instead monocarboaluminate (Mc) and hemicarboaluminate (Hc) phases form and more ettringite remains. Unfortunately due to the necessity of immersing the powder samples in isopropanol to stop hydration, ettringite could not be well quantified by XRD Rietveld Analysis. Neither can hemicarboaluminate (Hc) be quantified as the exact crystal structure is not yet known.

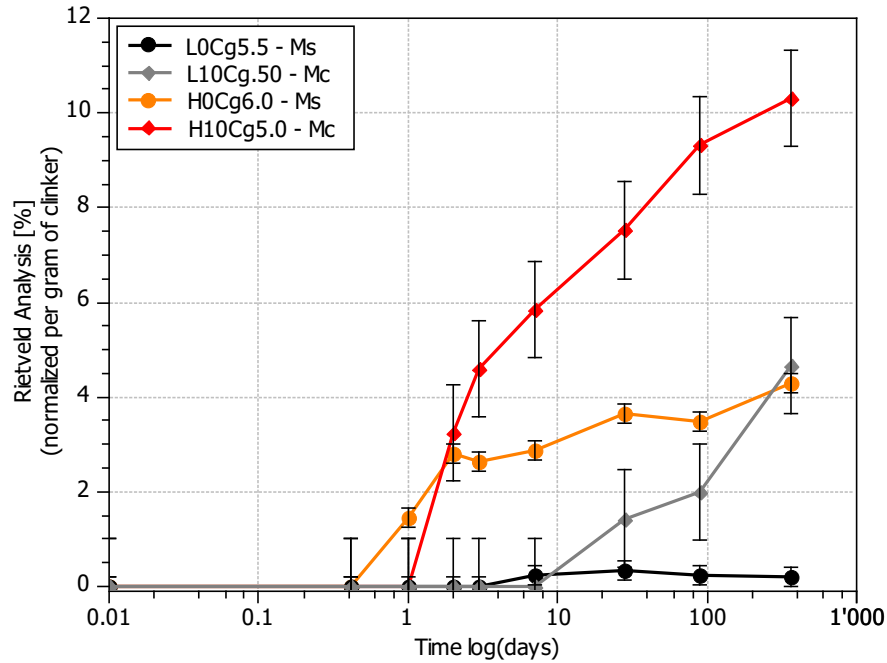


Figure 4.6: XRD Rietveld Analysis, monocarboaluminate and monosulfate quantification. Samples with low and high C_3A , 0 and 10% of limestone addition.

Figure 4.6 shows the evolution of monocarbonate (Mc) in the limestone containing cement compared to monosulfate (Ms) in the plain cements. The rate and amounts formed are strongly dependent on the C_3A content of the clinker. For the high C_3A system Mc and Hc are already visible at 2 days of hydration, while for low C_3A system the Mc and Hc are first visible at 7 days of hydration. Mc formation increases in both systems up to 720 days of hydration. Hc appears at the same time as Mc in both systems and continues to be presented up to 90 days. At 360 days no peak of Hc is visible in either system.

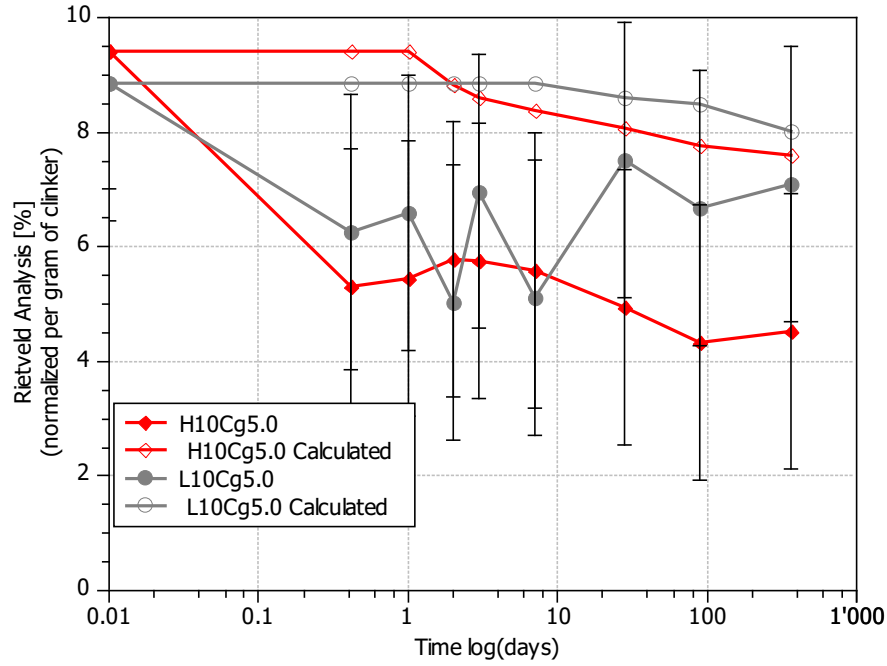


Figure 4.7: XRD Rietveld Analysis – calcite quantification and calculated calcite content.

Monosulfate is only formed in the samples without limestone and its formation also increases with C_3A content. For high C_3A system it is visible already at 1 day of hydration, while for low C_3A system it is visible from 3 days of hydration. Monosulfate continues to form up to 720 days of hydration and there is four times more monosulfate in the high C_3A system than in the low C_3A system.

In Fig. 4.7 the consumption of calcite by XRD analysis and calculated limestone consumption to produce Mc is presented. Results indicate that XRD Rietveld refinements underestimates the amount of calcite. There appears to be already a consumption of calcite at 1 day which is not reflected in Mc and Hc formation curves. For high C_3A system it is mainly consumed in the beginning up to 24 hours, later it is consumed in a small range. It should be noted for high C_3A that the error is about 2-5% which is presented in the table Fig. 3.5. According to the calculations only 1.5% of limestone is consumed up to 1 year of hydration in high C_3A system and for low C_3A system is only 1% of total limestone which is incorporated into Mc formation.

XRD Rietveld analysis for clinker phase hydration, ettringite and portlandite formation are combined in Annex LowHighL0L10H0H10allXRD [Section D.0.1](#).

4.1.3.1 GEMS predictions

GEMS predictions were done to calculate amount of phase formed during cement hydration, especially monocarboaluminate.

It has to be noted that in the GEMS model default C-S-H structures are:

$$[(CaO)_{0.83} \cdot (SiO_2) \cdot (H_2O)_{1.33}] - \textit{Tobermorite} \quad (4.1)$$

$$[(CaO)_{1.5} \cdot (SiO_2) \cdot (H_2O)_{1.83}] - \textit{Jennite} \quad (4.2)$$

In GEMS model the Ca/Si ratio for Tobermorite is 0.83 and for Jennite is 1.5.

SEM EDS analysis were done to determine the C-S-H composition. In [Fig. 4.8](#) an example of result for Ca/Si and Al/Si ratios determination method is presented. The average ratios for inner and outer C-S-H composition was chosen for further investigation. The results are presented in the table [Table 4.2](#). The experimental Ca/Si ratios are higher for all presented samples than in the GEMS model.

Table 4.2: C-S-H composition at 24 hours of hydration by SEM EDS analysis

Sample	Ratios		
	Ca/Si	Al/Si	S/Si
L0Cg5.5	1.97	0.233	0.11
L10Cg5.0	2.00	0.107	0.127
H0Cg6.0	2.04	0.1124	0.109
H10Cg5.0	2.04	0.127	0.120

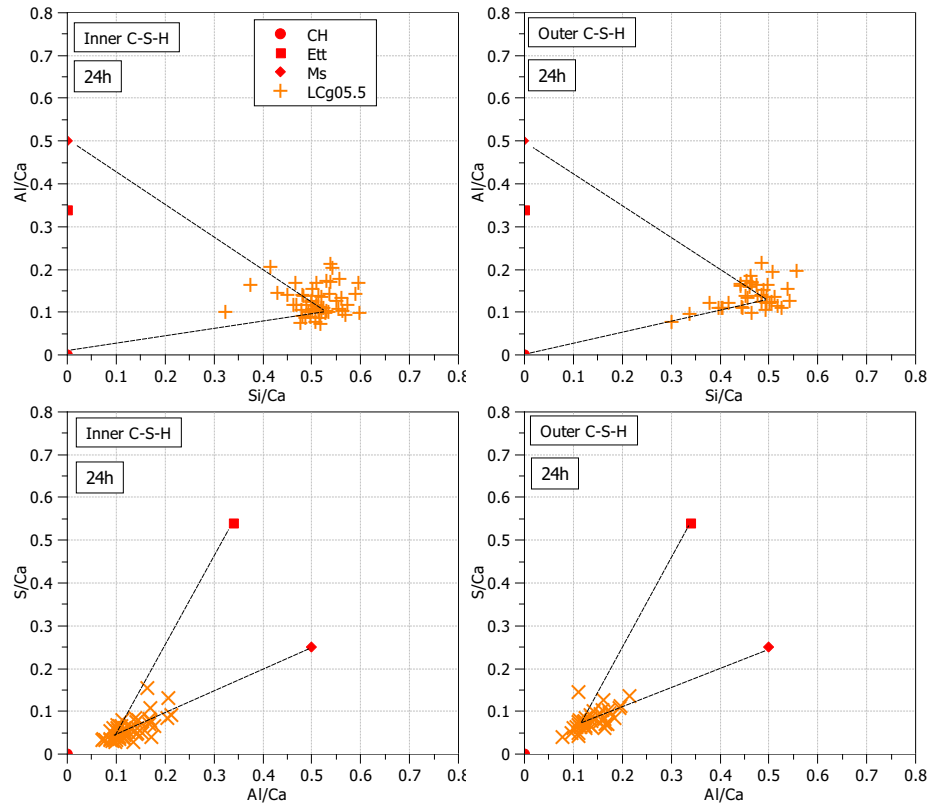


Figure 4.8: SEM EDS analysis – C-S-H composition at 24 hours of hydration for sample L0Cg5.5.

As an input in GEMS calculations the hydration of clinker phases: C_3S , C_2S , C_3A , C_4AF obtained by XRD Rietveld analysis were used. The phases predicted by GEMS are compared with data from XRD.

In Fig. 4.9 GEMS calculations data compared with XRD and GEMS calculation when Ca/Si ratio from SEM EDS analysis was included. Results show much better agreement between GEMS and XRD results.

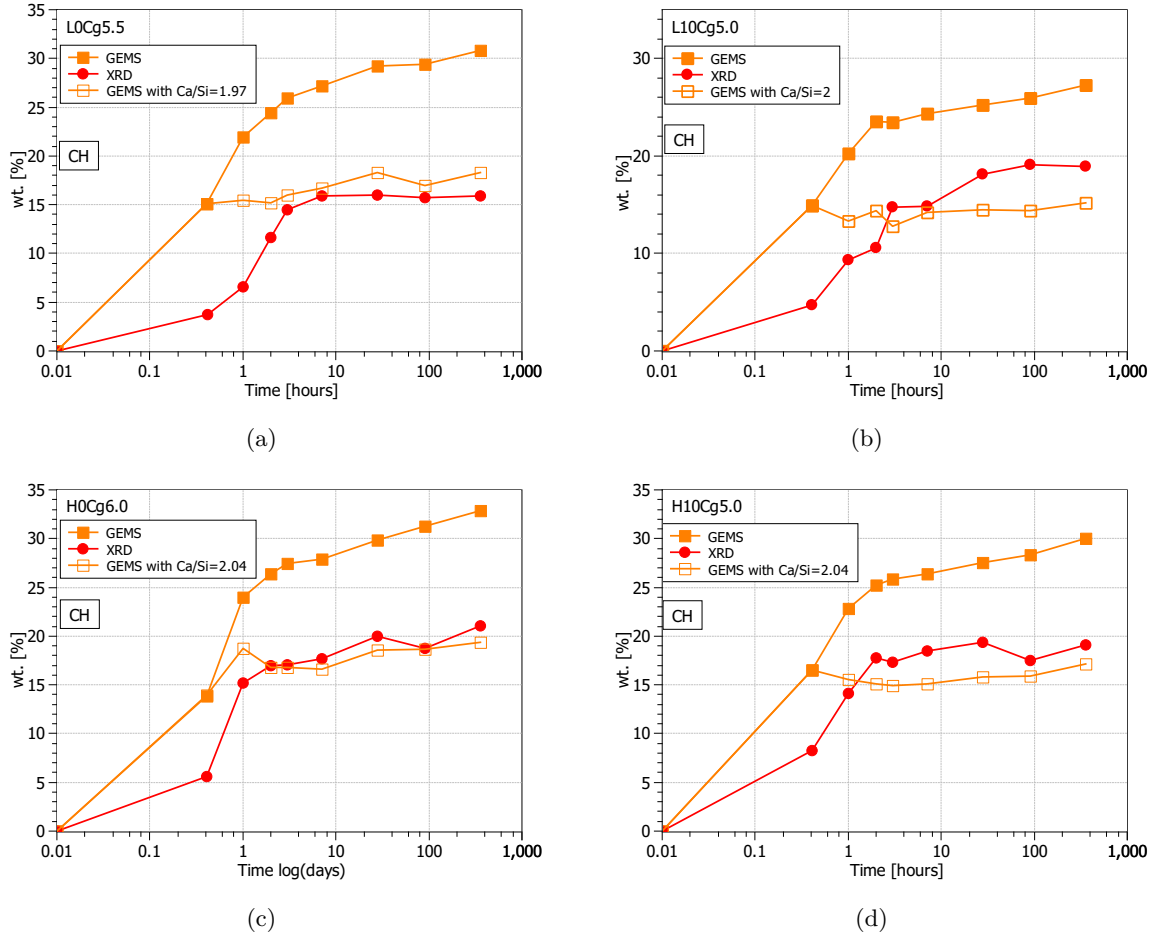


Figure 4.9: Portlandite formation by XRD Rietveld analysis, GEMS default settings, GEMS with fixed Ca/Si ratio obtained by SEM EDS analysis.

The GEMS predictions of monocarboaluminate formation (Fig. 4.10) show good agreement with XRD Rietveld analysis for sample with high C₃A clinker and 10% of limestone (Fig. 4.10 b). Sample with low C₃A clinker (Fig. 4.10 a) show significant disagreement in the monocarboaluminate formation in early ages, at 360 days the amount of monocarboaluminate predicted by GEMS and measured by XRD Rietveld analysis is similar.

One reason for the discrepancy could be the uptake of Al in C-S-H. This was adjusted in the GEMS calculations. Although the values are lower the kinetics of formation are still not well fitted for low C₃A system (Fig. 4.10 a). High C₃A cement system shows even better fit of monocarboaluminate formation (Fig. 4.10 b).

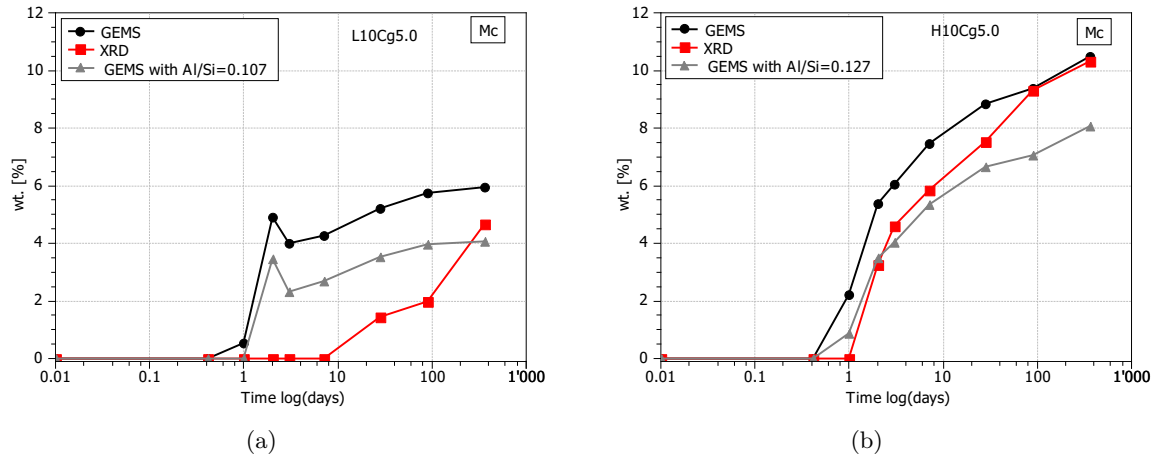


Figure 4.10: Monocarboaluminate formation by XRD Rietveld analysis and GEMS calculation with default C-S-H composition and with fixed Al/Si ratio.

4.1.4 Porosity

MIP shows that limestone has very little impact on the porosity. Porosity changes with C_3A and limestone addition (Figs 4.11, 4.12). First of all the total porosity is almost the same at every age with and without limestone addition for high C_3A clinker. For low C_3A system there are differences in the range of 2% for samples with and without limestone at each time of hydration, however the differences are in the range of error.

There is also little influence of limestone addition on the breakthrough diameter which is smaller with limestone addition at 10 hours of hydration in comparison to the sample without limestone. At later ages the breakthrough diameter is the same for sample with and without limestone for low C_3A system (Fig. 4.11) and still smaller for sample with limestone and with high C_3A clinker (Fig. 4.12).

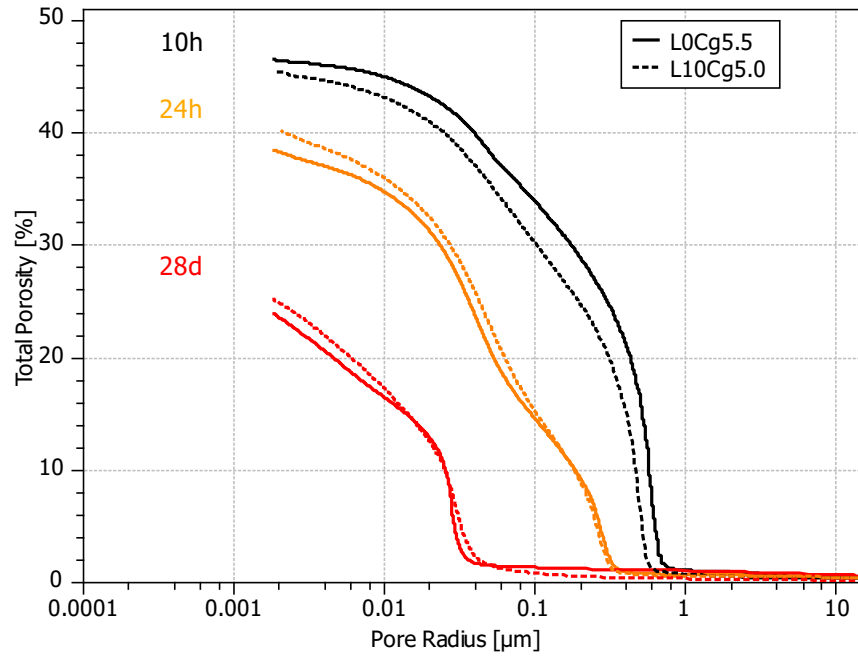


Figure 4.11: MIP data for cement with low C_3A (3%) clinker content and with 0 and 10% of limestone addition.

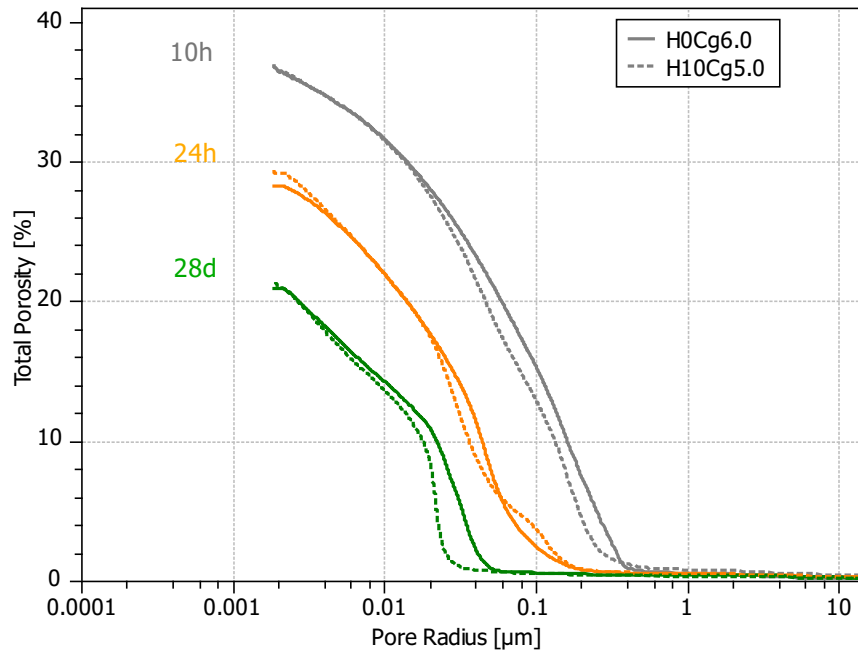


Figure 4.12: MIP data for cement with high C_3A (8%) clinker content and with 0 and 10% of limestone addition.

4.1.5 Microstructural development

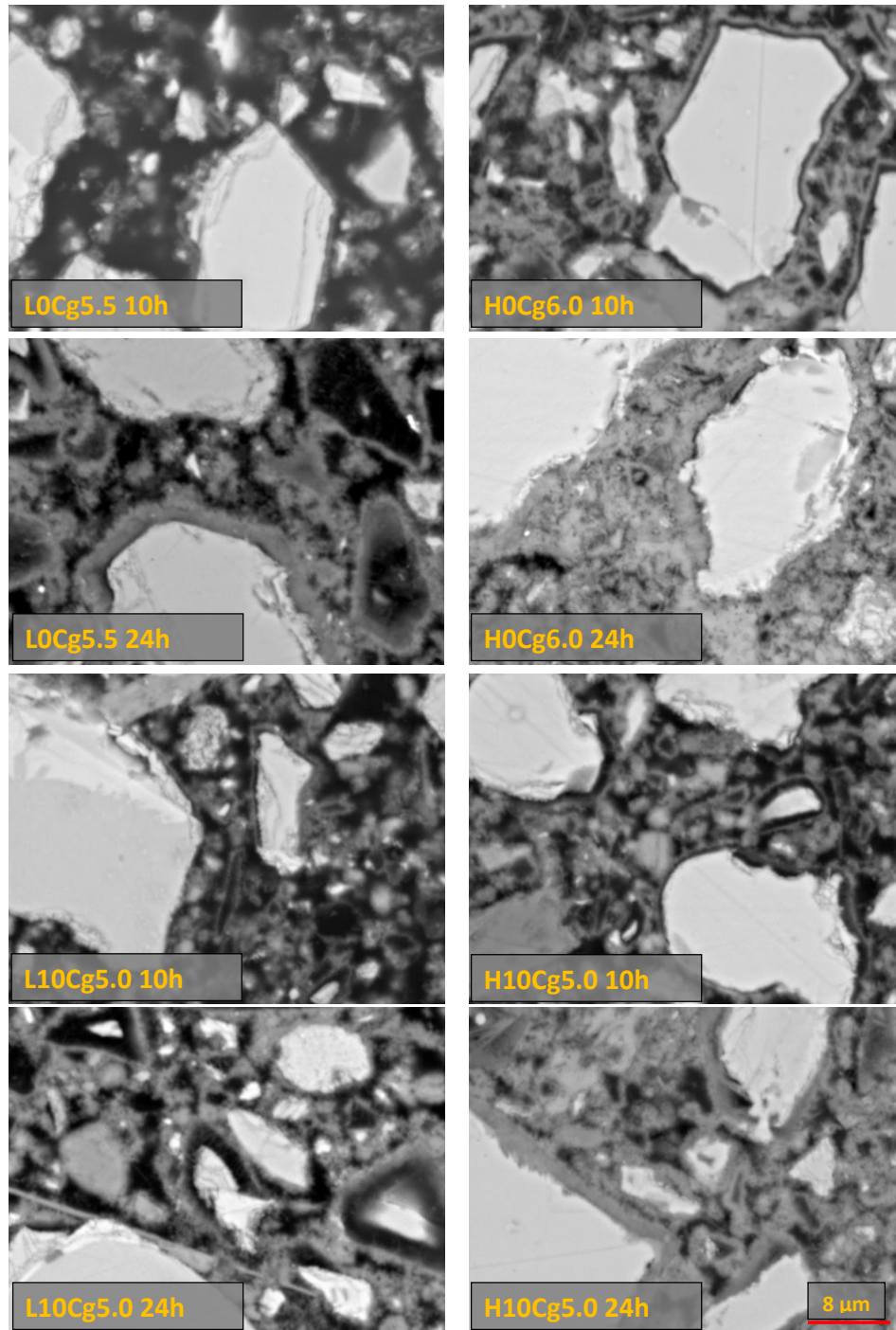


Figure 4.13: Scanning Electron Microscopy at 10 and 24 hours of hydration for samples with low (3%) and high (8%) C_3A clinker with 0 and 10% of limestone addition. Magnification=6000x, HV=15kV, WD=12.5mm.

SEM images of the systems (Fig. 4.13) show that C_3A and limestone can influence the microstructural development. Paste microstructure of high C_3A clinker cement appears denser in comparison to low C_3A system at early ages of hydration up to 24 hours of hydration. It seems that there is more hydration products in the system with high C_3A in comparison to low C_3A probably due to different C_3S content for low and high C_3A clinker (Fig. 3.3). With limestone the difference of the product formation is smaller between low and high C_3A system, due to shortening in induction period with limestone addition at low C_3A system and accelerating hydration reaction.

4.1.6 Summary – Hc and Mc formation with different C_3A content cements

- Limestone has an influence on the hydration kinetics and properties of cementitious materials however its effect is small and can vary from batch to batch of cement
- The formation of monocarbo- and hemicarboaluminate depends on the C_3A content
- With high C_3A content monocarboaluminate appears earlier and it is formed in larger amount up to 360 days of hydration. The amount of monocarboaluminate at 90 and 360 days is 9.3% and 10.3% respectively (Fig. 4.6)
- With low C_3A , monocarboaluminate is not visible until 7 days of hydration continuous to increase up to 360 days. The amount of monocarboaluminate at 90 days and 360 days is 1.98% and 4.67% respectively (Fig. 4.6)
- Ca/Si ratio is higher than in model C–S–H used in GEMS model
- Comparison between XRD Rietveld analysis and GEMS calculation suggest aluminum uptake into C–S–H
- Little influence of limestone is visible in the microstructural development, where there is a significant difference in microstructure between low and high C_3A clinker. The microstructure is denser in the system with high C_3A content and when limestone is incorporated the difference is smaller between low and high C_3A clinker system
- Because of the differences in product formation with limestone addition, porosity

and especially pore size distribution is influenced by limestone addition in both low and high systems. Total porosity is the same at high C_3A clinker for sample with and without 10% of limestone addition, while at low C_3A clinker differences between sample with without limestone is usually in a range of 2%. Breakthrough diameter is smaller for sample with 10% of limestone addition at 10 hours of hydration for low and high C_3A clinker

- The compressive strength is not influenced by limestone addition at early ages of hydration up to 24 hours . With limestone addition the compressive strength is decreased at later ages 28 and 90 days of hydration. However the difference between samples with and without limestone at 90 days of hydration in high C_3A system is lower than between samples with low C_3A system probably due to twice more amount of Mc in the sample with high C_3A clinker than with low C_3A clinker

4.2 Increasing limestone addition with high C₃A clinker cements

For samples with high C₃A (8%) clinker, 5, 10, 15, 20% of limestone addition. The composition of the samples and chemical composition is presented in the annex [Table A.3](#) and phase composition in the [Table A.7](#).

The gypsum addition for samples with increasing limestone content were determined by linear fit. First gypsum optimum for sample without limestone and with 10% of limestone was determined experimentally by increasing gypsum content in the cement and measuring compressive strength at 24 hours ([Table 5.2.1](#)). Gypsum content at which compressive strength at 24 hours of hydration was the highest was considered as the optimum gypsum. The optimum gypsum content for other limestone addition, 5, 15 and 20% were determined by linear fit of two experimentally determined points as presented in [Fig. 4.14](#). This indicates an optimum gypsum slightly below that from pure dilution, however it should be noted that determination of optimum gypsum is not very precise due to only three different gypsum additions available.

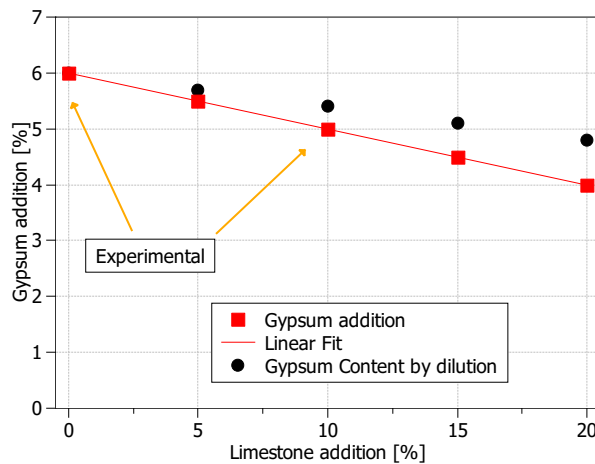


Figure 4.14: Indication of the optimum gypsum for each limestone addition

Table 4.3: Gypsum content by dilution and added gypsum content and SO₃/Al₂O₃ ratio

Sample	Gypsum _{Bydilution}	Gypsum _{Added}	SO ₃ /Al ₂ O ₃ _{Bydilution}	SO ₃ /Al ₂ O ₃ _{Added}
H0Cg6.0	6.0	6.0	0.98	0.98
H5Cg5.5	5.7	5.5	0.98	0.95
H10Cg5.0	5.4	5.0	0.98	0.91
H15Cg4.5	5.1	4.5	0.98	0.87
H20Cg4.0	4.8	4.0	0.98	0.82

The gypsum content by dilution is higher than the optimum gypsum content indi-

cated by linear fitting, therefore the SO_3/Al_2O_3 ratio decreases with limestone addition. The difference in the gypsum content by dilution and what was added and SO_3/Al_2O_3 ratio are presented in the [Table 4.3](#).

4.2.1 Compressive Strength

[Figure 4.15](#) shows the influence of limestone addition on the compressive strength of cement with high C_3A clinker cement.

The compressive strength decreases with limestone addition. The maximum decrease is in the range of 10MPa for the sample with 20% of limestone addition at 28 days of hydration. Up to 10% of limestone addition gives comparable values of compressive strength to the sample without limestone addition at 28 days of hydration.

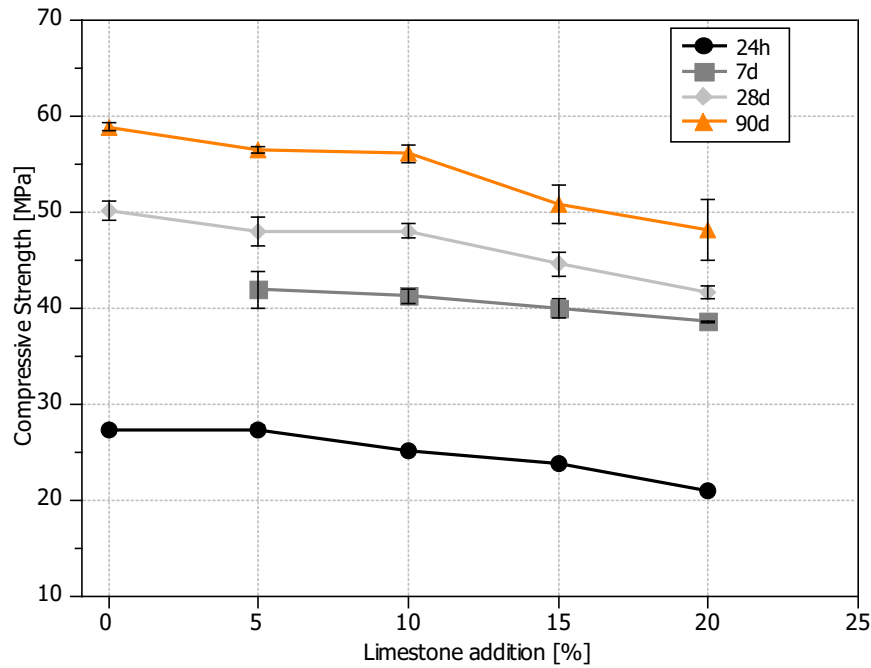


Figure 4.15: Compressive Strength of mortars with increasing limestone addition at different times of hydration.

4.2.2 Kinetics of the hydration

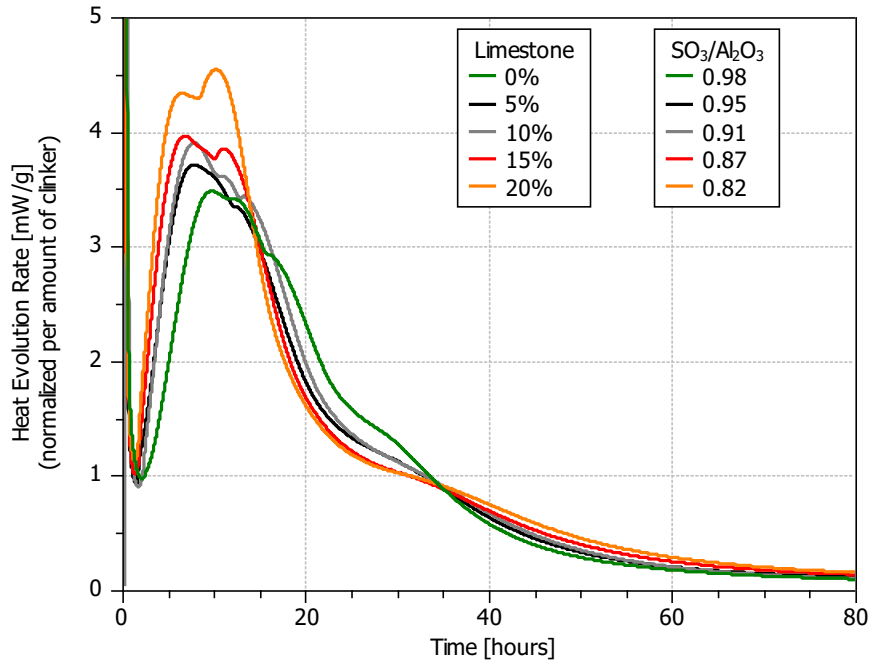


Figure 4.16: Isothermal Calorimetry with increasing limestone addition. Cement with high (8%) C₃A clinker, gypsum amount is in optimum for each sample.

In Fig. 4.16 the calorimetry data are presented. The samples are normalized with respect to total clinker content. Limestone addition has a significant effect on the kinetics of the cement hydration. It can be clearly seen that increasing amounts of limestone lead to increasing acceleration of the clinker hydration. There is an increase in the slope of the acceleration period (Fig. 4.18); an earlier onset of the aluminate reaction (Fig. 4.19) and a more pronounced reaction of the aluminate phase.

The increase in slope of the acceleration period is due to increased nucleation sites for C₃S hydration with limestone addition. Due to the clinker substitution by limestone and the same w/c ratio 0.40, there is also more space available for clinker reaction. The added gypsum relative to clinker decreases with limestone addition, and is the reason for the earlier onset of the aluminate reaction.

The total heat evolved is presented in the Fig. 4.17. With increasing limestone addition the total heat evolved relative to clinker increases, and the rate of reaction increases. This effect is visible from the beginning of the hydration and continues up to 80 hours of hydration. The reason for that is relatively more space for hydrates to grow with increasing limestone addition.

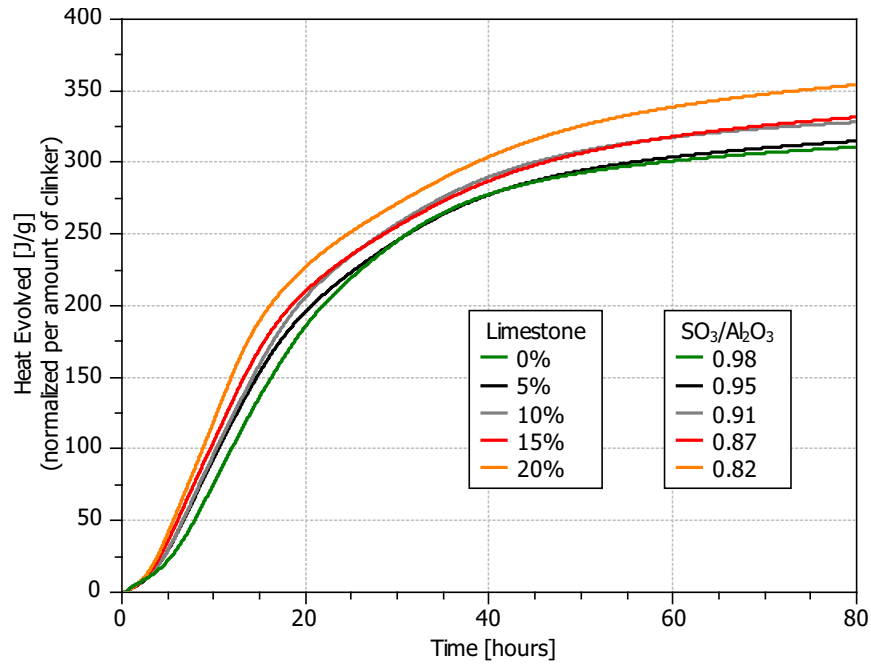


Figure 4.17: Isothermal Calorimetry with increasing limestone addition – cumulative curve. Cement with high (8%) C_3A clinker and increasing limestone addition gypsum amount is in optimum for each sample.

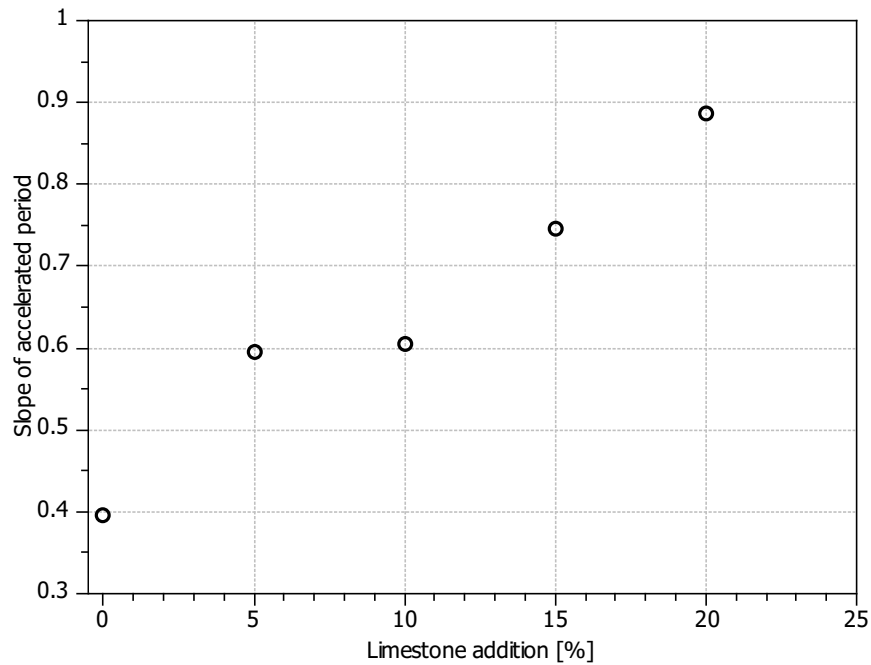


Figure 4.18: Slope of the acceleration period with limestone addition.

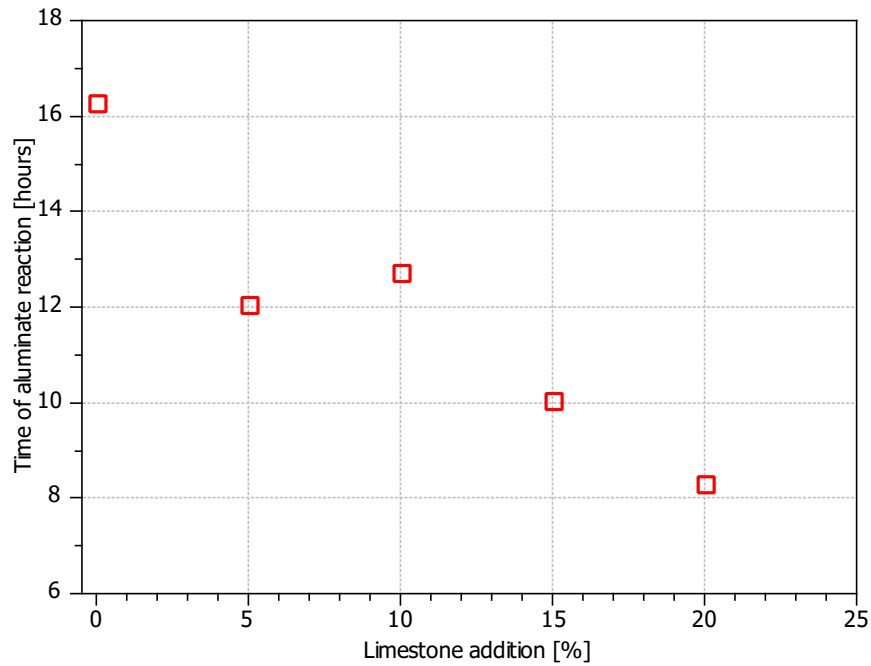


Figure 4.19: Time of the aluminate reaction with limestone addition.

4.2.3 Phase assemblage

In Fig. 4.20 the Thermo Gravimetric data not normalized with respect to clinker content at 24 hours of hydration are presented.

With increasing limestone addition the DTG curve shows three main effects. At 24 hours of hydration (Fig. 4.20) the region, which corresponds to C-S-H and AFm phases decomposition shows a slight decrease with limestone addition and suggests. The evolution of the peak in the first region which corresponds to C-S-H and AFm phases decomposition, does not correlate to the evolution of the CH decomposition peak which shows less differences between samples (Fig. 4.20). This could suggest that with limestone addition the composition of the C-S-H and formation of ettringite and carboaluminate phases changes.

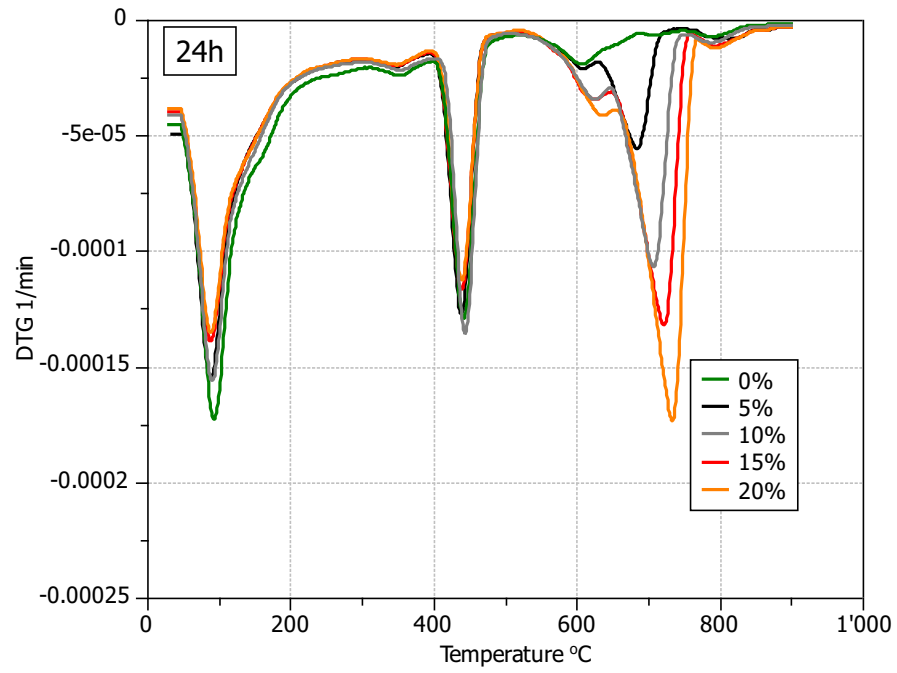


Figure 4.20: Thermal Gravimetry data for high C_3A clinker with increasing limestone addition, at 24 hours of hydration.

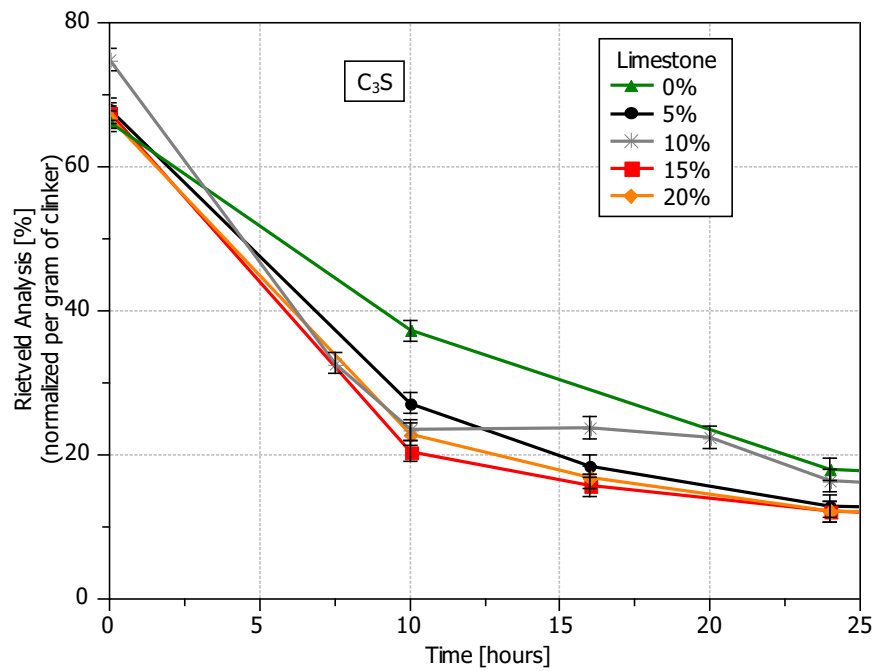


Figure 4.21: XRD Rietveld Analysis data for high C_3A clinker with increasing limestone addition. C_3S quantification.

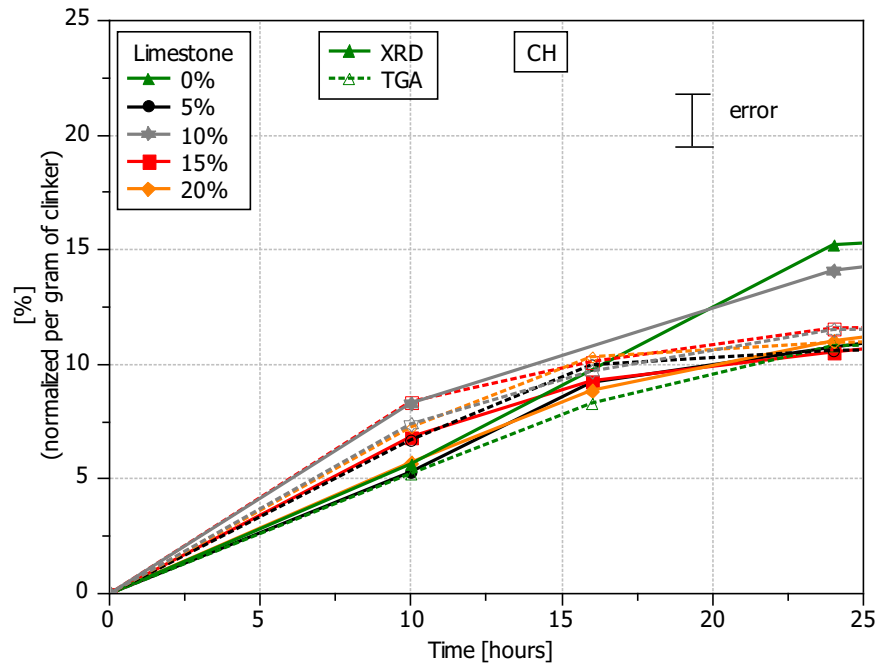


Figure 4.22: XRD Rietveld Analysis and TGA data for high C_3A clinker with increasing limestone addition. Portlandite (CH) quantification.

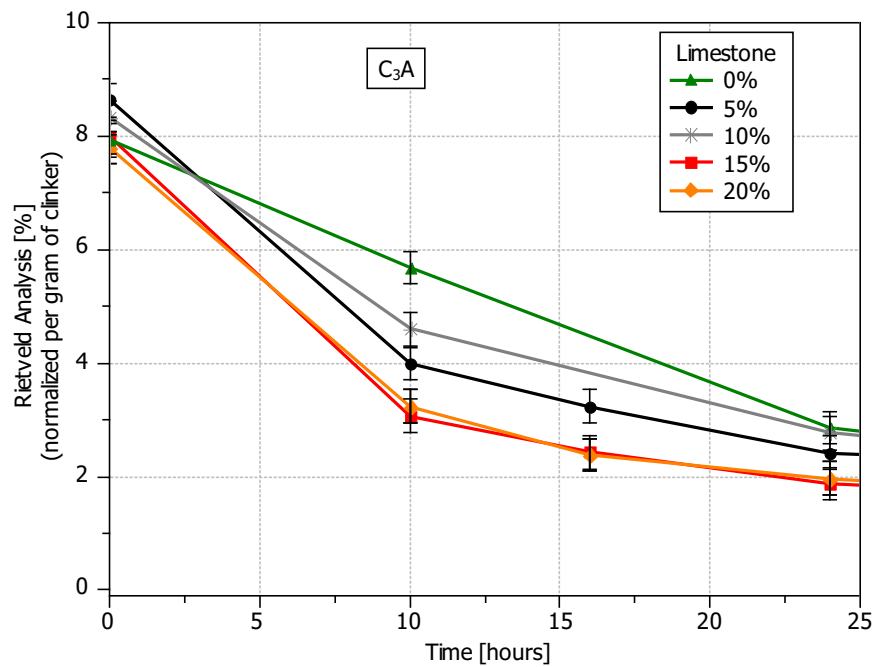


Figure 4.23: XRD Rietveld Analysis data for high C_3A clinker with increasing limestone addition. C_3A quantification.

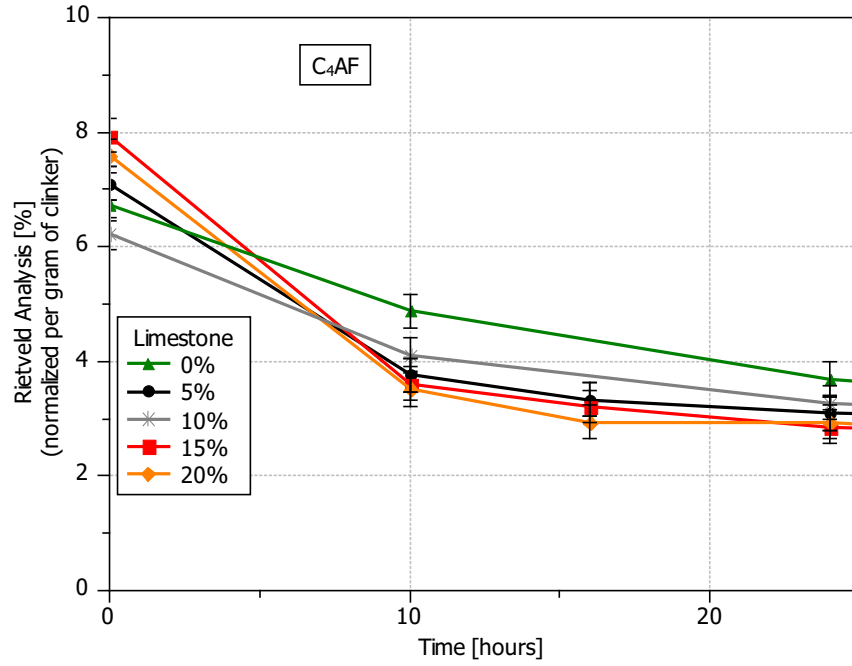


Figure 4.24: XRD Rietveld Analysis data for high C_3A clinker with increasing limestone addition. C_4AF quantification.

XRD Rietveld Analysis data show slight influence of limestone on the C_3S reaction at early ages up to 24 hours of hydration (Fig. 4.21) what confirms the calorimetry data of C_3S hydration acceleration. By 24 hours the C_3S consumption is similar. The portlandite formation increases with limestone addition, however there is not a lot of difference between different limestone additions as observed by TGA (Fig. 4.22). The result for sample with 0 and 10% of limestone addition, by XRD Rietveld analysis is out of the trend due to differences in batches of prepared cements and it was discussed before in Section 3.2.2.2.

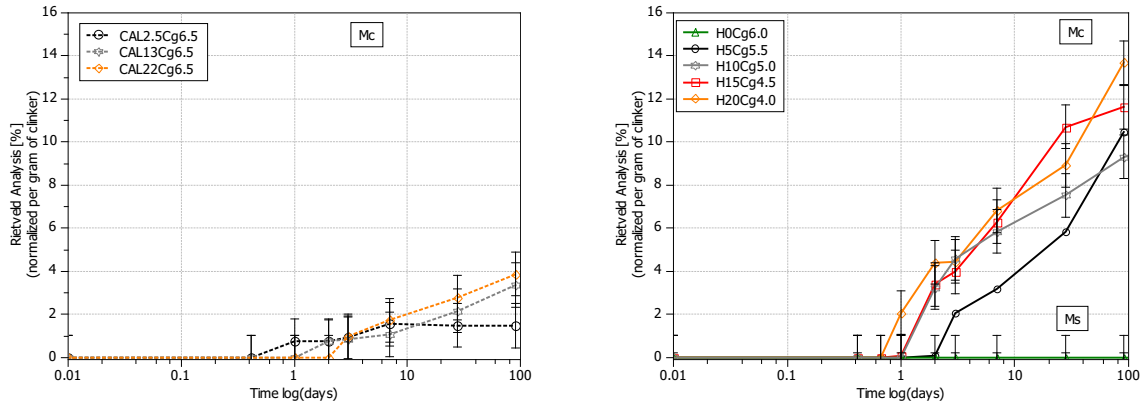
Limestone addition has a slight influence on the consumption of the other phases. C_3A consumption increases slightly with limestone addition up to 24 hours of hydration, but the difference between samples is in the range of error of the measurement (Fig. 4.23).

The situation is the same for C_4AF whose consumption slightly increases with limestone addition, however the difference is in the range of error of the measurement (Fig. 4.24).

4.2.3.1 Influence on the AFm phase formation

The previous results show that C₃A hydration is not significantly influenced by limestone addition by 24 hours of hydration (Fig. 4.23).

In Fig. 4.25 monocarboaluminate formation by XRD Rietveld analysis for high C₃A clinker cements (Fig. 4.25 b – laboratory cement) and for low C₃A clinker cements (Fig. 4.25 a – commercial cement) is presented.



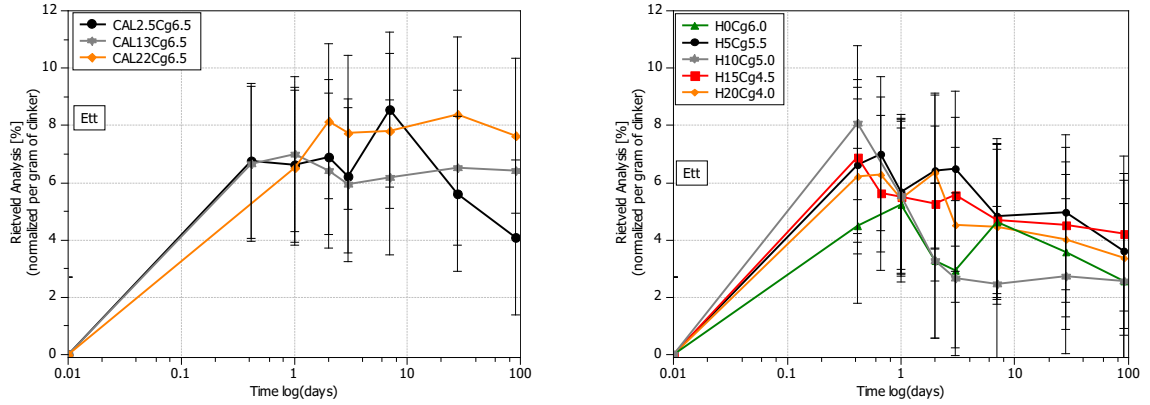
(a) Monocarboaluminate quantification by XRD Rietveld analysis. Low C₃A clinker cement with increasing limestone addition.

(b) Monocarboaluminate quantification by XRD Rietveld analysis. High C₃A clinker cement with increasing limestone addition.

Figure 4.25: XRD Rietveld Analysis. Low and high C₃A clinker with increasing limestone addition. Monocarboaluminate and monosulfate formation up to 90 days of hydration.

There is no monosulfate observed for samples with limestone addition up to 90 days of hydration. Increasing limestone addition does not influence formation of carboaluminate phases and in particular does not increase monocarboaluminate formation. The formation of monocarboaluminate is visible only since 2 day of hydration and there is more monocarboaluminate formed with limestone addition at each time of hydration due to slightly lower gypsum content with increasing limestone addition and more alumina available to react with limestone. Additionally with increasing limestone addition monocarboaluminate is formed earlier due to decreasing gypsum content with limestone addition and increasing C₃A to react with limestone (Fig. 4.25 b).

Low C₃A clinker cements show similar result to high C₃A clinker cements (Fig. 4.25 a). Only difference is in total amount of monocarboaluminate formed. For low C₃A clinker cements there is significantly less monocarboaluminate formed up to 90 days of hydration due to less aluminum in the system available to react with limestone (Fig. 4.25 b) and increasing SO₃/Al₂O₃ ratio with increasing limestone addition for this set of samples.



(a) Ettringite quantification by XRD Rietveld analysis. Low C₃A clinker cement with increasing limestone addition.

(b) Ettringite quantification by XRD Rietveld analysis. High C₃A clinker cement with increasing limestone addition.

Figure 4.26: XRD Rietveld Analysis. Low and high C₃A clinker with increasing limestone addition. Ettringite formation up to 90 days of hydration.

The formation of hemicarboaluminate is also influenced by limestone addition. With limestone addition it is better crystalline as determined by XRD pattern comparison (Fig. 4.27).

In the Fig. 4.26 ettringite formation up to 90 days of hydration is presented for low (Fig. 4.26 a) and high C₃A (Fig. 4.26 b) clinker cements. The ettringite formation is not significantly influenced by limestone additions. For high C₃A clinker cements at early ages, up to 7 days of hydration the ettringite formation is the same with all limestone additions. Around 7 days for sample with 5% of limestone addition and 28 days for samples with 15 and 20% of limestone addition the drop of about 2% of ettringite amount is observed and continuous later. Because there is no monosulfate observed with limestone addition the decrease in ettringite formation could be attributed to carboaluminate phases formation (Fig. 4.25 a). However difference in ettringite formation are in the range of error.

Low C₃A clinker cements (Fig. 4.26 a) show similar trend to high C₃A clinker cements, and ettringite formation is not significantly influenced by limestone addition. Slight differences in ettringite formation for low C₃A clinker cements with increasing limestone addition are caused by increasing SO₃/Al₂O₃ ratio, and more gypsum available to produce ettringite (Fig. 4.26 a).

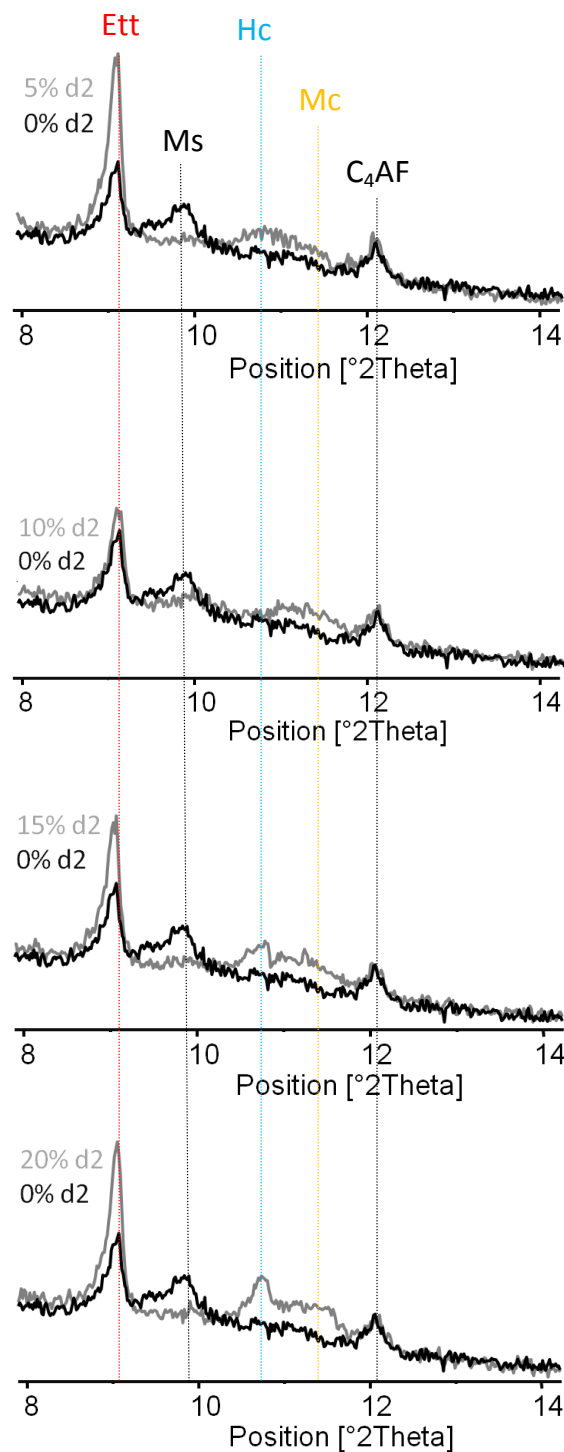


Figure 4.27: XRD patterns at 2 days of hydration. High C₃A clinker with increasing limestone addition. Ettringite, hemicarboaluminate and monocarboaluminate peak.

4.2.3.2 GEMS prediction of phase formation

Rate of hydration of clinker phases measured by XRD Rietveld analysis was used as an input in GEMS calculations. Phase formation by GEMS and XRD Rietveld analysis were compared.

In Fig. 4.28 monocarboaluminate formation prediction by GEMS is presented. Result show that regardless of limestone content monocarboaluminate formation predicted by GEMS is similar for all samples. Amount of monocarboaluminate does not increase with limestone addition. It indicates that limestone reaction and carboaluminate phase formation is controlled by aluminum availability. Slight differences are due to different gypsum content for each sample.

In Fig. 4.29 the comparison between XRD Rietveld analysis and GEMS calculation for sample with increasing limestone addition is presented. The gypsum/clinker ratio decreases for each limestone addition in comparison to sample without limestone due to optimized amount of gypsum for each sample. The best fit of monocarboaluminate formation by GEMS with XRD Rietveld analysis is for the sample with 10 and 20% of limestone addition (Fig. 4.29 b, d).

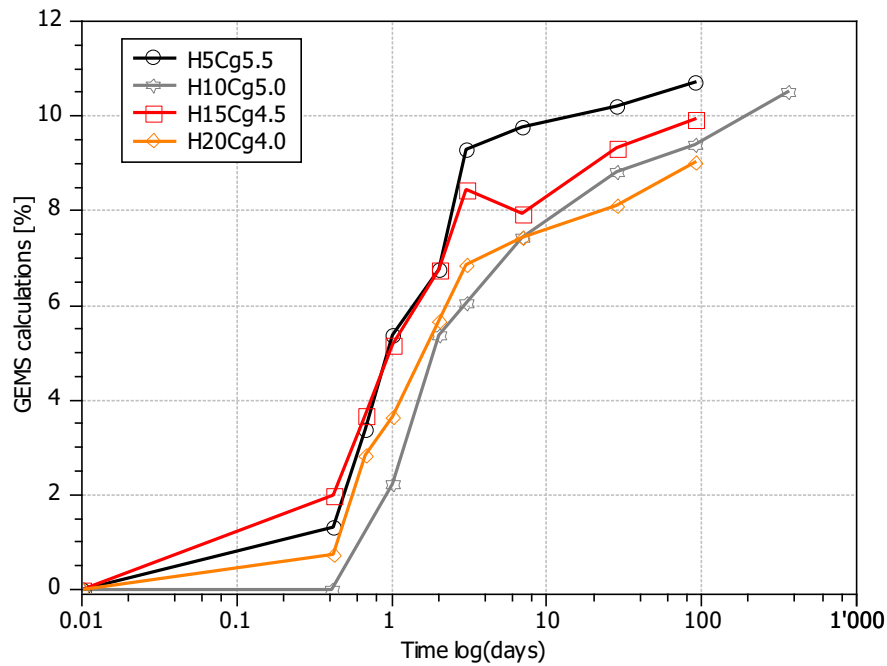
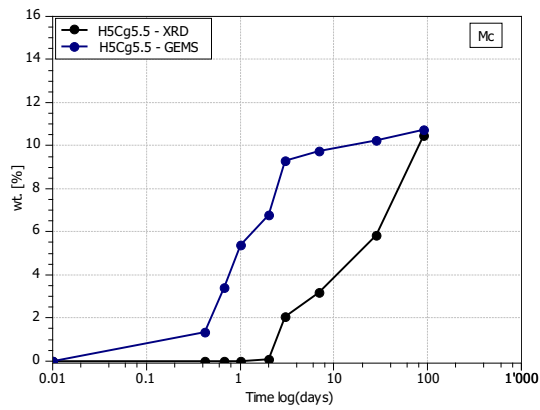
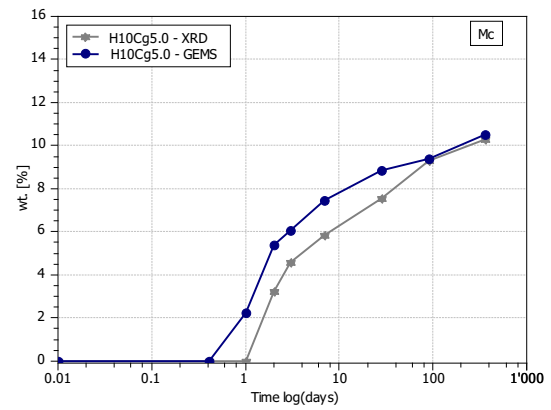


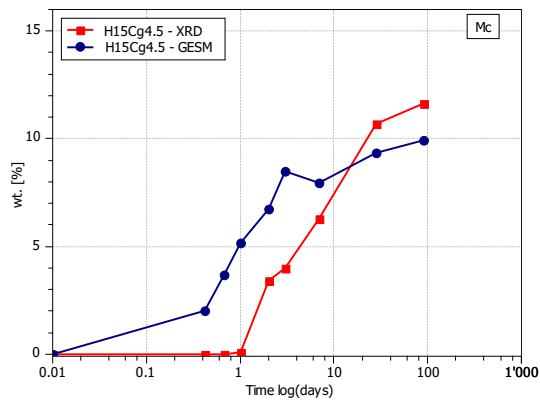
Figure 4.28: GEMS calculations data. Monocarboaluminate prediction formation for samples with increasing limestone addition.



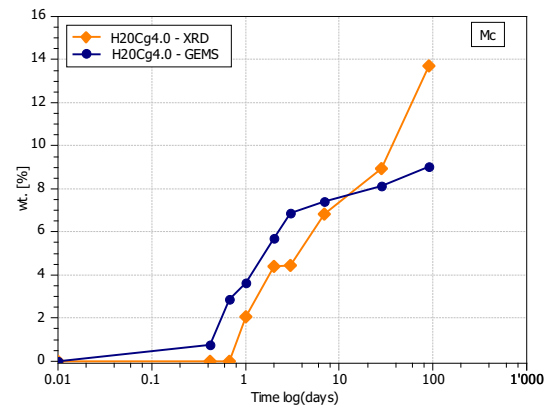
(a) H5Cg5.5



(b) H10Cg5.0



(c) H15Cg4.5



(d) H20Cg4.0

Figure 4.29: Monocarboaluminate formation by XRD Rietveld analysis and GEMS calculations. Samples with increasing limestone addition and gypsum at optimum content.

4.2.4 Porosimetry

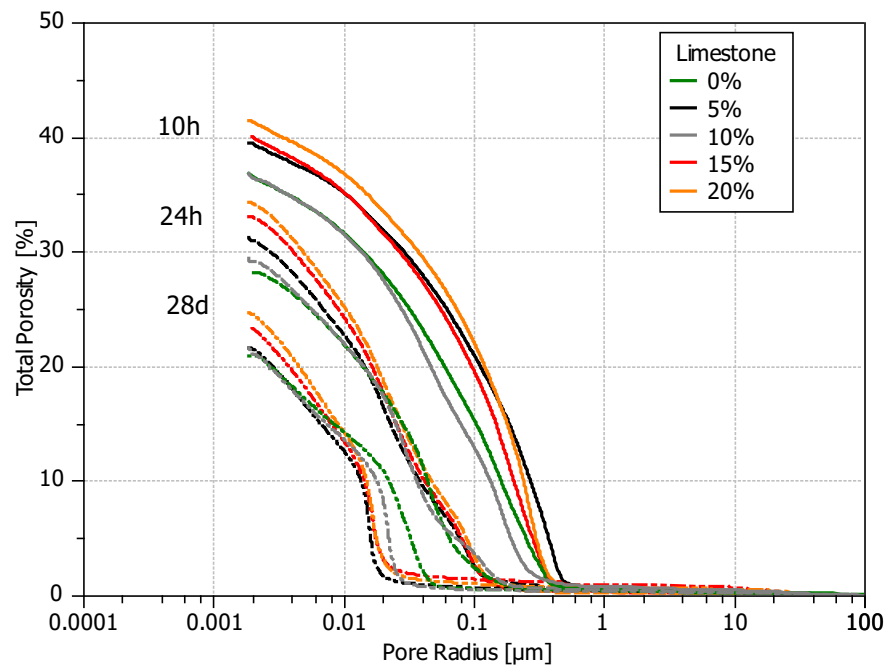


Figure 4.30: Mercury Intrusion Porosimetry (MIP) data at 10, 24 hours and 28 days of hydration. For samples with increasing limestone addition.

In the (Fig. 4.30) it can be seen that the limestone addition have little effect on the porosity. Total porosity is slightly higher with increasing limestone addition.

4.3 Summary

In this chapter the effect of increasing limestone addition on the hydration and properties of cements with different clinker content and with limestone addition were investigated. It was observed that limestone has an influence on the hydration and properties of cement and it depends on the C_3A content and gypsum addition in cement

Kinetics

- Regardless of the clinker composition limestone slightly steepers the accelerating period on the calorimetry curve. The total heat evolved increases with limestone addition

Compressive strength

- Compressive strength decreases with limestone addition

Phase assemblage

- With increasing addition of limestone slight increase in C_3S consumption
- Monocarboaluminate formation depends on aluminum availability
- C–S–H composition is different than model C–S–H, Ca/Si is higher than proposed by model and aluminum uptake occurs
- Crystallinity of hemicarboaluminate increases with limestone addition
- Ettringite formation is not influenced by limestone addition
- Calcite consumption does not increase with limestone content in the cement
- Porosity is slightly influenced by limestone addition. Total porosity increases with limestone addition at each time. Since 24 hours breakthrough diameter is the same for each limestone addition and at 28 days it is smaller than sample without limestone

All the results show that limestone has an influence on the hydration and properties of the cement however in which extend it depends on C_3A and gypsum content. Gypsum was shown to have significant influence on the hydration and properties development of cementitious materials.

Chapter 5

Influence of gypsum on hydration of PC and limestone cements

For typical modest additions of limestone, the level of sulfate has significant influence on strength and perhaps other properties of cementitious materials. Therefore it was decided to study the effects of gypsum addition. We need to understand the behavior and mechanisms of hydration with gypsum to better identify the influence of limestone in cement.

The importance of gypsum in improving compressive strength lies in its influence on the hydration reactions, which have a close influence on the hardening and microstructure development of the paste at early age. When Portland cement clinker is ground without addition of gypsum, the aluminate phases react rapidly to promote quick set. Because aluminate phases have advantages (works as flux in the cement kiln, binds Cl^- in the cement paste) and are always present in the clinker, gypsum is added to retard the initial hydration reaction.

There are questions about limestone influence on gypsum content when it is incorporated into the system as it reacts with C_3A to form carboaluminate phases. Therefore the limestone addition may effect the quantity of gypsum required to obtain proper retardation and maximize compressive strength.

Because of the lack of the precise information about the influence of gypsum on early hydration reactions and in order to prevent abnormal expansion due to overdose of gypsum addition in the cementitious materials, the amount of gypsum which is allowed to use in the cement system is limited by standard specification. The total SO_3 content is usually not more than 4.5% [46].

Optimum gypsum, the amount of gypsum which gives the highest compressive strength at a given time has been known since the 1950s when Lerch showed that, depending on the composition of the cement, gypsum can retard the initial hydration

and set or act as an accelerator [47]. After Lerch other researchers worked on the influence of gypsum on the mechanical properties [6] [13] [36] [37] [39] [82] [83]. All found that there is an optimum gypsum content below and above which compressive strength decreases. However, there are few studies to explain this behavior.

Lerch gave a few typical results of the rates of reaction of different cements, with low and high C_3A content cements with different gypsum and alkalis content. He noticed that cements show two main reaction peaks up to 24 hours of hydration. The first was the dissolution peak, and later after induction period a main reaction peak. He considered cements which contained the minimum quantity of gypsum required to give a curve with two peaks and no appreciable change with larger addition of gypsum during first 30 hours of reaction, to be cements properly sulfated [47]. This amount of gypsum could be indicated by the shape of calorimetry curve and those cements also showed the best compressive strength and the lowest shrinkage.

Two opposing effect of gypsum are involved in the existence of an optimum gypsum content in respect to strength. It was shown that gypsum accelerates the hydration reactions of pure C_3S [6] [37], alite [37] [39] and Portland Cement [82] [83] at early ages, up to 3 days [34]. On the other hand there are adverse effects when the amount of gypsum exceeds the optimum which have been attributed to the formation of excessive amounts of ettringite, and internal cracking [39]. There are also hypotheses that the addition of gypsum changes the quantity and quality of the C-S-H gel. Bentur [6] suggested that with gypsum addition the amount of gel formed during hydration increases but its intrinsic strength decreases, which is related to its C/S mole ratio.

In this section the results on gypsum addition in C_3S and in the cements with different clinker composition with and without limestone addition will be presented.

5.1 Influence of gypsum on the hydration of alite in the alite – gypsum – limestone system

Because of the complexity of the limestone, gypsum and different C_3A content, pure alite phase was prepared to investigate influence of limestone and gypsum on the hydration of alite. 8 mixes were prepared, alite with three different amounts of gypsum low 3.8, intermediate 6.0 and high 9.0, with 0 and 10% of limestone addition, and references sample without gypsum alite with water and with 0 and 10% of limestone. The composition of the mixes are presented in [Table 5.1](#).

Table 5.1: Alite, gypsum, limestone systems composition

Alite [%]	Gypsum	Limestone
100	0	0
96.2	3.8	0
94	6.0	0
91	9.0	0
90	0	10
86.2	3.8	10
84	6.0	10
81	9.0	10

5.1.1 Alite – gypsum – limestone systems – kinetics

Isothermal Calorimetry for all mixes were carried out to determine the kinetics of hydration of alite in the presence of gypsum and later also limestone addition.

There is no significant difference in the time of onset of the acceleration period of C_3S in the calorimetry curve. However the results show that with gypsum addition the hydration kinetics of alite are influenced. All the calorimetry curve show one main peak of silicate hydration and the peak is two times higher for samples containing gypsum in comparison to the samples without gypsum addition (Fig. 5.1). Between the different gypsum additions there are differences in the size of the main peak. The highest peak is for the sample with the lowest gypsum addition 3.8% and the samples with 6.0% and 9.0% of gypsum shows the same height of the main peak. The cumulative curve shows the same trend and with gypsum addition the total heat evolved is the highest for the sample with 3.8%. The total heat evolved for the samples with 6.0% and 9.0% of gypsum is the same and it is lower than sample with 3.8% of gypsum addition (Fig. 5.2).

With 10% of limestone addition in the system and increasing gypsum content slightly different trends in the alite hydration are observed. There is also one main peak of silicate hydration visible, and the size of the peak with gypsum addition is slightly higher for samples with gypsum in comparison to the sample of only alite and 10% of limestone mixed together (Fig. 5.3), and the height of the main peak increases up to 6.0% of gypsum and later decreases again. The cumulative curve however shows that mixes of alite with 10% of limestone shows the lowest total heat evolved up to 140 hours of hydration, but then shows the highest total heat evolved at later ages (Fig. 5.4). This unexpected result was repeated and confirmed. With gypsum addition the total heat evolved increases up to 6.0% addition and later decreases again with high

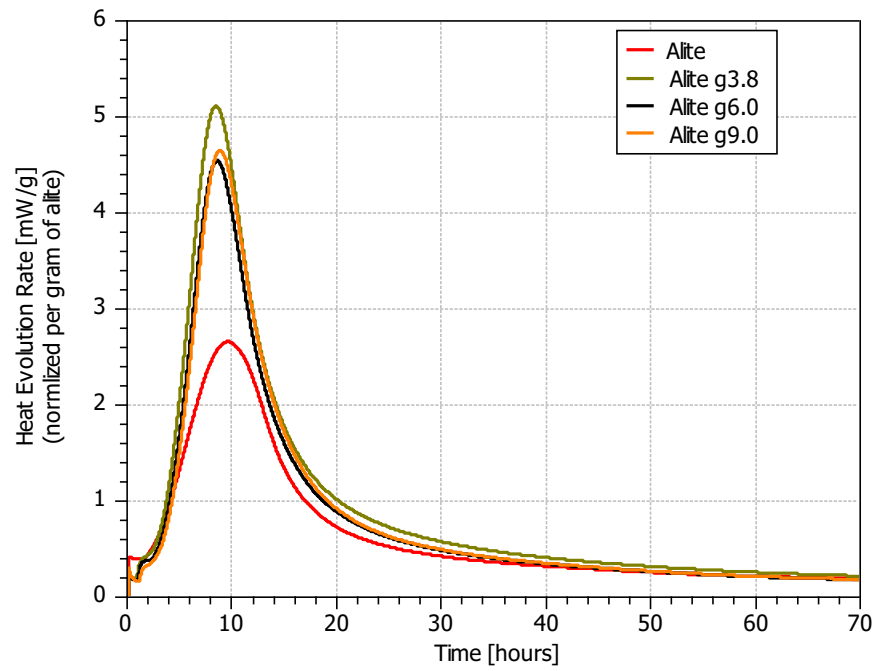


Figure 5.1: Isothermal Calorimetry Data for alite and gypsum mixes.

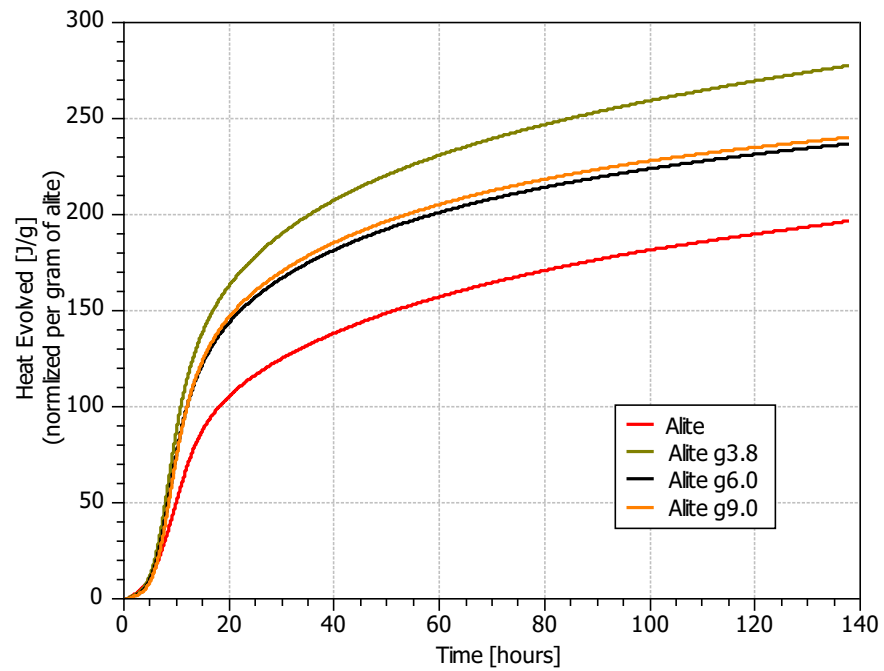


Figure 5.2: Isothermal Calorimetry Data for alite and gypsum mixes – cumulative curve.

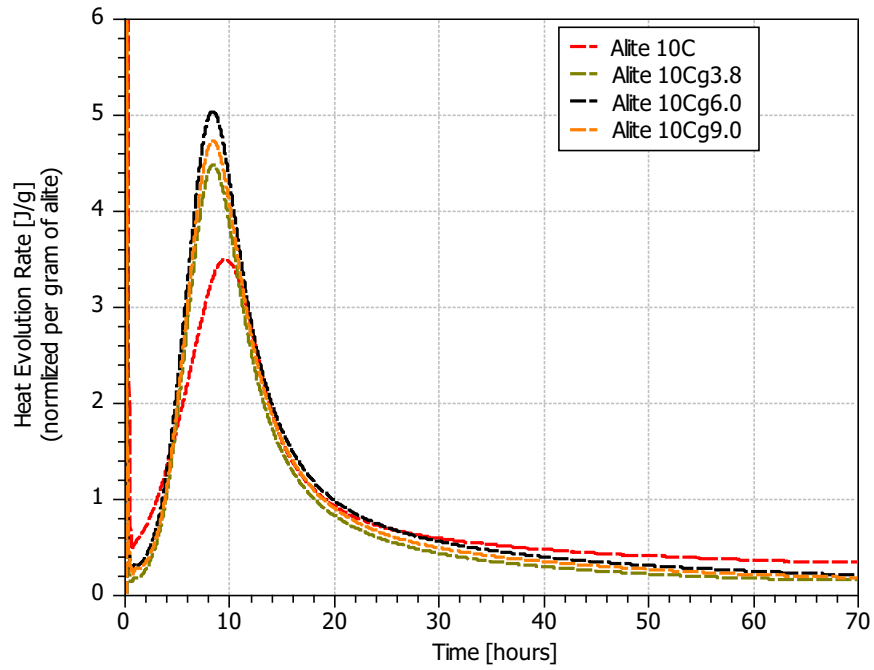


Figure 5.3: Isothermal Calorimetry Data for alite, gypsum and 10% of limestone mixes.

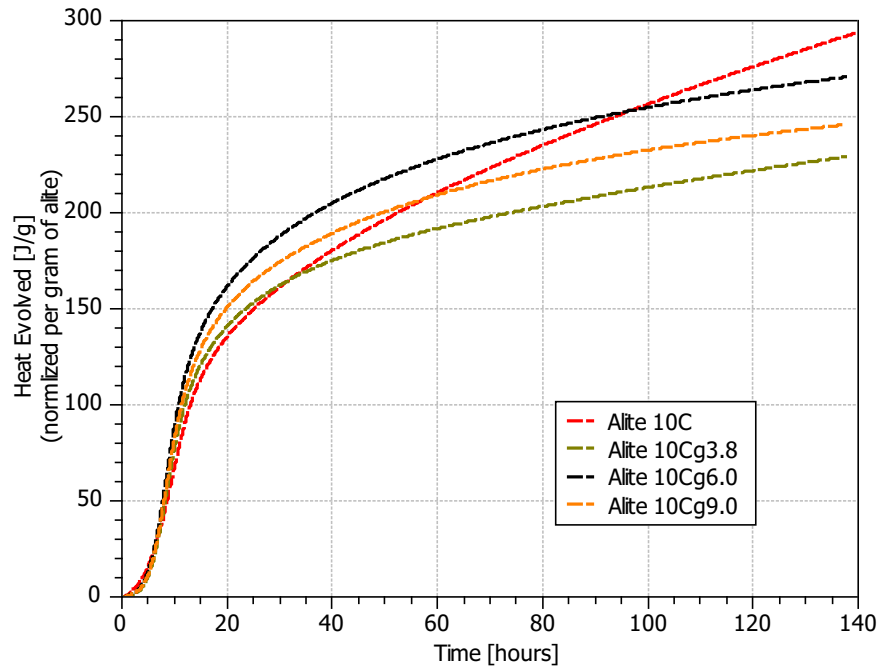


Figure 5.4: Isothermal Calorimetry Data for alite, gypsum and 10% of limestone mixes – cumulative curve.

9.0% of gypsum addition.

5.1.2 Phase assemblage of alite – gypsum – limestone mixes

The differences in microstructural development were investigated by Mercury Intrusion Porosimetry, TGA, XRD and SEM. Because of the limited amount of alite, the phase assemblage were done only on 7 days old samples reused after isothermal calorimetry tests.

XRD Rietveld Analysis show that with gypsum addition the consumption of alite increases significantly in comparison to the mix without gypsum, and increases in a narrow range with addition of gypsum (Fig. 5.5). With limestone addition the alite consumption additionally increases, therefore we can conclude that gypsum and limestone increase the alite hydration.

The quantity of amorphous phase also increases with gypsum addition and with 10% of limestone addition there is an additional increase in amorphous phase formation, quantified by XRD Rietveld Analysis (Fig. 5.6). However the portlandite amount quantified by XRD Rietveld Analysis decreases with gypsum addition and simultaneously with C_3S consumption and amorphous phase. This could be due to differences in composition of C–S–H formed in the matrix with gypsum and limestone addition or gypsum influence on the crystallization of portlandite.

The Mercury Intrusion Porosimetry shows only slight differences. The difference in the total porosity between samples is in the range of 7% (Fig. 5.7). The pore size distribution of hydrated alite it is not systematically influenced by gypsum or limestone addition after 7 days. The threshold is also not influenced by gypsum and limestone addition, and is similar for all alite mixes. The comparison with the cumulative curve of porosity for sample of cement paste with gypsum and limestone addition shows the pore distribution in pure alite is much coarser. The reasons for this are not clear.

TGA analysis were done to see the influence of gypsum and limestone on alite hydration. For all alite-gypsum-limestone two main regions are visible at 0–230°C C–S–H decomposition, and 400–550°C portlandite decomposition (Fig. 5.8). With limestone addition an additional peak at 700–850°C for calcite decomposition is visible (Fig. 5.9).

In the first region (0–230°C) the small peak of gypsum decomposition is visible for 6.0 and 9.0% of gypsum addition and based on its size we can conclude that there is more gypsum left in the alite systems when limestone is present in the system (Figs 5.8, 5.9).

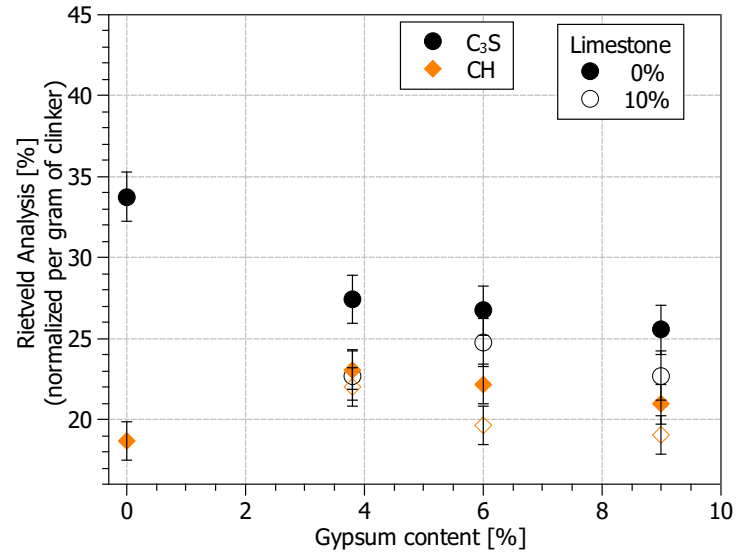


Figure 5.5: XRD Rietveld Analysis. C₃S and portlandite quantification in the system of alite-gypsum-limestone. 7 days of hydration.

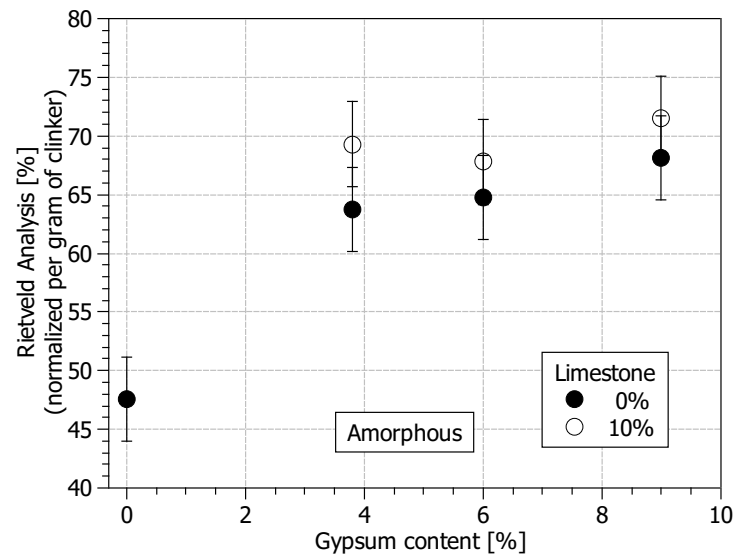


Figure 5.6: XRD Rietveld Analysis. Amorphous phase quantification in the system of alite-gypsum-limestone. 7 days of hydration.

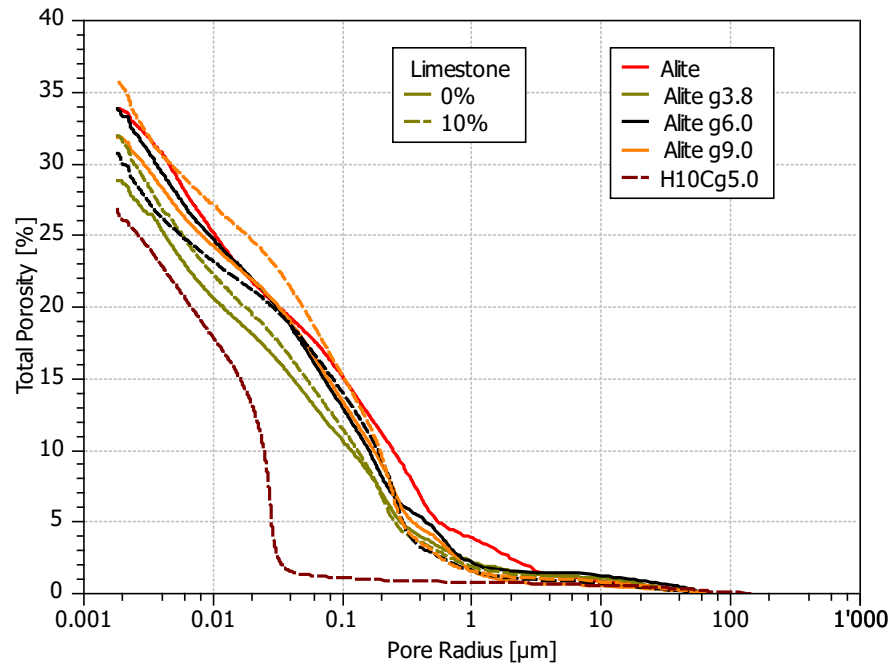


Figure 5.7: Mercury Intrusion Porosimetry. Alite, different amount of gypsum with 0 and 10% of limestone addition.

TGA results show that there is more water combined with increasing gypsum addition up to 9.0% of gypsum (however this is within the error) (Fig. 5.10) and less portlandite formed (Fig. 5.11). It suggests that the C-S-H formed is richer in Ca^{2+} with increasing gypsum content. With 10% of limestone addition the percent of water combined up to 550°C and portlandite content is lower than samples without limestone addition, however the trend with gypsum addition is the same for samples with 0 and 10% of limestone addition.

The SEM images do not show a significant influence of the gypsum addition on the microstructure development (Fig. 5.12). However it can be noticed that microstructure development is different for pure phases and cement system. There is coarser porosity and more uniform C-S-H in pure alite microstructure.

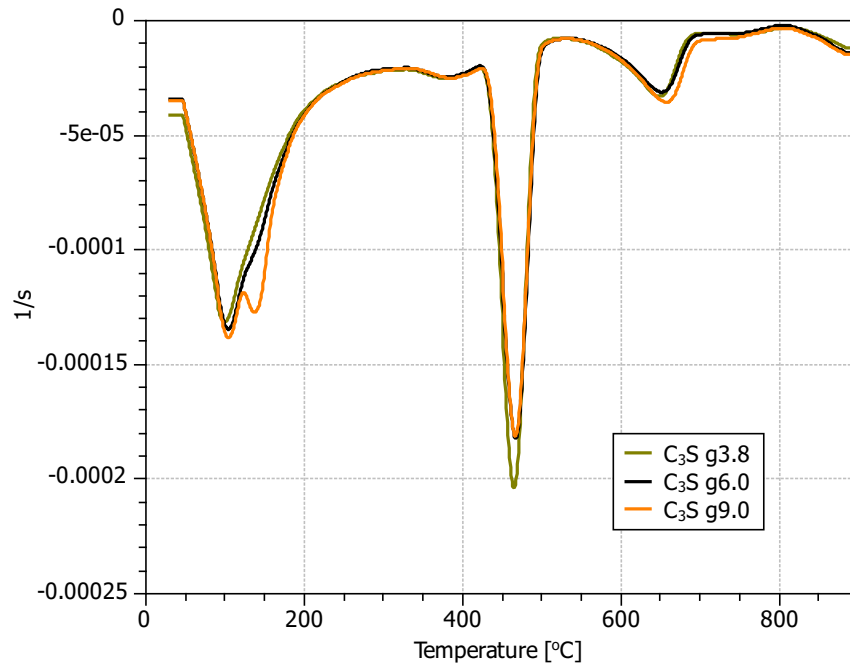


Figure 5.8: Thermogravimetric Analysis. Alite with different gypsum content and with 0% of limestone addition.

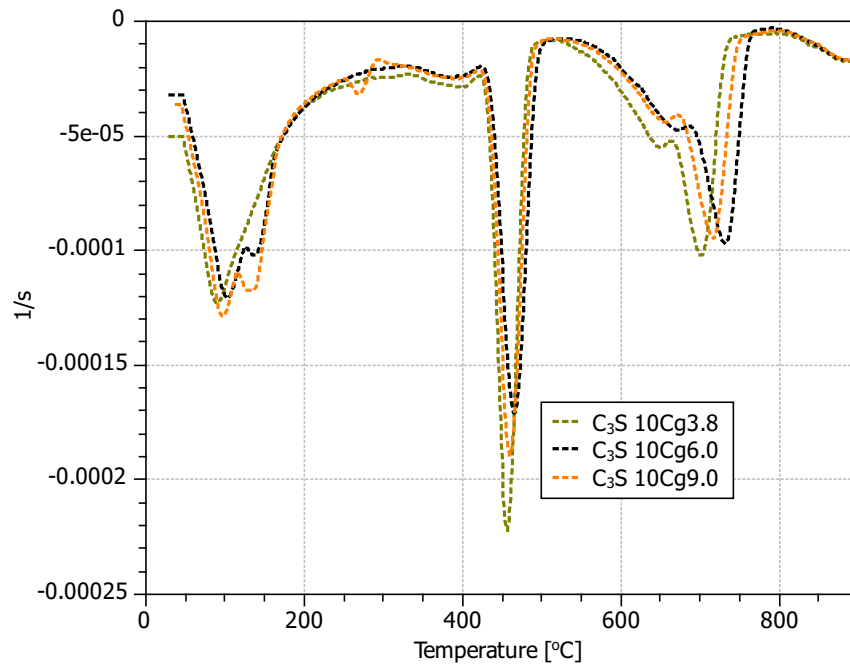


Figure 5.9: Thermogravimetric Analysis. Alite with different gypsum content and with 10% of limestone addition.

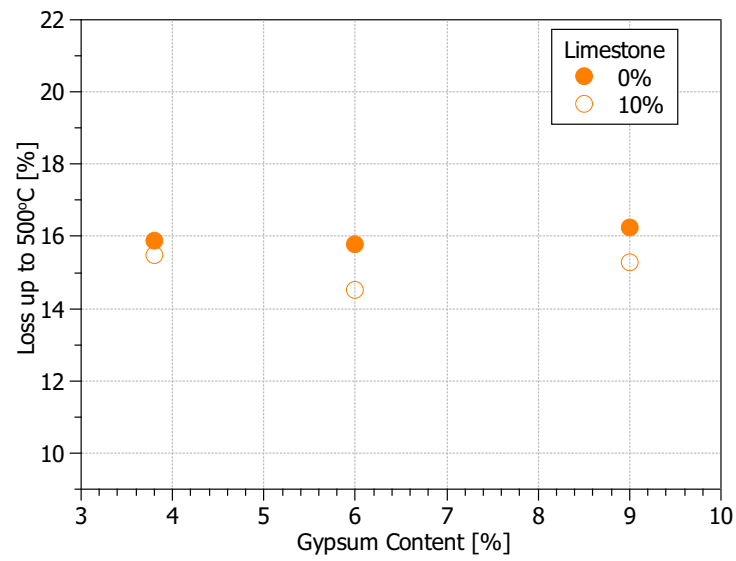


Figure 5.10: Thermogravimetric Analysis. Alite with different gypsum content and with 0 and 10% of limestone addition. Water loss up to 550°C.

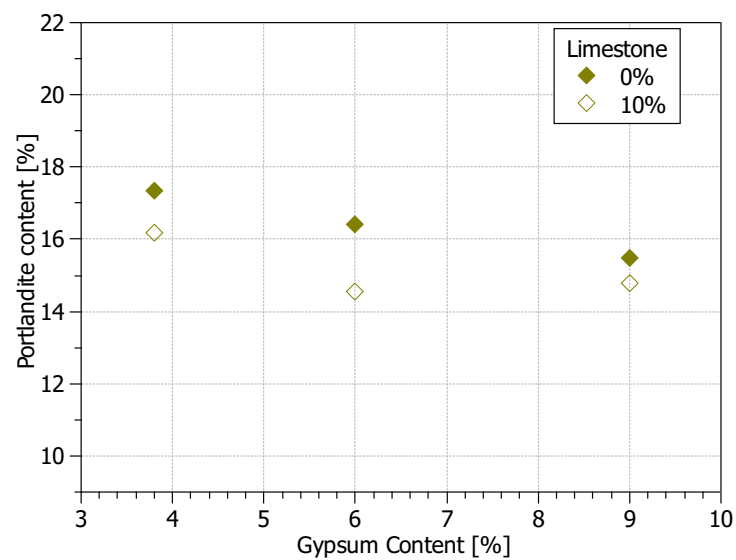


Figure 5.11: Thermogravimetric Analysis. Alite with different gypsum content and with 0 and 10% of limestone addition. Portlandite content.

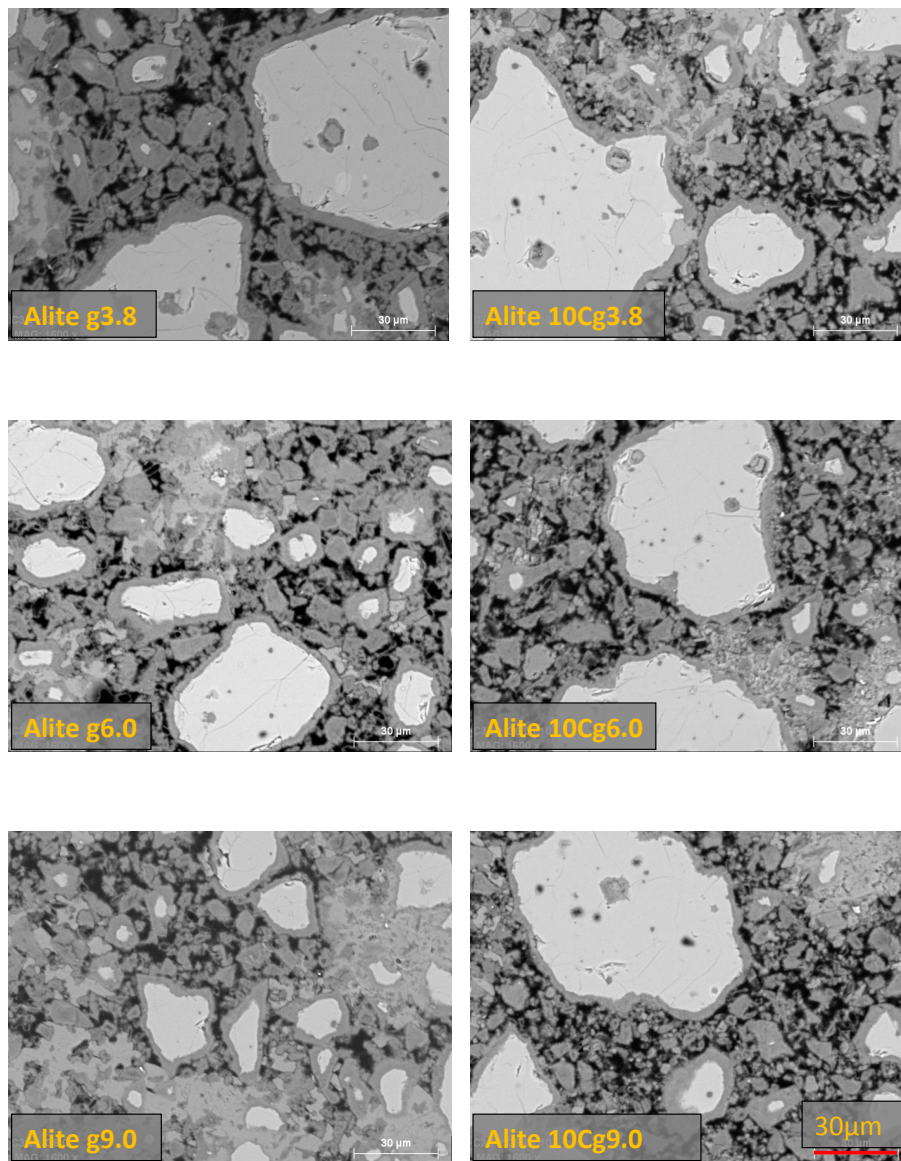


Figure 5.12: Scanning Electron Microscopy for samples alite – gypsum – limestone mixes. Magnification=1600x, HV=15kV, WD=12.5mm.

To conclude The gypsum addition has a direct influence on the alite hydration. Gypsum increases the rate of hydration of alite however there is little change in the length of induction period with increasing gypsum addition. There is more alite consumed with gypsum addition more C–S–H formed and more water combined, but less portlandite formed which suggest that the C–S–H formed has a different ratio between Si, Ca and H₂O. It seems that with gypsum addition there is less Ca²⁺ in the C–S–H formed. The porosity does not show significant differences with gypsum addition. However this needs to be confirmed experimentally.

With 10% of limestone addition the trends are the same but less pronounced. Limestone additionally seems to promote C₃S consumption and amorphous phase formation and the portlandite content is even smaller for samples with limestone.

5.2 Influence of gypsum on cement hydration

Two types of clinker with low (3%) and high (8%) C₃A content with different gypsum content and limestone addition, were investigated. The blends studied are shown in [Table 5.2](#).

Experiments were carried out in two sets. The first set concerned early compressive strength for all presented mixes and a preliminary study of hydration . After the first set of experiments selected samples were subjected to further investigations, especially late compressive strength.

Table 5.2: Composition of mixes with different gypsum content

Clinker	Low C ₃ A					High C ₃ A				
Gypsum [%]	2.2	3.9	5.5	6.0	9.0	3.8	5.5	6.0	9.0	
Limestone [%]	0	0	0	0	0	0	0	0	0	
	10	10	10	10	10	10	10	10	10	

5.2.1 Compressive strength

The existence of an optimum gypsum content for compressive strength is clearly visible at early age up to 24h (Figs 5.14, 5.16) and less at later ages (Figs 5.13, 5.15). At later ages it seems to increase continuously with gypsum.

The optimum gypsum depends on the clinker composition (Figs 5.14, 5.16), however there is only a slight difference in optimum gypsum with increasing C_3A content. For cement with low C_3A clinker (3% of C_3A) at 24 hours, the optimum gypsum is 5.5% while for high C_3A clinker (8% of C_3A) it is 6.0%. It might be expected that the SO_3/Al_2O_3 ratio is the same for the samples at optimum gypsum. However for the low C_3A system the SO_3/Al_2O_3 ratio at the optimum gypsum is 2.60 (Fig. 5.14) while for high C_3A system it is 0.98.

At 24 hours, for low C_3A clinker cements, a gypsum amount 1.6% lower than the optimum gives a 8% decrease in strength while 0.5% higher gypsum than optimum gives 29% decrease in strength (Fig. 5.14). In the cement with high C_3A amount of gypsum 2.2% less than optimum gypsum decreases strength about 19%, while increase in gypsum amount about 0.5% from optimum gypsum can decrease strength up to 50% (Fig. 5.16). Regardless of the clinker composition, cement is more sensitive to overdosing of gypsum than to a deficiency of the gypsum amount.

At 28 days both low and high C_3A clinker, (Figs 5.13, 5.15) show much lower variation in strength with gypsum addition at 28 days than at 24 hours. At 28 days the sample with 9% gypsum addition and high C_3A content shows the highest compressive strength.

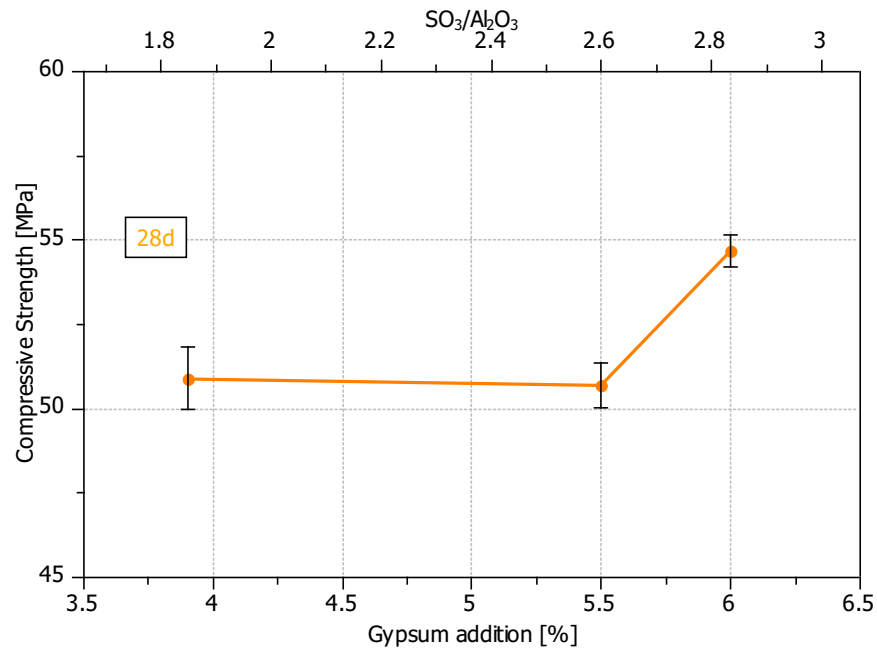


Figure 5.13: Compressive Strength of mortars at 28 days of hydration. Clinker with low (3%) C₃A content and increasing gypsum addition.

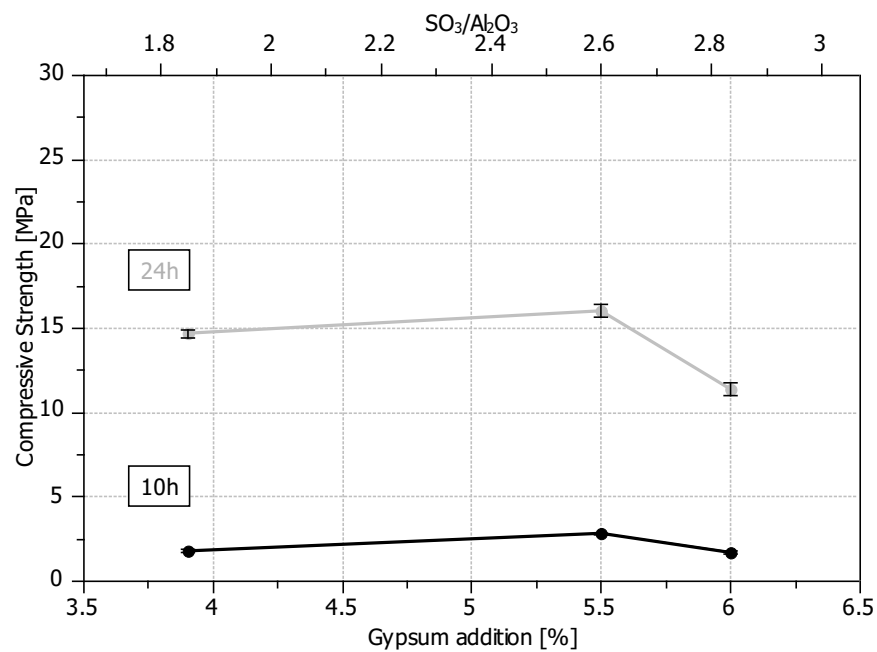


Figure 5.14: Compressive Strength of mortars at 10 and 24 hours of hydration. Clinker with low (3%) C₃A content and increasing gypsum addition.

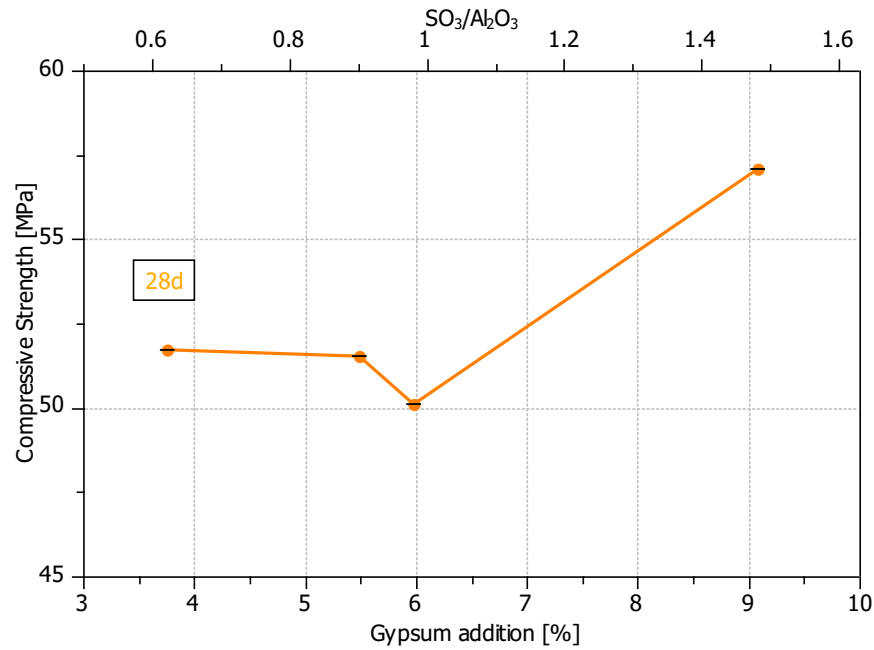


Figure 5.15: Compressive Strength of mortars at 28 days of hydration. Clinker with high (8%) C_3A content and increasing gypsum addition.

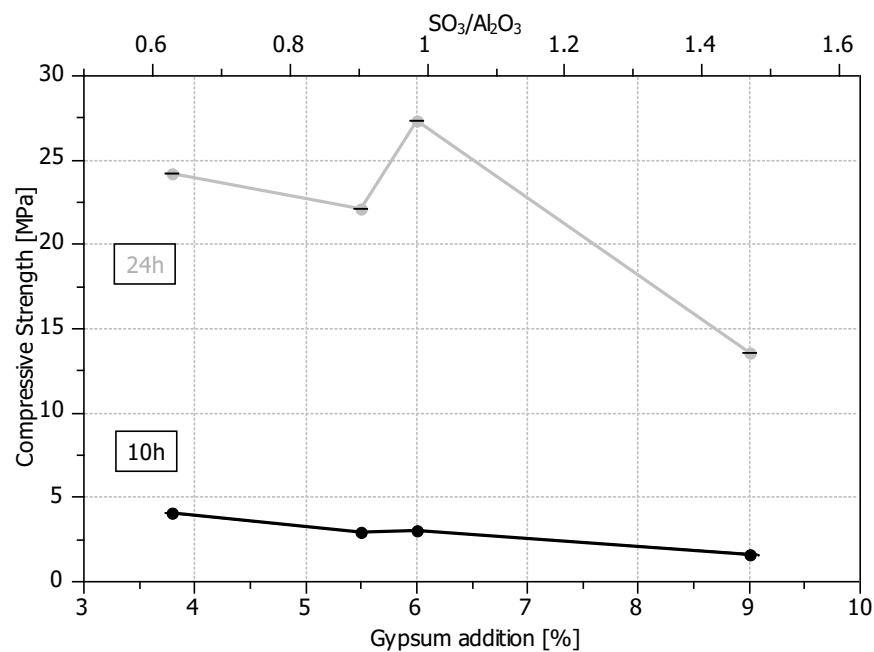


Figure 5.16: Compressive Strength of mortars at 10 and 24 hours of hydration. Clinker with high (8%) C_3A content and with increasing gypsum addition.

5.2.2 Hydration kinetics

The rate of heat liberation was determined for samples with low and high C_3A cements and increasing gypsum addition. The results are presented in Figs 5.17, 5.19. There is a delay of the aluminate peak with gypsum addition (Figs 5.17, 5.19). With the highest gypsum addition 9.0% the suppression of the hydration reaction of alite is visible. The sample with 9.0% of gypsum addition also shows the lowest total heat evolved (Figs 5.18, 5.20). With gypsum addition the total heat evolved increases up to optimum and later decreases again, regardless of the C_3A content.

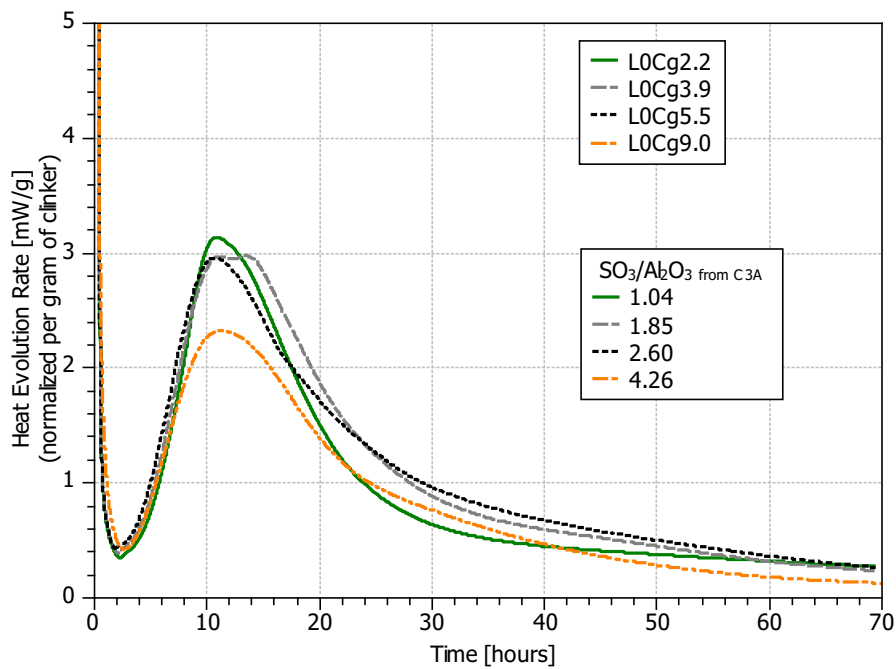


Figure 5.17: Isothermal Calorimetry data for low C_3A clinker with increasing gypsum content.

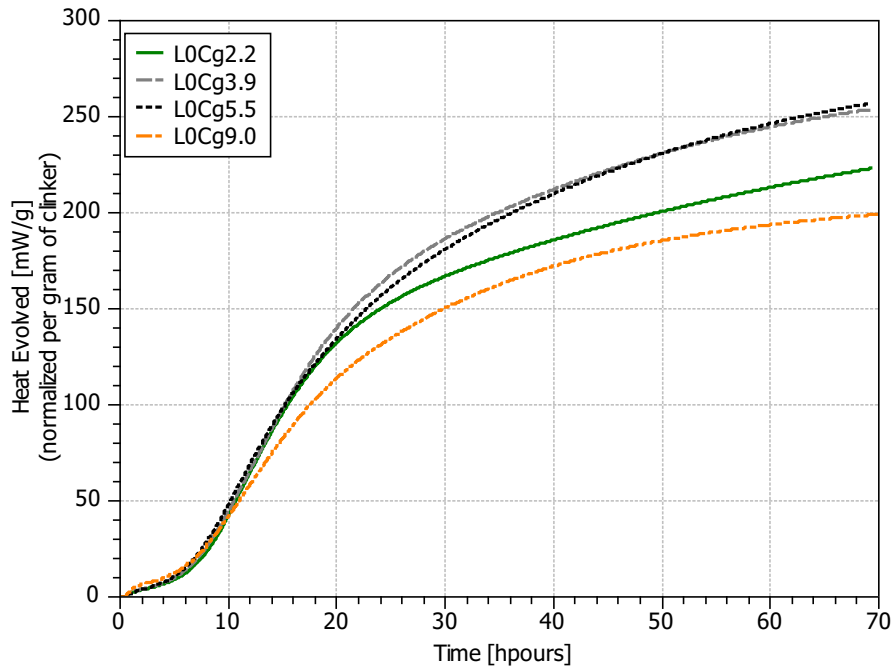


Figure 5.18: Isothermal Calorimetry data for low C_3A clinker with increasing gypsum content – Cumulative.

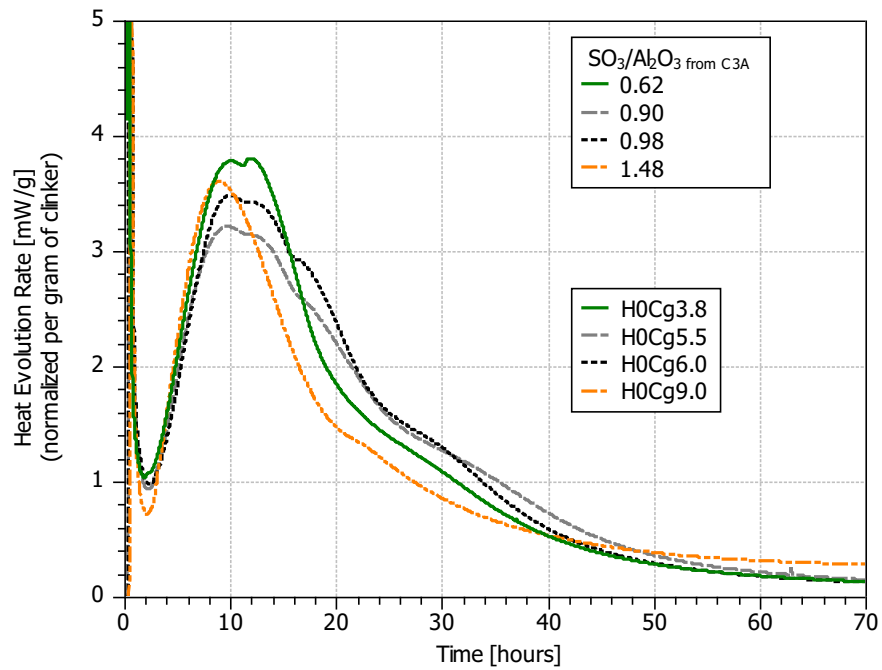


Figure 5.19: Isothermal Calorimetry data for high C_3A clinker with increasing gypsum content.

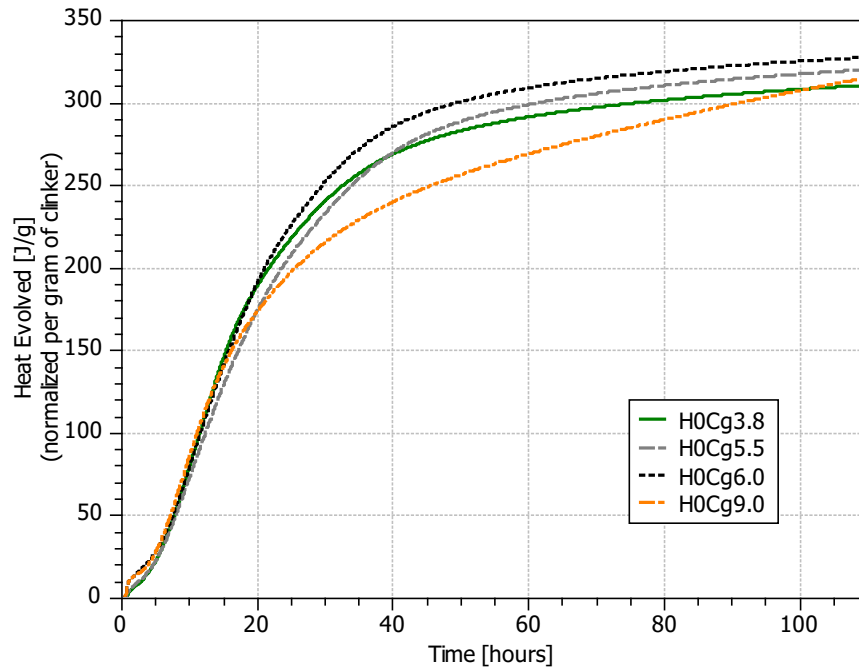


Figure 5.20: Isothermal Calorimetry data for high C_3A clinker with increasing gypsum content – Cumulative.

5.2.3 Development of phases (XRD, TGA)

In Figs 5.21 and 5.22 the C_3A consumption by XRD Rietveld Analysis is presented and ettringite formation for low and high C_3A cement with increasing gypsum addition. Regardless of the clinker composition, with gypsum addition the formation of ettringite increases for low C_3A and high C_3A cement. Even though ettringite formation increases, the C_3A consumption shows a similar rate for all gypsum additions. However the high error for measurement of such low amount is born in the results. Only samples with the highest gypsum content (regardless of C_3A) show a delay in C_3A reaction.

In Figs 5.23 and 5.24 the formation of monosulfate (Ms) is presented. With increasing gypsum addition the monosulfate formation tends to decrease for low and high C_3A clinker. Sample H0Cg6.0, which comes from different batch of cements (Fig. 5.24) shows a slight deviation from the general trend.

Even though differences in the C_3A consumption and ettringite formation with gypsum addition are visible they do not obviously explain the differences in the compressive strength at early age up to 24 hours.

In Figs 5.25, 5.26 the consumption of C_3S is presented. There are small differences in C_3S consumption with gypsum addition and with time of reaction, however there is no clear trend between gypsum addition and C_3S consumption. The error of the measurement by XRD Rietveld Analysis must be borne in mind.

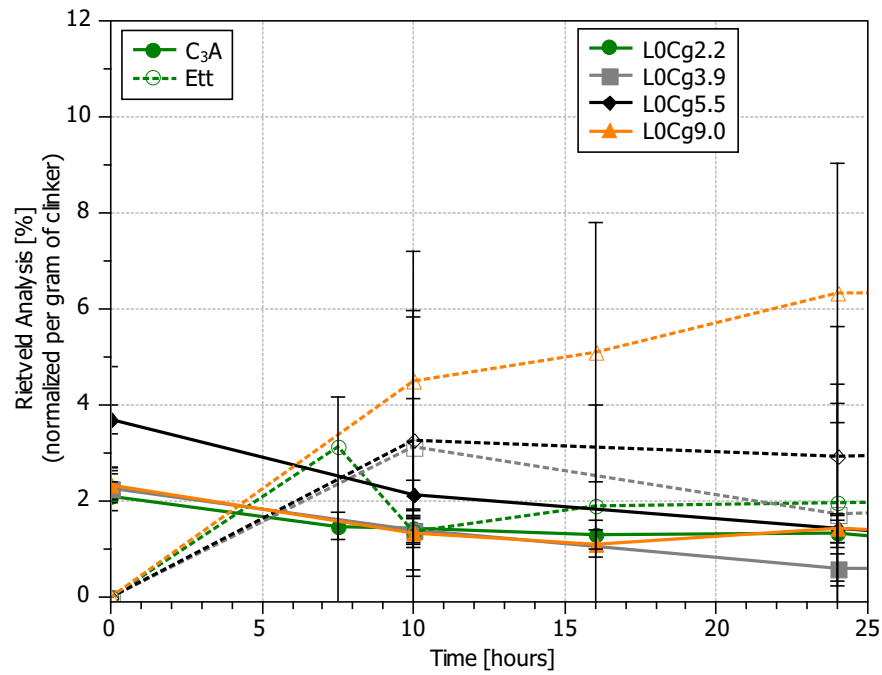


Figure 5.21: XRD Rietveld Analysis, ettringite formation and C₃A consumption up to 24 hours of hydration in low C₃A cement with increasing gypsum content.

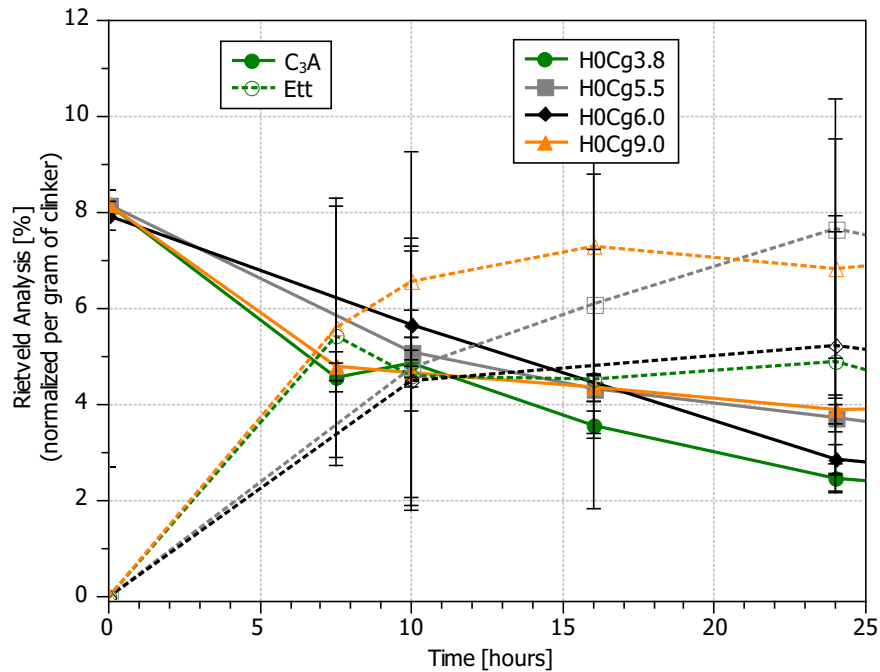


Figure 5.22: XRD Rietveld Analysis, ettringite formation and C₃A consumption up to 24 hours of hydration in high C₃A cement with increasing gypsum content.

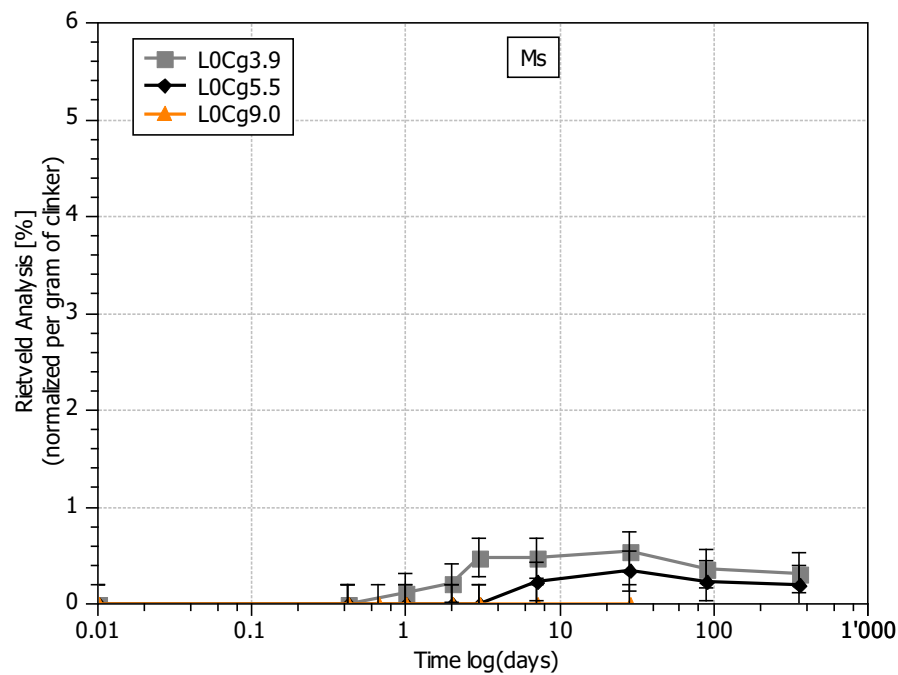


Figure 5.23: XRD Rietveld Analysis, monosulfate phase formation, low C_3A clinker with increasing gypsum addition.

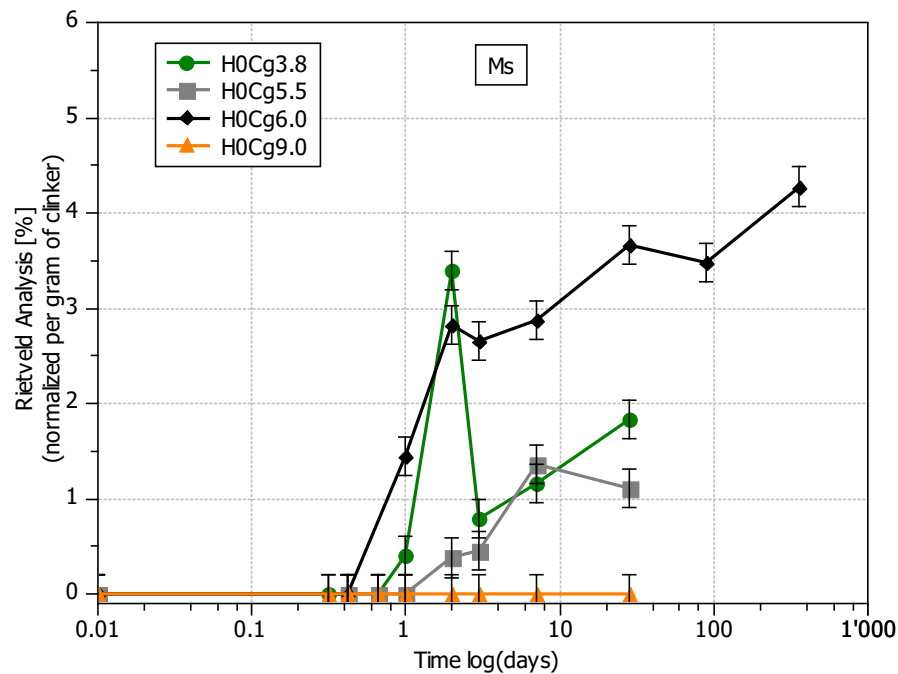


Figure 5.24: XRD Rietveld Analysis, monosulfate phase formation, high C_3A clinker with increasing gypsum addition.

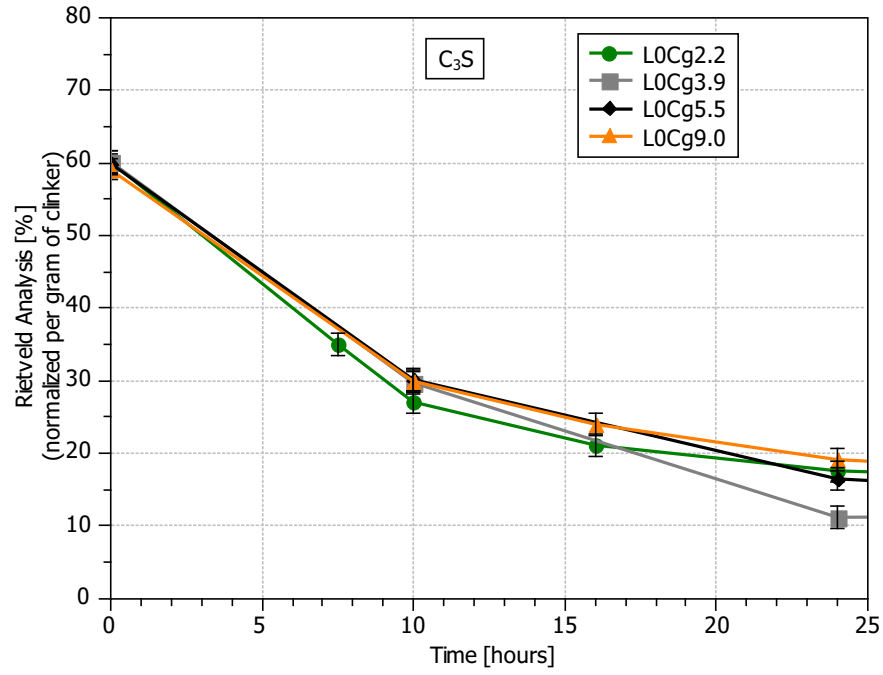


Figure 5.25: XRD Rietveld Analysis, C_3S phase consumption up to 24 hours of hydration, low C_3A clinker with increasing gypsum addition.

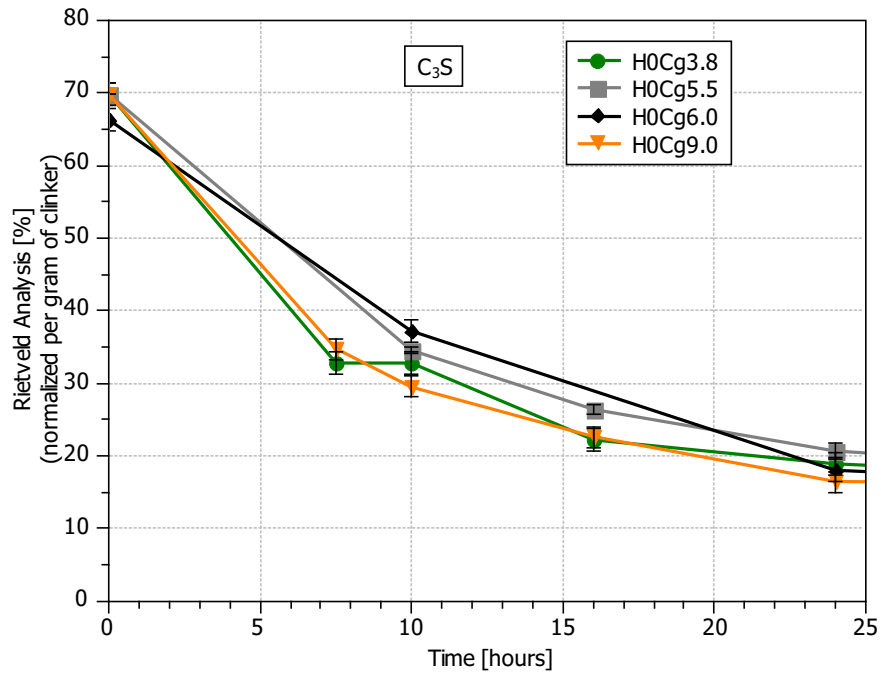


Figure 5.26: XRD Rietveld Analysis, C_3S phase consumption up to 24 hours of hydration, high C_3A clinker with increasing gypsum addition.

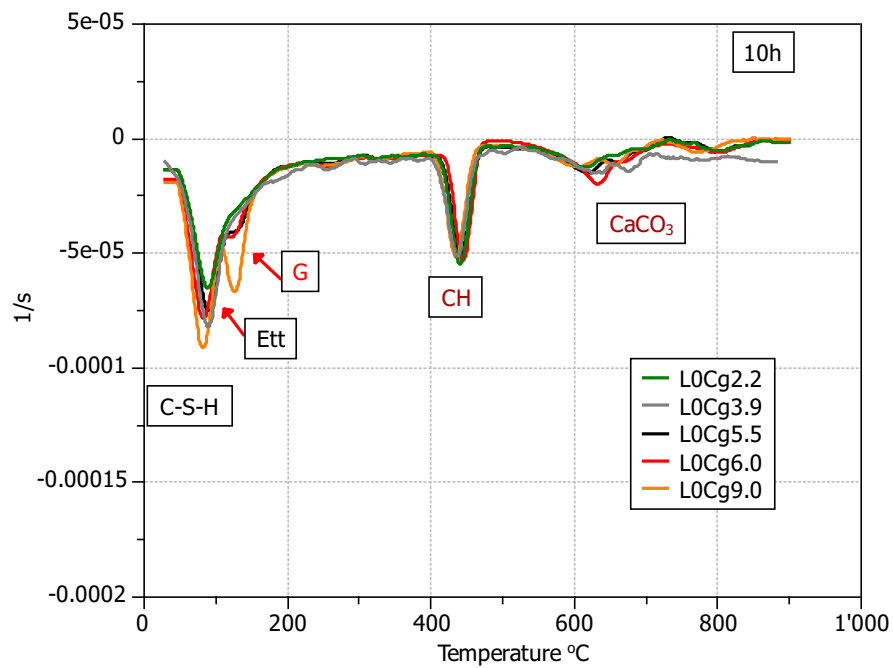


Figure 5.27: TGA at 10 hours of hydration of low C_3A clinker cement with increasing gypsum addition.

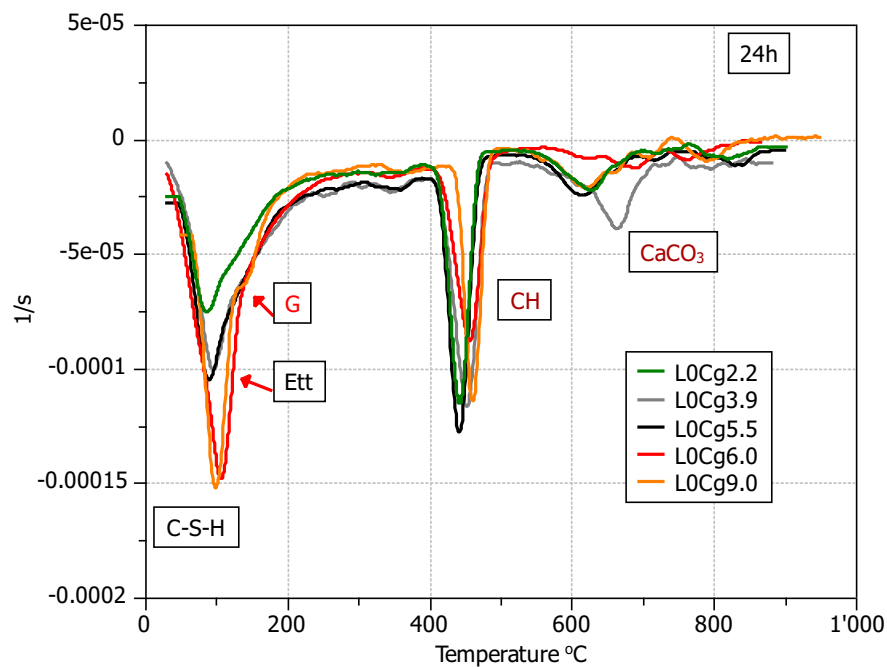


Figure 5.28: TGA at 24 hours of hydration of low C_3A clinker cement with increasing gypsum addition.

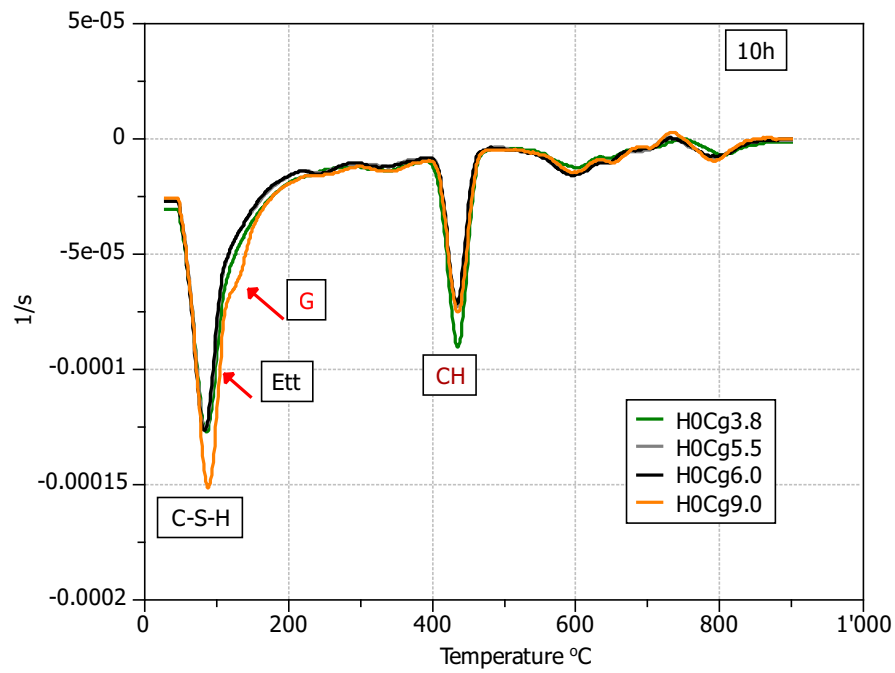


Figure 5.29: TGA at 10 hours of hydration of high C₃A clinker cement with increasing gypsum addition.

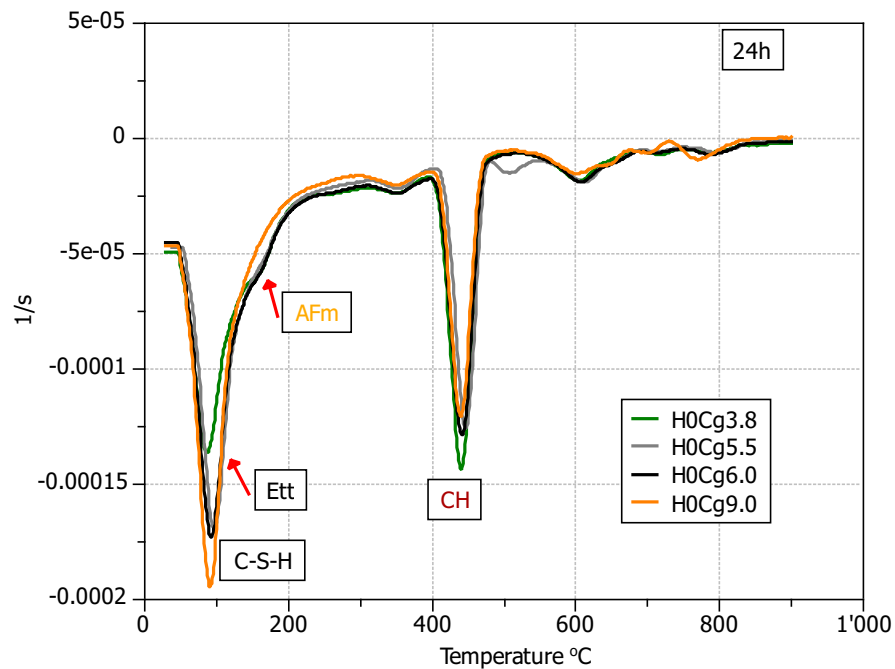


Figure 5.30: TGA at 24 hours of hydration of high C₃A clinker cement with increasing gypsum addition.

The sample at optimum (5.5%) gypsum for low C_3A clinker, shows the smallest rate of C_3S consumption at 24 hours. The sample at optimum gypsum for high C_3A clinker, with 6.0% of gypsum shows similar C_3S consumption with the highest C_3S consumption up to 24 hours of hydration (Fig. 5.25). Differences in C_3S consumption with gypsum addition are less visible for clinker with high C_3A than low C_3A .

In Figs 5.27 – 5.30, the Thermo Gravimetric Analysis data at 10 and 24 hours of hydration with increasing gypsum addition for low and high C_3A clinker cement are presented. At 10 hours of hydration the peak of the CH decomposition in the cement with low C_3A clinker is the same for all gypsum addition. At 24 hours of hydration there are variations in the region of the CH decomposition in the cement with low C_3A clinker but these do not show linear dependency of the C_3S hydration on gypsum addition (Fig. 5.28). In the cement with high C_3A clinker at 10 hours of hydration the CH decomposition peak is the highest for the lowest gypsum addition 3.8%, for all the other gypsum addition, the peak is the same (Fig. 5.29). At 24 hours of hydration the CH region decreases with gypsum addition (Fig. 5.30).

The sample with the highest gypsum addition 9.0%, and the lowest strength at 24 hours shows the sharpest peak in the region 30 – 230°C. This is due to increased ettringite formation with high gypsum addition. Moreover there is small peak of gypsum still visible at 24 hours of hydration for the highest gypsum addition. The sample with the highest compressive strength at 24 hours, for low C_3A clinker cement, with 5.5% of gypsum addition has a relatively smaller peak than the samples with 6.0 and 9.0% of gypsum addition peak in the first region.

Even though calorimetry indicates some systematic effects of increasing gypsum addition, XRD and TGA do not have the precision to really tell how these effects impact the phase assemblage.

5.2.4 Porosimetry

In the literature there are many papers correlating compressive strength and porosity [58]. The increase in strength with gypsum addition in the literature was attributed to increase in density of the reaction product, the improvement in the gel quality with gypsum addition [83], or to an increase in the degree of hydration, or in the amount of combined water [58].

Later it was reported the the density of C–S–H gel is independent of the SO_3 content [82]. Odler found [58] that differences in strength with different gypsum content could be related to porosity changes in the samples. Sersale and Cioffi [80] found that the total porosity was the main microstructural parameter governing the influence of SO_3 content on compressive strength.

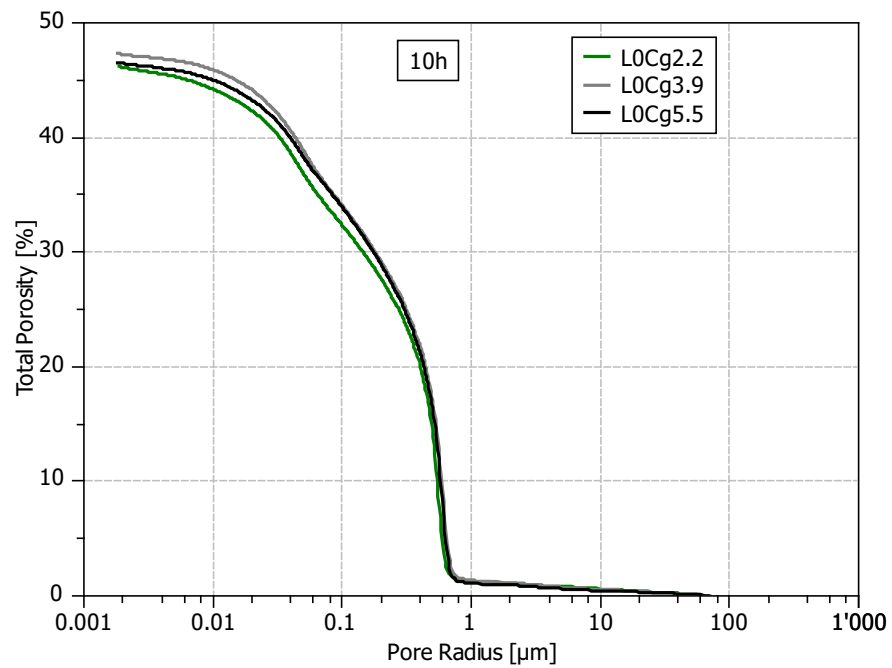


Figure 5.31: Mercury Intrusion Porosimetry at 10 hours of hydration. Low C_3A clinker with increasing gypsum addition.

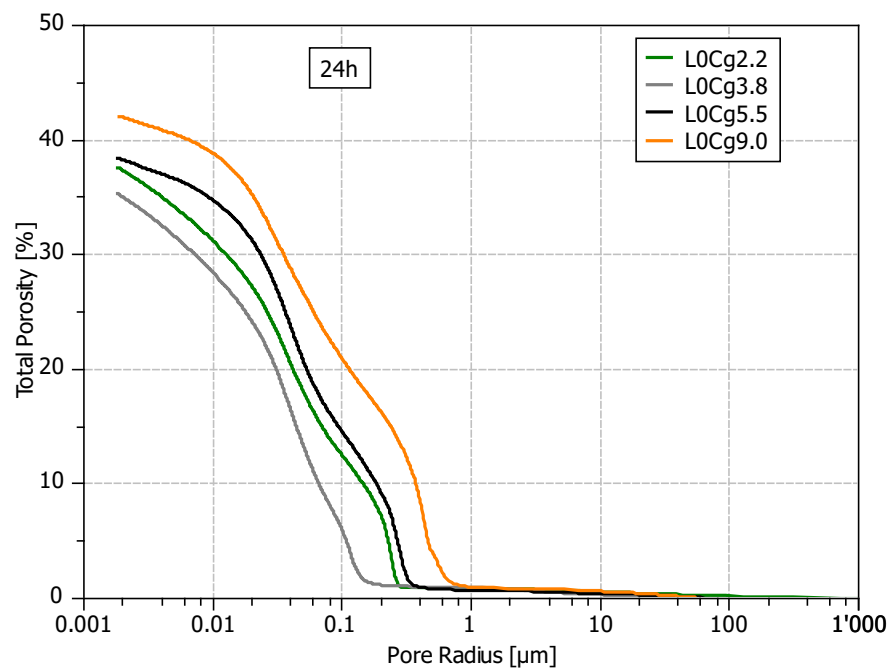


Figure 5.32: Mercury Intrusion Porosimetry at 24 hours of hydration. Low C_3A clinker with increasing gypsum addition.

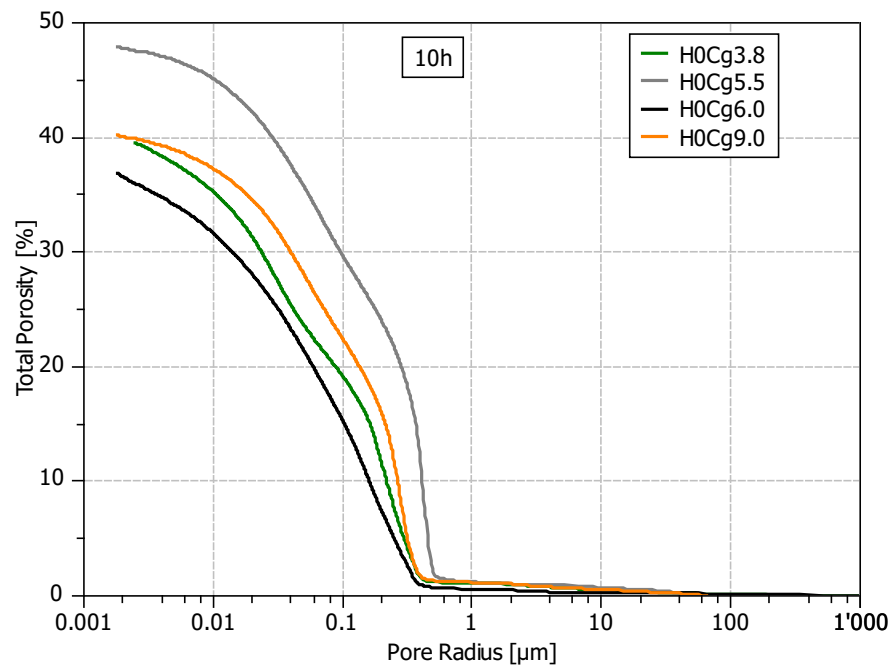


Figure 5.33: Mercury Intrusion Porosimetry at 10 hours of hydration. High C_3A clinker with increasing gypsum addition.

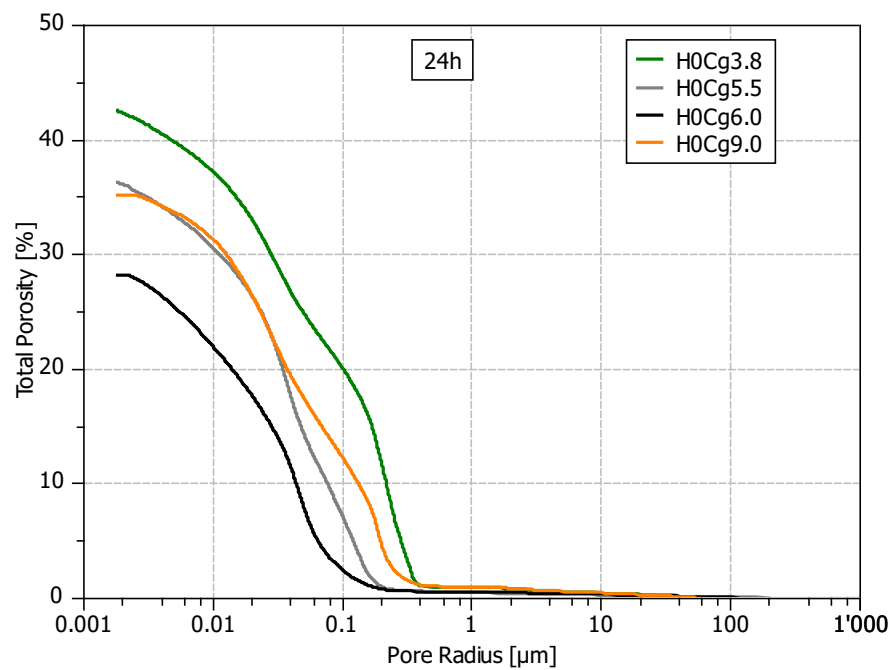


Figure 5.34: Mercury Intrusion Porosimetry at 24 hours of hydration. Low C_3A clinker with increasing gypsum addition.

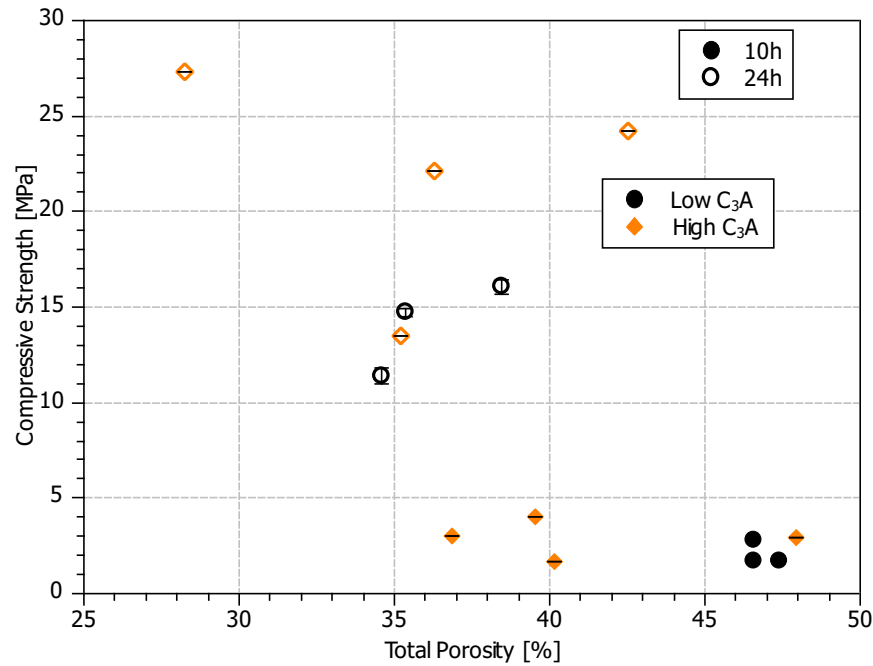


Figure 5.35: Total porosity vs. Compressive strength at 10 and 24 hours of hydration. Low and high C₃A clinker with increasing gypsum addition.

In Figs 5.31 – 5.34 the mercury intrusion porosimetry at 10 and 24 hours of hydration with increasing gypsum addition is presented. The low C₃A clinker cement at 10 hours of hydration shows no difference in the total porosity and pore size distribution (Fig. 5.31), while high C₃A clinker at 10 hours of hydration shows differences in total porosity between samples with gypsum addition in the range of 20% but without a clear relationship with increasing or decreasing gypsum addition (Fig. 5.33). At 24 hours of hydration for low C₃A clinker the total porosity decreases with gypsum addition up to 3.8% of gypsum addition and later increases again (Fig. 5.32). High C₃A clinker with gypsum addition at 24 hours of hydration the total porosity decrease up to optimum and later increases again (Fig. 5.34). Additionally sample H0Cg6.0 comes from different batch of cements what can have influence on the results as discussed Fig. 3.2.2.2.

Gypsum has similar influence on threshold of the samples. There is no clear relationship with gypsum addition.

There is also no clear relationship between total porosity and compressive strength. In the Fig. 5.35 the total porosity vs. compressive strength for samples with low and high C₃A clinker are presented. There is less difference in total porosity with gypsum addition for low C₃A clinker cement than for high C₃A clinker.

5.2.5 Microstructure

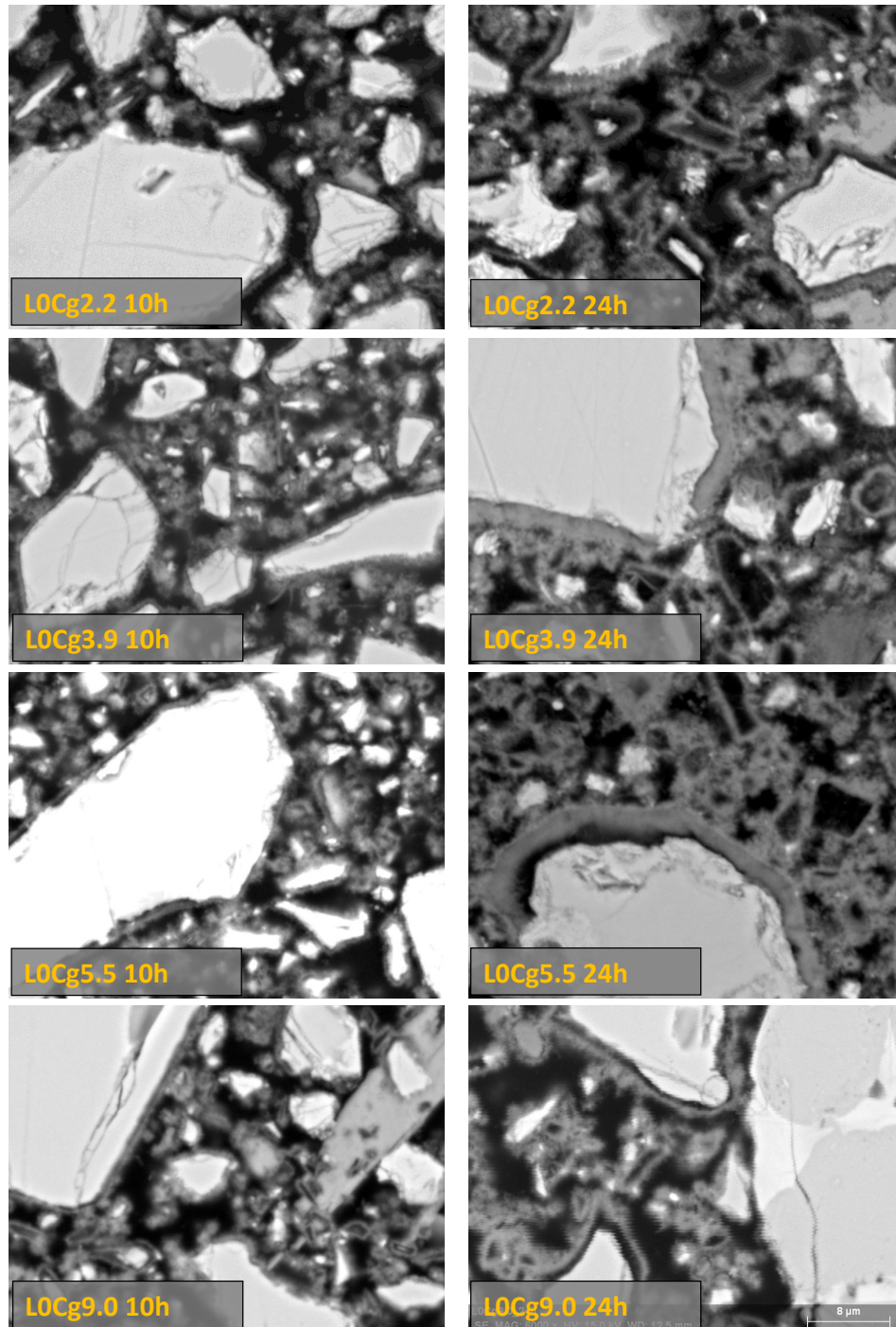


Figure 5.36: Scanning Electron Microscopy at 10 and 24 hours of hydration for samples with low C_3A clinker and increasing gypsum addition. Magnification=6000x, HV=15kV, WD=12.5mm.

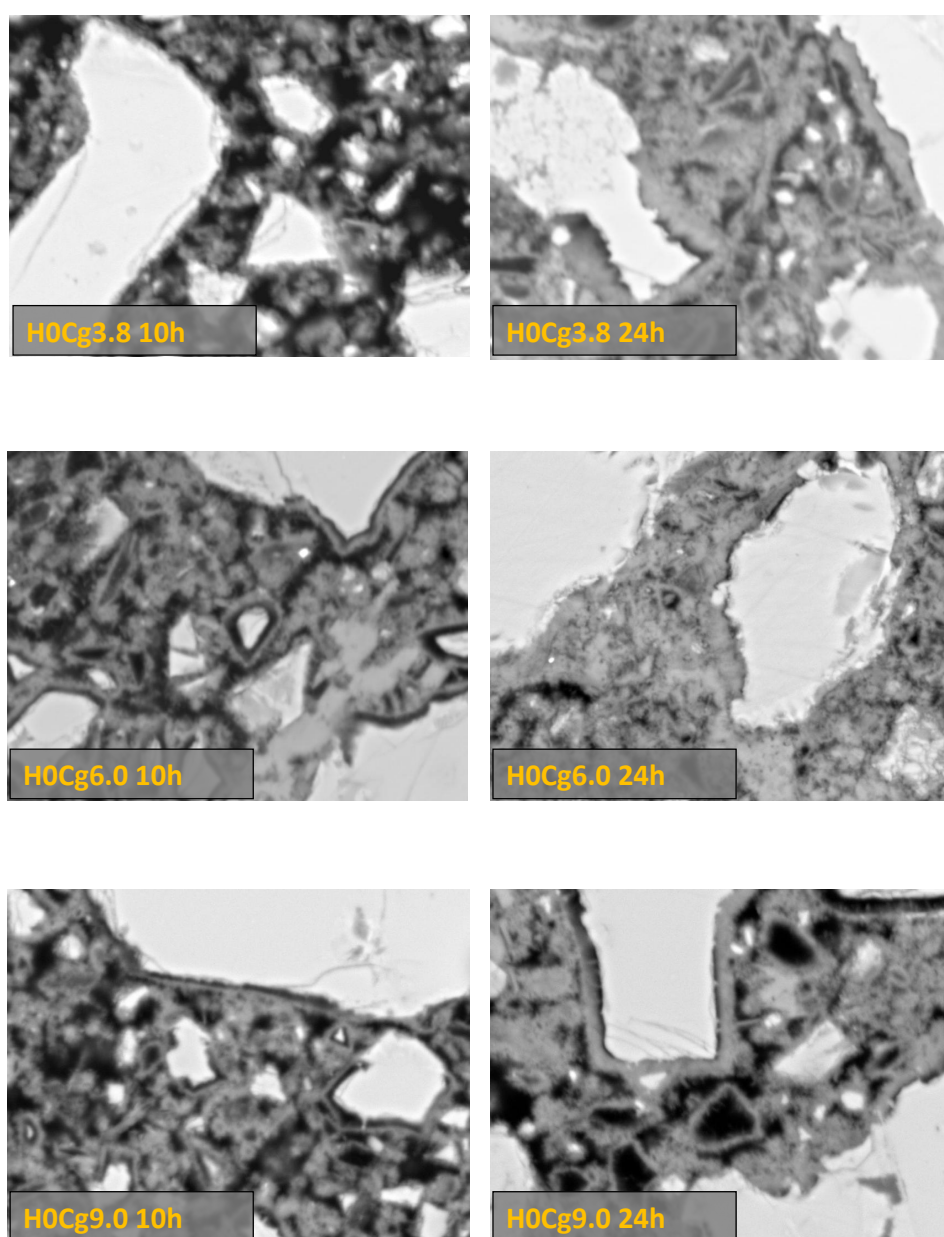


Figure 5.37: Scanning Electron Microscopy at 10 and 24 hours of hydration for samples with high C_3A clinker and increasing gypsum addition. Magnification=6000x, HV=15kV, WD=12.5mm.

With gypsum addition some differences in microstructure are observed concerning space filling. The main difference is in the C-S-H rim formation around cement grains (Figs 5.36, 5.37).

From the microstructural point of view in low and high C_3A clinker cement the most important difference are at early ages.

At 10 hours of hydration the product formed around grains is already visible and the shell is more pronounced around smaller grains than bigger grains. At the highest gypsum addition there is larger number of small shells of dimensions around $1\mu m$. The differences in the rim formation with increasing gypsum addition is the most visible at 24 hours of hydration. With increasing gypsum addition up to optimum, the thickness of the shell formed around the cement grains increases and there is better connectivity between cement grain and growing hydration product Fig. 5.36. At 24 hours of hydration with the highest gypsum addition, the thickness of the rim does not increase significantly compared to 10 hours of hydration, and the connectivity between cement grain and hydration product is significantly less good compared to lower gypsum addition. This phenomena was found in both high and low C_3A clinker and seemed to be significant in determining compressive strength of the cements with increasing gypsum content.

5.2.6 Summary - Influence of gypsum

Gypsum has a direct influence on cement hydration.

- There is an optimum gypsum up to which compressive strength increases and later decreases again
- Optimum gypsum depends on the cement composition. Slightly increases with C_3A content and decreases with limestone addition
- Regardless of C_3A content cement systems are more sensitive to the overdose of the gypsum content than on underdosing
- With increasing gypsum addition acceleration in accelerating period is observed
- With increasing gypsum addition a delay in aluminate reaction is observed
- Significantly above optimum gypsum clear suppression of the hydration reaction, below the optimum effects are not clear

- Porosity does not show clear relationship with gypsum addition and depends on the cement composition and time of hydration

5.3 Influence of limestone on gypsum optimum

5.3.1 Influence of limestone on the compressive strength

The compressive strengths for the blends, with and without 10% of limestone addition are shown in figures 5.38 – 5.41.

With 10% limestone addition there is little effect on the optimum gypsum. The optimum gypsum at 24 hours for clinker with low C_3A cement is the same with and without 10% of limestone addition and it is 5.5% relative to clinker. Optimum gypsum for high C_3A cement and 10% of limestone is 5.5%, relative to clinker content and for sample without limestone is 6.0%. The SO_3/Al_2O_3 decreases from 0.99 for cement without limestone to 0.90 to cement with 10% of limestone addition (Fig. 5.41).

For the samples without limestone addition when the amount of gypsum is lower or higher than optimum gypsum the compressive strength decreases significantly and with limestone addition the effect is less pronounced. Therefore with limestone addition the system is less sensitive to changes in gypsum content.

At 28 days the optimum gypsum is the same for samples with low C_3A clinker cement (Fig. 5.38). The highest compressive strength at 28 days for high C_3A clinker shows sample with 9.0% of gypsum addition (Fig. 5.40).

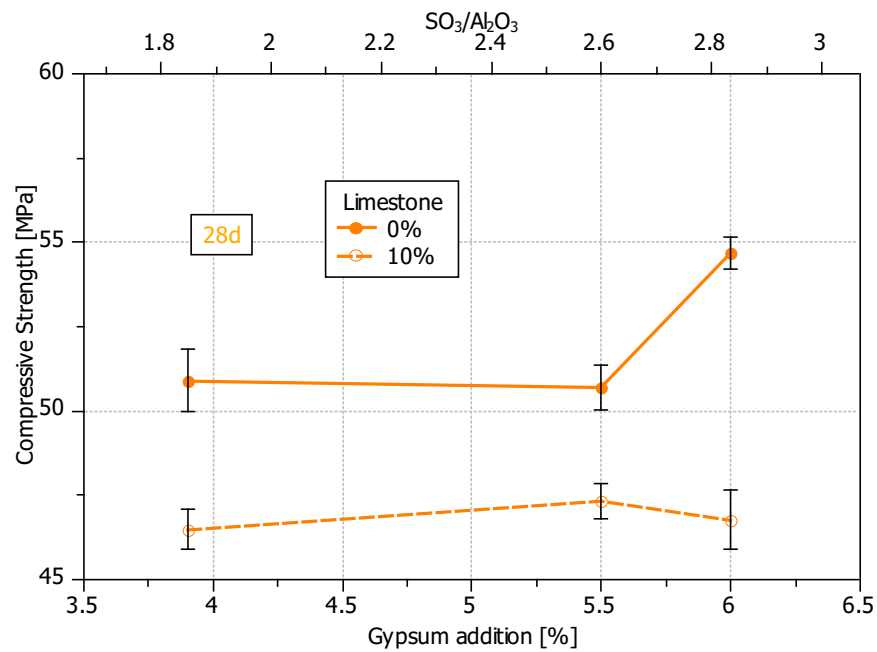


Figure 5.38: Compressive Strength of mortars at 28 days of hydration. Clinker with low (3%) C₃A content with 0 and 10% limestone addition.

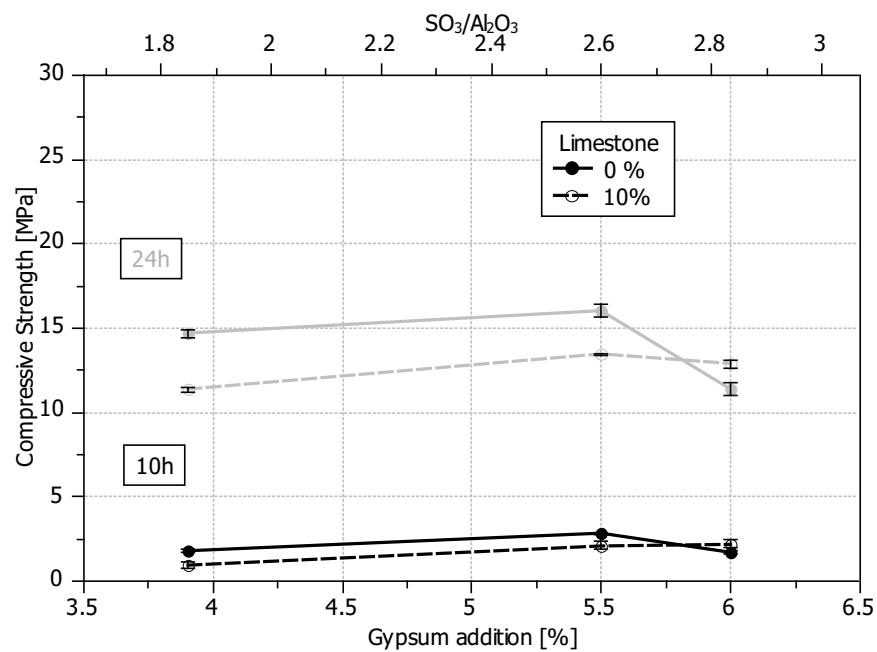


Figure 5.39: Compressive Strength of mortars at 10 and 24 hours of hydration. Clinker with low (3%) C₃A content, with 0 and 10% limestone addition.

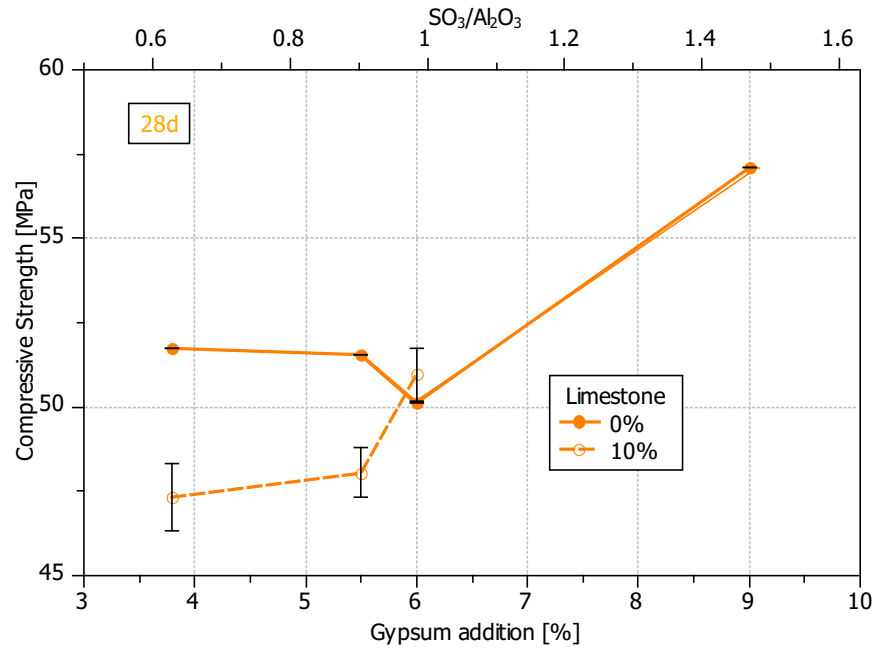


Figure 5.40: Compressive Strength of mortars at 28 days of hydration. Clinker with high (8%) C₃A content with 0 and 10% of limestone addition.

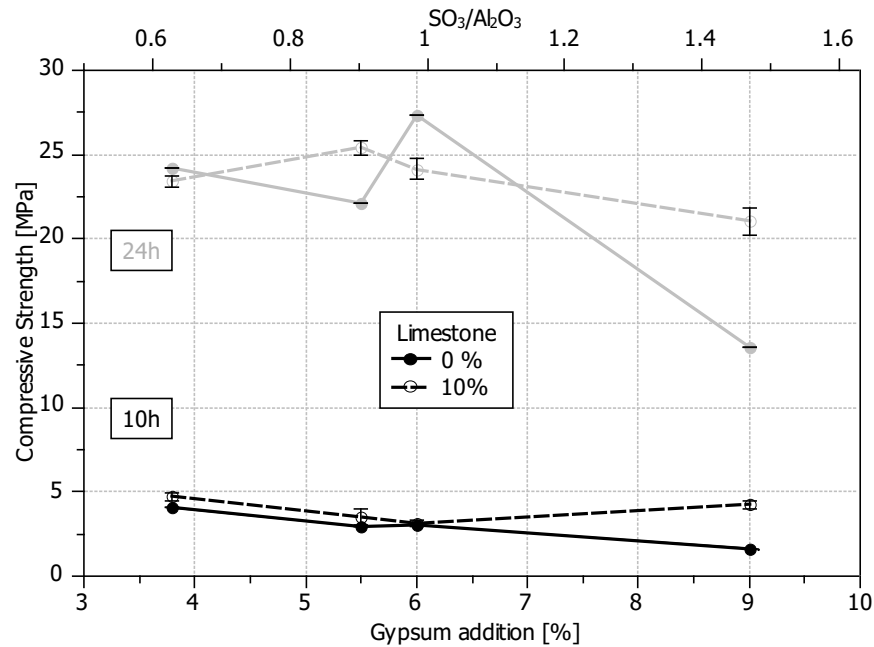


Figure 5.41: Compressive Strength of mortars at 10 and 24 hours of hydration. Clinker with high (8%) C₃A content with 0 and 10% of limestone addition.

5.3.2 Influence of Limestone on the kinetics

With 10% of limestone addition there is no acceleration with gypsum addition. For both clinker types and all gypsum additions the acceleration period is the same (Figs 5.42, 5.43). Again the systems appear less sensitive to the gypsum addition, as was observed for compressive strength. With gypsum addition the shift of the aluminate peaks occurs, up to the highest gypsum addition 9.0% where no aluminate peaks occurs in the period of main reaction. At the highest levels of gypsum addition the C_3S reaction is suppressed and this is more pronounced in the cements with low C_3A clinker in comparison to high C_3A clinker.

The comparison of the calorimetry curve for each gypsum addition with and without limestone addition shows that in general limestone accelerates the hydration reaction (regardless of the C_3A content) (Fig. 5.44). The effect of limestone is diminished with increasing levels of gypsum and with the highest gypsum addition the effect of limestone is very slight.

With gypsum addition the total heat evolved increases up to optimum gypsum and then decreases again. For the highest gypsum addition the total heat evolved is the lowest regardless of the C_3A content and limestone addition. With 10% of limestone total heat evolved relative to clinker content additionally increases for each gypsum addition for low and high C_3A clinker (Figs 5.45 – 5.46).

When limestone is added to the system. The comparison of samples without and with 10% of limestone for particular gypsum addition shows that limestone addition also shortens the induction period for all gypsum additions (Fig. 5.44) and the height of the silicate peak each time is slightly higher for the sample with 10% of limestone addition.

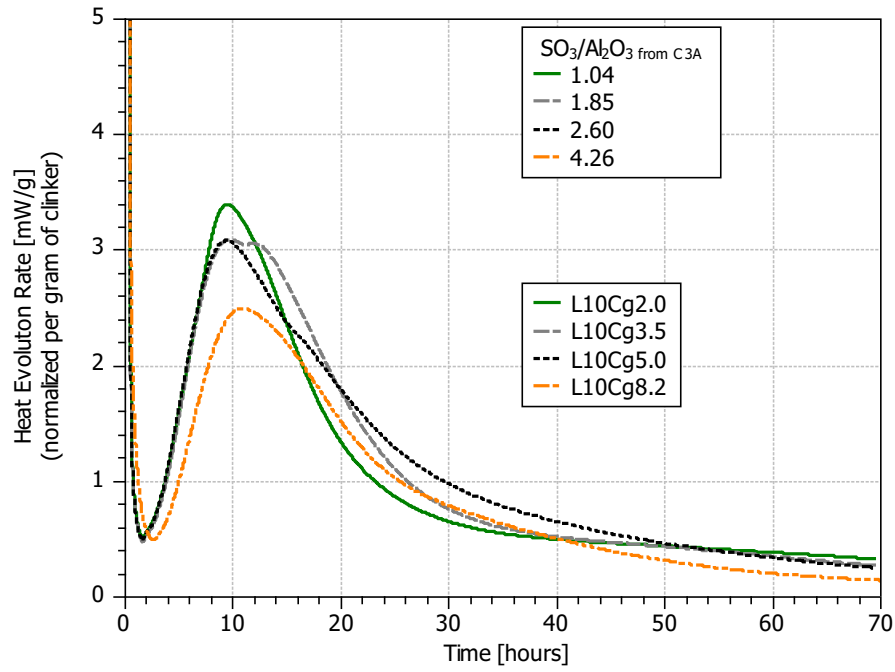


Figure 5.42: Isothermal Calorimetry data – Heat Evolution Rate. Clinker with low (3%) C₃A content and with 10% of limestone addition.

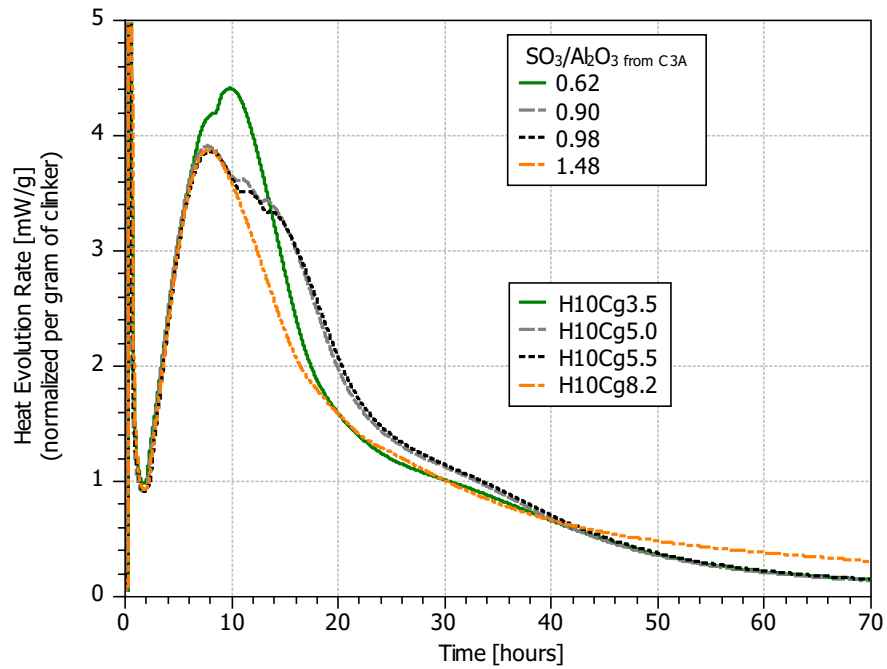


Figure 5.43: Isothermal Calorimetry data – Heat Evolution Rate. Clinker with high (8%) C₃A content and with 10% of limestone addition.

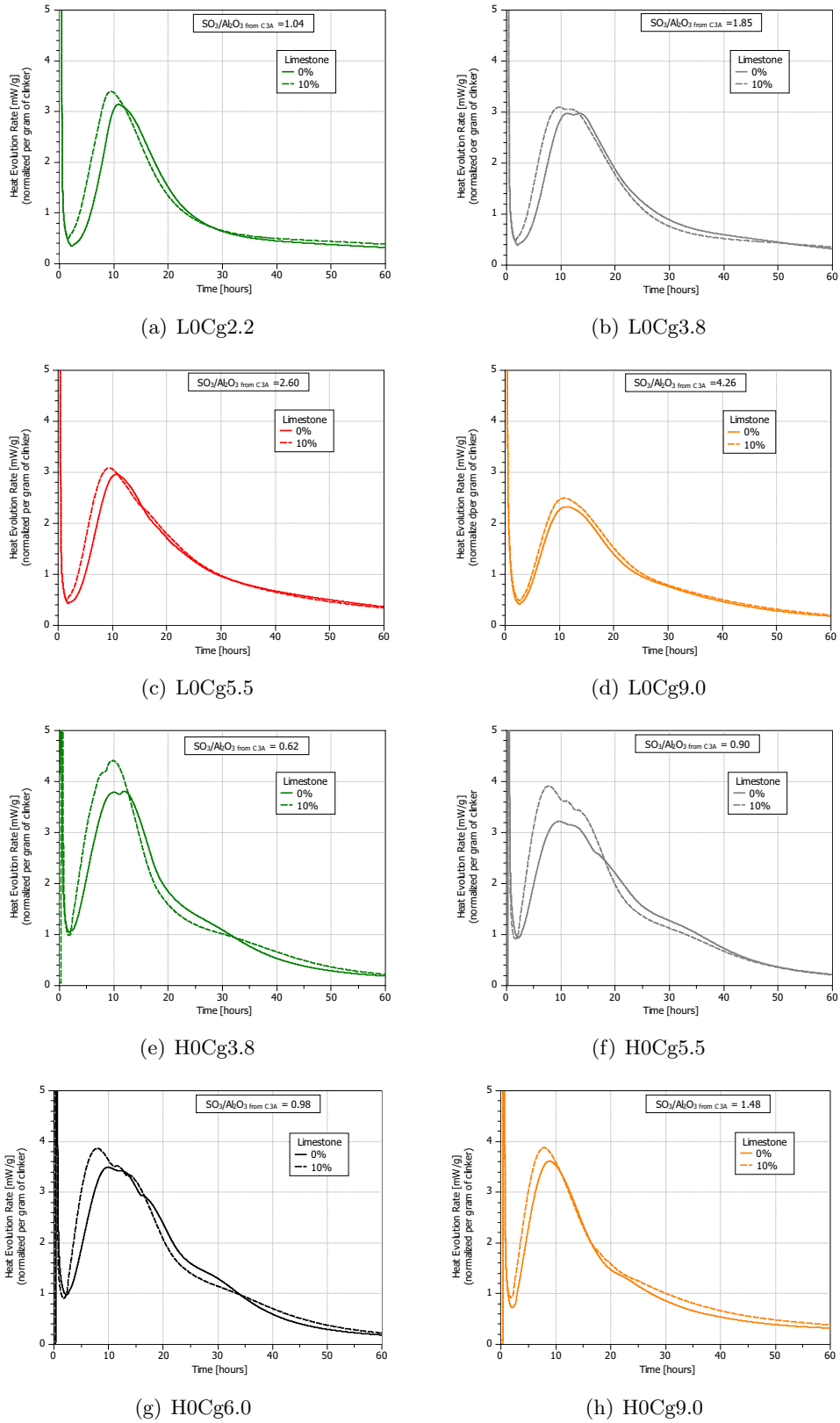


Figure 5.44: Isothermal Calorimetry data for samples with low and high C_3A clinker, 0 and 10% of limestone addition and increasing gypsum content.

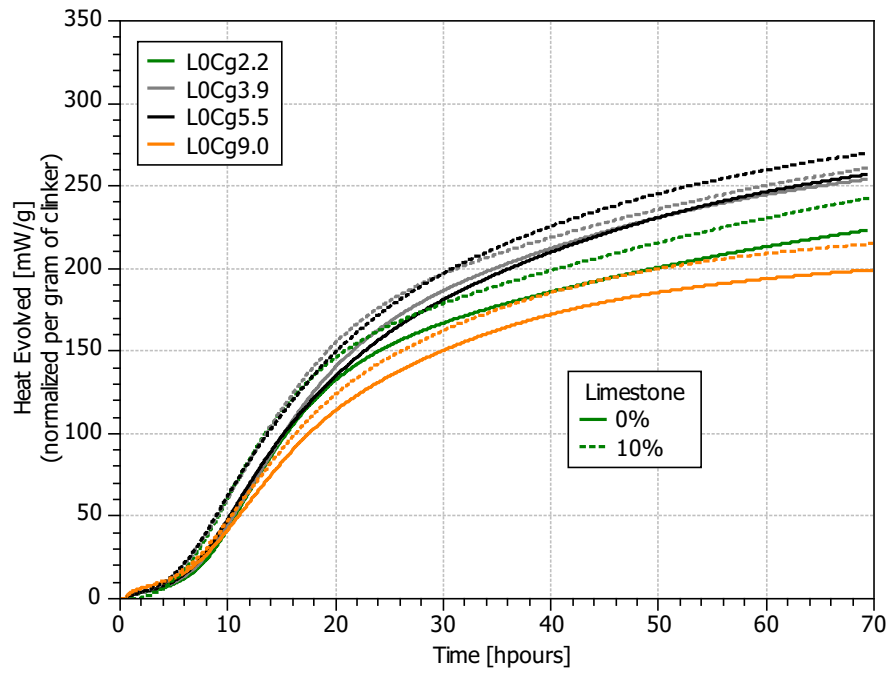


Figure 5.45: Isothermal Calorimetry data – Cumulative Curve. Clinker with low (3%) C₃A content with increasing gypsum content and with 0 and 10% of limestone addition.

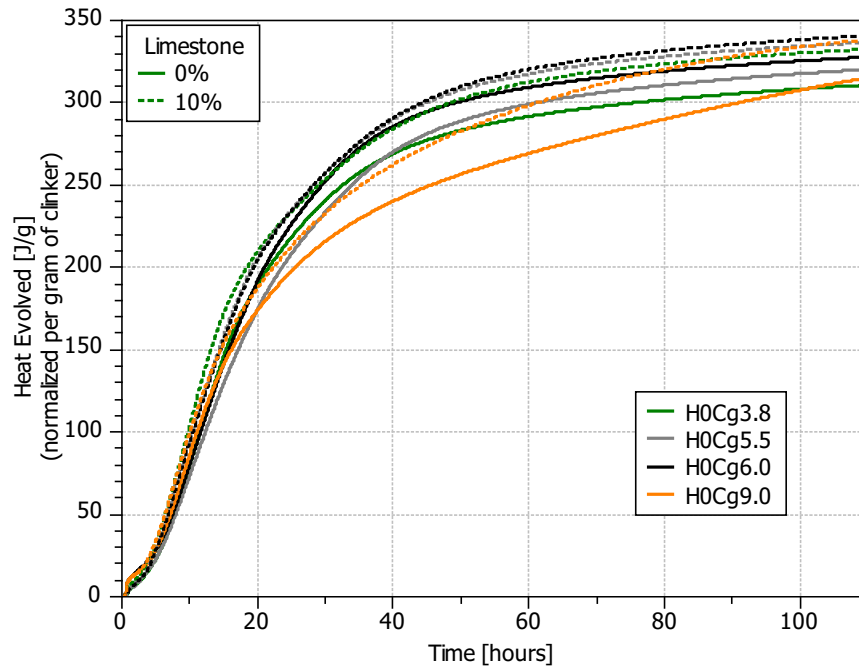


Figure 5.46: Isothermal Calorimetry data – Cumulative. Clinker with high (8%) C₃A content with increasing gypsum content and with 0 and 10% of limestone addition.

5.3.3 Influence of limestone on the phase assemblage

Limestone addition slightly increases C_3A consumption for high C_3A clinker cements at each gypsum addition (Annex Figs F.4, F.5, F.6). For low C_3A clinker cement, 10% of limestone addition only slightly increases the hydration at 5.5% of gypsum addition (Annex Fig. F.2).

When limestone is in the system no monosulfoaluminate (Ms) was observed. With limestone addition there is formation of hemi- and monocarboaluminate which depends on the C_3A and gypsum content (Figs 5.47, 5.48). With gypsum addition, regardless of the C_3A content the formation of monocarboaluminate (Mc) is delayed and its amount decreases.

The C_3S consumption slightly increases with 10% of limestone addition for high C_3A clinker cement (Fig. F.10). In Figs 5.50, 5.50 % of C_3S hydrated at certain time in the function of gypsum addition is presented. Low C_3A clinker cement show that with gypsum addition C_3S hydration slightly decreases at 10 hours of hydration, increases up to 3.8% of gypsum and with higher gypsum amounts decreases, and slightly increases at 28 days of hydration (Fig. 5.50). 10% of limestone addition slightly increases C_3S consumption for low C_3A clinker cements, especially at 24 hours and 28 days of hydration.

High C_3A clinker cement show increase in C_3S hydration with gypsum addition at each time. Sample with 6.0% of gypsum and 0% of limestone shows slightly different trend at 10 hours of hydration, however this sample comes from different batch of cements (Fig. 5.50). Additionally 10% of limestone addition increases C_3S hydration at each time of hydration for high C_3A clinker cements (Fig. 5.50).

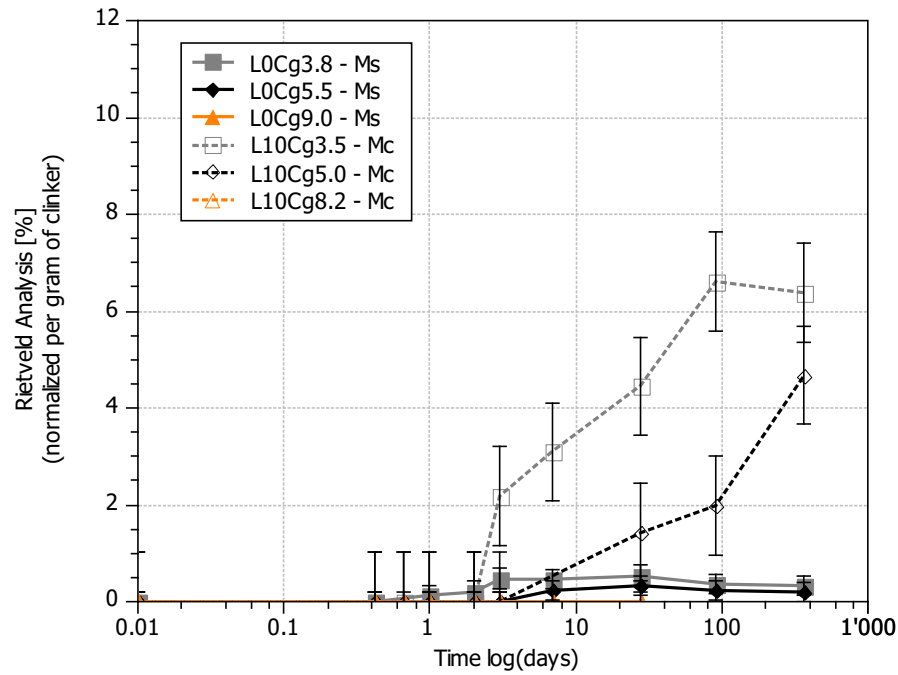


Figure 5.47: XRD Rietveld Analysis, monosulfate (Ms) and monocarboaluminate (Mc) quantification. Sample with low C_3A clinker cement, increasing gypsum addition, 0 and 10% of limestone addition.

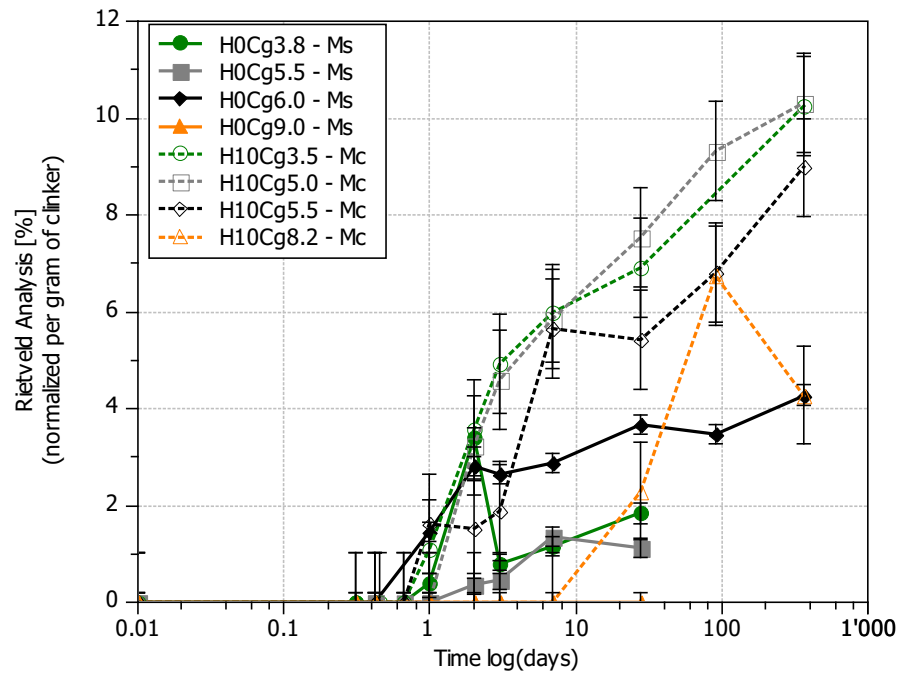


Figure 5.48: XRD Rietveld Analysis, monosulfate (Ms) and monocarboaluminate (Mc) quantification. Sample with high C_3A clinker cement, increasing gypsum addition, 0 and 10% of limestone addition.

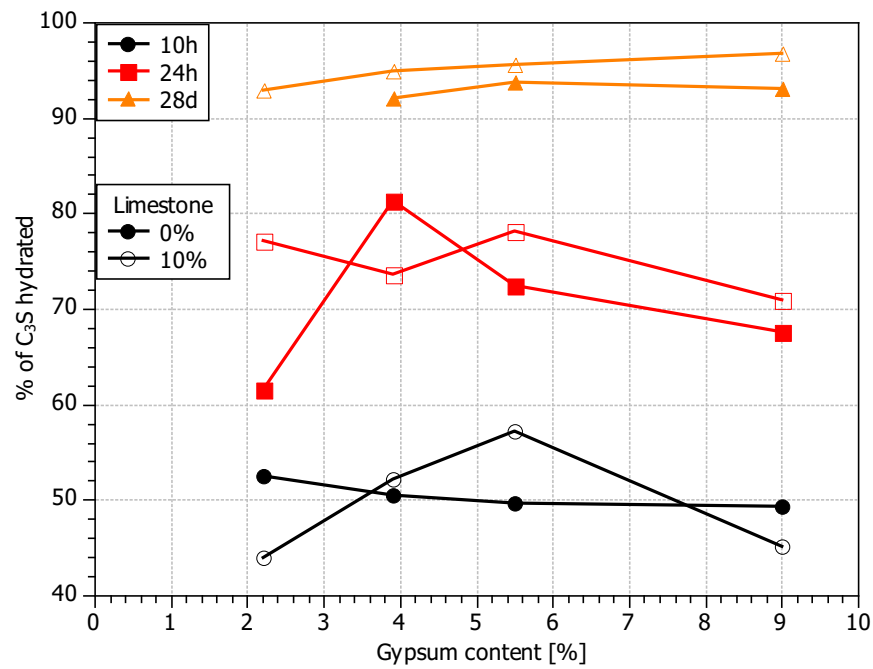


Figure 5.49: % of C_3S hydrated in function of gypsum addition. Low C_3A clinker cements with 0 and 10% of limestone.

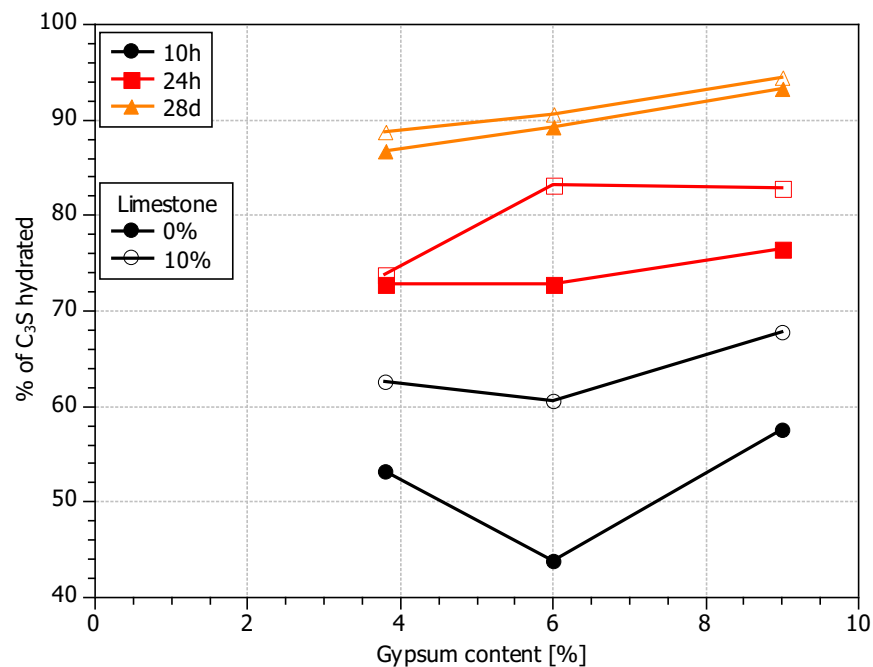


Figure 5.50: % of C_3S hydrated in function of gypsum addition. High C_3A clinker cements with 0 and 10% of limestone.

5.3.4 Influence of limestone on the porosity and microstructure development

In Figs 5.51 – 5.54 the MIP data at 10 and 24 hours of hydration for low and high C_3A clinker with 0 and 10% of limestone addition are presented. Even though limestone slightly increases C_3S and C_3A consumption, the formation of ettringite increases and additionally carboaluminate phases are formed the total porosity does not show a clear trend with limestone addition, only compensates presence of limestone. The porosity depends on the C_3A , gypsum content.

At 10 hours of hydration for low C_3A clinker cement with increasing gypsum addition limestone addition sometimes increases and sometimes decreases total porosity (Fig. 5.51). At 24 hours of hydration for low C_3A clinker cement 10% of limestone addition increases the total porosity.

For high C_3A clinker at 10 and 24 hours of hydration the total porosity decreases with 10% of limestone addition, only for sample with 6.0% the total porosity at both times is higher with limestone addition (Figs 5.53, 5.54).

In general, with 10% of limestone addition the differences in porosity are less pronounced and low and high C_3A clinker systems are less sensitive to the changes in gypsum addition.

Similar results can be observed by SEM. The differences in the formation of C–S–H shells around cement grains with gypsum addition are less pronounced when 10% of limestone addition is in the system (Figs 5.55, 5.56).

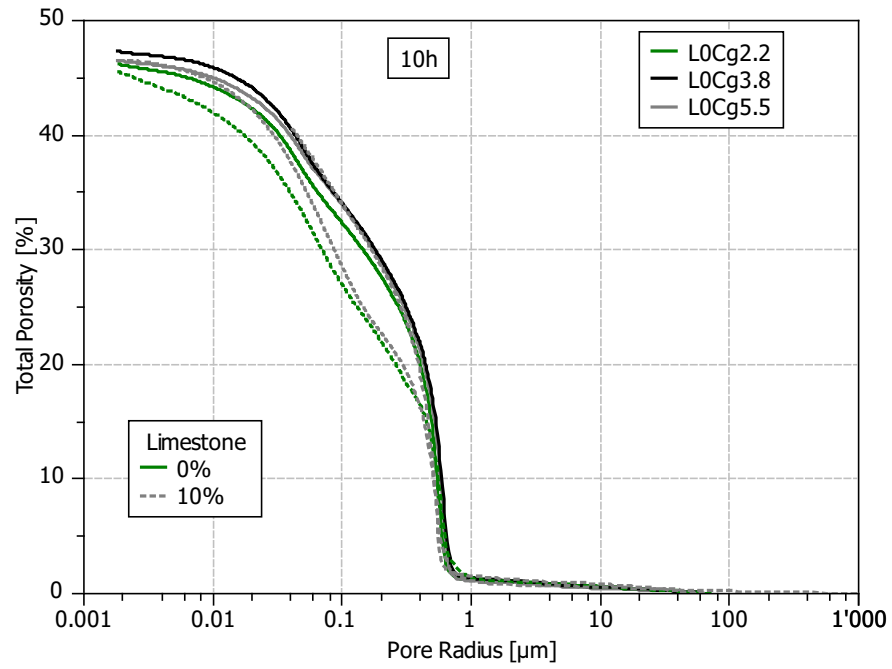


Figure 5.51: MIP data at 10 hours of hydration. Sample with low C_3A clinker cement, increasing gypsum addition, 0 and 10% of limestone addition.

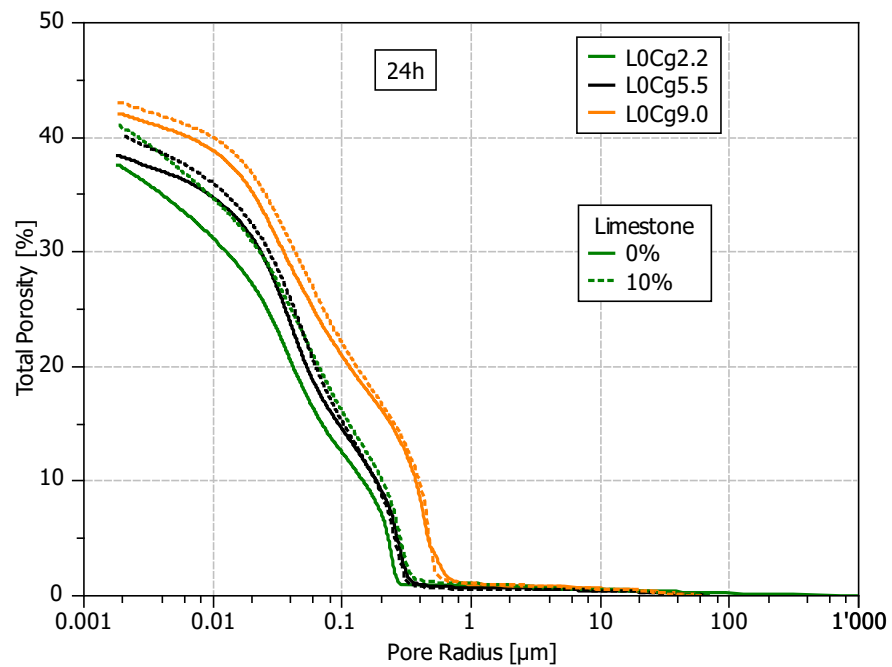


Figure 5.52: MIP data at 24 hours of hydration. Sample with low C_3A clinker cement, increasing gypsum addition, 0 and 10% of limestone addition.

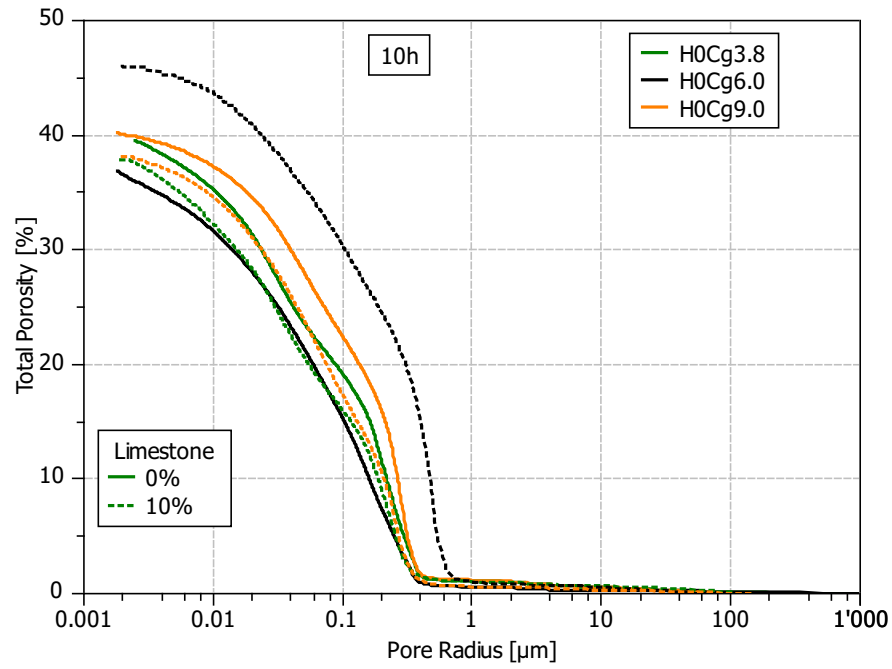


Figure 5.53: MIP data at 10 hours of hydration. Sample with high C_3A clinker cement, increasing gypsum addition, 0 and 10% of limestone addition.

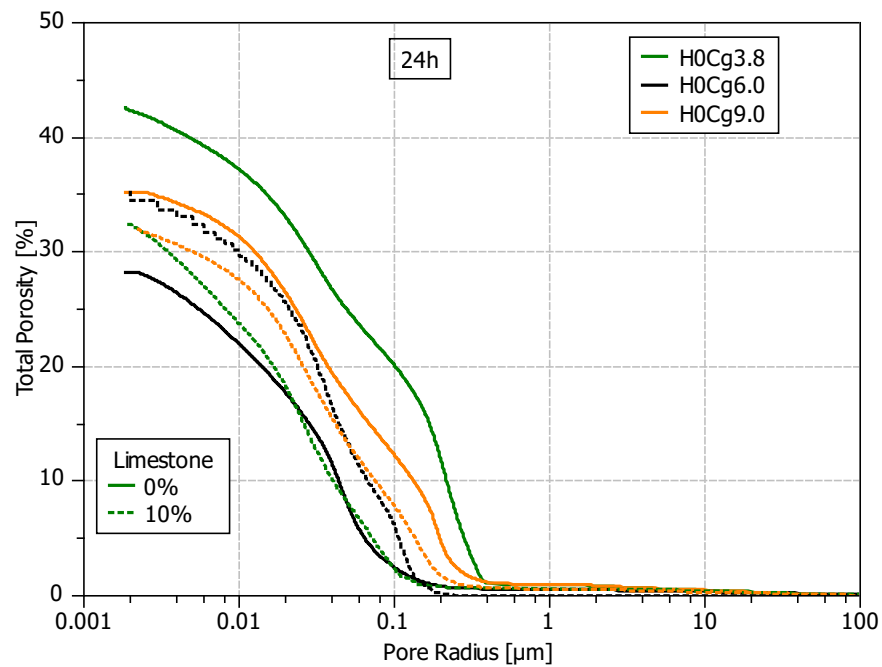


Figure 5.54: MIP data at 24 hours of hydration. Sample with high C_3A clinker cement, increasing gypsum addition, 0 and 10% of limestone addition.

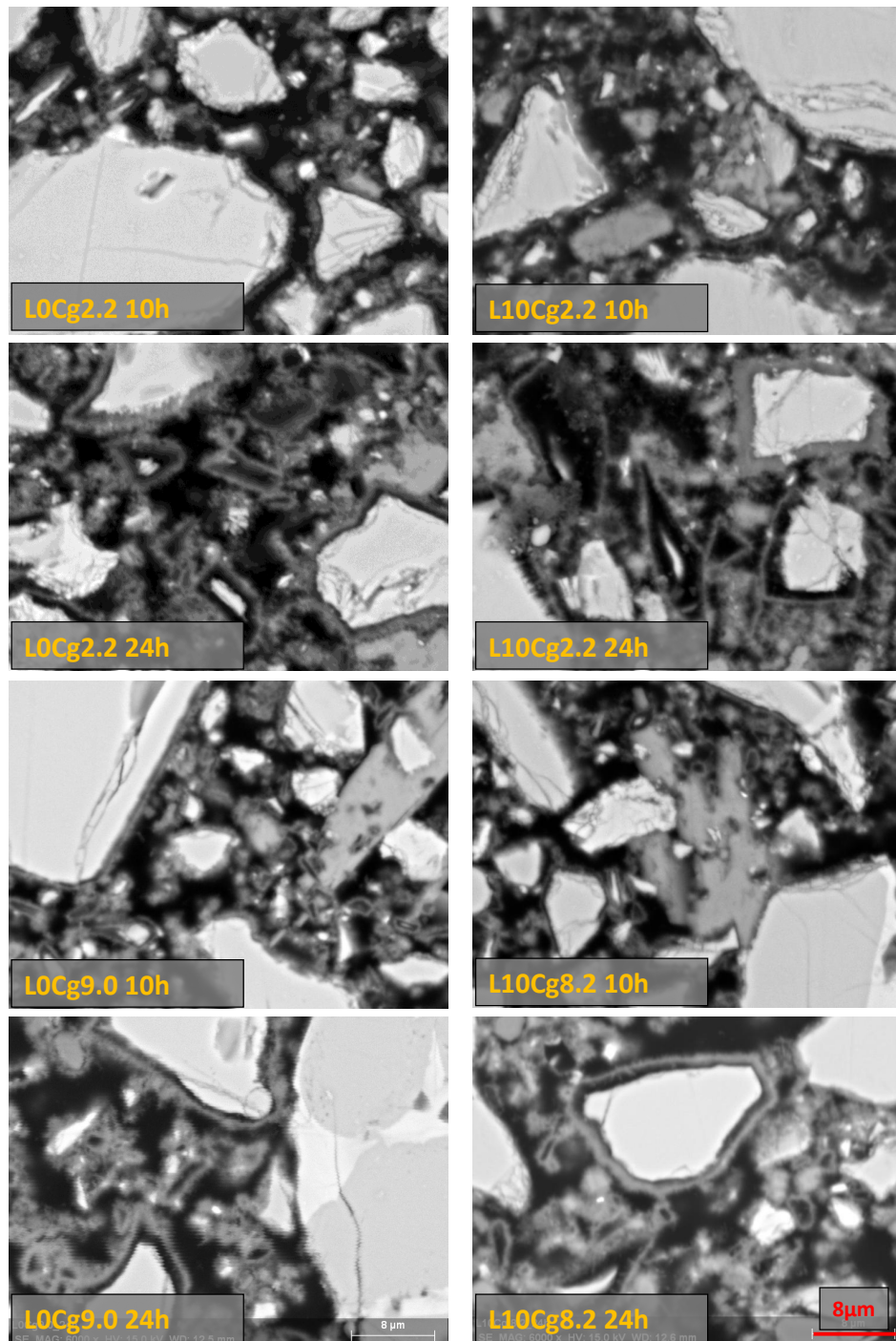


Figure 5.55: Scanning Electron Microscopy at 10 and 24 hours of hydration for samples with low C_3A clinker, increasing gypsum addition, 0 and 10% of limestone addition. Magnification=6000x, HV=15kV, WD=12.5mm.

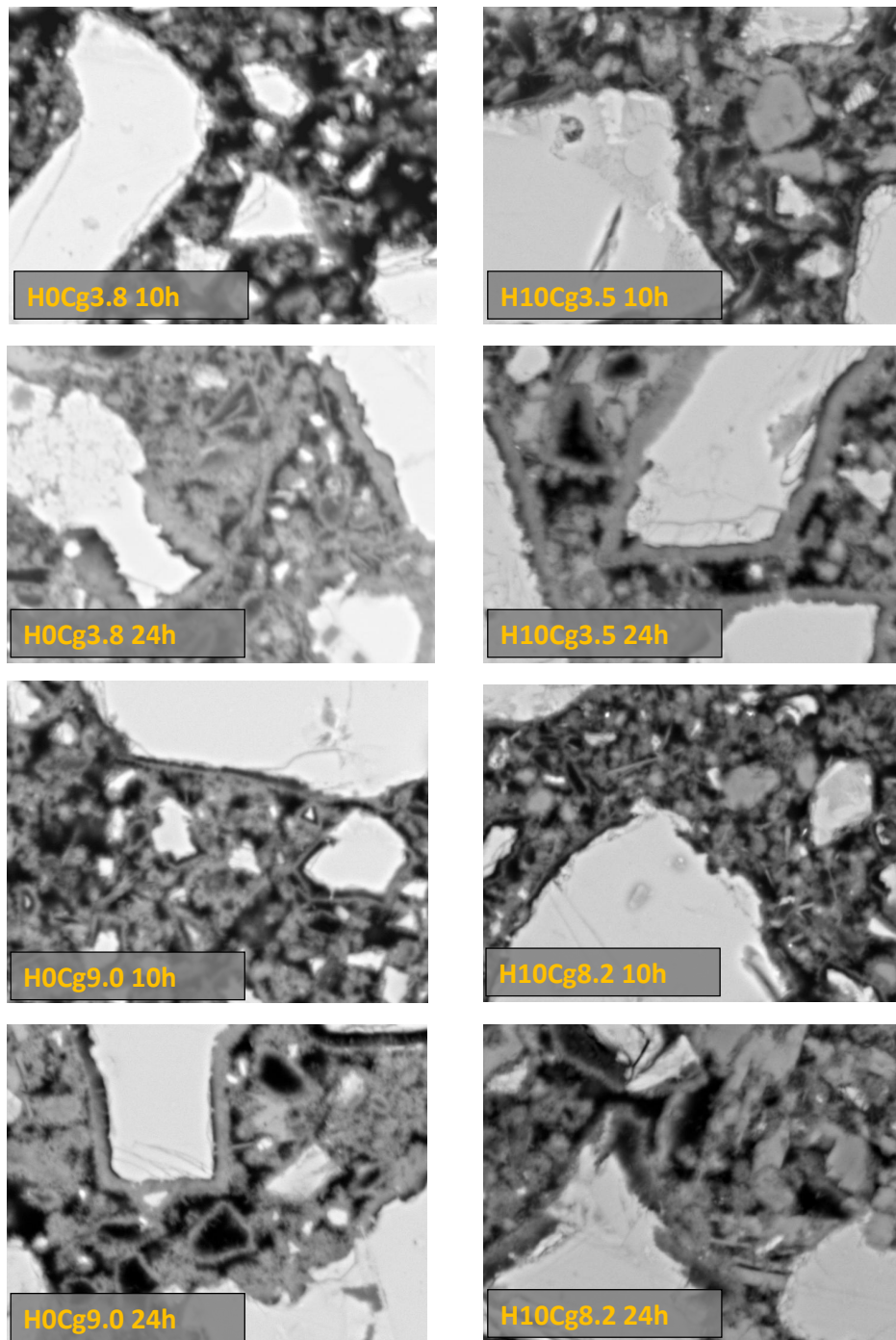


Figure 5.56: Scanning Electron Microscopy at 10 and 24 hours of hydration for samples with high C_3A clinker, increasing gypsum addition, 0 and 10% of limestone addition. Magnification=6000x, HV=15kV, WD=12.5mm.

5.4 GEMS vs XRD, aluminium gypsum and calcium uptake into C-S-H

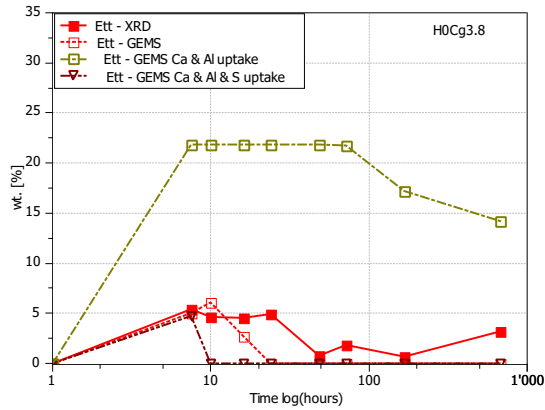
In this part the GEMS calculations were done. As an input to GEMS calculations, the degree of hydration of clinker phases at each time of hydration measured by XRD Rietveld analysis was used. Formation of phases by XRD Rietveld analysis and GEMS calculation was compared.

In the previous chapter [Chapter 4.1](#) it was shown that the Ca/Si ratio of the C-S-H should be fixed from EDS measurement. Also there is an uptake of a certain amount of aluminum into C-S-H. The XRD Rietveld analysis data were found to be in agreement with GEMS prediction when Al/Si ratio obtained by SEM EDS analysis was fixed in the C-S-H. In the end there was good agreement between XRD and GEMS calculations for monocarboaluminate formation especially for high C₃A clinker systems.

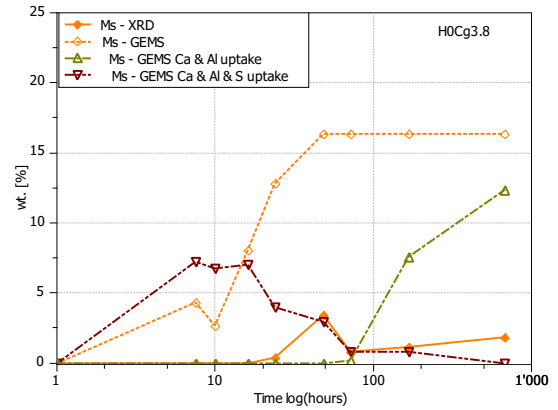
In present section GEMS calculations were done with three different approaches. First approach was to predict phase formation inputting clinker phases hydration from XRD Rietveld analysis and comparison of both. As it was expected phase formation predicted by GEMS was different from XRD Rietveld analysis measurement. Therefore the second approach and Ca and Al uptake into C-S-H was included in the GEMS calculations. In the third approach, additionally beside Ca and Al also S uptake into C-S-H was included. Ratios of C-S-H composition for each sample were determined experimentally by SEM EDS analysis. The results of comparison between XRD Rietveld analysis, GEMS calculations are presented in the [Fig. 5.57](#) – systems without limestone and [Fig. 5.58](#) – systems with 10% of limestone.

For high C₃A system without limestone addition, aluminate and sulfate uptake into C-S-H influences ettringite and monosulfate formation. When aluminate uptake is included ettringite formation increases significantly for sample with low gypsum content ([Fig. 5.57 a](#)) and slightly for sample with optimum and high gypsum content ([Fig. 5.57 c, e](#)). This is because the S/Al ratio increases so there is more ettringite rather than monosulfate ([Fig. 5.57 b, d, f](#)).

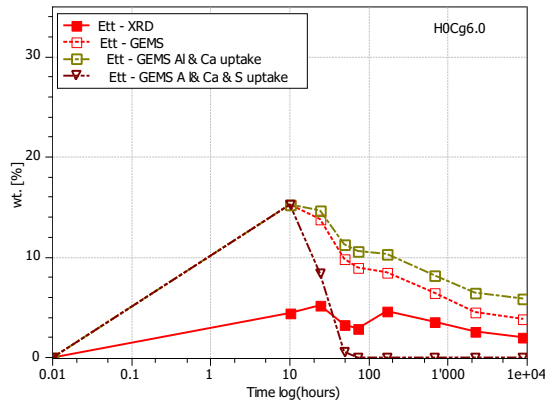
When the sulfate uptake is also included, ettringite formation significantly decreases for all gypsum additions ([Fig. 5.57 a, c, e](#)). The S/Al ratios decrease and overall there is less Al to form ettringite and monosulfate. Monosulfate formation however increases for the highest gypsum addition ([Fig. 5.57 f](#)), slightly increases and later decreases for optimum gypsum sample ([Fig. 5.57 d](#)), and decreases for low gypsum sample ([Fig. 5.57 b](#)).



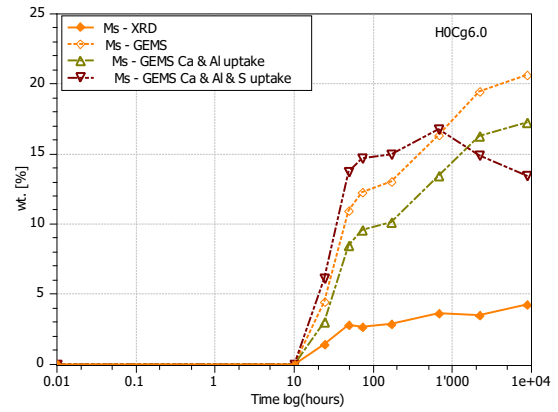
(a) H0Cg3.8 – Ettringite quantification.



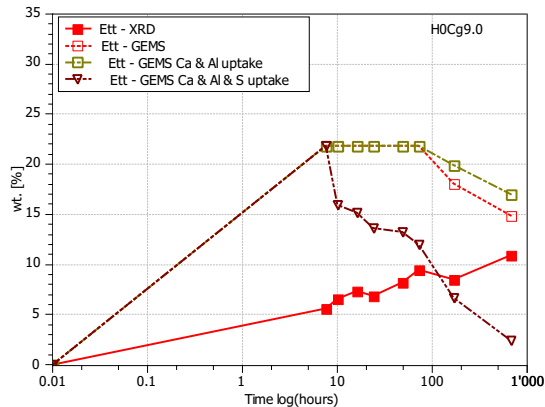
(b) H0Cg3.8 – Monosulfate quantification.



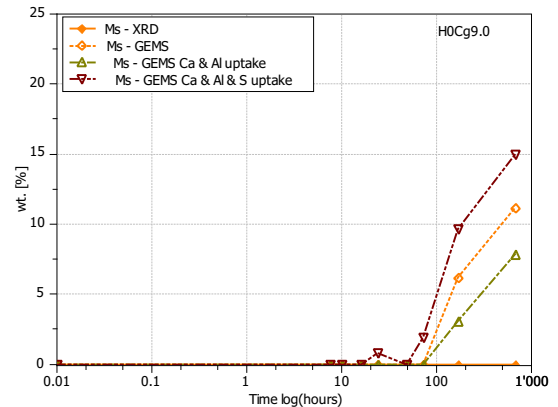
(c) H0Cg6.0 – Ettringite quantification.



(d) H0Cg6.0 – Monosulfate quantification.

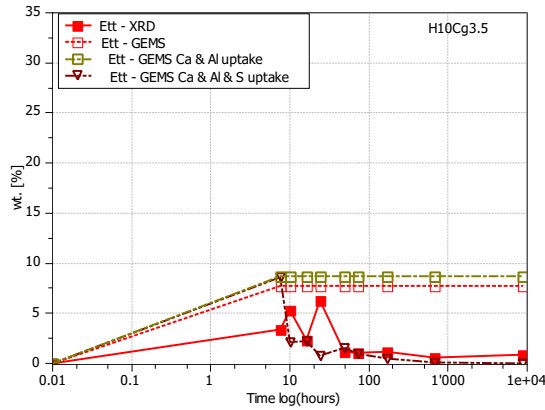


(e) H0Cg9.0 – Ettringite quantification.

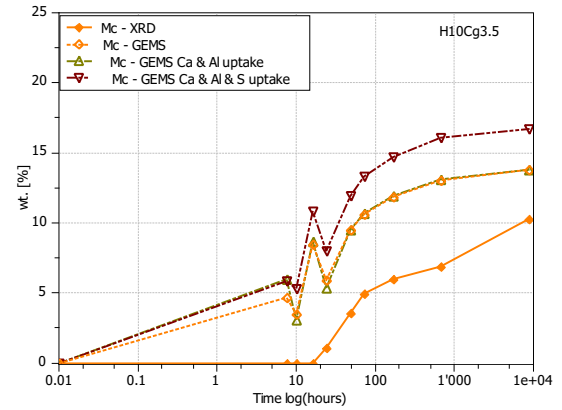


(f) H0Cg9.0 – Monosulfate quantification.

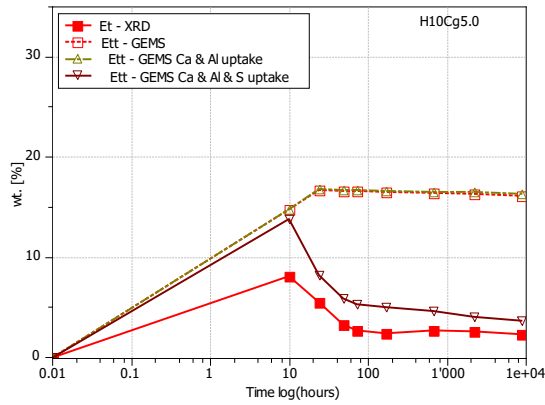
 Figure 5.57: Comparison of XRD Rietveld analysis and GEMS calculation of ettringite and monosulfate. Systems with high C₃A clinker, 0% of limestone and increasing gypsum content.



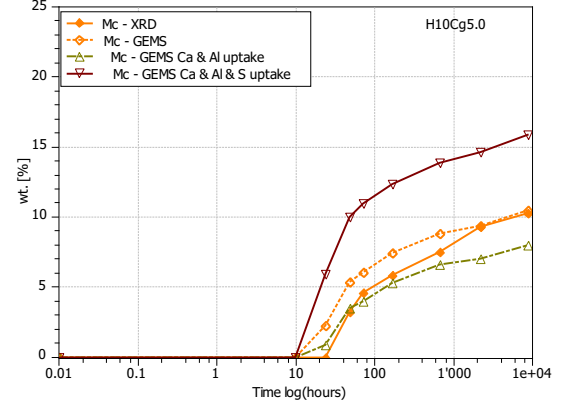
(a) H10Cg3.5 – Ettringite quantification.



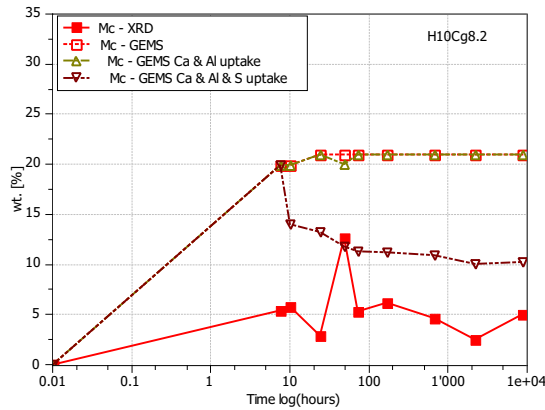
(b) H10Cg3.5 – Monocarboaluminate quantification.



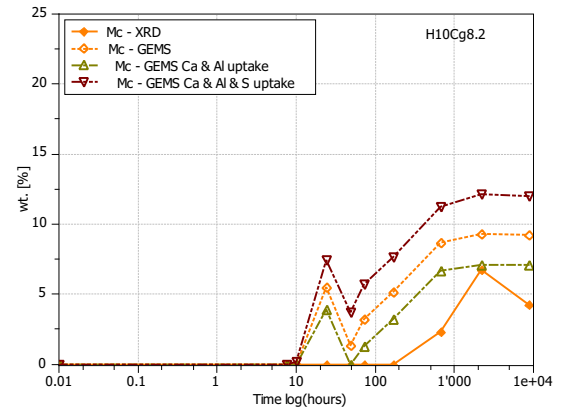
(c) H10Cg5.0 – Ettringite quantification.



(d) H10Cg5.0 – Monocarboaluminate quantification.



(e) H10Cg8.2 – Ettringite quantification.



(f) H10Cg8.2 – Monocarboaluminate quantification.

Figure 5.58: Comparison of XRD Rietveld analysis and GEMS calculation of ettringite and monocarboaluminate. Systems with high C_3A clinker, 10% of limestone and increasing gypsum content.

In the limestone cement systems ettringite and monocarboaluminate are influenced by aluminate and sulfate uptake. Aluminate uptake does not influence ettringite formation (Fig. 5.58 a, c, d). Lack of alumina however influences monocarboaluminate formation especially at optimum gypsum (Fig. 5.58 d) and with the highest gypsum addition (Fig. 5.58 f). Its formation is significantly lower when aluminate uptake is included. The low gypsum addition sample shows only slight changes in monocarboaluminate formation at early age, later the formation is similar due to small gypsum amount and still high aluminate content to produce monocarboaluminate (Fig. 5.58 b).

When sulfate uptake is also included in samples with limestone addition ettringite is significantly influenced and its formation significantly decreases (Fig. 5.58 a, c, e) and in the same time monocarboaluminate formation increases due to more alumina available for its formation (Fig. 5.58 b, d, f). When aluminate and sulfate uptake is included into GEMS calculations ettringite formation prediction is closer to XRD Rietveld analysis data.

5.5 Summary

In this chapter influence of gypsum on the cement hydration and properties, with different C_3A content and limestone addition were investigated. The following conclusion can be drawn:

Alite system

- Studies of alite – gypsum – limestone system shows that gypsum has a direct influence on the alite hydration. With gypsum addition there is more C_3S consumed more C–S–H formed and more water combined but less portlandite formed what suggests that C–S–H formed has a different ratio between Si, Ca and H_2O

Influence of gypsum

- There is an optimum gypsum (the amount of gypsum at which the compressive strength at 24 hours is the highest) below and above which the compressive strength is significantly lower
- Optimum gypsum depends on the cement composition, and increases slightly increase with C_3A content and decreases with limestone addition
- Low C_3A systems are less sensitive on the overdosing of gypsum content and more

sensitive on to underdosing of gypsum content

- High C_3A systems are more sensitive on the overdosing the gypsum amount and less sensitive on to underdosing
- Gypsum has a direct influence on the kinetics of the hydration reaction:
 - acceleration in accelerating period up to optimum gypsum later decelerations
 - delay of aluminate reaction
- With gypsum addition there is more ettringite formed, while C_3A consumption is similar at each gypsum addition up to optimum
- There are only slight changes in C_3S hydration with gypsum addition
- Total porosity and threshold values does not show clear relationship with gypsum addition, it depends more on the cement composition and limestone addition and time of the hydration
- C–S–H composition is different than used in GEMS model, there is an aluminum and sulfate uptake into C–S–H
- There is no clear correlation between total porosity and compressive strength

Influence of limestone on gypsum

- With 10% of limestone addition the optimum gypsum decreases slightly depending on the C_3A content.
- With 10% of limestone addition the systems are less sensitive to changes in gypsum amount:
 - the compressive strength show smaller loss from optimum gypsum regardless to clinker composition
 - the acceleration period on the calorimetry curve is the same for each gypsum addition up to optimum, regardless to clinker composition. For very high gypsum addition the suppression of the reaction is also visible
- 10% of limestone addition increases acceleration period at each gypsum addition

- 10% of limestone addition increases total heat evolved at each gypsum addition
- With 10% of limestone addition the formation of ettringite increases at each gypsum addition
- With 10% of limestone addition the C_3A consumption changes and it depends on the gypsum content and clinker composition
- With 10% of limestone addition Mc is formed at each gypsum addition instead of Ms, and Mc formation increases with gypsum addition
- C_3S consumption increases with limestone addition at each gypsum addition
- 10% of limestone addition decreases total porosity, however it depends on the cement composition

Chapter 6

Influence of the temperature on hydration and properties of PC and limestone cement

The curing temperature has an important influence on the strength of mortars and concrete. In the laboratory most tests are performed at ambient temperature 20–25°C, while the conditions in the field are often below or above this temperature and moreover with temperature differences between day and night. Therefore it is useful to understand the behavior of cementitious materials during hydration at different temperatures.

It is widely accepted that concrete exposed to high temperatures during early age hydration has increased early strength and decreased later strength [25]. With temperature the initial hydration is accelerated which causes more rapid precipitation of hydration products during the first hours of hydration [25] and increase in strength. The increased hydration rate leads to higher density C–S–H [97]. With decreasing temperature the hydration slows down, and a less dense C–S–H is formed, so there is lower coarse porosity in the cement matrix [24] [42].

In this section the influence of temperature on the hydration of cement with different C_3A , gypsum and 0, 10% of limestone will be discussed. The hydration kinetics, phases assemblage, porosity and mechanical properties, at different temperatures will be presented.

6.1 Influence of the temperature on the kinetics

With increasing temperature the reaction kinetics increase. In Figs 6.1 – 6.6 the isothermal calorimetry data for low C_3A clinker with different gypsum addition and without 0 and 10% of limestone are presented, and on the Figs 6.7 – 6.12 the data for high C_3A clinker with different gypsum content and with 0 and 10% of limestone addition are presented.

The hydration is accelerated with temperature regardless of the C_3A content, gypsum addition and limestone addition. The acceleration at 30°C in comparison to 20° is visible at early ages. On the cumulative curve the total heat starts to be the same for samples at 20 and 30 °C around 70 hours for low C_3A clinker and around 50 hours for high C_3A clinker, with the small variation depending on the gypsum content.

The hydration at 10°C is slowed down in comparison to 20°C and on the cumulative curve for 10 ° the total heat evolved reaches the same value as 20° around 250 hours (~10days) for low C_3A clinker and around 150 hours for high C_3A clinker. Only samples with the highest gypsum addition 9.0% and high C_3A content show no common point for 10 and 20°C on cumulative curve, 20 and 30°C show similar trend and common point on the cumulative curve at 100 hours (Fig. 6.12).

Limestone addition accelerates the hydration reaction at each temperature regardless of C_3A content and gypsum content. For high C_3A clinker the total heat evolved is higher at each temperature with 10% of limestone addition, up to 6.0% of gypsum addition. For 9% of gypsum addition this effect is less pronounced because of high gypsum addition and higher influence of gypsum addition on the hydration.

For low C_3A clinker limestone addition increases the length of acceleration period at each temperature up to 6.0% of gypsum addition. The total heat evolved is not always higher with limestone addition and in the low C_3A clinker it depends on the temperature and gypsum content in the sample.

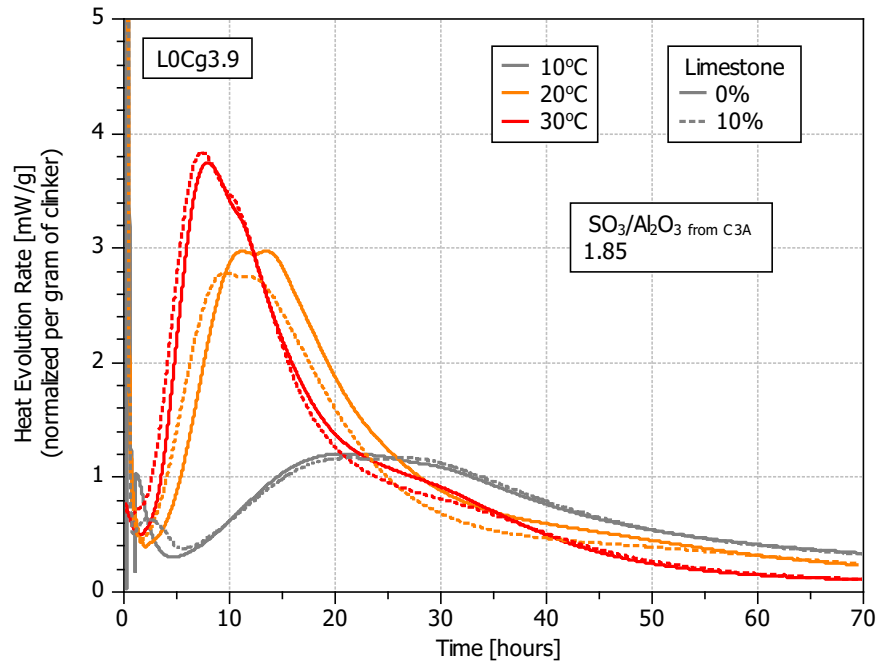


Figure 6.1: Isothermal Calorimetry Data at different temperatures. Sample with low C_3A content, 3.8% of gypsum 0, 10% of limestone addition.

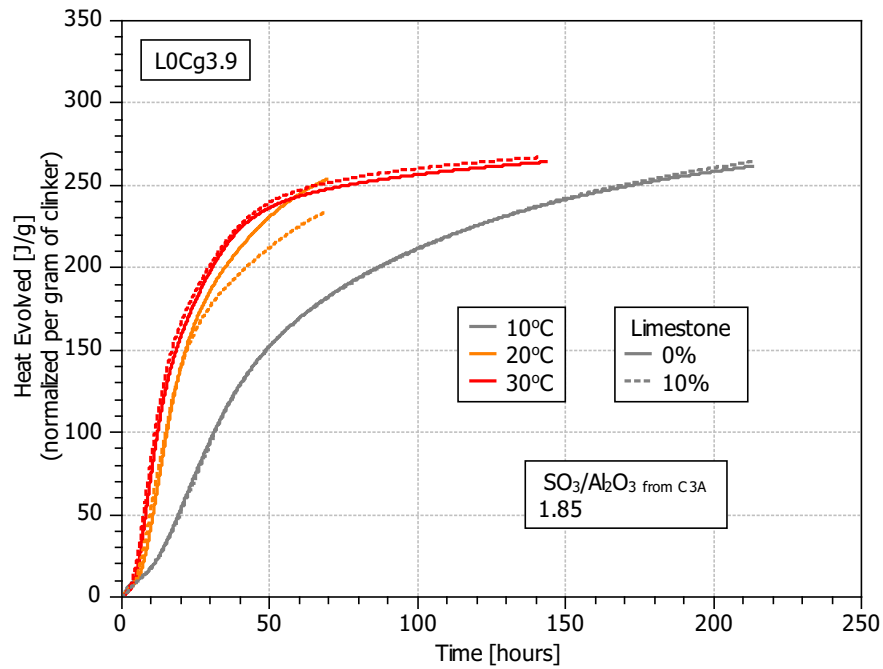


Figure 6.2: Isothermal Calorimetry Data at different temperatures. Cumulative curve. Sample with low C_3A content, 3.8% of gypsum, 0, 10% of limestone addition.

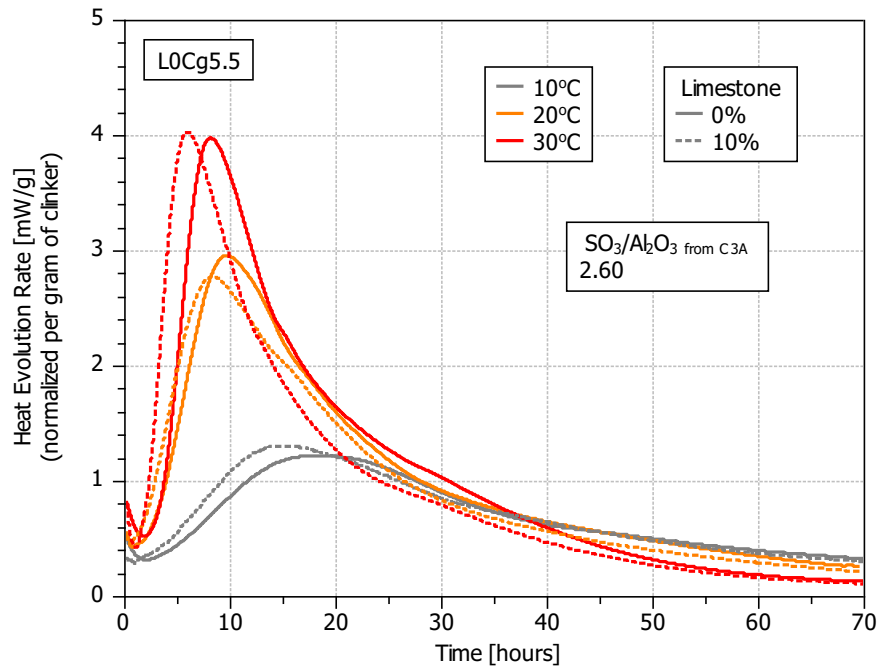


Figure 6.3: Isothermal Calorimetry Data at different temperatures. Sample with low C_3A content, 5.5% of gypsum, 0, 10% of limestone addition.

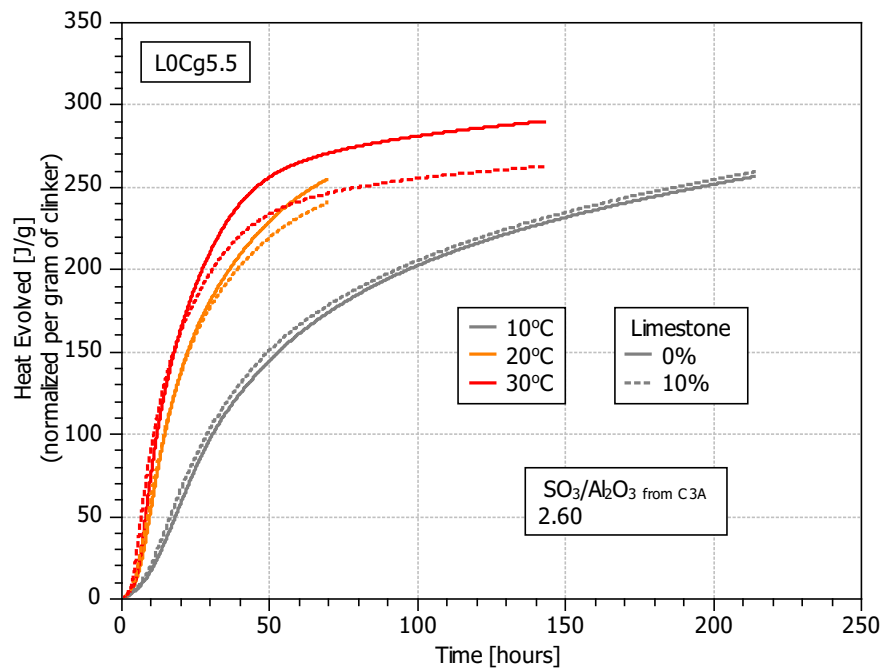


Figure 6.4: Isothermal Calorimetry Data at different temperatures. Cumulative curve. Sample with low C_3A content, 5.5% of gypsum, 0, 10% of limestone addition.

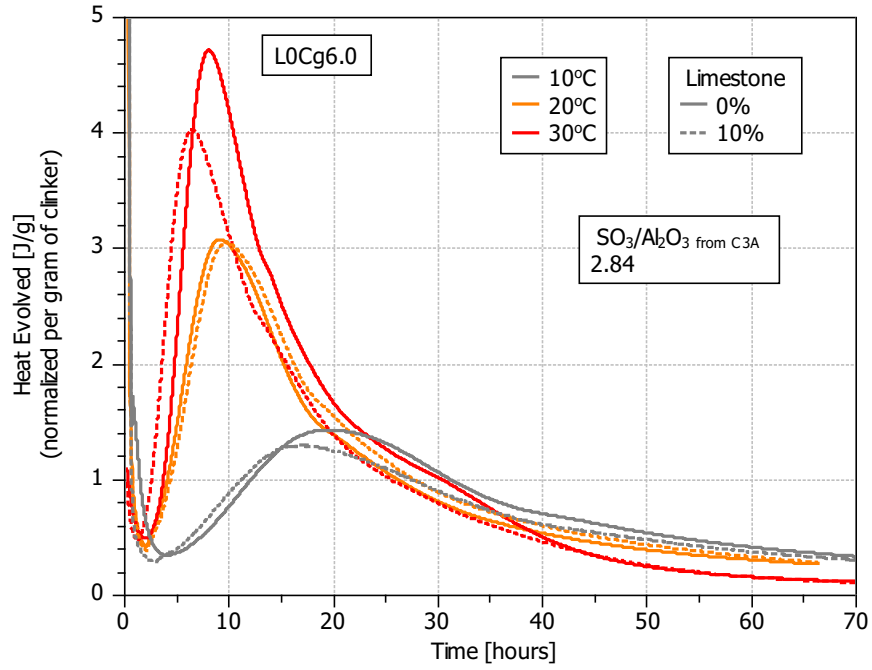


Figure 6.5: Isothermal Calorimetry Data at different temperatures. Sample with low C₃A content, 6.0% of gypsum, 0, 10% of limestone addition.

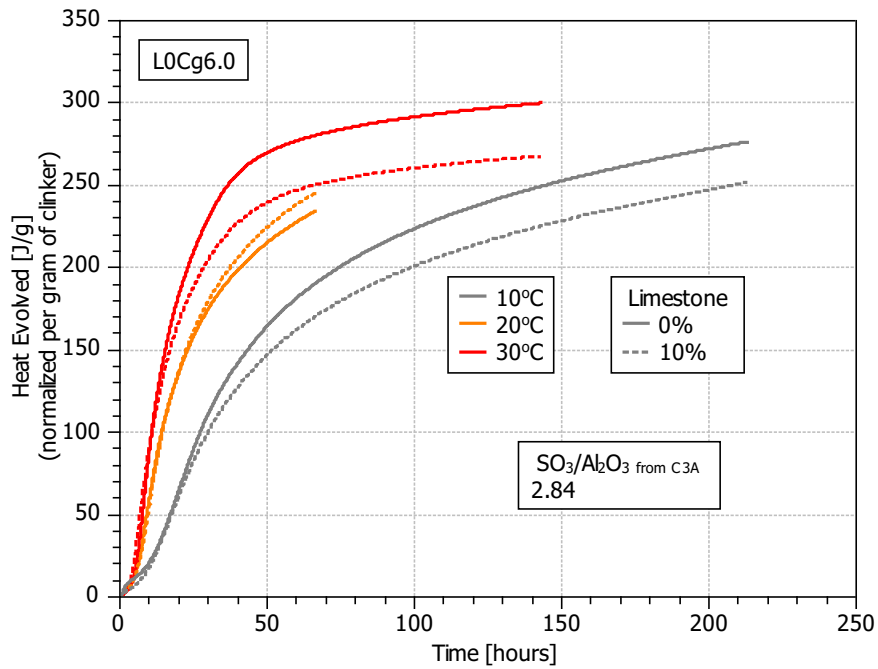


Figure 6.6: Isothermal Calorimetry Data at different temperatures. Cumulative curve. Sample with low C₃A content, 6.0% of gypsum, 0, 10% of limestone addition.

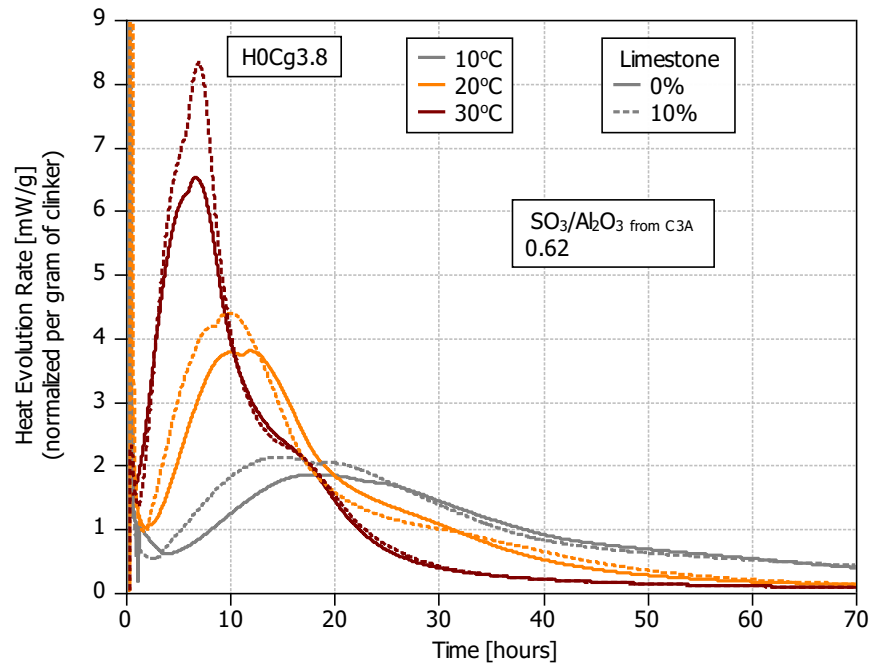


Figure 6.7: Isothermal Calorimetry Data at different temperatures. Sample with high C_3A content, 3.8% of gypsum, 0, 10% of limestone addition.

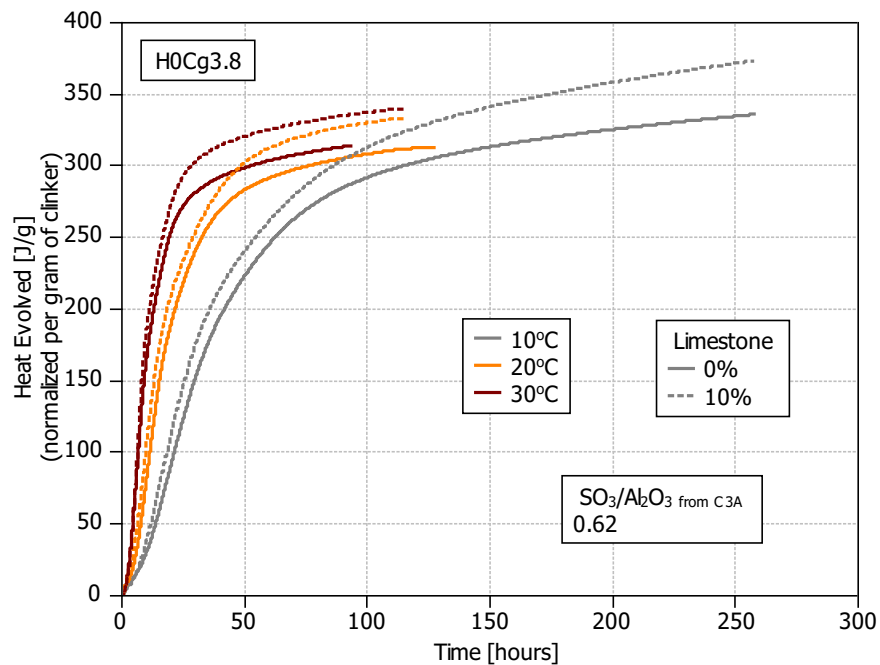


Figure 6.8: Isothermal Calorimetry Data at different temperatures. Sample with high C_3A content, 3.8% of gypsum, 0, 10% of limestone addition.

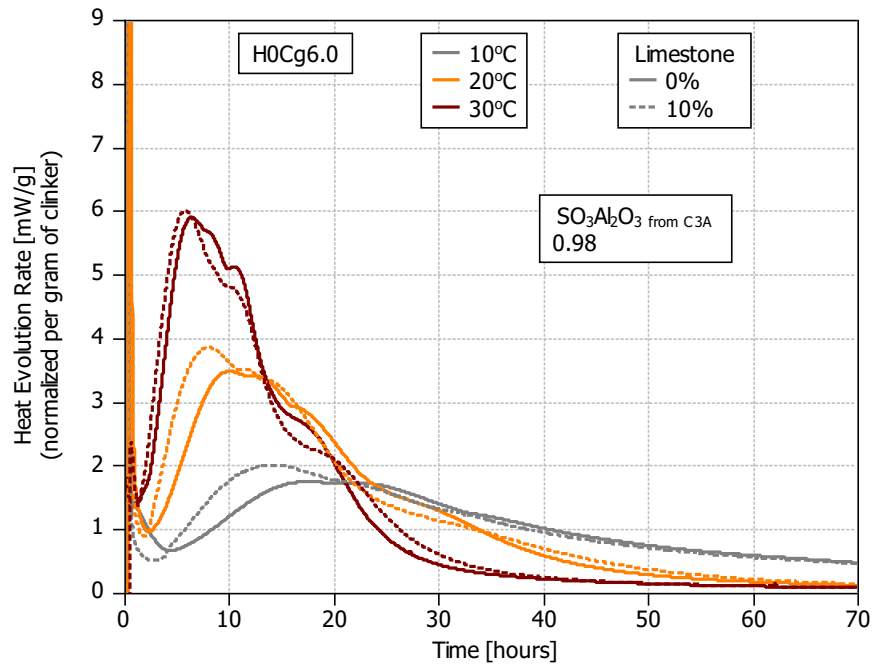


Figure 6.9: Isothermal Calorimetry Data at different temperatures. Sample with high C_3A content, 6.0% of gypsum, 0, 10% of limestone addition

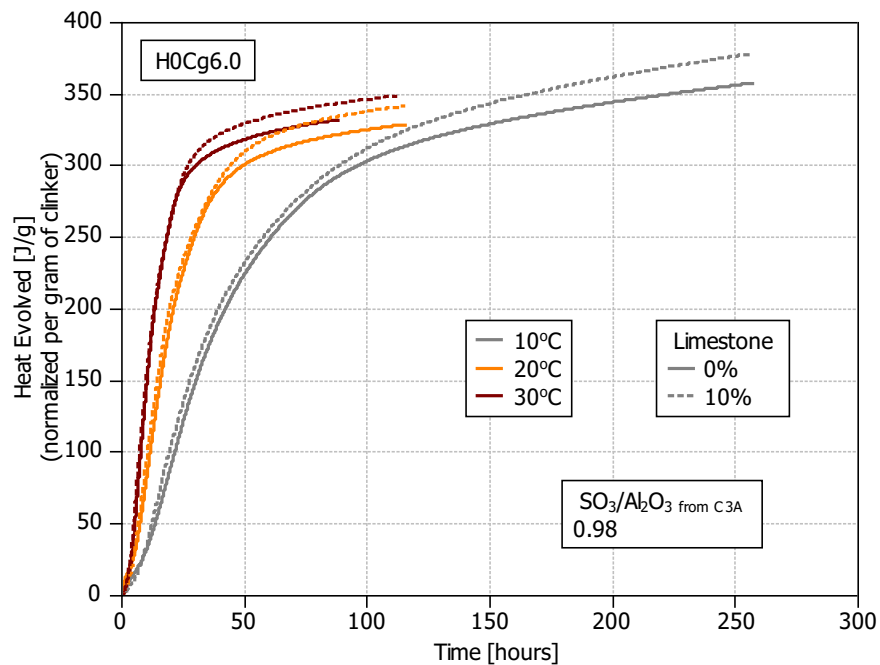


Figure 6.10: Isothermal Calorimetry Data at different temperatures. Sample with high C_3A content, 6.0% of gypsum, 0, 10% of limestone addition.

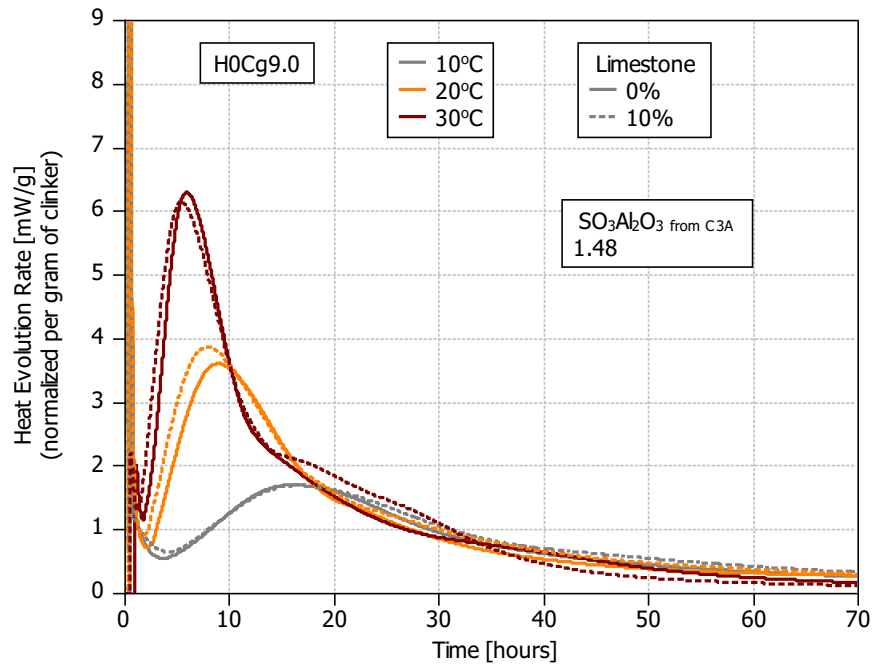


Figure 6.11: Isothermal Calorimetry Data at different temperatures. Sample with high C_3A content, 9.0% of gypsum, 0, 10% of limestone addition.

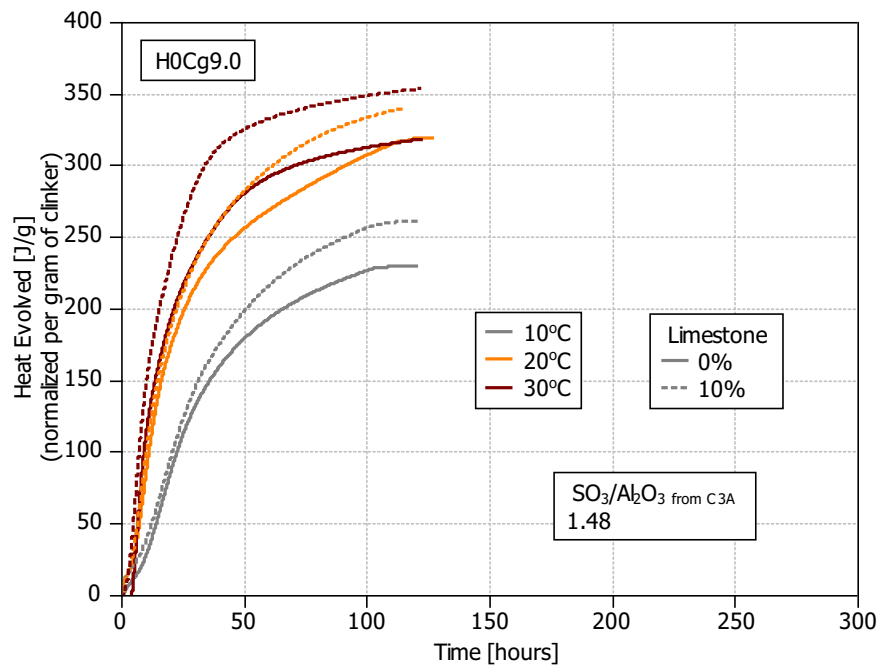


Figure 6.12: Isothermal Calorimetry Data at different temperatures. Sample with high C_3A content, 9.0% of gypsum, 0, 10% of limestone addition.

6.2 Influence of the temperature on the compressive strength

The increase in hydration reaction causes an increase in compressive strength especially at early age (Figs 6.13 – 6.14). At 10 hours of hydration the differences in strength are the most pronounced. The values of compressive strength of samples hydrated at 10°C are extremely low while samples kept at 30°C show the values of compressive strength three times higher than samples hydrated at 20°C (Fig. 6.13). At 24 hours the differences in strength between samples hydrated at different temperatures are smaller, especially between 20 and 30°C. At 24 hours samples hydrated at 10°C still shows low compressive strength (Fig. 6.14).

With 10% of limestone addition at 10 hours of hydration, compressive strength is the same for samples hydrated at 10°C in comparison with samples without limestone, slightly higher for samples hydrated at 20°C and significantly lower for samples hydrated at 30°C (Fig. 6.13).

At 24 hours of hydration, with 10% of limestone addition, the samples at each temperature show the same or slightly higher compressive strength up to optimum gypsum and above the optimum show smaller strength than samples without limestone addition. The optimum gypsum is not influenced by temperature and it is the same at 20, 10 and 30° (Fig. 6.14).

At 28 days of hydration, the differences in compressive strength between samples hydrated in different temperatures are in the range of 10MPa. There is no clear trend with temperature and the compressive strength depends on the gypsum addition. The highest strength at optimum gypsum (6% without limestone and 5.5% with 10% of limestone) is shown by samples hydrated at 10°C (Fig. 6.15).

With temperature the hydration is accelerated. Two approaches were used to determine the same maturity of hydrated systems, Isothermal Calorimetry Data and degree of hydration from XRD Rietveld Analysis.

- Isothermal Calorimetry approach – The compressive strength at 20°C was taken at 10 and 24 hours of hydration. On the calorimetry curve performed at 20°C it corresponds to the moment of the top of the first peak (10h) and after the third small peak (24h). The same moments on the calorimetry curve were chosen for samples hydrated at different temperatures. All process is illustrated in the Fig. 6.16.
- Degree of hydration by XRD Rietveld – The X-ray diffraction was performed on the powdered samples, later Reitveld Analysis to determine the degree of hydra-

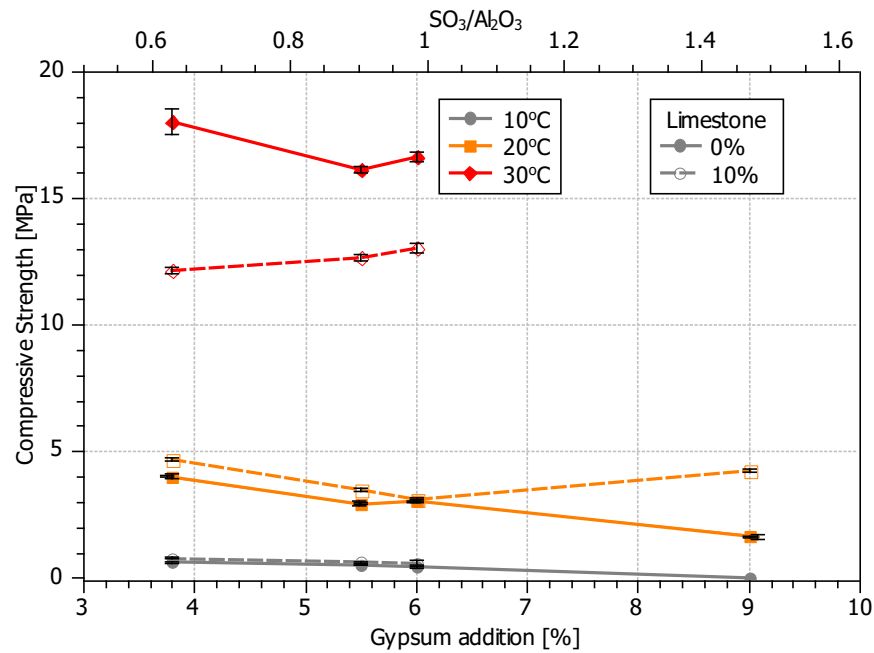


Figure 6.13: Compressive Strength at 10h of hydration and different temperatures. Samples with high C₃A clinker, different gypsum content and with 0 and 10% of limestone addition.

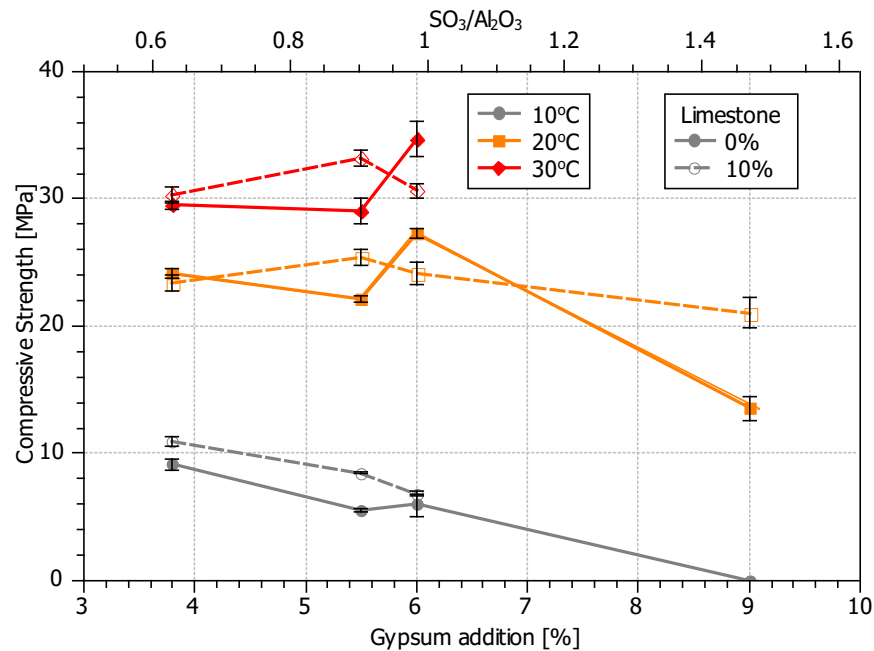


Figure 6.14: Compressive Strength at 24h of hydration and different temperatures. Samples with high C₃A clinker, different gypsum content and with 0 and 10% of limestone addition.

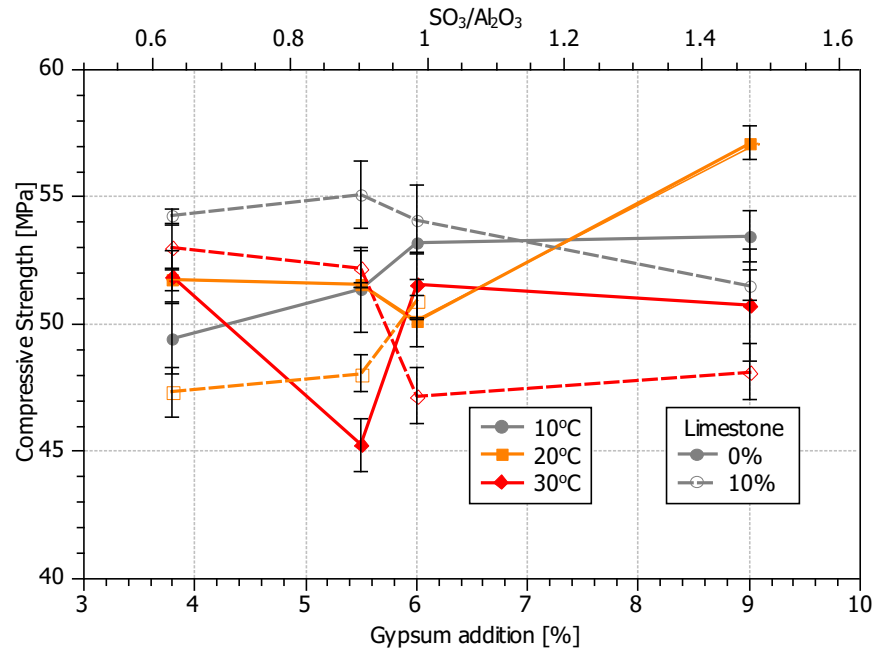


Figure 6.15: Compressive Strength at 28d of hydration and different temperatures. Samples with high C₃A clinker, different gypsum content and with 0 and 10% of limestone addition.

Table 6.1: Maturity of the system at different temperatures indicated by Isothermal Calorimetry and Degree of Hydration from XRD Rietveld Analysis

	The Same Maturity time [h]	20°C	10°C	30°C
Calo		10	16	6
XRD		10	16	6
Calo		24	40	16
XRD		24	46	24

tion of hydrated samples. The maturity of the system at different temperature was determined by choosing the time of the same value of degree of hydration at 20°C at 10 hours and 24 hours for 10 and 30°C. The process is presented in the Fig. 6.17

The corresponding maturity values for different temperature are in agreement at 10 hours of hydration between calorimetry and XRD method. The maturity at 24 hours show differences between calorimetry and XRD method. All results are combined in the Table 6.1.

The compressive strength at the same maturity of the system were measured. Two times of maturity for sample hydrated at 20°C were chosen 10 and 24h and correspond-

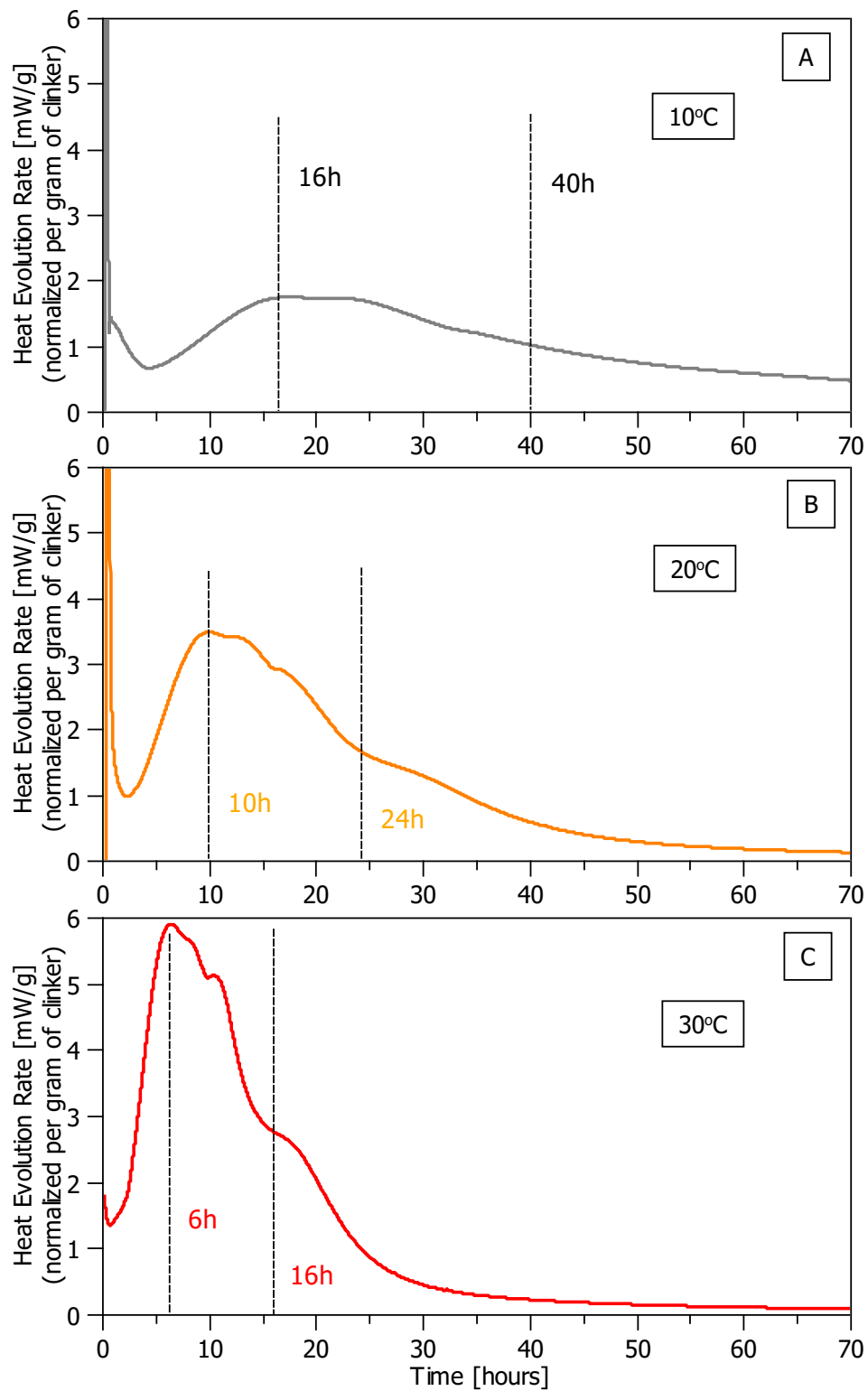


Figure 6.16: Isothermal Calorimetry Data – Maturity of the system at different temperatures.

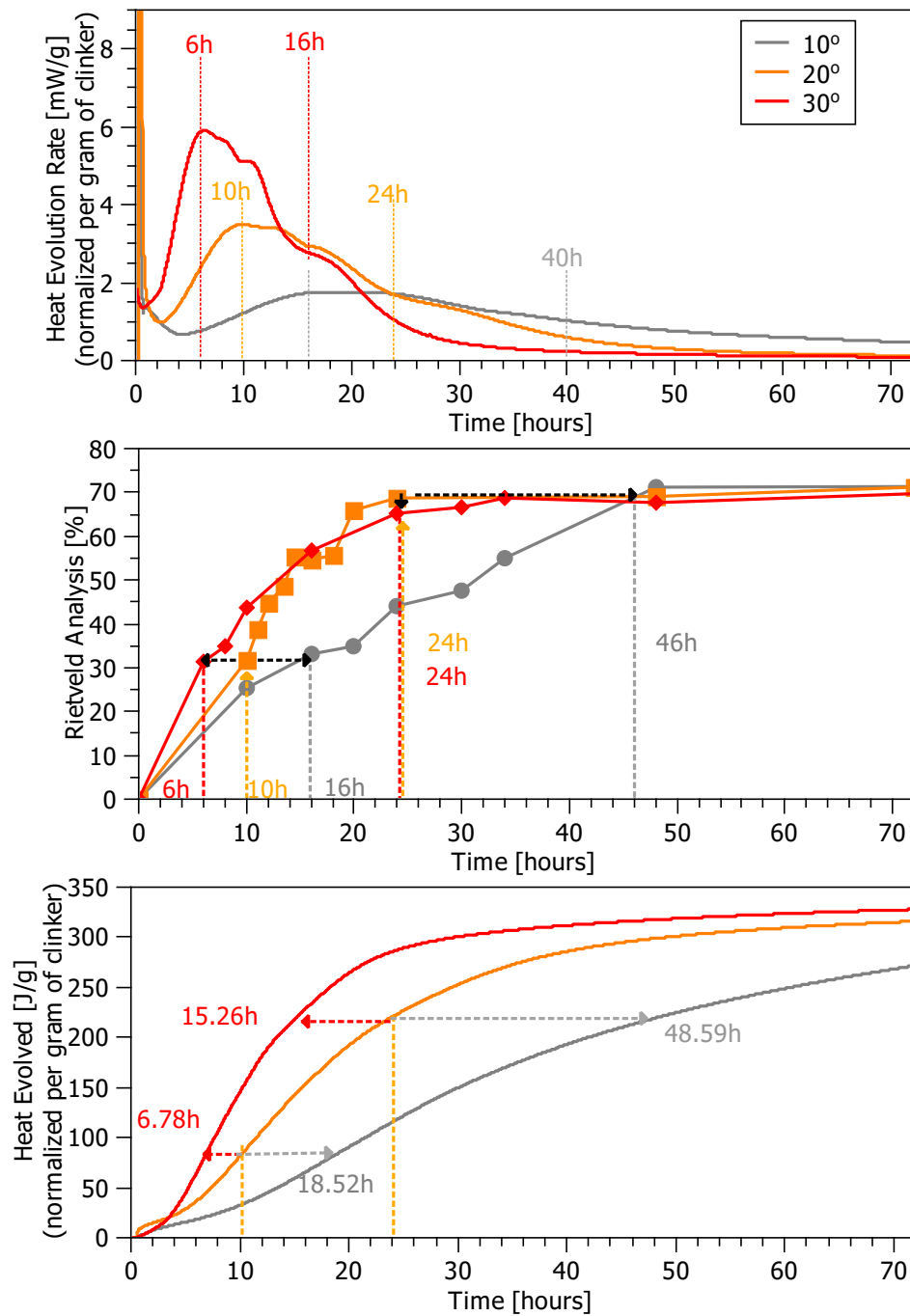


Figure 6.17: Isothermal Calorimetry Data, and X-ray Diffraction, Rietveld Analysis Data – Maturity of the system at different temperatures by degree of hydration.

ing maturity at 10 and 30°C was determined using Isothermal Calorimetry and XRD Rietveld Analysis, as described above.

Results show that samples hydrated at 20 and 30°C show similar compressive strength at 10 hours of hydration and samples hydrate at 10°C show much lower compressive strength than samples hydrated at 20°C (Fig. 6.18). Moreover at each temperature the highest strength at 10 hours of hydration show samples with the lowest 3.8% of gypsum addition with and without limestone addition.

In Fig. 6.19 the compressive strength results for samples with the same maturity are presented. Results show that optimum gypsum is not influenced when the temperature is higher than 20°C, and samples cured at 30° show the same value for optimum gypsum. Samples hydrated at 10°C show the highest compressive strength for sample with the lowest 3.8% of gypsum addition without limestone. With limestone at 10°C the optimum gypsum is the same as for sample hydrated at 20°C.

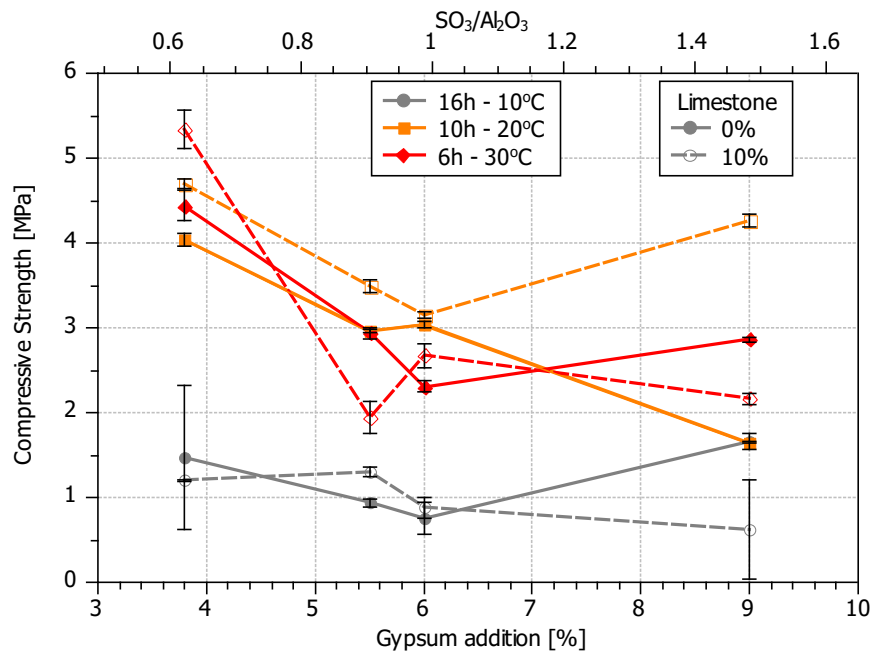


Figure 6.18: Compressive Strength – corresponding maturity at different temperatures to 10h maturity at 20°C, by calorimetry and XRD.

The differences in strength cannot also be explained by differences in total porosity. The result obtained by Mercury Intrusion Porosimetry shows that with temperature the total porosity changes. The samples hydrated at 20°C have the lowest porosity for each gypsum addition with and without 10% of limestone addition.

There is no clear relationship between total porosity and compressive strength. In Fig. 6.23 the total porosity vs compressive strength is presented. The same maturity

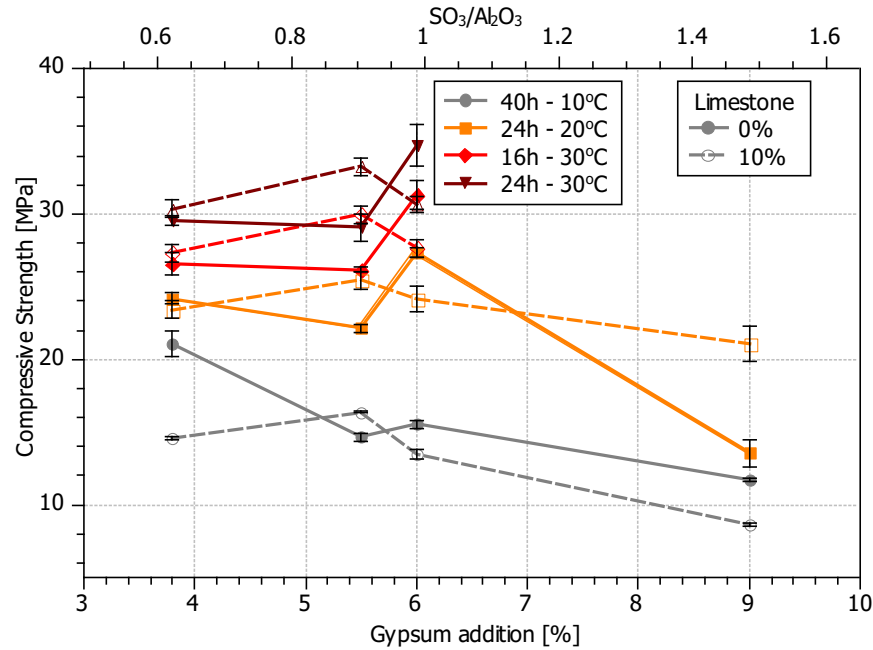


Figure 6.19: Compressive Strength – corresponding maturity at different temperatures to 24h maturity at 20°C, by calorimetry and XRD.

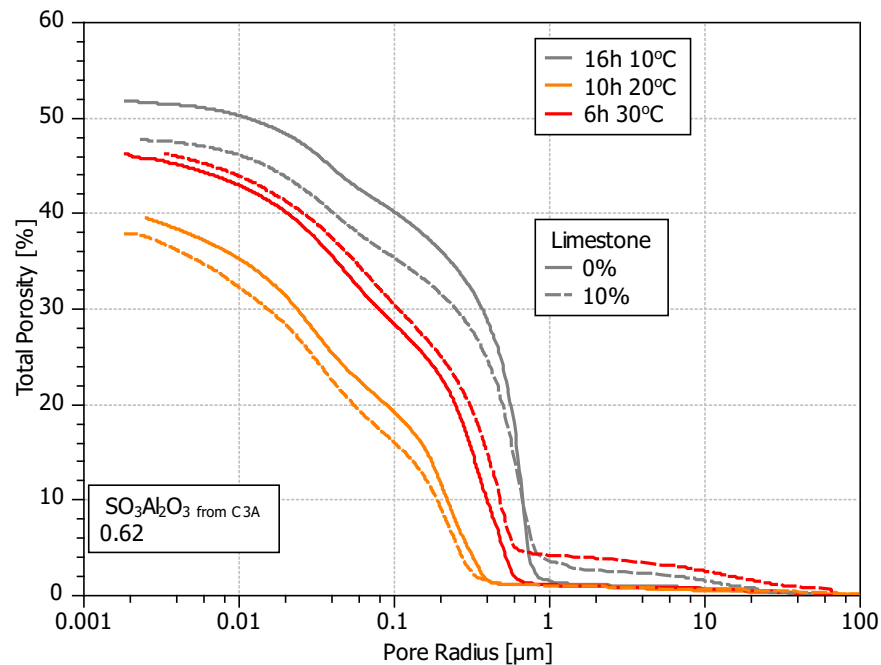


Figure 6.20: Mercury Intrusion Porosimetry – Sample with 3.8% of gypsum and high C_3A content, $SO_3/Al_2O_3 = 0.62$. Corresponding maturity at 10 and 30 °C to 10h maturity at 20°C.

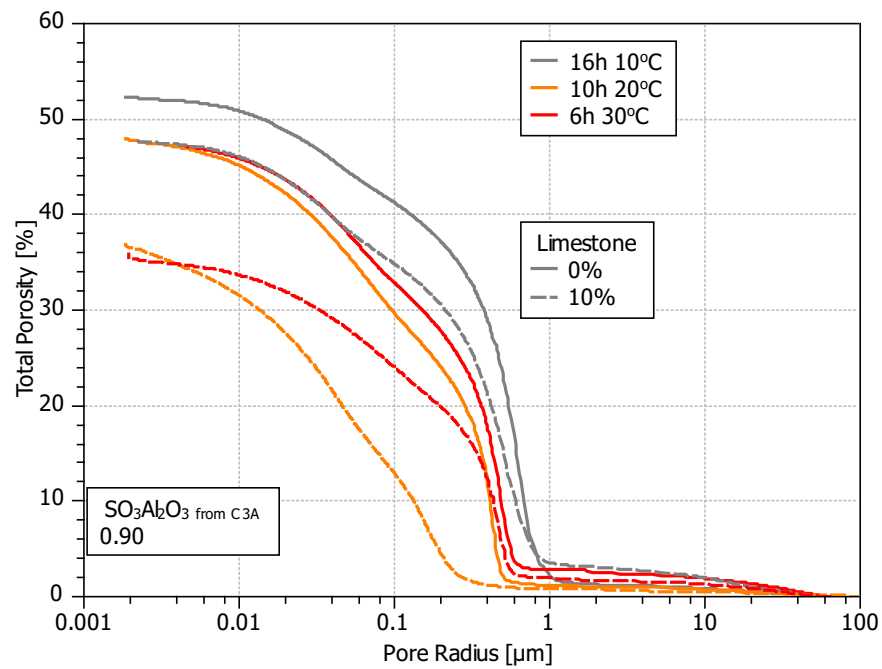


Figure 6.21: Mercury Intrusion Porosimetry – Sample with 5.5% of gypsum and high C_3A content, $SO_3/Al_2O_3 = 0.90$. Corresponding maturity at 10 and 30 °C to 10h maturity at 20°C.

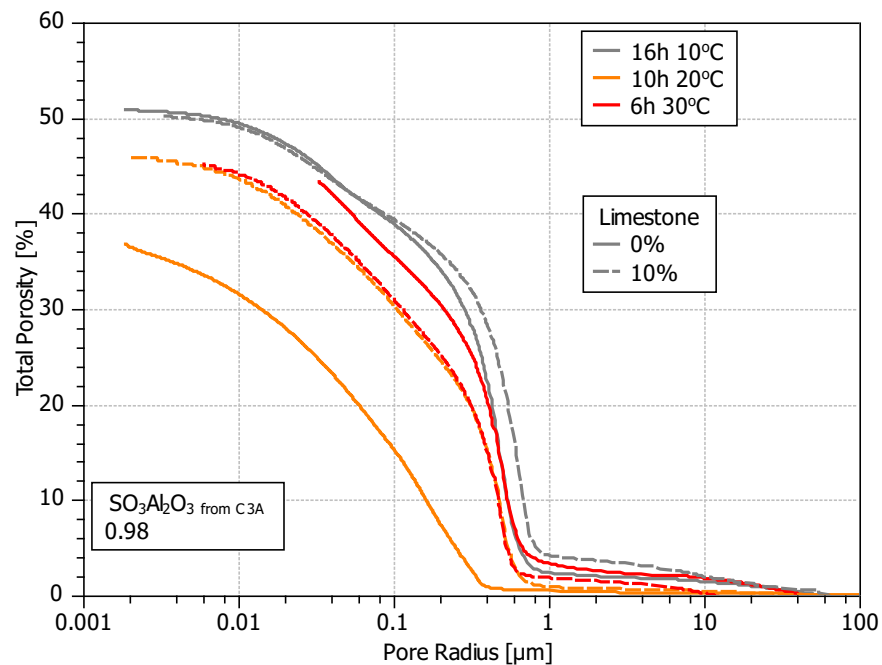


Figure 6.22: Mercury Intrusion Porosimetry – Sample with 6.0% of gypsum and high C_3A content, $SO_3/Al_2O_3 = 0.99$. Corresponding maturity at 10 and 30 °C to 10h maturity at 20°C.

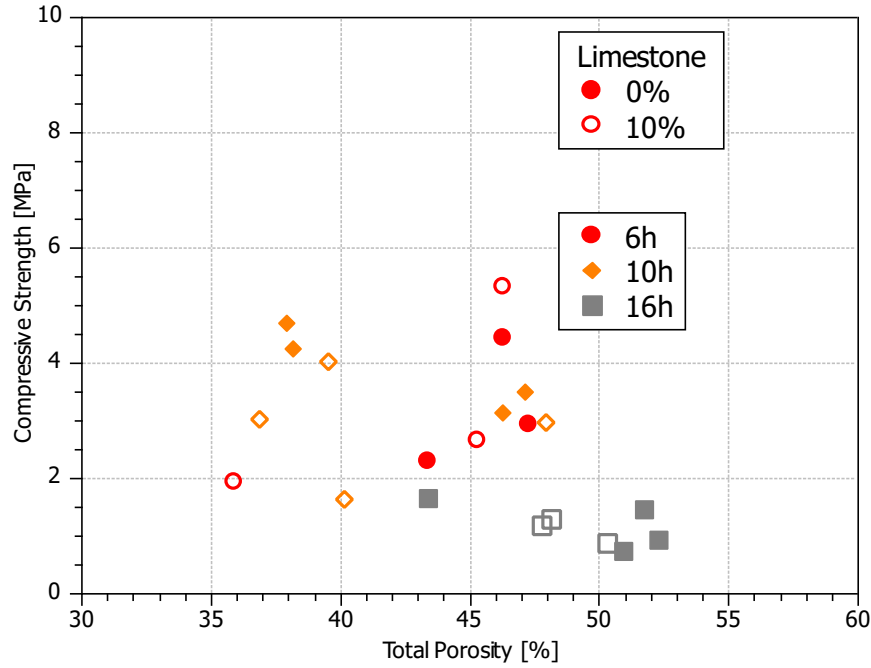


Figure 6.23: Total Porosimetry vs. Compressive Strength at different temperatures.

of the samples according to Isothermal Calorimetry and XRD Rietveld Analysis does not show the same compressive strength with similar total porosity and vice versa. These results show that hydration reaction and development of compressive strength is a complex process which is not fully understood.

6.3 Activation Energy

The Activation energy indicates the sensitivity of the rate of reaction to temperature and can be calculated from Arrhenius equation (Eq. 6.1).

$$k = \exp\left(\frac{-E_a}{RT}\right) \quad (6.1)$$

Where:

R – gas constant (8.314 J/mol/K)

T – temperature at which reaction occurs (K)

k – rate of heat evolution (W)

E_a – activation energy (J/mol)

Because the hydration of the cement it is mix of reactions occurring simultaneously the expression of "apparent" activation energy is used.

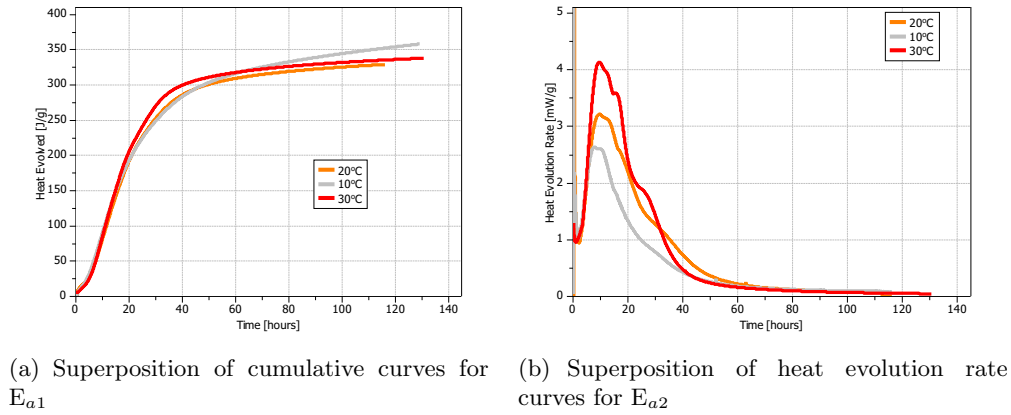


Figure 6.24: Examples of superposition of calorimetry curves for calculating activation energy.

There are several methods to calculate activation energy. The differences in results from each method are significant, which makes results difficult to compare. The best methods description and comparison can be found in the literature and especially in the paper [64].

The activation energy can be calculated by the concept of equivalent age. The most common equation used to compute equivalent age is proposed by Friesleben Hansen and Pederson and is presented below (Eq. 6.2)

$$t_e(T_r) = \sum_0^t e^{-\frac{E_a}{R} \left(\frac{1}{T_c} - \frac{1}{T_r} \right)} \cdot \Delta t \quad (6.2)$$

Where:

$t_e(T_r)$ – equivalent age at reference temperature

T_r and T_c – reference temperature and temperature of the concrete

6.3.1 Activation Energy for different cement systems

The differences in activation energy for cements with different clinker composition, gypsum and limestone addition were investigated. Two clinkers with low and high C_3A content, increasing gypsum content and with 0 and 10% of limestone addition were investigated.

The method used was Maturity Method. This method consists superposing the first part of cumulative heat using the Eq. 6.3 and α is the age conversion factor obtained to superpose the cumulative curves (Fig. 6.24 a).

$$t_e = \alpha \cdot t \quad (6.3)$$

Table 6.2: Calculated Activation Energy

Low C ₃ A cements			High C ₃ A cements		
Sample	E _{a1} [kJ/mol]	E _{a2} [kJ/mol]	Sample	E _{a1} [kJ/mol]	E _{a2} [kJ/mol]
L0Cg3.9	32.94	33.72	H0Cg3.8	40.17	51.07
L0Cg5.5	32.25	22.85	H0Cg5.5	37.87	42.18
L0Cg6.0	30.18	30.81	H0Cg6.0	37.87	41.50
			H0Cg9.0	37.87	47.78
L10Cg3.5	32.94	32.94	H10Cg3.5	35.86	30.93
L10Cg5.0	32.20	35.89	H10Cg5.0	35.86	35.07
L10Cg5.5	29.65	34.58	H10Cg5.5	35.86	25.17
			H10Cg8.2	38.56	45.23

The Activation energy results were obtained and compared with the results of Activation energy obtained by superposing the slopes of the differential calorimetric curves using Eq. 6.4 with β as a factor of calorimetric curves shift (Fig. 6.24 b).

The sensitivity of the fitting is moderately high and the deviation from the fitting value about 0.1 gives an error of 2–8 [kJ/mol].

$$t_e = \alpha \cdot (t + \beta) \quad (6.4)$$

Activation Energy for each system was calculated using Eq. 6.5

$$E_a = \frac{\ln(\alpha) \cdot R}{\frac{1}{T} - \frac{1}{T_r}} \quad (6.5)$$

The comparison of the results is presented in the table Table 6.2. The both methods gives comparable results Fig 6.25 and Fig. 6.26. The difference in the Activation Energies for sample without and with limestone are more pronounced using second fitting method. Fitting the differential calorimetry curve was found to be more sensitive to the addition of limestone in the cement.

Activation energy show similar results with increasing gypsum and 10% of limestone addition. There are only slight changes between samples. Low C₃A system (Fig. 6.25) show less scattering of the results than high C₃A system (Fig. 6.26).

For high C₃A clinker cements more dispersion was expected due to simultaneous reactions however still generally the E_a is similar for all samples.

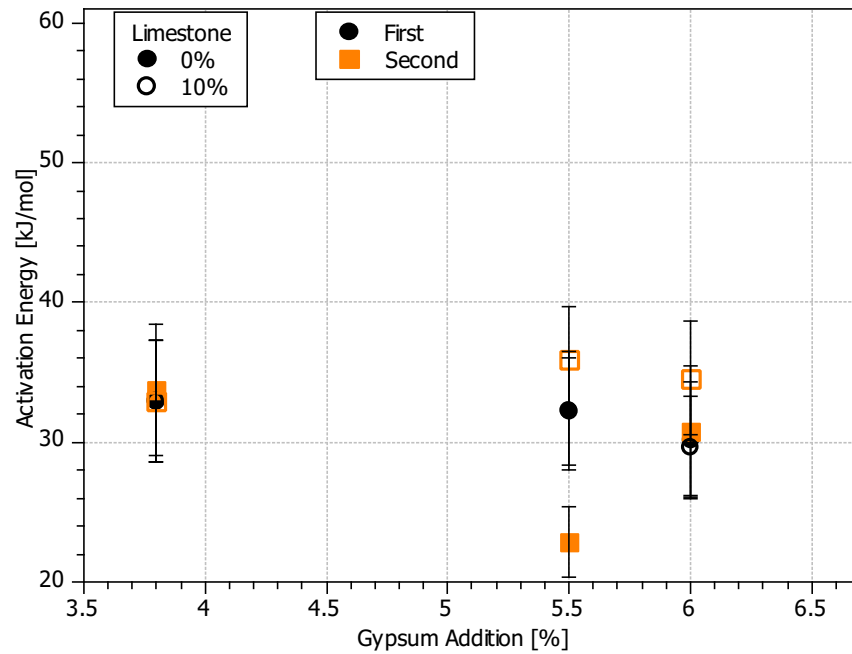


Figure 6.25: Activation Energies results for low C_3A clinker.

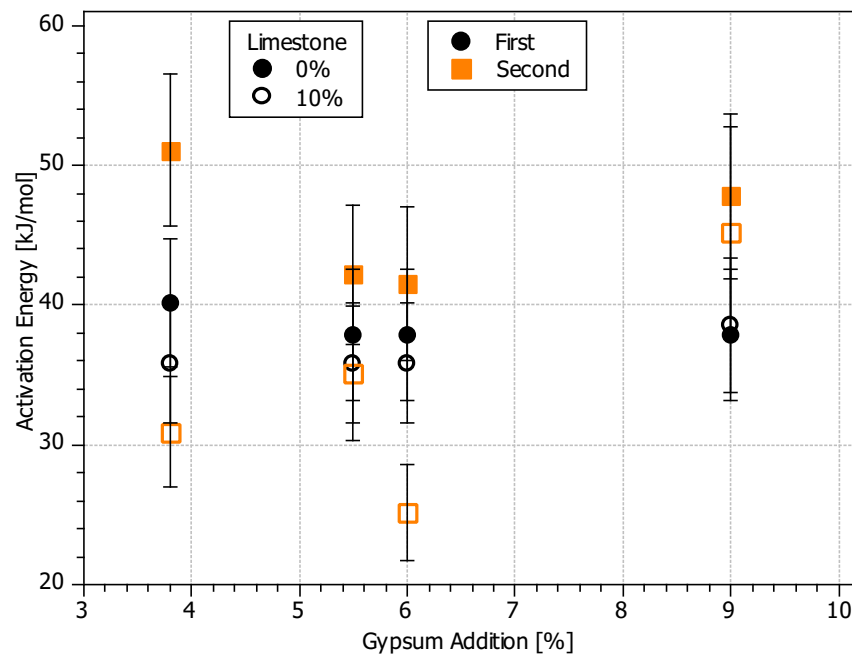


Figure 6.26: Activation Energies results for high C_3A clinker.

6.4 Summary

- Temperature accelerates the hydration reaction
- Compressive strength increases with temperature
- Compressive strength done at the same maturity of the system (Calo, XRD) at different temperature depends on the cement composition, however the highest strength at 24 hours is equivalent to sample cured at 30°C
- At 28 days the highest compressive strength show sample cured at 10°C
- Temperature has an influence on the porosity. At each time of hydration the highest total porosity shows sample cured at 10°C and the lowest sample cured at 20°C
- Activation Energy is similar for all cement mixes

Chapter 7

Influence of limestone and gypsum on the durability of cementitious materials

The durability aspect of the cementitious materials, especially with supplementary cementitious materials is a main concern of the cement industry.

It has been claimed that systems with limestone are more susceptible to sulfate attack, however it depends on many parameters such as limestone content and clinker composition. Therefore in this chapter the influence of limestone on the sulfate attack with clinker with different C_3A content and gypsum content will be investigated. The expansion curves and microstructural investigation will be presented.

Additionally sorptivity of the same systems as exposed to the sulfate attack will be presented.

7.1 Sulfate attack

7.1.1 State of the art

Blended cements containing limestone are not allowed in applications where sulfate attack may occur. As a limestone can be source of the CO_3^{2-} which is the main constituent of the thaumasite form of sulfate attack [7], due to their high calcite content.

In general sulfate attack is a damage of construction material after exposure to the external sulfate source such as soil or water rich in sulfate ions. The reaction of hydrates and cement components with sulfate ions result in a set of overlapping and complex chemical and physical processes which lead to damage of construction. AFm phase, unhydrated alumina phases and CH interact with aggressive solution to

form expansive compounds such as ettringite and gypsum which produce cracks, loss of strength and softening. Another kind of sulfate attack, attributed to thaumasite formation, concern cement and concretes containing limestone [5][11].

The observed expansion as a results of sulfate attack is not totally well understood and it can not be directly linked to the formation of one of secondary sulfate phase. Most likely it is an effect of overlapping different physical and chemical reactions in the system.

There is many theories concerning sulfate attack mechanism. The most recent one is that crystallization pressure developed in pores generates initial stress and consequently expansion of the matrix [75].

The primary phases as effect of sulfate attack in the cement are ettringite and gypsum. Ettringite was the phase first considered as a cause of the sulfate attack damages [15] [53]. However strong correlation between formation of ettringite and expansion was not found [12]. However the choice of low C_3A clinker cements is made as a sulfate resistant cements and gypsum formation and its effects are diminished.

Mehta et al. [54] studied the sulfate resistance of C_3A free cements – alite cements. In the end gypsum was found to be the reason of deterioration of the system. Similar in the study of Tian and Cohen showed that C_3S pastes and mortars are susceptible to the sulfate attack and expansion and large amount of gypsum formation was found [90]. Additionally Santhanam et al. showed that gypsum and ettringite contribute to expansion of Portland cements with high C_3S content [73].

The mechanisms of thaumasite formation is still not well understood, however it is known that thaumasite ($CaSiO_3 \cdot CaCO_3 \cdot CaSO_4 \cdot 15H_2O$) forms at low temperature and requires sulfate and carbonate ions, a source of calcium silicate and excess of humidity. It can also be preceded by the formation of ettringite. Because thaumasite formation requires C–S–H with carbonate and sulfate ions it may also form in ordinary Portland cement or even in the sulfate resistant cements [4].

Temperature has a significant influence on the thaumasite formation. Thaumasite formation is attributed to low temperature $5^{\circ}C$ [5] [43] [62], however it is also observed in higher temperatures [87] [50] [62].

The formation of thaumasite is promoted in low pH [5] [18] [92], however formation in high pH was also observed [98].

The formation of thaumasite depends in general on the relative solubility products of thaumasite, ettringite, gypsum, calcite, portlandite, and if $MgSO_4$ is present also brucite, which vary with temperature and pH of the solution (variation of ions present in solution) [98].

It was also found that clinker structure can affect the performance of limestone

incorporated mortars. Clinker with higher C_3S/C_2S ratio and dendritic interstitial phase structure seems to be more susceptible to sulfate attack [67] [91] [94].

It was found that with increasing limestone addition the systems were less sulfate resistant [87] however deterioration level depends on the type of sulfate solution and sulfate concentration [87]. Even at 20°C the deterioration is strongly associated with thaumasite formation regardless to sulfate solution [87]. The deterioration was an effect of thaumasite and gypsum formation [87].

7.1.2 Influence of limestone on the sulfate attack

Two types of cement system, low and high C_3A with different gypsum content (3.5–5.5%) and limestone addition were investigated. Additionally laboratory made and commercial cements and their sulfate resistance were compared. The expansion curves are presented on the (Figs 7.2, 7.3, 7.4).

7.1.2.1 Methods

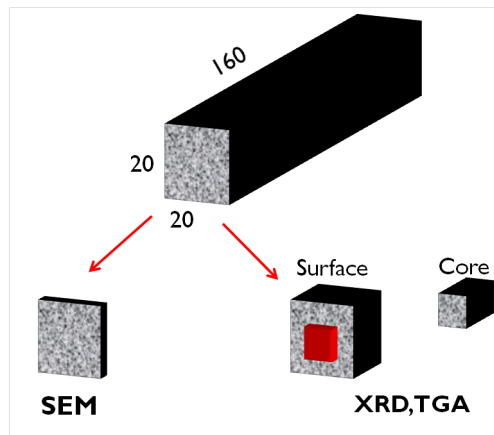


Figure 7.1: Sulfate attack experiment - sampling.

The experiment was containing following steps:

- Mixing of the mortars in the w:s:c ratio 1:2:3, and w/c ratio was 0.5
- Casting in the 40x40x160mm prism with a metal pin, from each end of length 250mm and diameter 3mm
- Demoulding and storing in the humidity box for 28 days
- Cutting the surfaces and reducing the diameters to 20x20x160mm
- Immersing into sulfate solution of 3g/l of Na_2SO_4 . Solution/sample volume ratio – 2.34

The sulfate solution was exchanged each second week of the experiment. At certain times the piece of sample was cut and immersed into isopropanol for 7 days to stop the hydration. Later it was tested using SEM, XRD, TGA. The sampling procedure is presented in the Fig. 7.1.

In the Fig. 7.2 samples with low C_3A clinker 0 and 10% of limestone addition and increasing gypsum are presented. It can be observed that in low C_3A clinker cement 10% of limestone addition doesn't influence the expansion rate of samples up to 2 years of curing in the Na_2SO_4 sulfate solution. Also different gypsum addition have no influence in the samples with low C_3A clinker.

The samples with high C_3A clinker show higher expansion when 10% of limestone is in the system in comparison to the sample without limestone, however the expansion occurs later with limestone addition (Fig. 7.3). With increasing gypsum content the expansion and destruction of the mortar occurs earlier. After 600 days of curing in the Na_2SO_4 solution all samples with limestone addition are destroyed.

In general samples with high C_3A content show higher expansion than samples with low C_3A content (Figs 7.2, 7.3).

Commercial cements show the same behavior (Fig. 7.4), where samples with high C_3A clinker and 10% of limestone addition was destroyed after 1 year of curing in the sulfate solution and samples with low C_3A clinker and different limestone addition are showing small continuous expansion up to 800 days of curing in the sulfate solution. With increasing limestone addition there is no significant difference in the expansion for cement with low C_3A content clinker and the samples expand in the same way.

In the Fig. 7.5 the expansion rate for different samples and their destruction level comparison is presented. The results show that the same expansion rate can effect in different destruction effect and it depends on the cement composition.

In the low C_3A clinker cement limestone addition (up to 22%) does not decrease resistance of the mortars to the sulfate attack (Fig. 7.4). The difference between samples with increasing limestone addition and low C_3A clinker is in the range of error.

7.1.2.2 Microstructure investigation

The sulfate attack mechanism was investigated using several techniques. Microstructural investigations on samples with the same age (6 months, 1 year, 480 days) but different expansions and the same expansions but different times were performed.

The formation of phases was mostly followed by XRD analysis. Using XRD it is difficult to detect thaumasite because main peak of thaumasite could be confused with ettringite peak on the XRD pattern, therefore thaumasite identification is based on the peaks characteristic only for thaumasite phases such as peak at 16, 23.5, and 28 2θ .

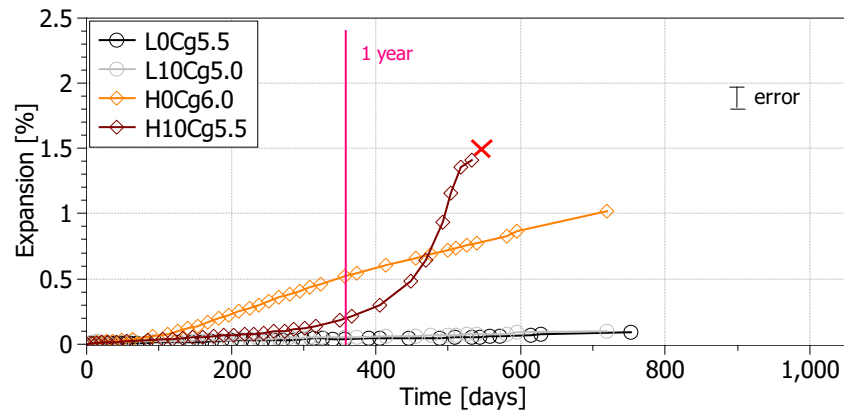


Figure 7.2: Expansion – Laboratory Cement. Samples with low C_3A content (3%), 0 and 10% of limestone addition and different gypsum content.

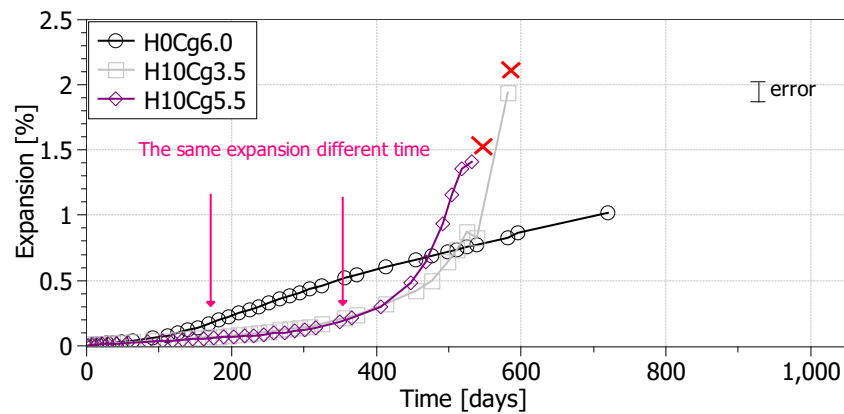


Figure 7.3: Expansion – Laboratory Cement. Samples with high C_3A content (8%), 0 and 10% of limestone addition and different gypsum content.

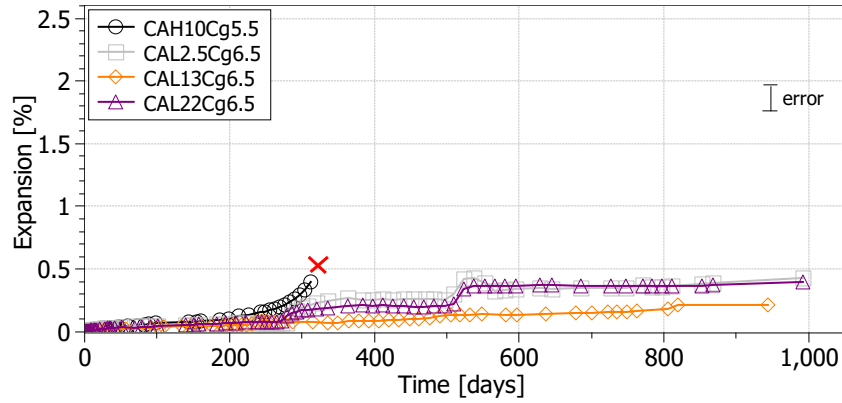


Figure 7.4: Expansion – Commercial Cement. Samples with low and high C_3A content, different limestone addition and 6.5% of gypsum content.

Additionally the absence of ettringite effects in absence of the peaks at 15.8, 18.9, 22.9, 25.5 2θ . However even though the differentiation between ettringite and thaumasite is not straightforward.

The XRD investigation showed that if thaumasite is formed after long times of exposure to the sulfate environment and in the current experiments it is observed at 480 days. Up to 360 days only ettringite was observed in the samples exposed to the sulfate attack (Fig. 7.7).

Samples with the same expansion level at different times (Fig. 7.3) do not show the same phase assemblage by XRD (Fig. 7.6). Sample H10Cg5.5 exposed for 360 days to the sulfate solution shows additionally formation of gypsum in comparison to the sample H0Cg6.0 exposed 180 days. At 480 days of exposure to the sulfate attack both samples show similar phases assemblage but sample H10Cg5.5 shows twice the expansion of sample H0Cg6.0 (Fig. 7.3). Sample H10Cg5.5 shows slight thaumasite formation in the cover of the sample (Fig. 7.7).

Additionally comparison of samples with low and high C_3A clinker with 0 and 10% of limestone addition at 360 days of exposure to the sulfate shows different expansion but only slight differences in the phase assemblage by XRD (Figs 7.8, 7.9).

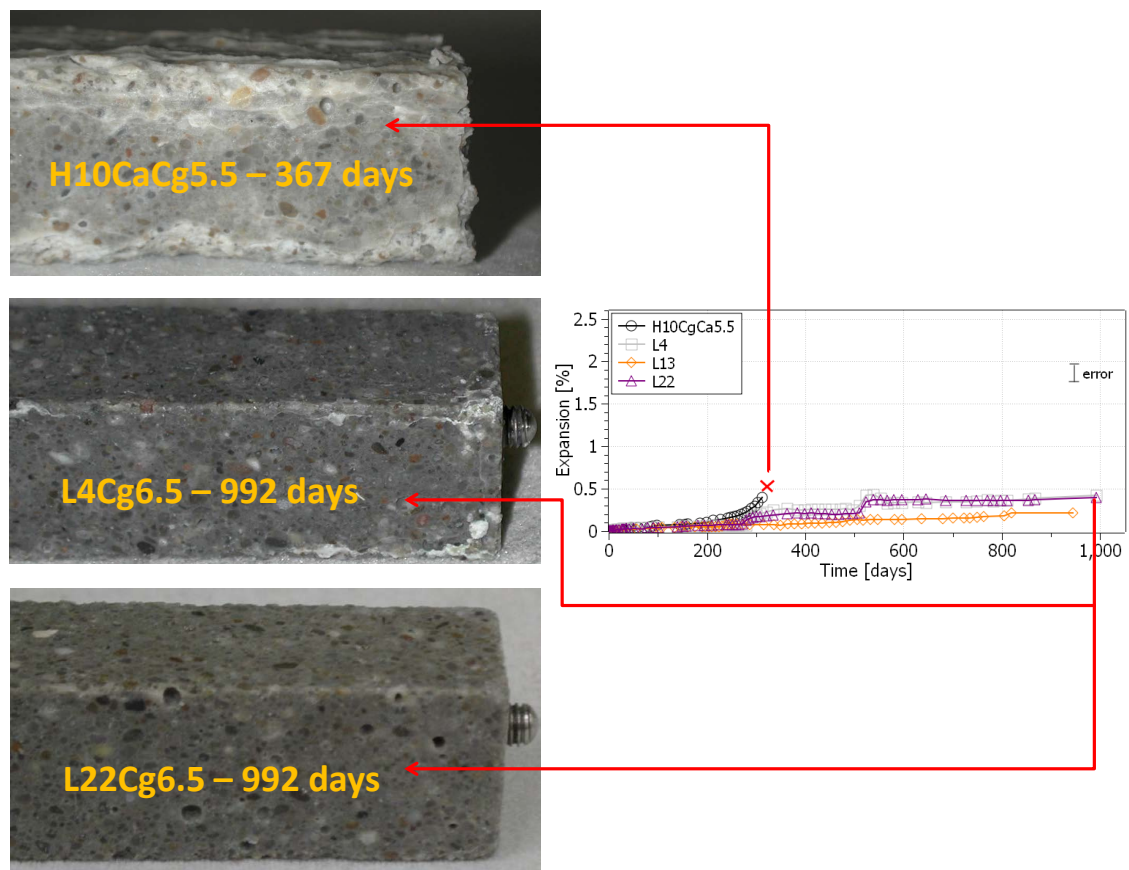


Figure 7.5: The same value of expansion and different level of destruction– Commercial Cement. Samples with low and high C_3A content, different limestone addition and gypsum content.

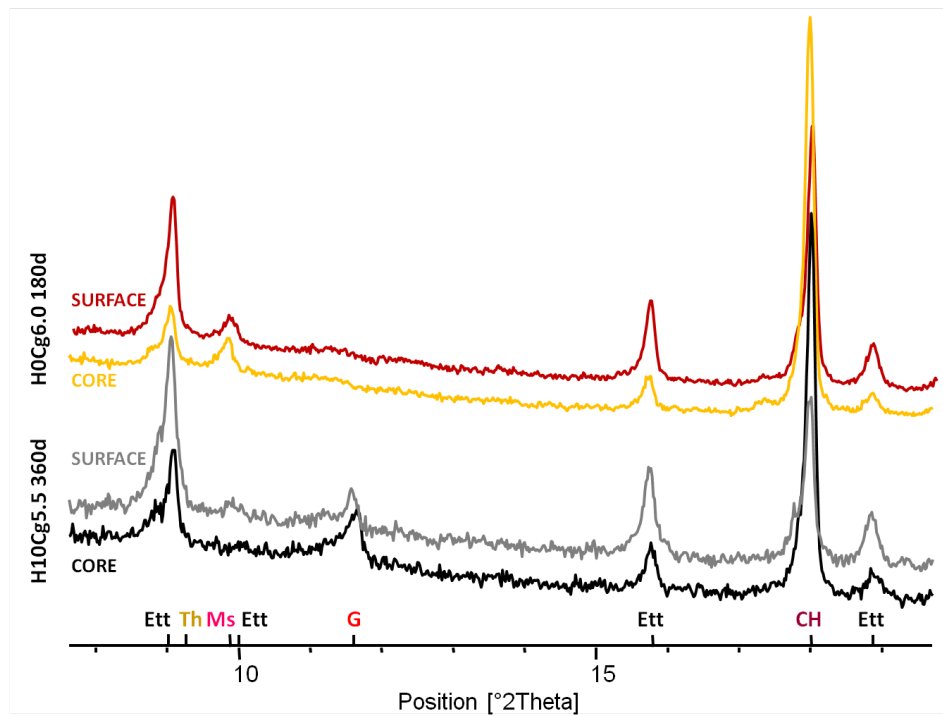


Figure 7.6: XRD Pattern for samples with the same level of expansion and different time of exposure, 180 and 360 days. High C_3A clinker.

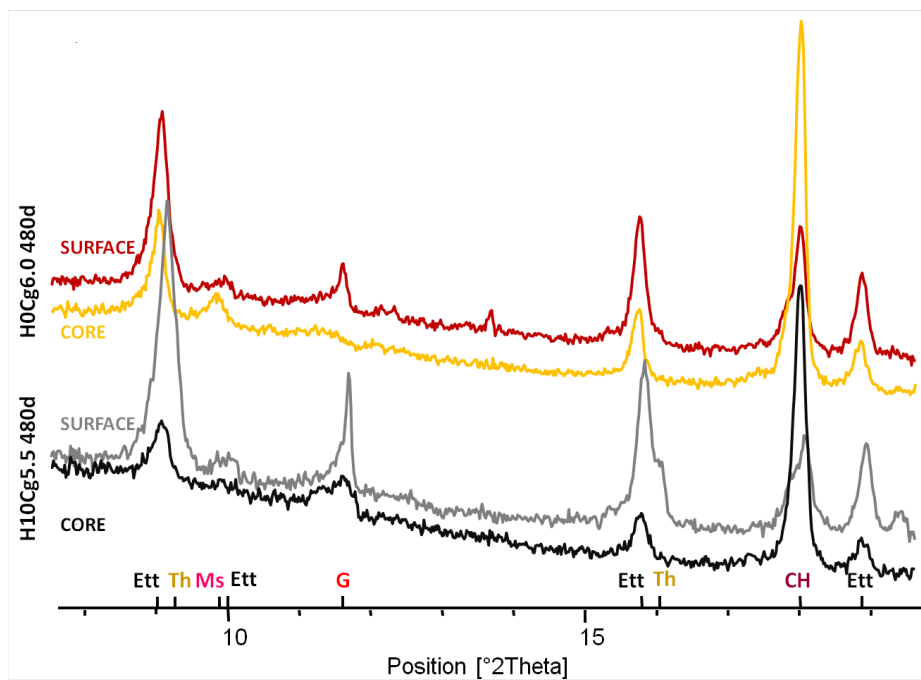


Figure 7.7: XRD Pattern for samples at the same time (480 days) but different expansion level. High C_3A clinker.

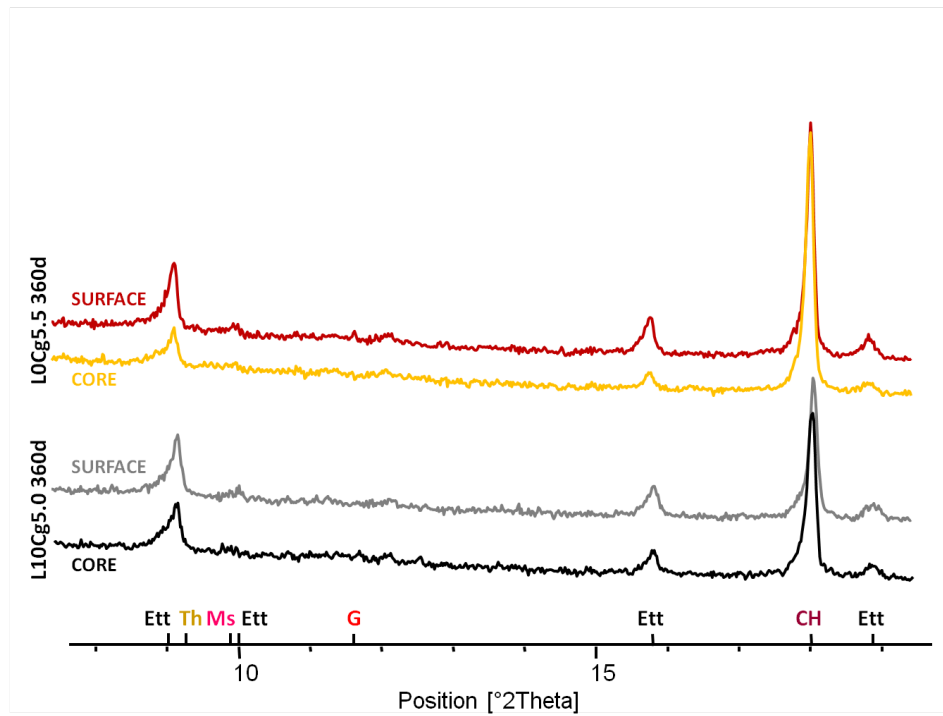


Figure 7.8: XRD Patterns for samples at 360 days in sulfate solution. Low C_3A clinker.

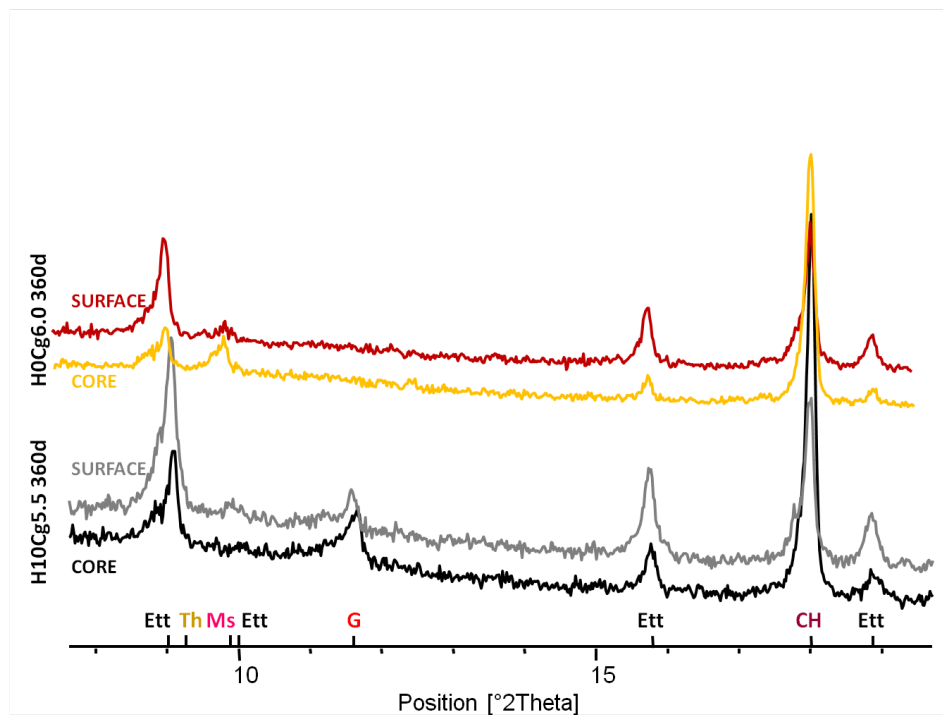


Figure 7.9: XRD Patterns for samples at 360 days in sulfate solution. High C_3A clinker.

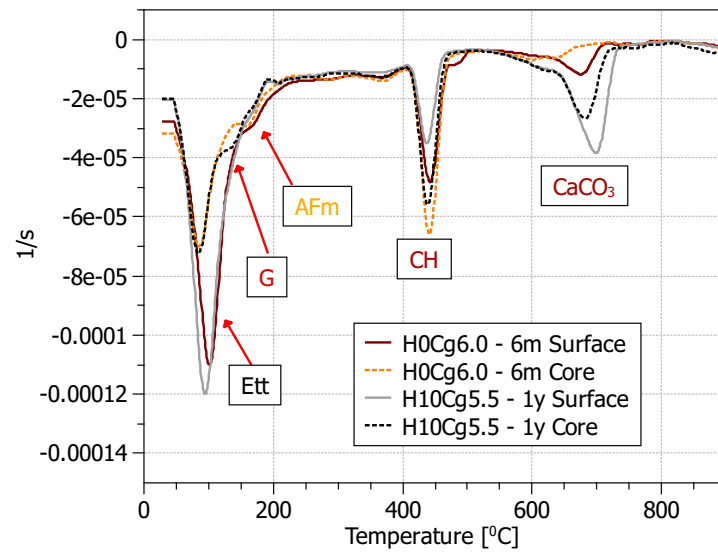


Figure 7.10: TGA, derivative curves for samples with the same level of expansion and different time of exposure, 180 and 360 days. High C₃A clinker.

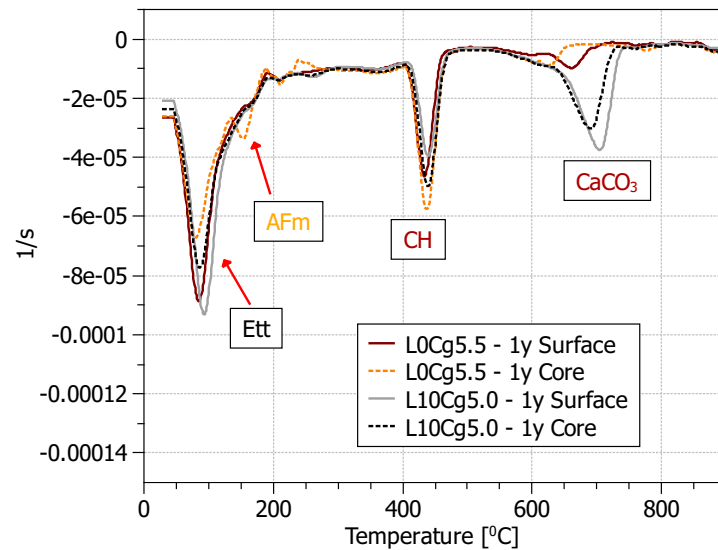


Figure 7.11: TGA, derivative curves for samples at the same time (480 days) but different expansion level. High C₃A clinker.

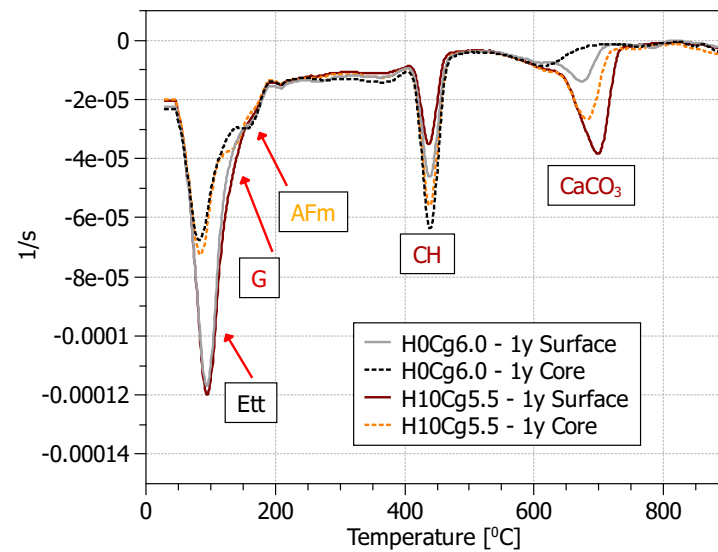


Figure 7.12: TGA, derivative curves for samples at 360 days in sulfate solution. Low C_3A clinker.

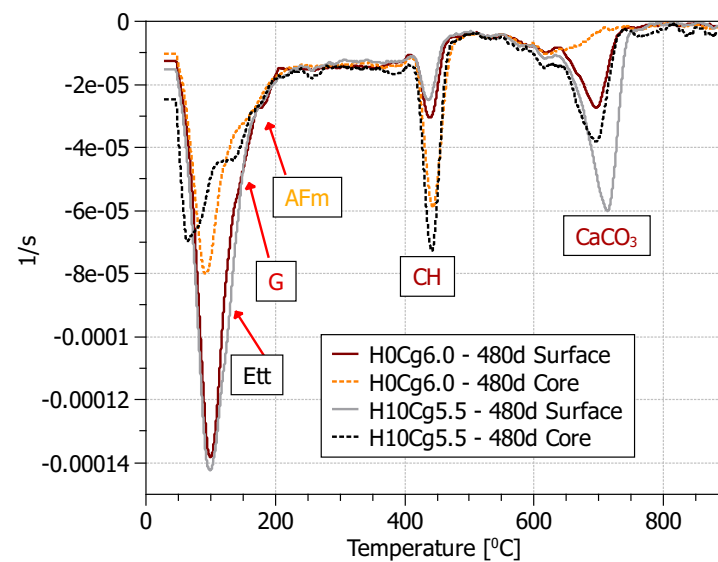


Figure 7.13: TGA, derivative curves for samples at 480 days in sulfate solution. High C_3A clinker.

The biggest difference is in gypsum formation, which is more visible in the samples with high C_3A (Fig. 7.9). The XRD results however can not be quantified quantitatively because of the grains of sand present in the sample. Therefore TGA was used to see the difference in the amount of phases in the samples exposed to the sulfate attack (Figs 7.10, 7.11, 7.12, 7.13).

There are only slight differences in the phase amounts between samples with the same level of expansion at different times. The expansion starts usually on the surface of the sample, and here the effects are the most visible. H10Cg5.5 cured for 1 year at sulfate solution shows slightly more ettringite, less portlandite in comparison to the sample H0Cg6.0 cured for 6 months in sulfate solution (Fig. 7.10).

TGA investigation shows additional phases present in the system which were not well visible by XRD analysis. The difference between surface and core of the sample is more pronounced. At each time of measurement there is more ettringite formed in the cover in comparison to the core of the same sample. In the core there was always more portlandite in comparison to the cover due to leaching on the surface of the sample. Additionally when high C_3A clinker was in the cement also AFm and calcite was formed in the cover while in the core those phases were not present. With 10% of limestone addition ettringite and gypsum were phases visible in the surface and in the core gypsum was visible. Gypsum was not observed for sample without limestone for both low and high C_3A clinker. Also thaumasite is difficult to detect by TGA because decomposition peaks overlap with other phases. Additionally XRD shows only slight amount of thaumasite therefore it is even more difficult to observe by TGA.

Results show that thaumasite is only the last stage of the sulfate attack and it is not the cause of the sulfate attack damages. It was present at most in the sample which was showing the highest damages due to sulfate attack.

SEM analysis and profile analysis were done to see the sulfate distribution in the samples exposed to the sulfate attack. The pictures observation show that there are gaps around aggregates (Fig. 7.15). Additionally sulfate profile pictures shows that sulfate easier penetrates sample with limestone. However if this is an effect of the sulfate attack already or the reason of destruction it is not clear.

Sulfates profile show that there is much more sulfate in the sample with H10Cg5.5 even if the sample at 1 year has the same expansion than sample H0Cg6.0 at 6 months of exposure (Fig. 7.14).

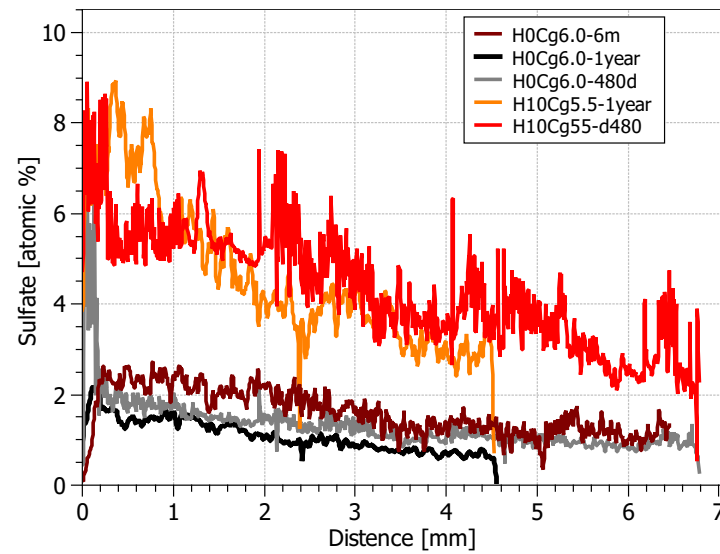
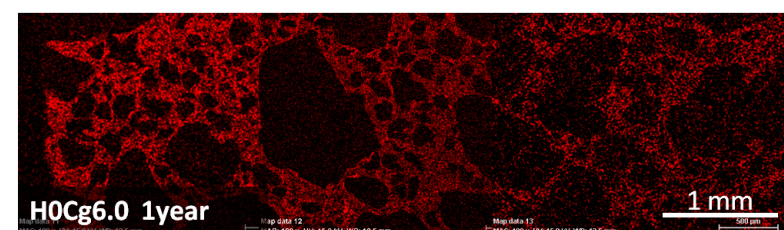
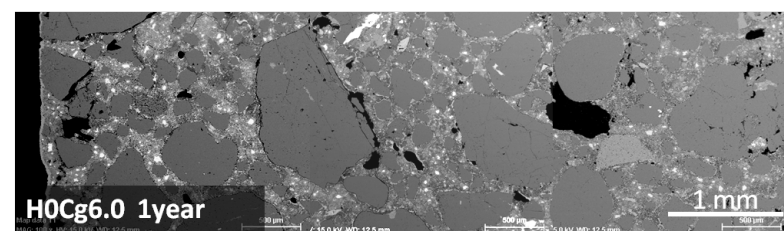
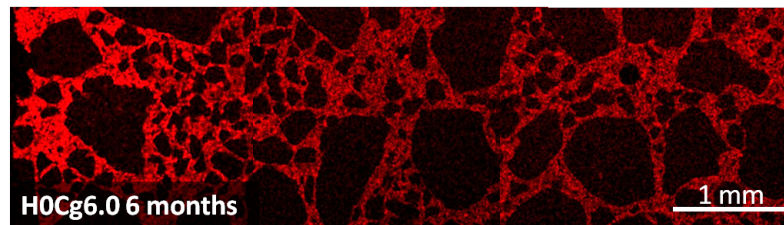
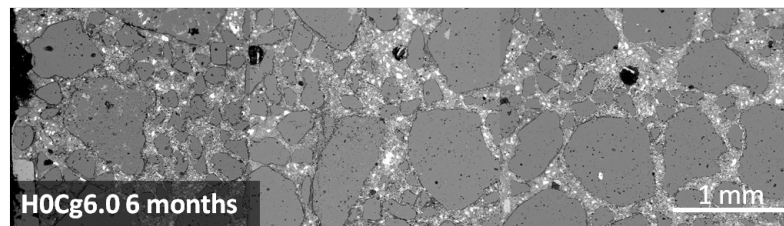


Figure 7.14: SEM, sulfate concentration in the samples.



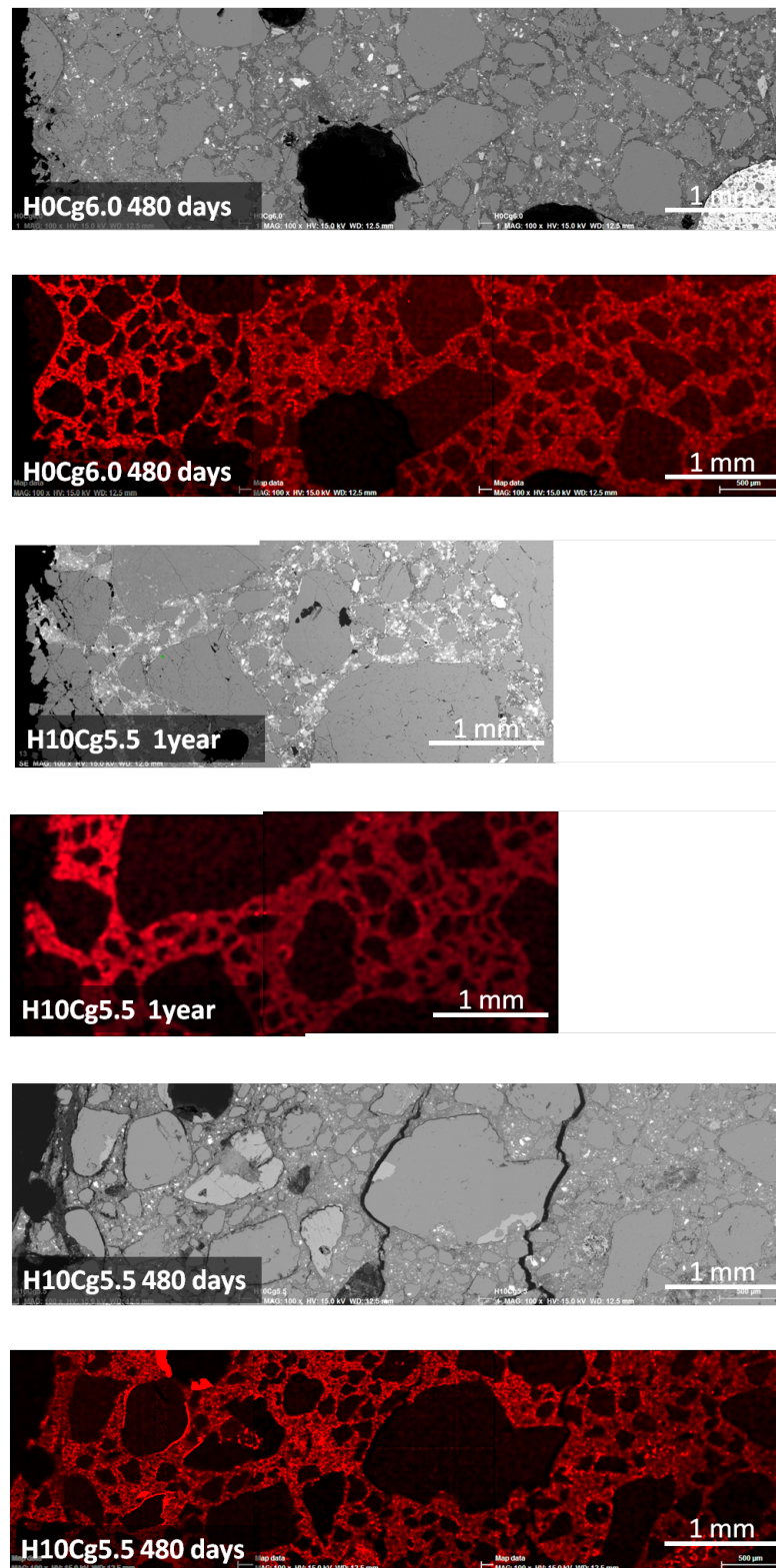


Figure 7.15: SEM pictures (gray pictures) and sulfate profile (colored pictures). Mag:100x, HV:15kV, WD:12.5mm.

7.2 Sorptivity

The method used to measure the sorptivity is explained in the [section ??](#).

In the Figs 7.16, 7.17, 7.18 the sorptivity curves for laboratory and commercial samples, with low and high C_3A clinker, with 0 and 10% of limestone addition and different gypsum content are presented.

The drying process of the mortar cylinders of the 60mm diameter and height of 50mm is a long process, which can take up to 1 year. Tested samples were only dried for 30 days in isopropanol and later 30 days in a desiccator to shorten this period. However results show that this period was too short and some inconsistencies in the results are observed.

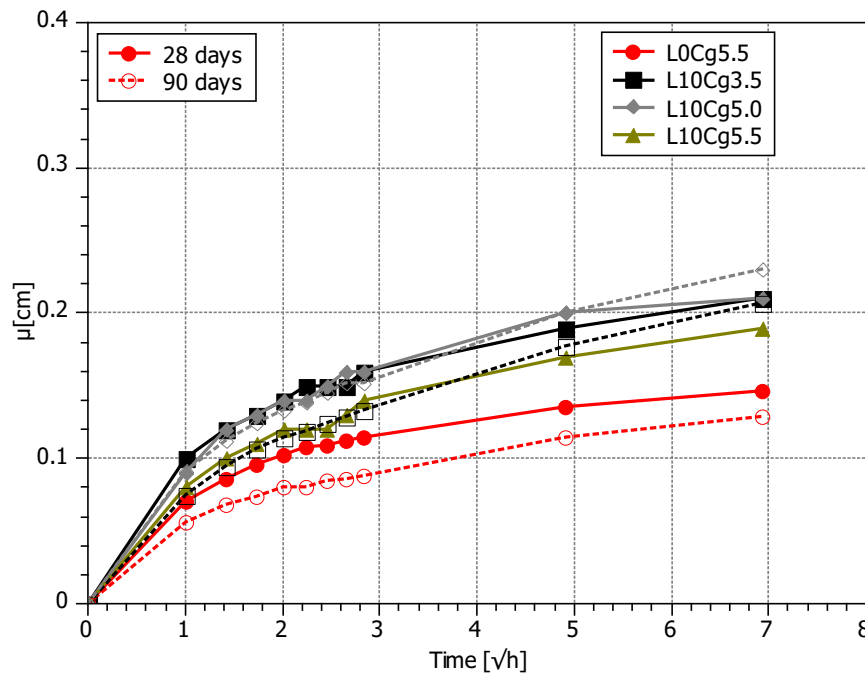


Figure 7.16: Sorptivity data at 28 and 90 days of hydration. Low C_3A clinker with 0 and 10% of limestone.

The results show that sorptivity is increasing with limestone addition and with increasing gypsum content sorptivity decreases. However there are some inconsistencies in results therefore it is difficult to draw clear conclusions.

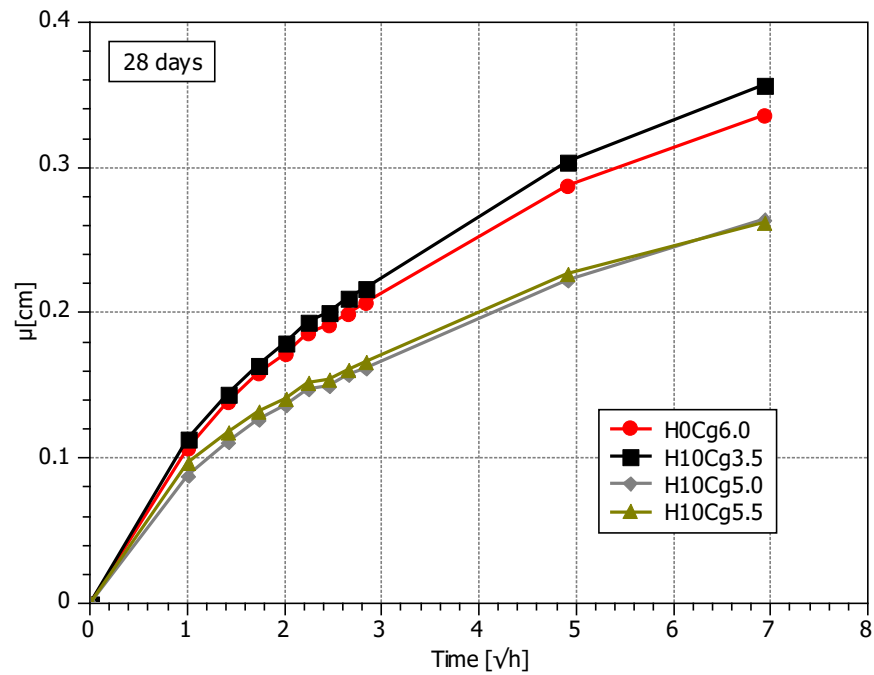


Figure 7.17: Sorptivity data at 28 days of hydration. High C_3A clinker with 0 and 10% of limestone.

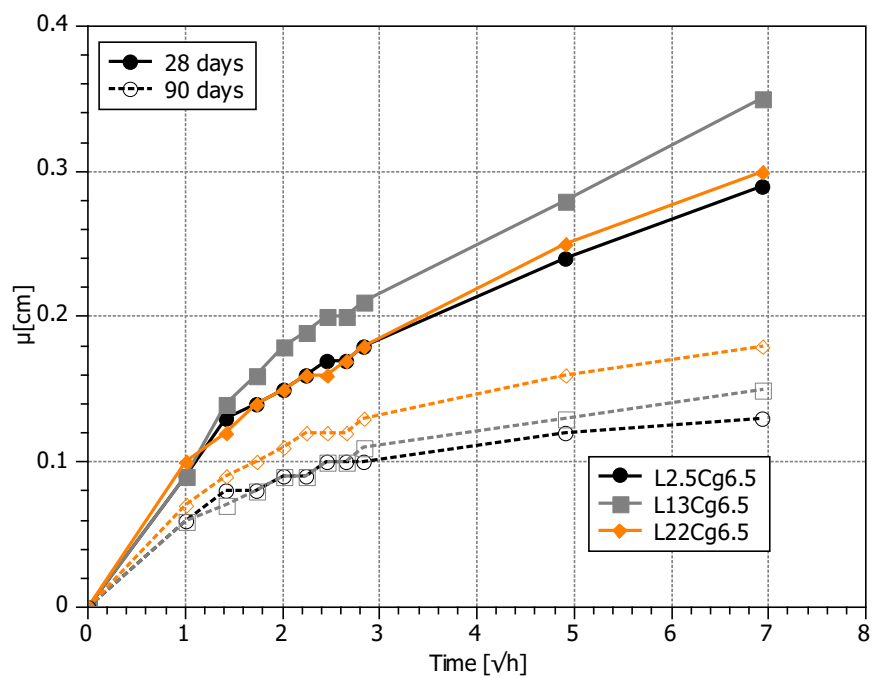


Figure 7.18: Sorptivity data at 28 and 90 days of hydration. Commercial Cements.

7.3 Summary

In this chapter durability of cement with limestone and different gypsum content are discussed. Mechanism of sulfate attack and limestone influence on the sulfate attack and sorptivity is presented.

Sulfate attack

- Limestone samples are more susceptible to sulfate attack only if high C_3A content of clinker is used in cement
- Limestone does not have a direct influence on the deterioration of the mortars exposed to the sulfate attack
- In the cement with low C_3A (3%) clinker substitution by limestone up to 22% does not decrease the cement resistant to the sulfate attack
- Thaumasite was observed in a little amount and after long exposure to the sulfate solution (480 days) just before samples was total destroyed, therefore it was concluded, as proposed by Schmidt [78] that thaumasite is only last stage product of the sulfate attack but not a cause of the samples deterioration

Sorptivity

- Sorptivity increases with limestone and decreases with increasing gypsum addition, however the results are inconsistent due to incomplete drying of the sample

Chapter 8

Main findings and future perspective

This thesis focused on influence of limestone on the hydration and properties of cements with low and high C_3A clinker and different gypsum content.

The first part concentrated on the general influence of limestone on the hydration of the clinker phases and the phases assemblage, when 0 and 10% of limestone is in the system and gypsum at optimum and how increasing limestone addition from 0–20% of limestone addition, can influence the hydration of cements.

The second part concentrated on the influence of gypsum on cement hydration and properties and how 10% of limestone addition influences the gypsum effect in the cement system. In this part also the effect of temperature was investigated.

Finally some investigations of durability were made.

The main findings and future perspective are presented below.

8.1 Main findings

8.1.1 Methods

Wide range of methods was used in the study. The main development was a:

- new way of samples treatment for XRD Rietveld Analysis was developed, samples compaction by continuous displacement of the spatula. This method avoids prefer orientation of the susceptible phases. Additionally this method allows to better qualify the hemi- and monocarboaluminate.

8.1.2 Hc and Mc formation

The influence of limestone depends on many aspects especially clinker composition and gypsum content in the cement. However the general influence of limestone and the

cement hydration and properties are:

- Substitution of clinker by any amount of limestone addition results in monocarboaluminate phases formation during cement hydration.
- The formation of monocarboaluminate (Mc), its time and amount depends on the aluminum availability to react with limestone:
 - With increasing C_3A content, the Mc amount increases. For high C_3A cement it is visible at 2 days of hydration and at the 720 days 4.5% of monocarboaluminate is measured in the system. For low C_3A cements it is visible at 7 days of hydration and at the 720 days 1.6% of monocarboaluminate is measured in the system. Monocarboaluminate is formed only after all gypsum is used to produce ettringite.
- The formation of monocarboaluminate (Mc) is always accompanied by hemicarboaluminate (Hc) formation.
- The formation of Hc is observed up to 28 days (low C_3A clinker) and 90 days (high C_3A clinker) later disappears, possible due to its carbonation to monocarboaluminate.

8.1.3 Ettringite formation

Ettringite is a difficult phase to quantify by XRD Rietveld Analysis due to decomposition after treatment in isopropanol therefore visible differences in ettringite formation between samples are generally not significant. The following conclusions about ettringite formation can be drawn:

- Ettringite formation is visible earlier when limestone is in the system and the amount of ettringite formed is higher. There is more sulfate available to form ettringite.

8.1.4 C–S–H composition

- Ca/Si ratio in C–S–H of hydrated cement was found to be higher than in model C–S–H used in GEMS calculations. Additionally there is an uptake of certain amount of Al and S into C–S–H.

8.1.5 Kinetics

The kinetics of the hydration are influenced by many aspects such as C_3A , gypsum, limestone content.

Influence of clinker

- It has to be noticed that in the present study the low and high C_3A clinker also had significant differences in C_3S content and different SO_3/Al_2O_3 ratios, therefore some of the differences between cements are more attributable to higher C_3S content and lower SO_3/Al_2O_3 in high C_3A clinker in comparison to low C_3A clinker cement. However with high C_3A in comparison to low C_3A :
 - Acceleration in accelerating period due to higher C_3S content
 - Shortening of the induction period due to higher C_3S content
 - Higher heat evolution rate for silicate and aluminate reaction
 - More peaks visible

Effect of gypsum

- With increasing gypsum addition a steeper accelerating period is observed, however no visible increase in C_3S consumption by XRD Rietveld Analysis is measured. Increasing gypsum addition causes a delay in the aluminate reaction and additional peaks in aluminate region are observed.
- With very high gypsum addition there is a visible suppression of the hydration reaction. The heat rate and total heat evolved are lower. The same effect is observed for all cement compositions.

Effect of limestone

- With addition of 10% of limestone there are small differences in kinetics which vary from batch to batch of the cement.
- In general there is a small increase in the accelerating period with 10% of limestone addition.
- With increasing limestone addition up to 20%, an increase in accelerating period is observed for heat evolution normalized per gram of clinker. There is an earlier aluminate reaction with increasing limestone addition is due to decreasing SO_3/Al_2O_3 ratio with increasing limestone addition in those set of samples.

8.1.6 Porosity

- Effects of low limestone (10%) addition on the porosity are slight at early ages and at later ages the differences are insignificant.
- There are significant differences in porosity when gypsum content in cement varies (2.2–9.0). However there is no clear relationship with gypsum addition and total porosity, it depends on the cement composition and time of hydration.

8.1.7 Compressive strength

Limestone addition

- Compressive strength is not influenced by 10% limestone addition at early age up to 24 hours of hydration. At later ages limestone slightly decreases compressive strength.
- High C_3A clinker cement produces twice more monocarboaluminate in comparison to low C_3A clinker cement which contributes to compressive strength and lower decrease in strength for high C_3A clinker cement than for low C_3A clinker cement when 10% of limestone is added.
- With increasing limestone addition compressive strength decreases.

Gypsum addition

- There is an optimum gypsum at which compressive strength is the highest. Samples with the optimum gypsum content and the highest compressive strength do not always shows the highest peak in rate of heat evolution for silicate reaction nor the highest total heat evolved.
- Optimum gypsum depends on the cement composition. Slightly increases with C_3A content and slightly decreases with limestone addition.
- Regardless of the C_3A content, systems are more sensitive to the overdosing of gypsum than to underdosing.
- With 10% of limestone addition there is smaller loss in strength when gypsum content is different from optimum.

8.1.8 Alite–gypsum–limestone system

In pure systems of alite, gypsum and limestone have a direct influence on the alite hydration.

8.1.9 Temperature influence

- Temperature accelerates the hydration reactions as an effect compressive strength increases with temperature especially in early age. At 28 days the highest compressive strength is shown by sample cured at 10°.
- The activation Energy is similar for all cement mixes.

8.1.10 Durability

Limestone is not responsible for a deterioration of the mortars exposed to sulfate attack. Samples with limestone addition are only more susceptible for the sulfate attack when high C₃A clinker is used in cement.

8.2 Perspective

In this study we tried to look at the affect of C₃A content. however there were several other differences between the two cements, notably their C₃S content. Therefore in order to have a more systematic understanding of the influence of C₃A more similar clinkers or model systems should be studied.

Regarding the effect of gypsum, it was very difficult to quantify the differences between samples with different gypsum contents. The variation in the amount of phases formed and porosity was usually less than the precision of the measurement techniques. The micrographs indicated that there were differences in the distribution of hydration products, for example size of gaps between reacting grains and hydrate shells. However we could not find any way to reliably quantify these effects. It would be interesting to test hypotheses about the hydrate distribution by modelling, but this requires a reliable method for calculating mechanical properties which does not exist at present time.

The optimum amount of gypsum for low C₃A and high C₃A clinkers was similar, 5.5 and 6.0% respectively. Therefore SO₃/Al₂O₃ for low C₃A clinker was 2.5 times higher than for high C₃A (SO₃/Al₂O_{3_{low}} = 2.60, SO₃/Al₂O_{3_{high}} = 0.98). If gypsum is regulating only C₃A reaction, as is generally accepted in the cement science the

$\text{SO}_3/\text{Al}_2\text{O}_3$ ratio should be the same for each cement at optimum gypsum. The reason for differences in $\text{SO}_3/\text{Al}_2\text{O}_3$ for optimum gypsum should be investigated further.

Main subject of present study was limestone addition in cement. Up to 20% of clinker was substituted by limestone addition. At this level the compressive strength significantly decreased. However the total heat evolved per gram of clinker measured by calorimetry curve increased up to 20% of limestone addition, Therefore it would be interesting to prepare the same cement mixes where limestone would be substituted by inert filler to distinguish to which extent the effects of limestone are due to its chemical reaction.

Limestone influence on the hydration and properties was investigated with the same for all mixes and limestone additions water/cement(clinker+gypsum+limestone) ratio . Water available for clinker reaction was increasing with increasing limestone addition. Moreover the workability of mixes with limestone cement were very good. Therefore it would be interesting to prepare cement pastes at constant workability and investigate how the properties of cement with increasing limestone addition are influenced, especially kinetics, compressive strength and porosity.

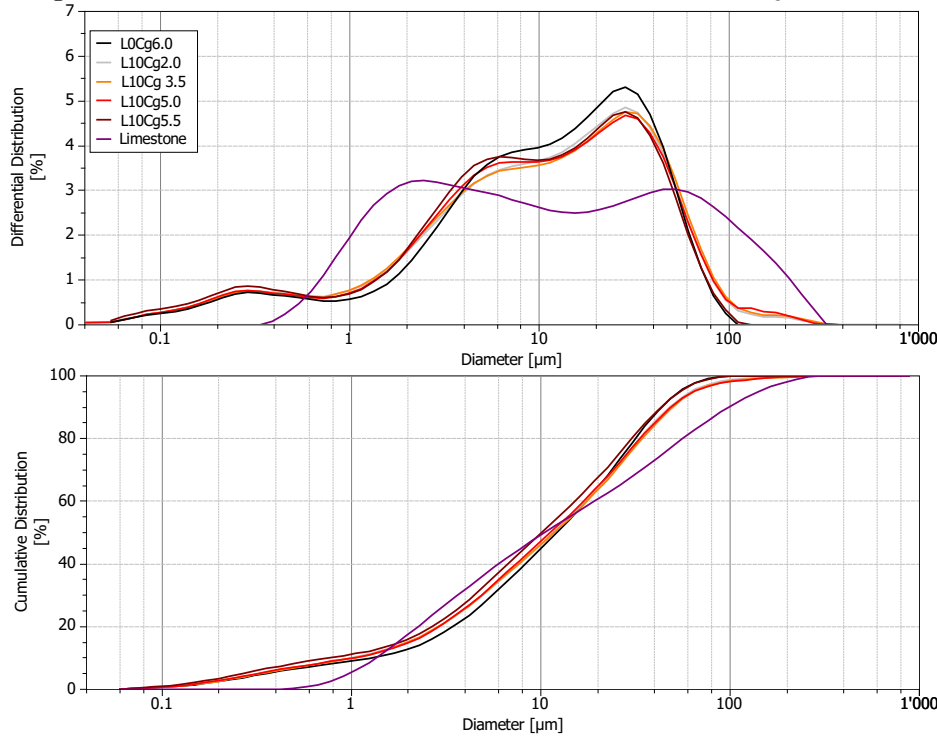
In terms of durability a more complete study is needed. Here we had problems with conditioning samples to obtain good measurements of sorptivity. MIP did not indicate significant changes in porosity. Performance in sulfate solutions did not change dramatically as C_3A is the dominant influence but the pattern of failure was changed. It would be interesting to investigate these effects further.

Appendices

Appendix A

Materials

Figure A.1: Particle size distribution. Cements with low C₃A content.



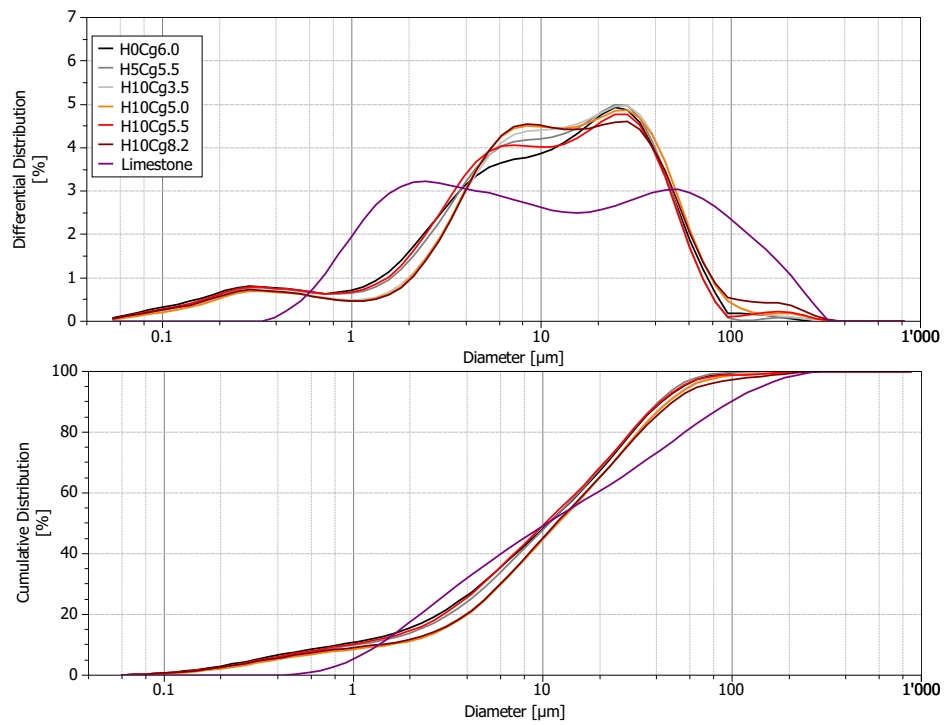


Figure A.2: Particle size distribution. Cements with high C_3A content.

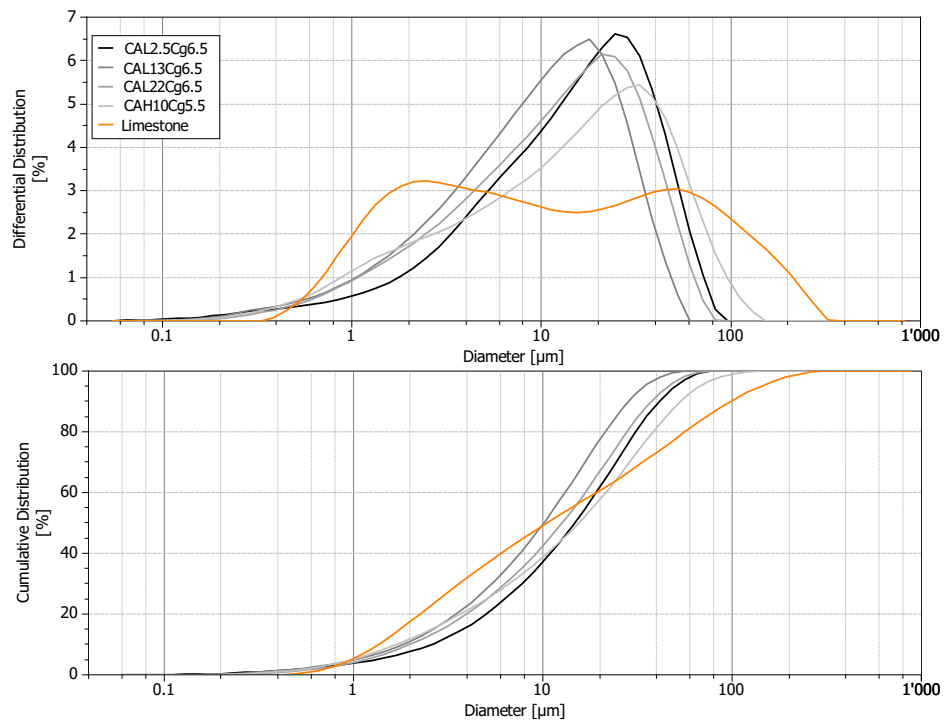


Figure A.3: Particle size distribution. Commercial Cements.

Table A.1: Laboratory Cements Composition. Cements without limestone

Name	Components	[%]	$G_{ypsum}/C_{clinker}$	SO_3/Al_2O_3	CaO	SiO ₂	Al ₂ O ₃	Fe ₂ O ₃	SO ₃	MgO	Na ₂ O	K ₂ O	Cl	LOI
Low C ₃ A clinker (3%)														
L0Cg2.2	clinker gypsum	97.8 2.2	0.023	1.04	62.32	21.99	3.65	4.40	2.19	1.78	0.24	0.89	0.01	2.16
L0Cg3.9	clinker gypsum	96.1 3.9	0.041	1.85	61.85	21.89	3.64	4.38	2.93	1.75	0.22	0.88	0.01	2.08
L0Cg5.5	clinker gypsum	94.5 5.5	0.058	2.60	61.66	21.46	3.58	4.30	3.72	1.74	0.20	0.87	0.01	2.10
L0Cg6.0	clinker gypsum	94.0 6.0	0.064	2.84	62.34	21.76	3.87	4.49	3.51	1.91	0.17	0.90	0.01	0.74
L0Cg9.0	clinker gypsum	91.0 9.0	0.099	4.26	62.37	21.12	3.63	4.49	4.14	1.82	0.23	0.88	0.01	0.78
High C ₃ A clinker (8%)														
H0Cg3.8	clinker gypsum	96.2 3.8	0.040	0.62	63.16	20.03	5.6	2.33	3.30	2.68	0.300	1.25	0.01	0.85
H0Cg5.5	clinker gypsum	94.5 5.5	0.058	0.90	62.83	19.71	5.57	2.40	3.88	2.64	0.187	1.24	0.01	1.09
H0Cg6.0	clinker gypsum	94.0 6.0	0.064	0.98	62.70	19.76	5.5	2.28	4.18	2.63	0.244	1.23	0.01	1.01
H0Cg9.0	clinker gypsum	91.0 9.0	0.099	1.48	61.86	19.10	5.38	2.32	5.64	2.58	0.422	1.16	0.01	1.07

Table A.2: Laboratory Cements Composition. Cements with limestone

Name	Components	[%]	$C_{\text{gypsum}}/C_{\text{clinker}}$	SO_3/Al_2O_3	CaO	SiO ₂	Al ₂ O ₃	Fe ₂ O ₃	SO ₃	MgO	Na ₂ O	K ₂ O	Cl	LOI
Low C ₃ A clinker (3%)														
L10C _g 2.0	clinker	88.0												
	gypsum	2.0	0.023	1.04	60.99	20.41	3.38	4.03	2.06	1.70	0.20	0.82	0.01	6.05
	limestone	10												
L10C _g 3.5	clinker	86.5												
	gypsum	3.5	0.041	1.85	60.73	19.96	3.3	3.95	2.80	1.67	0.20	0.81	0.01	6.23
	limestone	10												
L10C _g 5.0	clinker	85.0												
	gypsum	5.0	0.058	2.60	60.51	19.66	3.25	3.88	3.57	1.65	0.19	0.79	0.01	6.09
	limestone	10												
L10C _g 5.5	clinker	84.5												
	gypsum	5.5	0.064	2.84	61.43	20.18	3.45	4.18	3.09	1.81	0.18	0.81	0.01	4.62
	limestone	10												
L10C _g 8.2	clinker	81.8												
	gypsum	8.2	0.099	4.26	63.46	20.42	3.54	4.22	4.34	1.81	0.21	0.86	0.01	0.78
	limestone	10												
High C ₃ A clinker (8%)														
H10C _g 3.5	clinker	86.5												
	gypsum	3.5	0.040	0.62	62.07	18.60	5.18	2.24	2.87	2.54	0.253	1.14	0.01	4.74
	limestone	10												
H10C _g 5.0	clinker	85.0												
	gypsum	5.0	0.059	0.90	61.98	18.12	5.04	2.18	3.66	2.46	0.147	1.10	0.01	4.91
	limestone	10												
H10C _g 5.5	clinker	84.5												
	gypsum	5.5	0.065	0.98	61.86	18.08	5.00	2.16	3.75	2.46	0.242	1.09	0.01	5.01
	limestone	10												
H10C _g 8.2	clinker	81.8												
	gypsum	8.2	0.100	1.48	60.78	17.82	4.96	2.12	4.87	2.45	0.310	1.09	0.01	5.30
	limestone	10												

Table A.3: Laboratory Cements Composition. Cements with increasing limestone addition.

Name	Components	[%]	G_{yps}/C_{lin}	SO_3/Al_2O_3	CaO	SiO ₂	Al ₂ O ₃	Fe ₂ O ₃	SO ₃	MgO	Na ₂ O	K ₂ O	Cl	LOI
High C ₃ A clinker (8%)														
H5Cg5.5	clinker	89.5												
	gypsum	5.5	0.061	0.95	62.72	19.38	5.36	2.23	3.52	2.54	0.295	1.058	0.00	2.55
	limestone	5												
H15Cg4.5	clinker	80.5												
	gypsum	4.5	0.056	0.87	61.59	18.08	4.98	2.12	3.25	2.41	0.146	0.981	0.00	6.40
	limestone	15												
H20Cg4.0	clinker	76.0												
	gypsum	4.0	0.053	0.82	61.03	17.42	4.74	2.03	3.19	2.32	0.089	0.957	0.00	8.46
	limestone	20												

Table A.4: Commercial Cements Composition

Name	Components	[%]	G_{yps}/C_{lin}	SO_3/Al_2O_3	CaO	SiO ₂	Al ₂ O ₃	Fe ₂ O ₃	SO ₃	MgO	Na ₂ O	K ₂ O	Cl	LOI
Low C ₃ A clinker (3%)														
CAL2.5Cg6.5	clinker	91.0												
	gypsum	6.5	0.061	1.55	62.44	20.9	4.41	2.61	4.11	1.82	0.300	0.940	0.01	2.06
	limestone	2.5												
CAL13Cg6.5	clinker	80.5												
	gypsum	6.5	0.081	1.37	60.85	18.40	3.85	2.42	4.13	1.62	0.270	0.720	0.01	7.32
	limestone	13												
CAL22Cg6.5	clinker	71.5												
	gypsum	6.5	0.091	1.22	60.45	17.57	3.56	2.17	3.89	1.57	0.290	0.650	0.01	10.05
	limestone	22												
High C ₃ A clinker (8%)														
CAH10Cg5.5	clinker	84.5												
	gypsum	5.5	0.065	0.87	60.05	18.73	4.86	2.11	4.66	2.15	0.310	1.140	0.01	5.52
	limestone	10												

Table A.5: XRD analysis of laboratory cement – Low C₃A clinker

	L0Cg2.2	L0Cg3.9	L0Cg5.5	L0Cg6.0	L0Cg9.0	L10Cg3.5	L10Cg5.0	L10Cg5.5	L10Cg6.0	L10Cg9.0
Alite	60.48	63.56	58.67	57.23	63.19	56.11	51.70	52.29	53.55	54.40
Belite	20.73	14.90	18.68	21.92	16.29	11.84	16.59	15.78	19.30	14.60
Aluminate cub.	1.22	1.37	0.88	0.90	1.53	1.33	1.34	1.10	1.34	1.42
Aluminate orth.	2.23	1.85	2.03	2.50	1.69	2.12	1.15	1.59	1.60	1.20
Total C₃A	3.43	3.22	2.91	3.40	3.22	3.45	2.49	2.69	2.94	2.62
Ferrite	11.88	12.11	12.16	12.55	13.39	12.28	11.25	10.79	11.31	11.95
Gypsum	0.89	2.35	3.53	2.91	3.97	1.26	2.19	2.57	3.02	3.53
Hemihydrate	0.00	0.00	0.49	0.57	0.00	0.41	1.20	0.00	0.53	0.00
Anhydrite	0.56	0.82	0.74	0.58	0.00	1.22	0.68	0.84	0.68	0.49
Total	1.54	3.18	4.75	4.06	3.97	2.90	4.08	3.42	4.22	3.53
Arcanite	1.08	1.13	1.48	0.00	0.00	2.37	2.91	1.91	0.00	0.00
Free Lime	0.00	1.07	0.63	0.00	0.00	0.00	0.00	0.73	0.00	0.00
Periclase	0.84	0.83	0.71	0.83	0.00	0.53	0.56	0.66	0.83	0.00
Calcite	0.00	0.00	0.00	0.00	0.00	10.05	10.10	10.95	7.12	11.7
Quartz	0.00	0.00	0.00	0.00	0.00	0.32	0.43	0.72	0.68	

Table A.6: XRD analysis of laboratory cement – High C₃A clinker

	H0Cg3.8	H0Cg5.5	H0Cg6.0	H0Cg9.0	H10Cg3.5	H10Cg5.0	H10Cg5.5	H10Cg8.2
Alite	74.33	72.99	72.60	70.92	67.01	65.73	65.74	64.09
Belite	7.37	7.53	7.49	6.10	6.11	6.13	5.42	4.77
Aluminate cub.	8.47	8.40	8.36	8.87	7.28	7.29	7.24	5.86
Aluminate orth.	0.00	0.00	0.00	0.00	0.00	0.00	0.00	1.62
Total C₃A	8.47	8.40	8.36	8.87	7.28	7.29	7.24	7.48
Ferrite	6.24	5.56	5.53	5.94	6.21	4.76	5.28	5.52
Gypsum	2.30	4.71	5.14	7.27	2.03	3.84	3.96	6.79
Hemihydrate	0.00	0.00	0.00	0.00	0.00	0.00	0.00	0.00
Anhydrite	0.00	0.00	0.00	0.00	0.00	0.00	0.44	0.84
Total gypsum	2.30	4.71	5.14	7.27	2.03	3.84	4.40	7.63
Arcanite	0.00	0.00	0.00	0.00	0.00	0.00	0.00	0.00
Free Lime	0.00	0.00	0.00	0.00	0.00	0.00	0.00	0.00
Periclase	1.02	0.81	0.87	0.90	0.87	0.00	0.80	
Calcite	0.00	0.00	0.00	0.00	10.51	12.26	11.13	10.51
Quartz	0.00	0.00	0.00	0.00	0.00	0.00	0.00	0.00

Table A.7: XRD analysis – laboratory cement High (8%) C₃A clinker and increasing limestone content and commercial cement

	Laboratory Cements			Commercial Cements			
	H5Cg5.5	H15Cg4.5	H20Cg4.0	CAL2.5Cg6.5	CAL13Cg6.5	CAL22Cg6.5	CAH10Cg5.5
Alite	63.50	56.43	51.68	63.39	55.80	49.10	52.68
Belite	9.29	7.50	7.36	10.55	8.26	9.71	12.22
Aluminate cub.	6.67	5.94	5.29	2.61	0.92	1.18	5.29
Aluminate orth.	1.29	0.97	1.15	1.68	2.40	2.40	1.15
Total C₃A	7.93	6.91	6.44	4.29	3.58	3.58	6.44
Ferite	6.69	6.49	5.66	9.10	9.05	6.62	5.58
Gypsum	3.34	3.02	2.98	4.22	4.22	4.95	1.07
Hemihydrate	0.00	0.00	0.00	0.92	1.32	0.83	3.13
Anhydrite	0.86	0.86	0.69	1.25	1.33	1.14	1.26
Total gypsum	4.2	3.88	3.67	6.39	6.87	6.92	5.46
Arcanite	1.69	1.75	2.05	2.20	1.78	1.14	2.88
Free Lime	0.00	0.00	0.38	0.00	0.64	0.00	0.00
Periclase	0.00	1.33	1.13	1.03	0.61	0.79	1.03
Calcite	5.20	15.06	20.53	2.50	13.00	21.49	11.43
Quartz	0.00	0.67	1.10	0.56	0.67	1.10	0.00

Appendix B

Methods

Table B.1: Phases structures used in the XRD Rietveld Refinement

Phase	Chemical Formula	Crystal system	ICSD	References
Alite	C_3SiO_5	Monoclinic/ M_3	94742	de la Torre et al., 2002 [19]
Belite	C_2SiO_4	Monoclinic/ β	79550	Tsurumi et al., 1994 [93]
Tricalcium aluminate	$\text{C}_3\text{Al}_2\text{O}_6$	Cubic	1841	Mondal et al., 1975 [56]
Tricalcium aluminate	$\text{C}_{8.5}\text{NaAl}_6\text{O}_{18}$	Orthorhombic	1880	Nishi et al., 1975 [57]
Ferrite	C_2AlFeO_5	Orthorhombic	9197	Coleville et al., 1971 [17]
Limne	CaO	Cubic	75785	Huang et al., 1994 [35]
Periclase	MgO	Cubic	104844	Taylor, 1984 [88]
Calcite	CaCO_3	Rhombohedral	79674	Wartchow, 1989 [96]
Gypsum	$\text{CaSO}_4 \cdot 2\text{H}_2\text{O}$	Monoclinic	2059	Cole et al., 1974 [16]
Hemihydrate	$\text{CaSO}_4 \cdot 0.5\text{H}_2\text{O}$	Monoclinic	73263	Abreil et al., 1993 [1]
Anhydrite	CaSO_4	Orthorhombic	40043	Hawthorne et al., 1975 [33]
Arcanite	K_2SO_4	Orthorhombic	2827	McGinnety, 1972 [52]
Portlandite	Ca(OH)_2	Rhombohedral	15471	Petch, 1961 [60]
Etringite	$\text{C}_3\text{A}(\text{C}\bar{\text{S}})_3\text{H}_32$	Hexagonal P	16045	Goetz-Neunhoeffer et al., 2006 [30]
Monosulfate	$\text{C}_4\text{A}\bar{\text{S}}\text{H}_12$	Hexagonal	100138	Allmann, 1977 [2]
Monocarboaluminate	$\text{C}_4\text{A}\bar{\text{C}}\text{H}_11$	Triclinic P	59327	Francois et al., 1998 [28]
Hemicarboaluminate	$\text{C}_4\text{AbarC}_{0.5}\text{H}_{11.5}$	Rhombohedral	PDF041-0221	Pöllmann et al., 1989 [63]
Calcium Silicate Hydrate	$\text{Ca}_{1.5}\text{SiO}_{3.5}\text{xH}_2\text{O}$	Unknown	PDF033-0306	Mohan et al., 1980 [55]

Appendix C

SEM EDS analysis

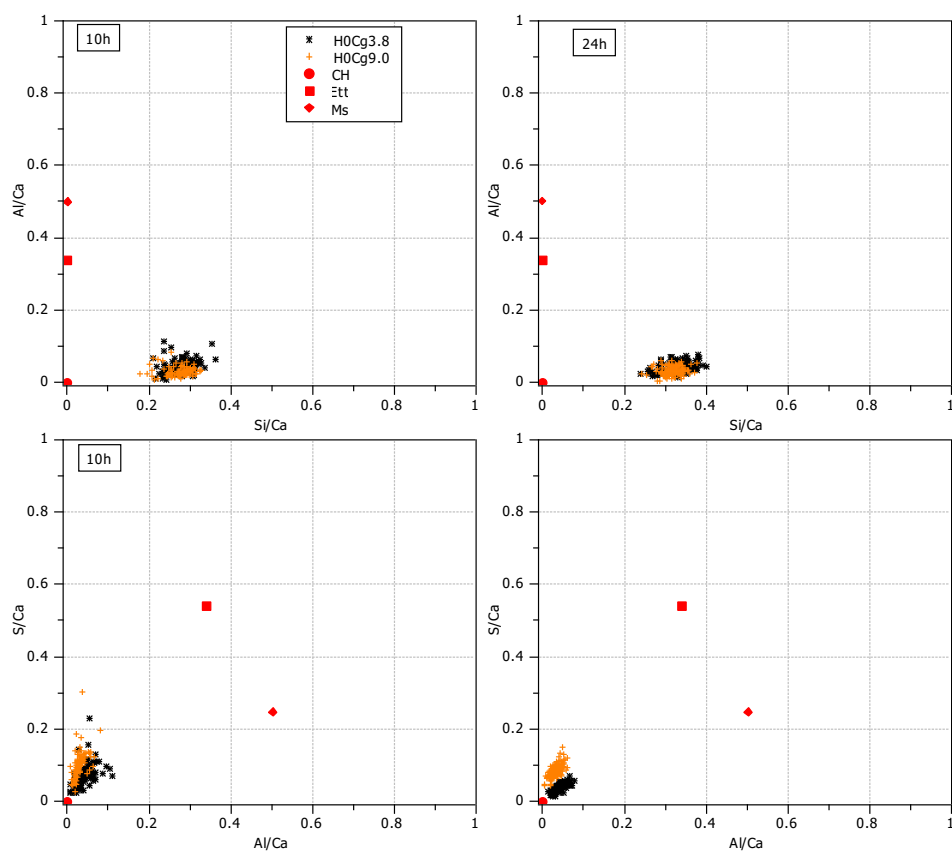


Figure C.1: Inner C–S–H composition by SEM EDS analysis. High C_3A clinker, 3.8 and 9.0 % of gypsum at 10 and 24 hours of hydration.

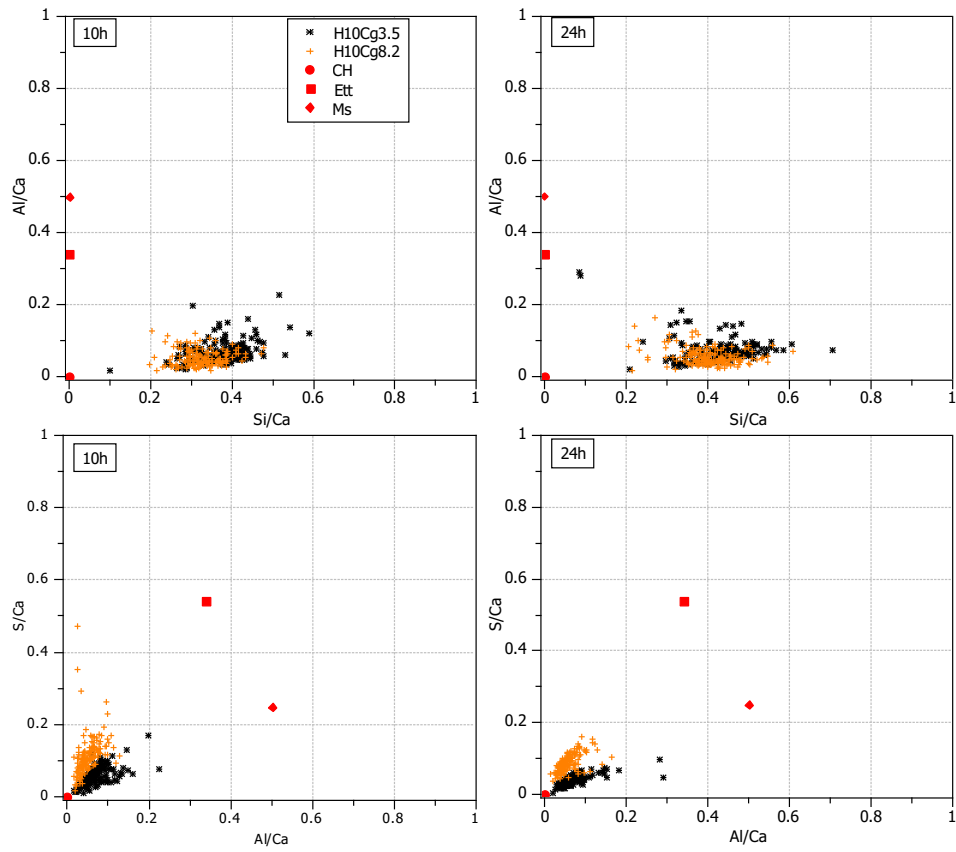


Figure C.2: Inner C-S-H composition by SEM EDS analysis. High C_3A clinker, 10% of limestone addition and different gypsum content at 10 and 24 hours of hydration.

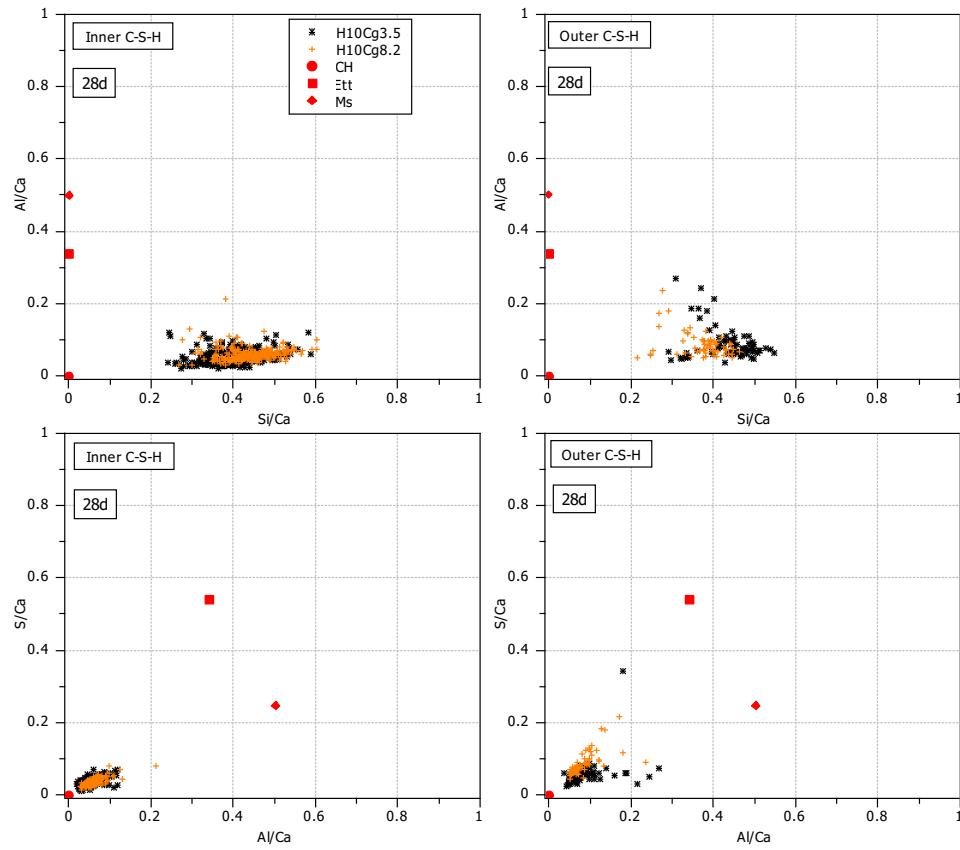


Figure C.3: Inner and outer C-S-H composition by SEM EDS analysis. High C_3A clinker, 10% of limestone addition and different gypsum content at 28 days of hydration.

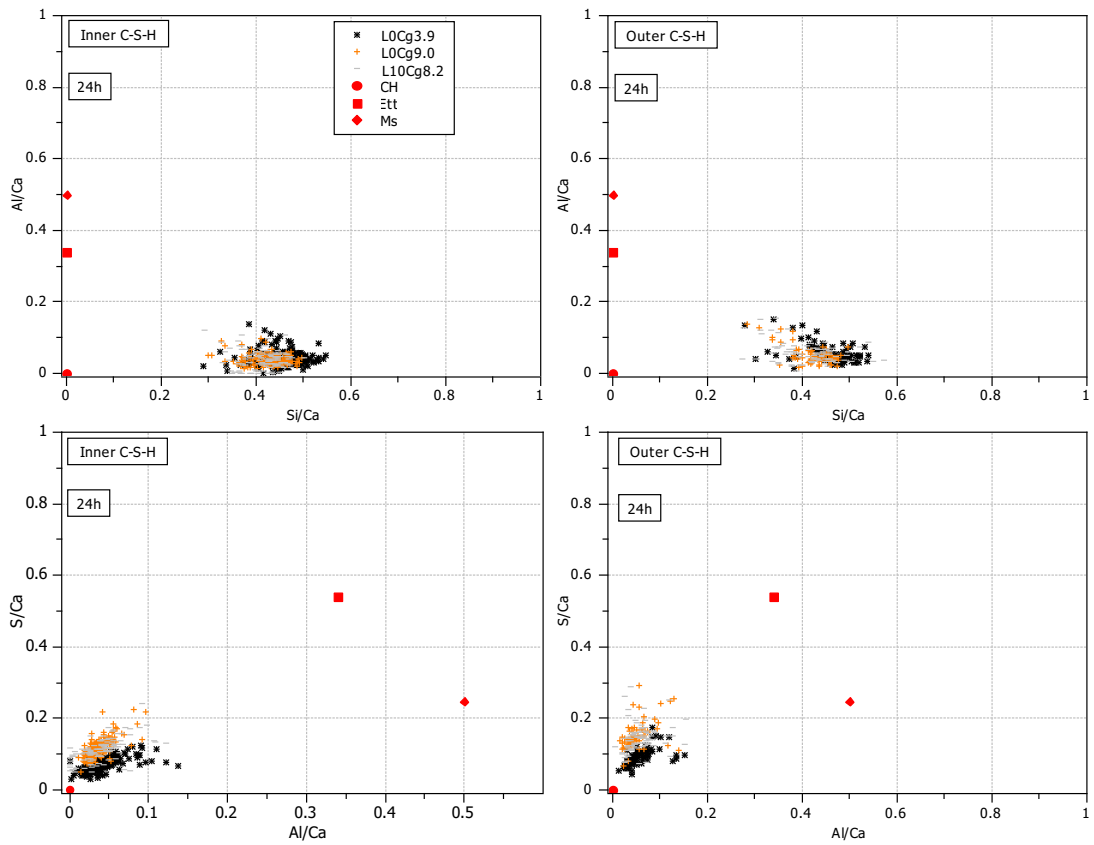


Figure C.4: Inner and outer C-S-H composition by SEM EDS analysis. Low C_3A clinker, 0 and 10% of limestone addition and different gypsum content at 24 hours of hydration.

Appendix D

Influence of limestone on cement hydration

D.0.1 Influence of C_3A content on hemi- and monocarboaluminate formation

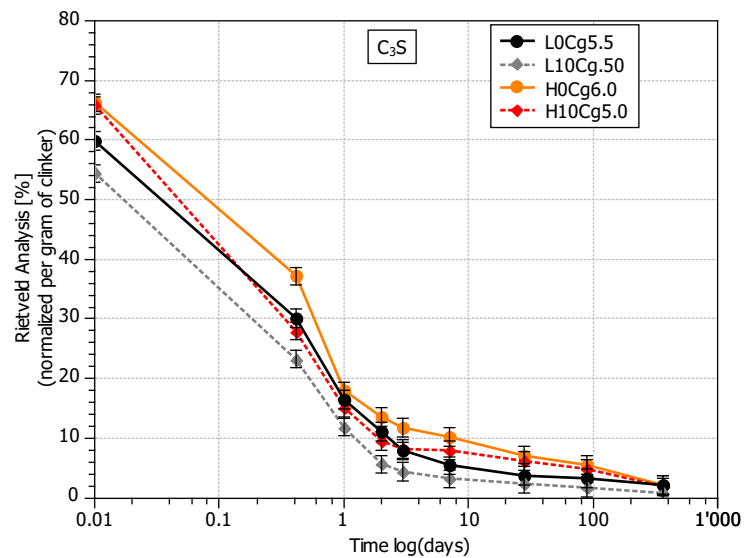


Figure D.1: XRD Rietveld analysis – C_3S quantification.

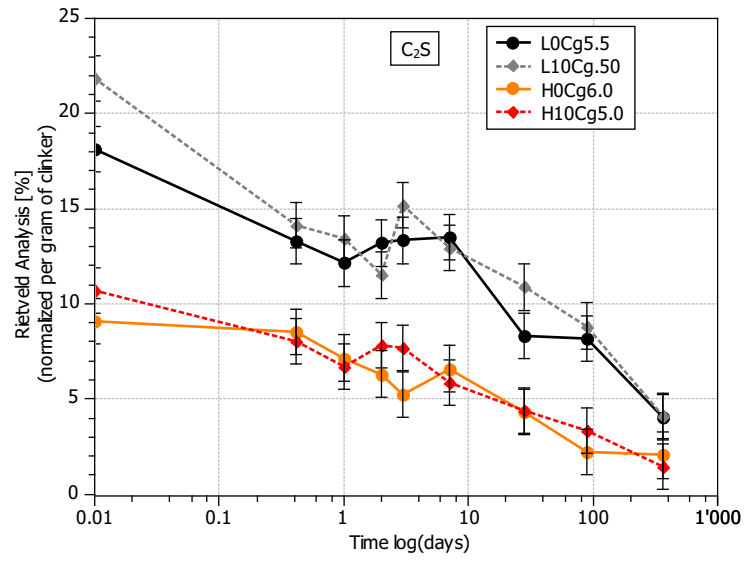


Figure D.2: XRD Rietveld analysis – C₂S quantification.

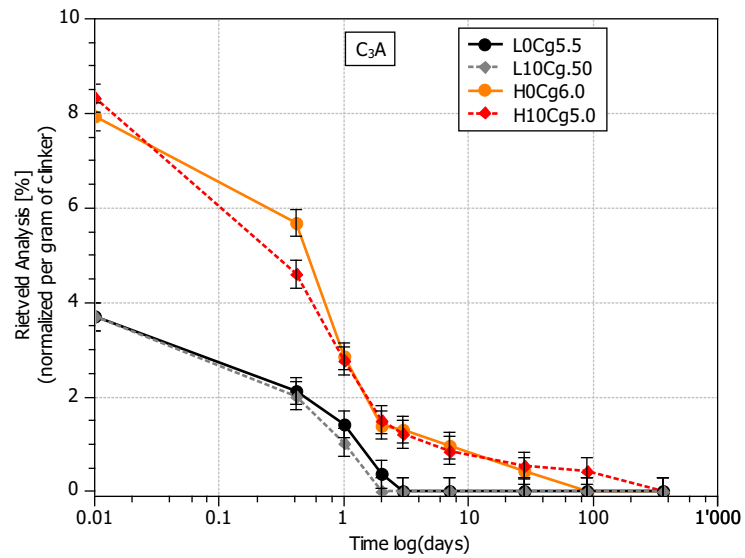


Figure D.3: XRD Rietveld analysis – C₃A quantification.

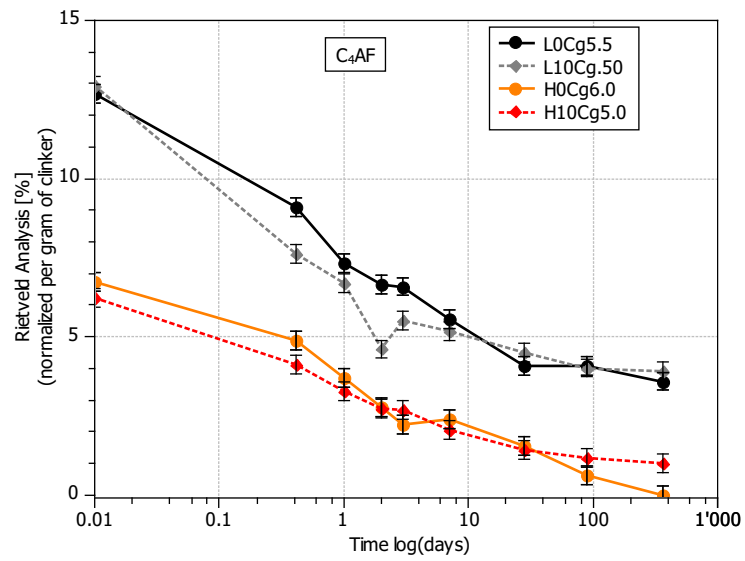


Figure D.4: XRD Rietveld analysis – C₄AF quantification.

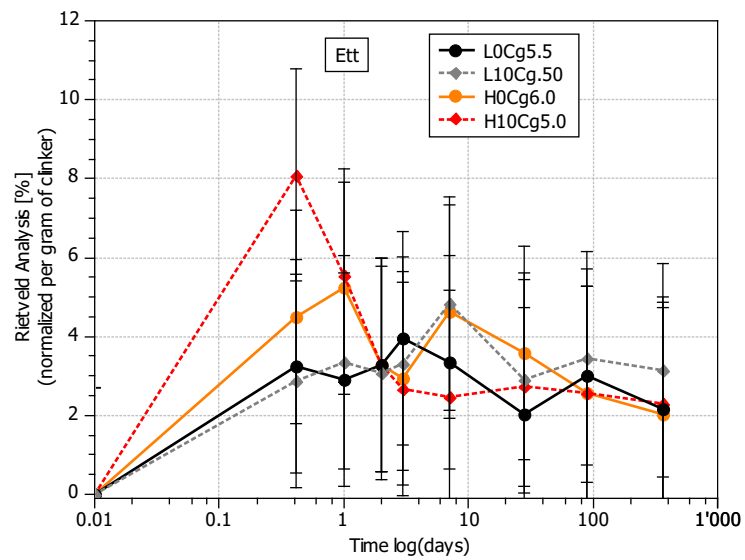


Figure D.5: XRD Rietveld analysis – ettringite quantification.

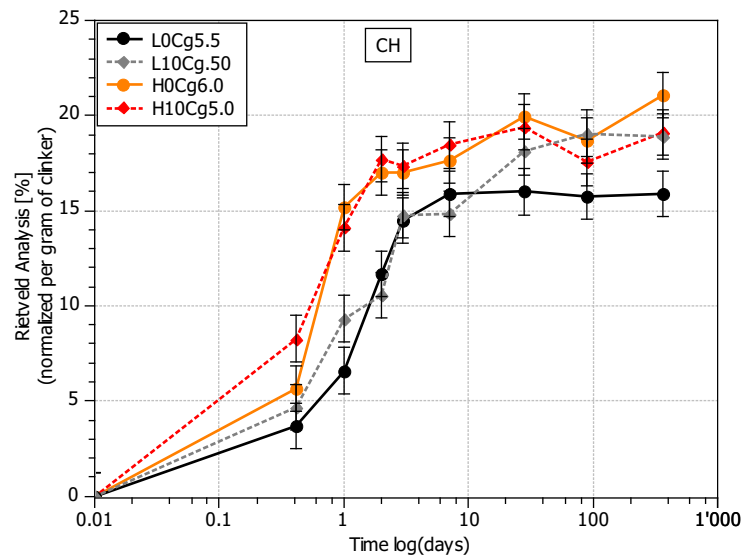


Figure D.6: XRD Rietveld analysis – portlandite quantification.

D.0.2 Commercial cements

D.0.2.1 Kinetics

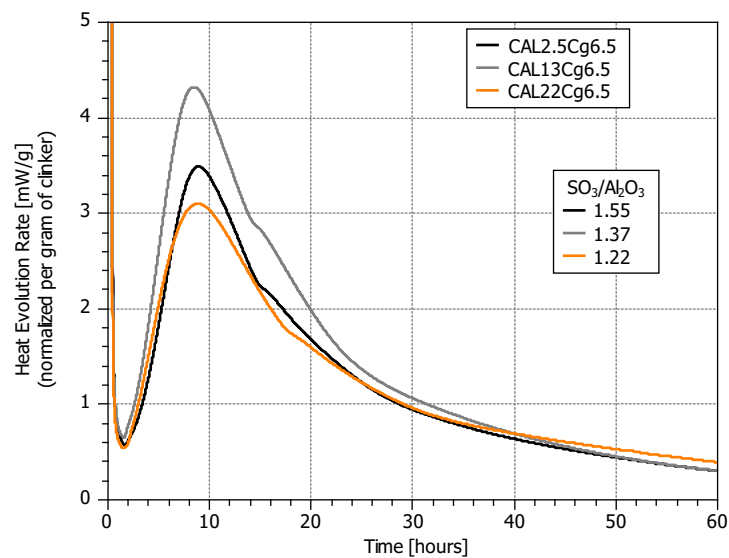


Figure D.7: Heat Evolution Rate for samples with low C_3A content and increasing limestone content.

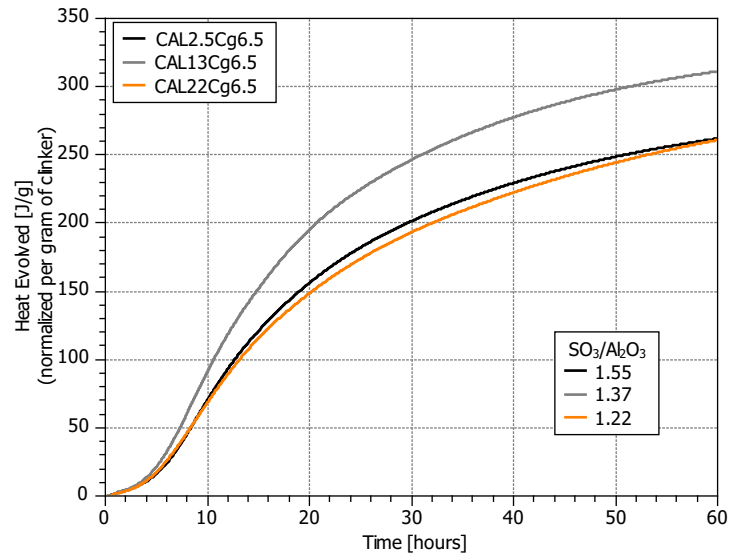


Figure D.8: Heat Evolved for samples with low C_3A clinker and increasing limestone content.

D.0.2.2 Phase assemblage

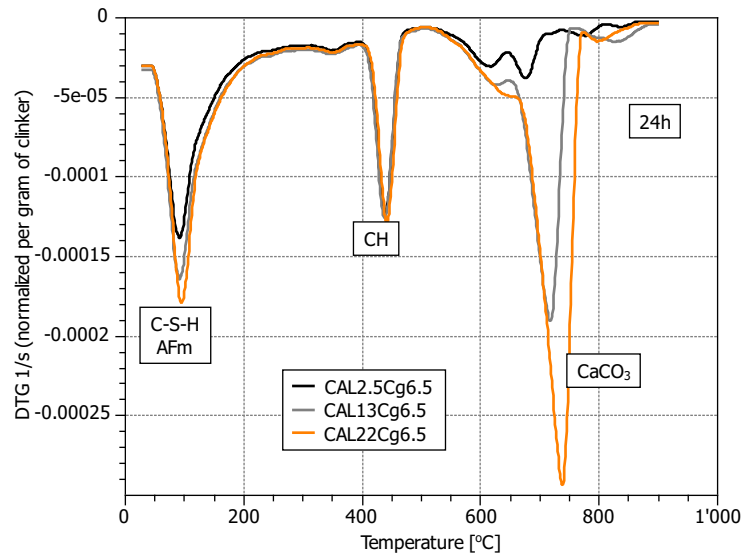


Figure D.9: Thermal Gravimetry data at 24 hours of hydration. Commercial cements with low C_3A content and increasing limestone addition.

D.0.2.3 Porosity

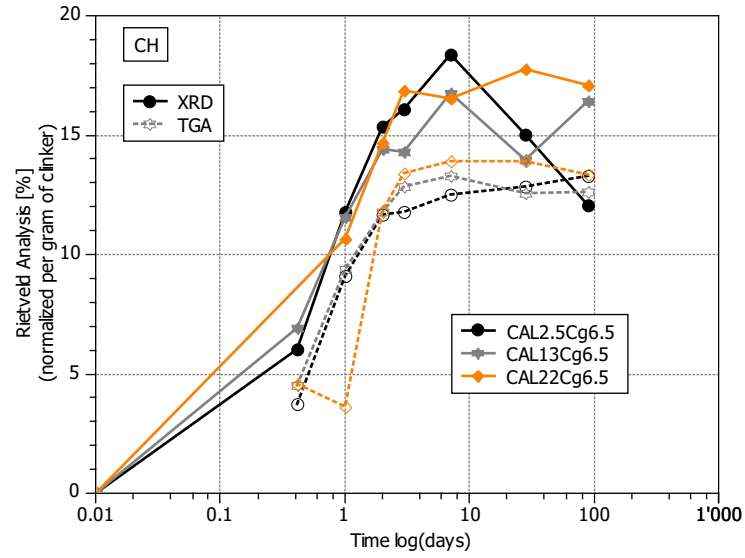


Figure D.10: Portlandite quantification by XRD Rietveld Analysis and TGA analysis. Commercial cements with low C_3A content and increasing limestone addition.

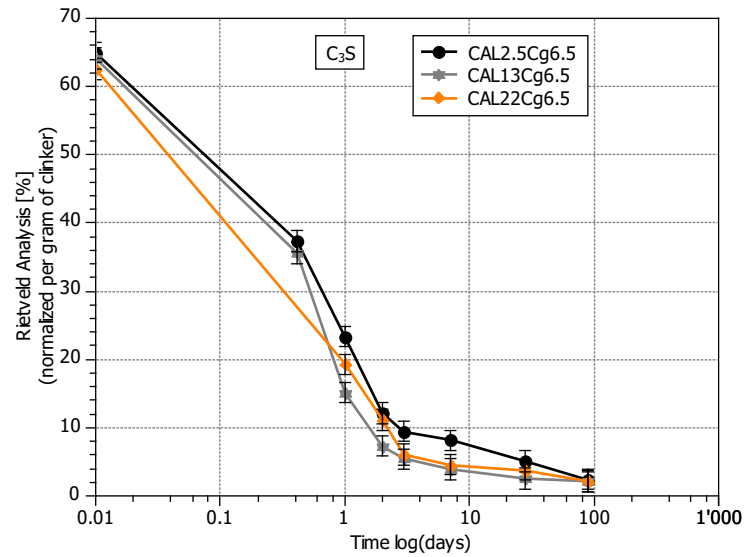


Figure D.11: XRD Rietveld Analysis. C_3S quantification. Commercial cements with low C_3A content and increasing limestone addition.

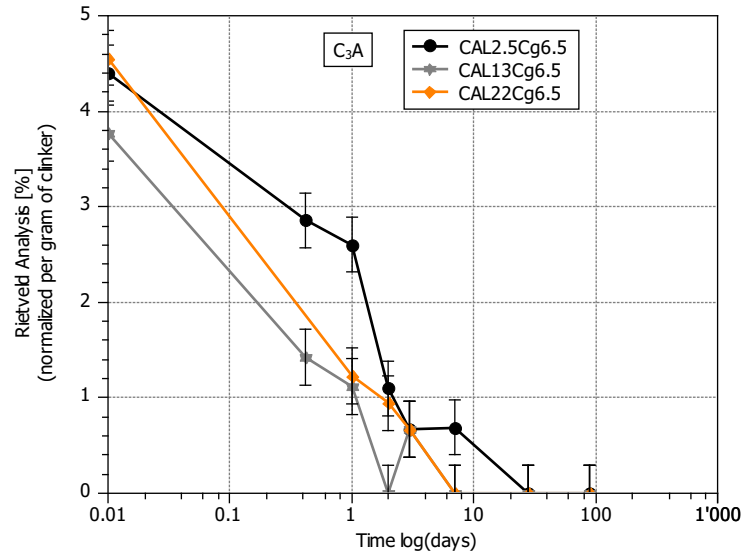


Figure D.12: XRD Rietveld Analysis. C_3A quantification. Commercial cements with low C_3A content and increasing limestone addition.

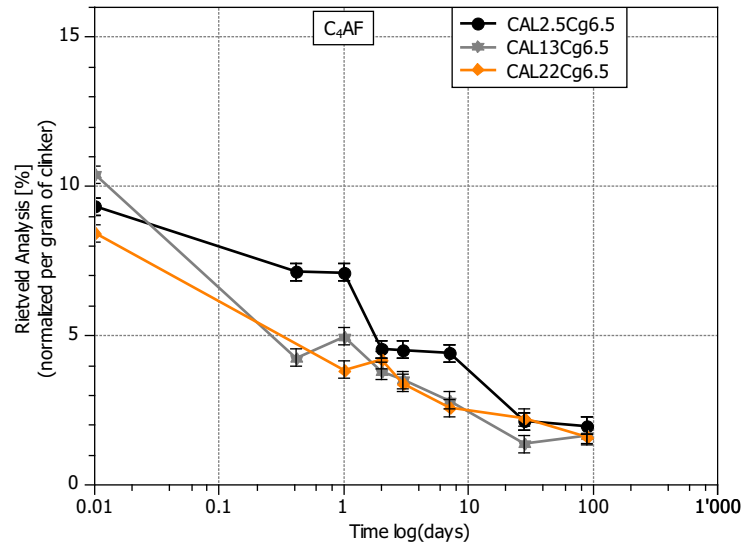


Figure D.13: XRD Rietveld Analysis. C_4AF quantification. Commercial cements with low C_3A content and increasing limestone addition.

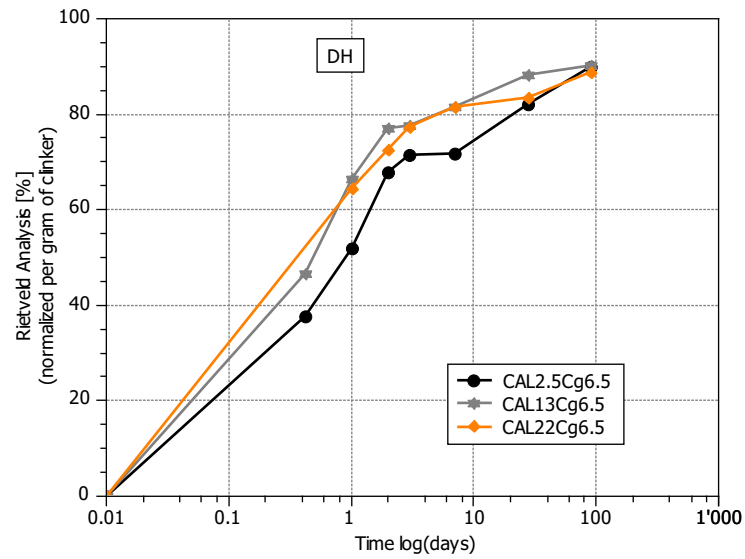


Figure D.14: XRD Rietveld Analysis. Degree of hydration. Commercial cements with Low C_3A content and increasing limestone addition.

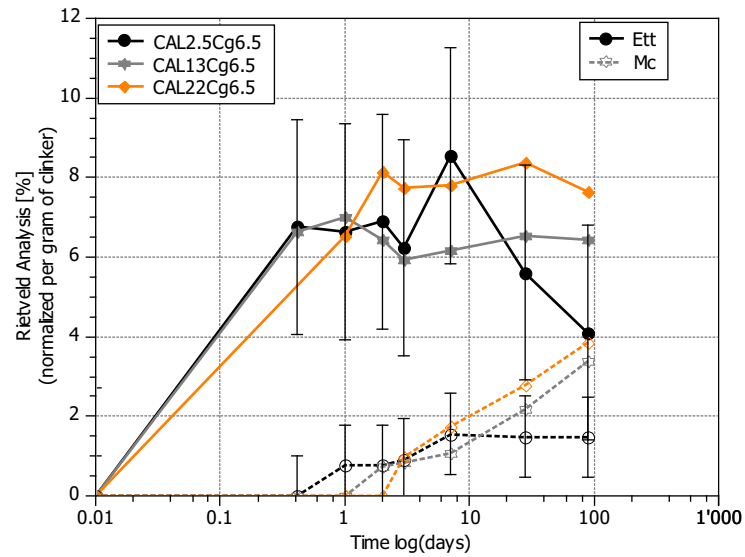


Figure D.15: XRD Rietveld Analysis. Ettringite (Ett) and monocarboaluminate (Mc) quantification. Commercial cements with low C_3A content and increasing limestone addition.

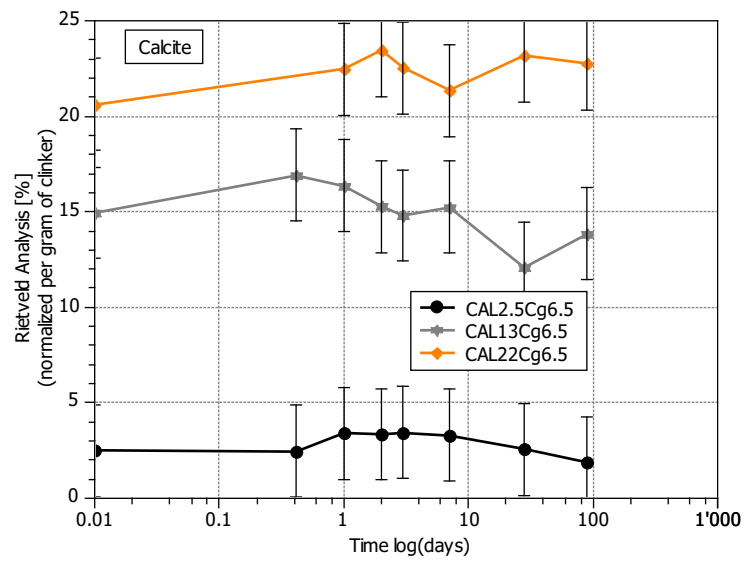


Figure D.16: XRD Rietveld Analysis. Calcite quantification. Commercial cements with low C_3A content and increasing limestone addition.

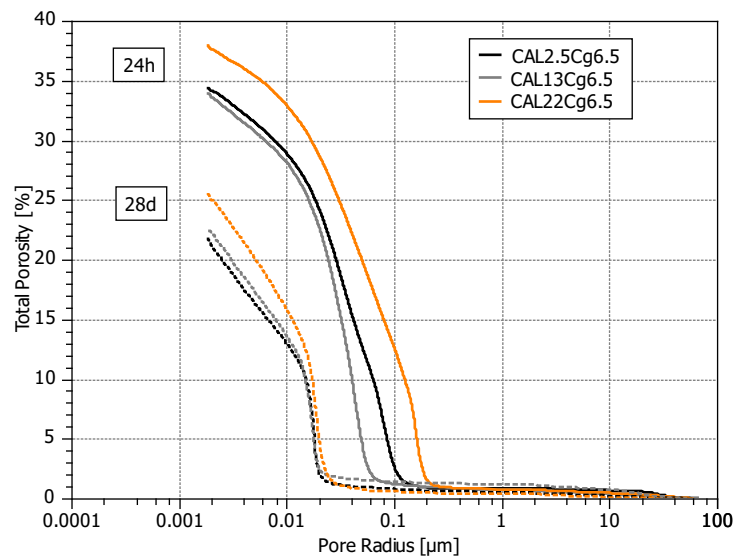


Figure D.17: MIP at 24 hours and 28 days of hydration.

Appendix E

Comparison of Laboratory and commercial cements

E.1 Cement composition and particle size distribution

Table E.1: Laboratory vs. Commercial Cements. Compared samples

Laboratory cement	Commercial cements
Sample	Sample
L0Cg6.0	CAL2.5Cg6.5
L10Cg5.5	CAL13Cg6.5
	CAL22Cg6.5
H0Cg6.0	
H10Cg5.5	CAH10Cg5.5

Table E.2: Laboratory vs. Commercial Cements. Clinkers composition

Clinker	[%]	C ₃ S	C ₂ S	C ₃ A cub.	C ₃ A orth.	C ₄ AF
Low C ₃ A _{lab}		56.4	22.3	1.6	1.0	17.0
Low C ₃ A _{commercial}		69.57	11.58	2.86	1.84	9.98
High C ₃ A _{lab}		68.3	11.5	7.3	0.2	9.0
High C ₃ A _{commercial}		63.39	14.70	6.98	2.33	6.71

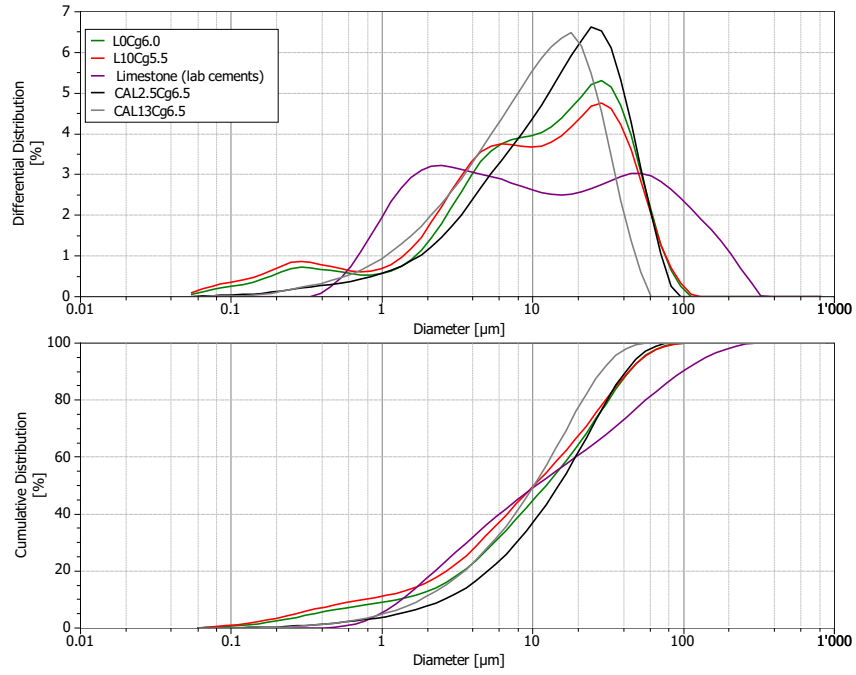


Figure E.1: Particle size distribution of laboratory and commercial cements. Cements with low C_3A content.

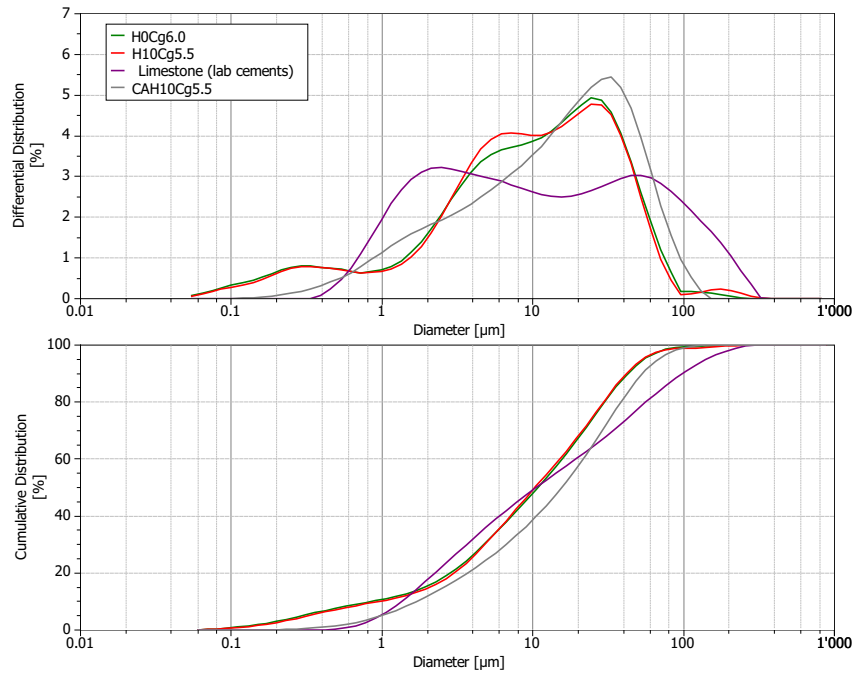


Figure E.2: Particle size distribution of laboratory and commercial cements. Cements with high C_3A content.

E.2 Kinetics of hydration

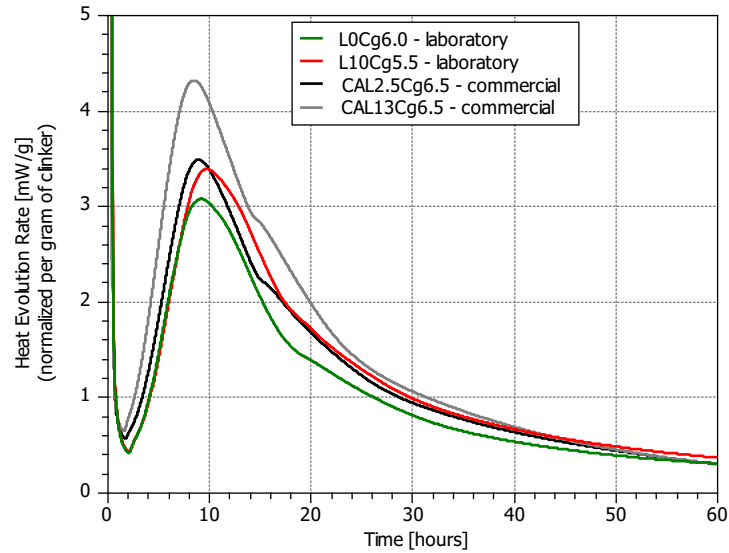


Figure E.3: Heat Evolution Rate up to 60 hours of hydration. Cements with low C_3A content. Comparison between laboratory and commercial cements.

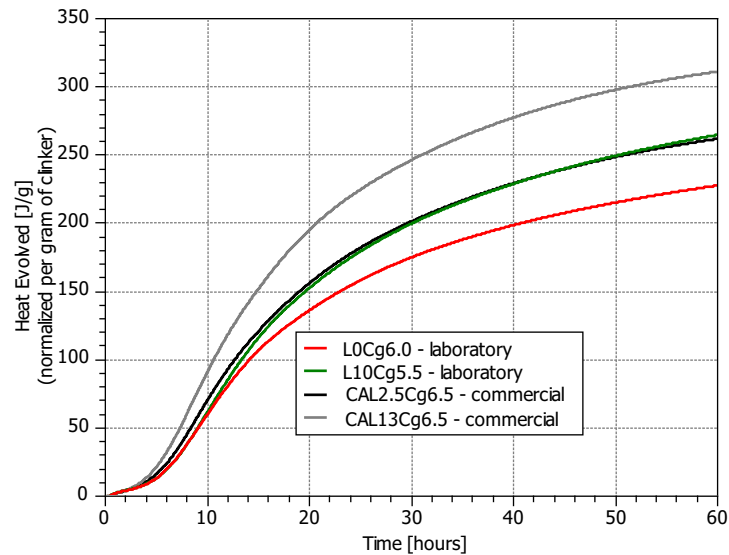


Figure E.4: Total Heat Evolved up to 60 hours of hydration. Cements with low C_3A content. Comparison between laboratory and commercial cements

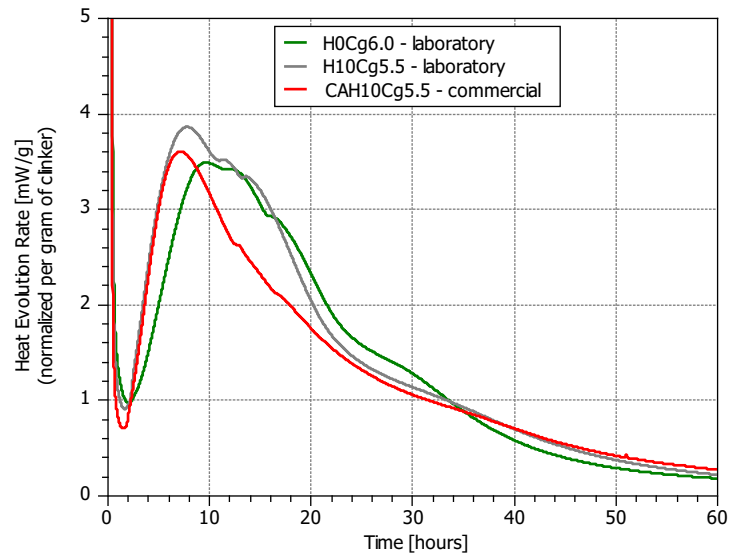


Figure E.5: Heat Evolution Rate up to 60 hours of hydration. Cements with high C_3A content. Comparison between laboratory and commercial cements

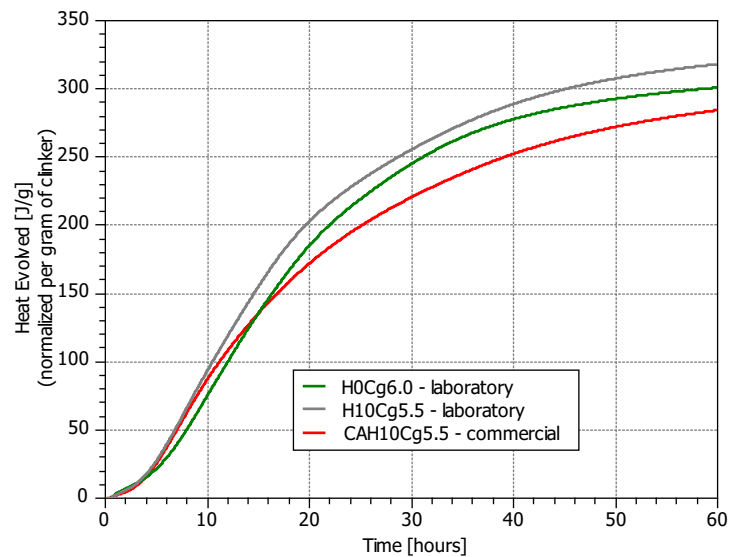
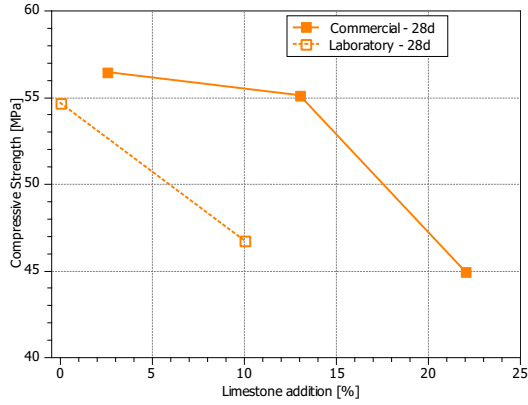
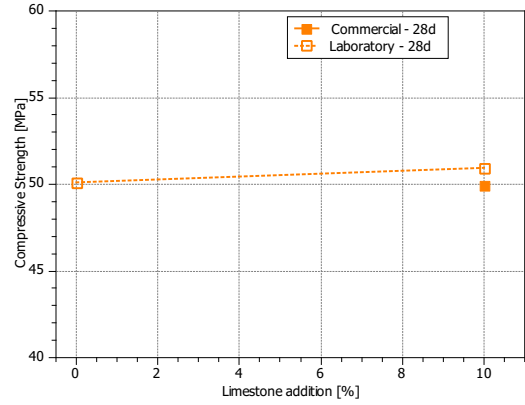


Figure E.6: Total Heat Evolved up to 60 hours of hydration. Cements with high C_3A content. Comparison between laboratory and commercial cements

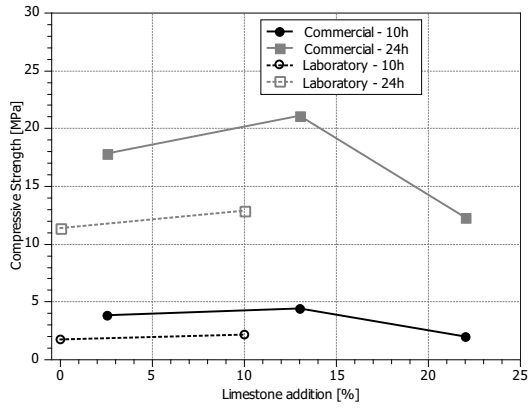
E.3 Compressive strength



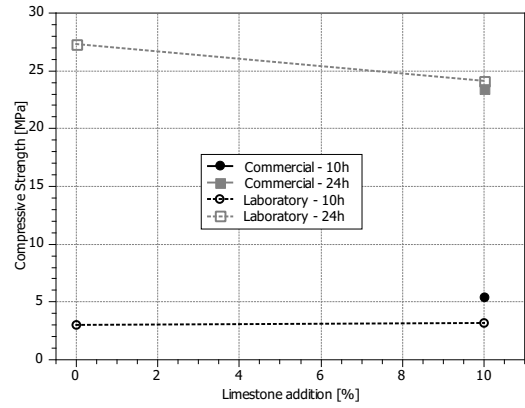
(a) Low C_3A , 28 days



(b) High C_3A , 28 days



(c) Low C_3A , 10 and 24 hours



(d) High C_3A , 10 and 24 hours

Figure E.7: Compressive strength. Clinker with low (3%) C_3A content with different gypsum addition and with 0 and 10% of limestone addition.

Appendix F

Gypsum influence on hydration

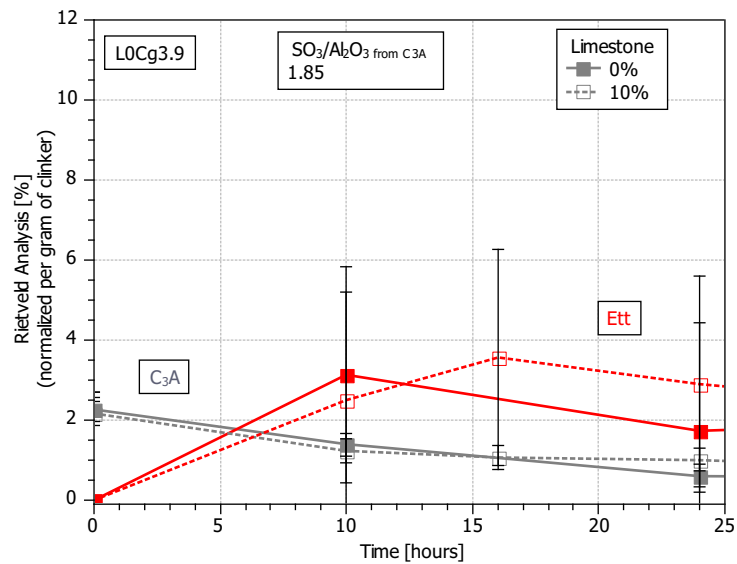


Figure F.1: XRD Rietveld Analysis, C_3A and ettringite quantification. Sample with low C_3A clinker cement, 3.8% of gypsum addition, 0 and 10% of limestone addition.

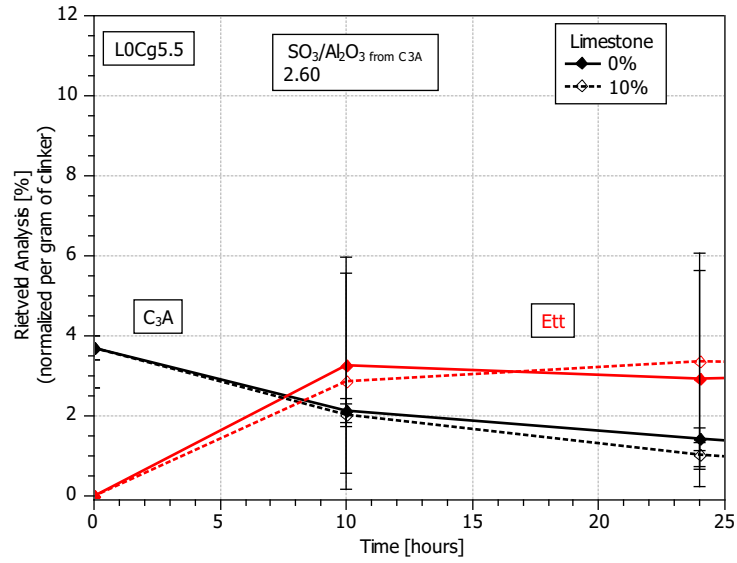


Figure F.2: XRD Rietveld Analysis, C₃A and ettringite quantification. Sample with low C₃A clinker cement, 5.5% of gypsum addition, 0 and 10% of limestone addition.

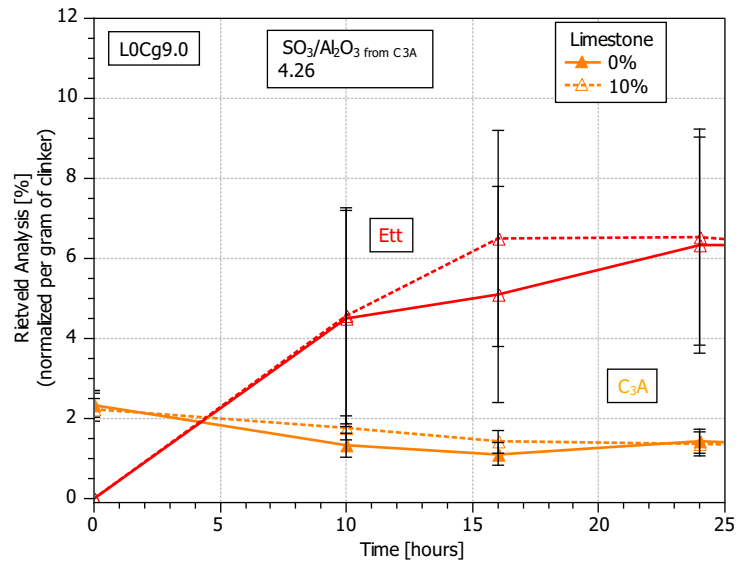


Figure F.3: XRD Rietveld Analysis, C₃A and ettringite quantification. Sample with low C₃A clinker cement, 9.0% of gypsum addition, 0 and 10% of limestone addition.

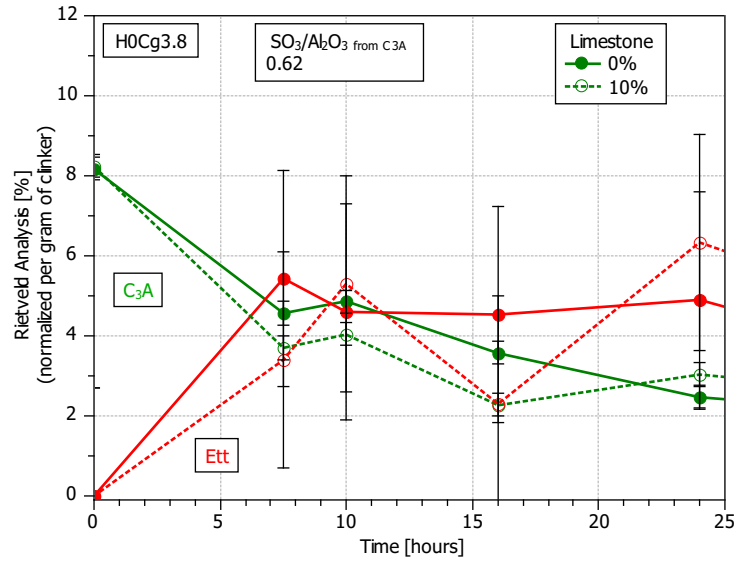


Figure F.4: XRD Rietveld Analysis, C₃A and ettringite quantification. Sample with high C₃A clinker cement, 3.8% of gypsum addition, 0 and 10% of limestone addition.

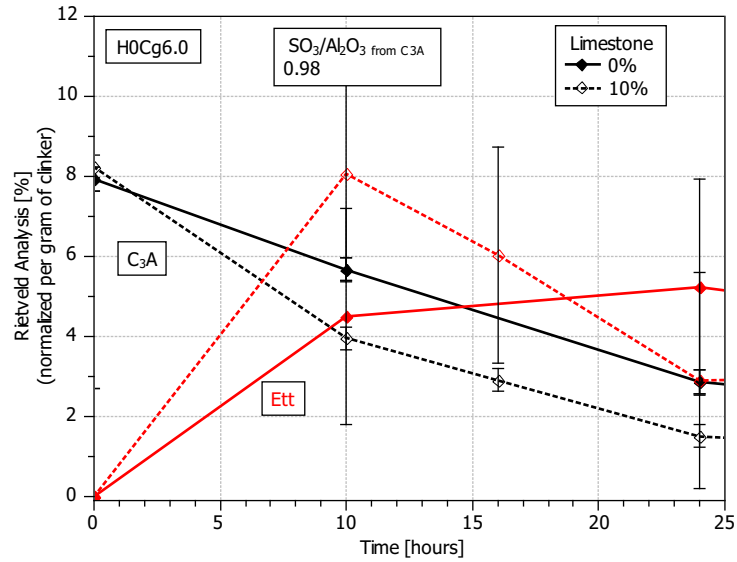


Figure F.5: XRD Rietveld Analysis, C₃A and ettringite quantification. Sample with high C₃A clinker cement, 6.0% of gypsum addition, 0 and 10% of limestone addition.

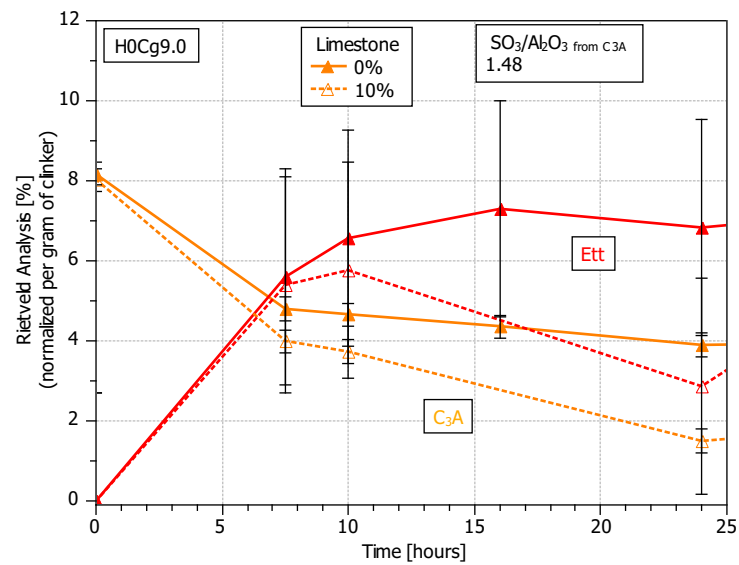


Figure F.6: XRD Rietveld Analysis, C₃A and ettringite quantification. Sample with high C₃A clinker cement, 9.0% of gypsum addition, 0 and 10% of limestone addition.

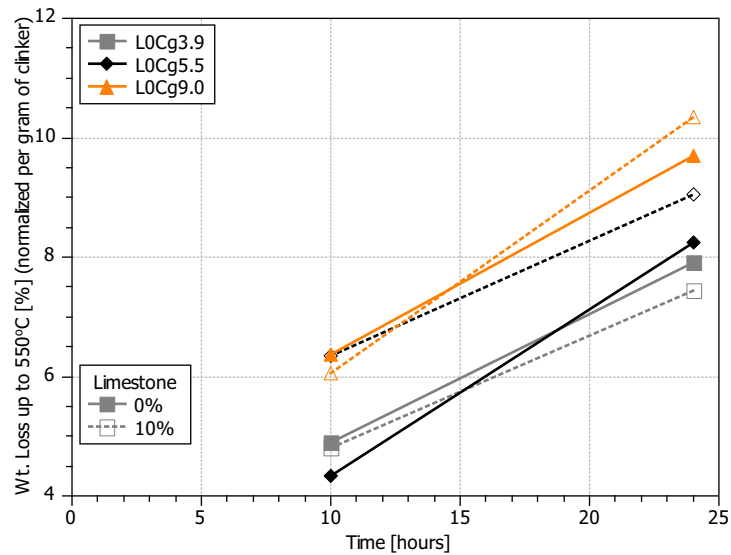


Figure F.7: Thermo Gravimetric Analysis, water loss up to 550°C. Sample with low C₃A clinker cement, increasing gypsum addition, 0 and 10% of limestone addition.

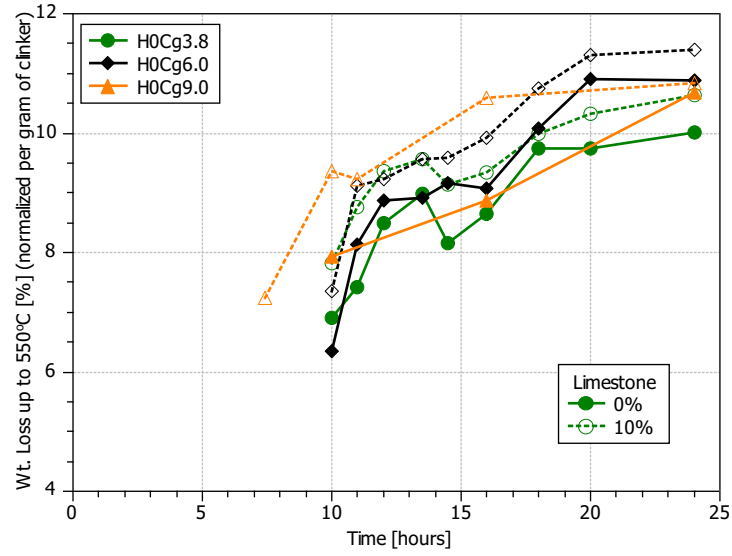


Figure F.8: Thermo Gravimetric Analysis, water loss up to 550°C. Sample with high C_3A clinker cement, increasing gypsum addition, 0 and 10% of limestone addition.

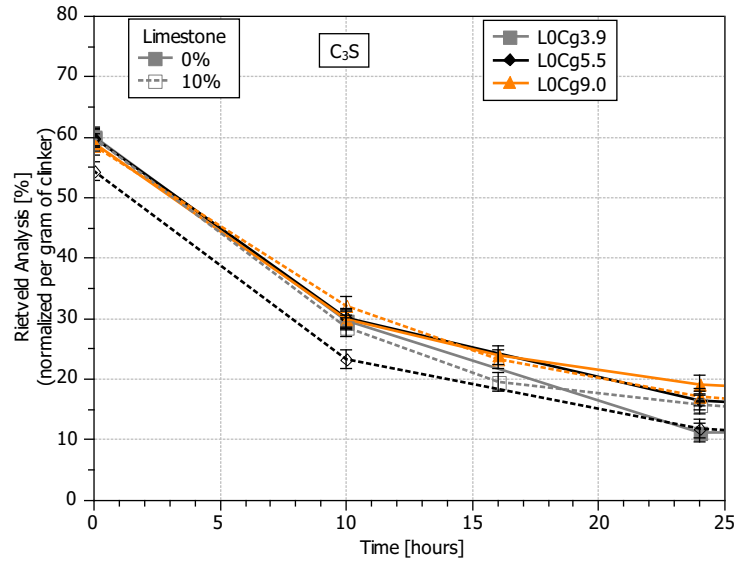


Figure F.9: XRD Rietveld Analysis, C_3S quantification. Sample with low C_3A clinker cement, increasing gypsum addition, 0 and 10% of limestone addition.

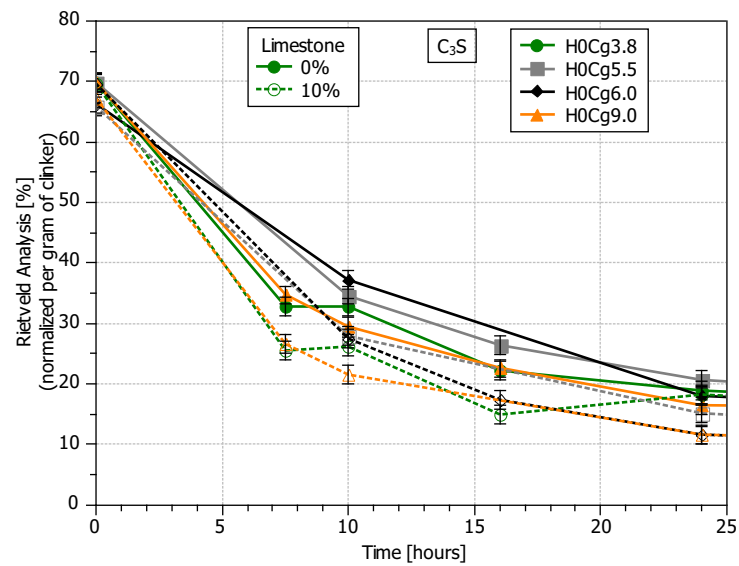


Figure F.10: XRD Rietveld Analysis, C₃S quantification. Sample with high C₃A clinker cement, increasing gypsum addition, 0 and 10% of limestone addition.

Bibliography

- [1] ABRIEL, W., AND NESPER, R. Bestimmung der Kristallstruktur von $\text{CaSO}_4(\text{H}_2\text{O})_0 \cdot 5$ mit Roentgenbeugungsmethoden und mit Potentialprofil-Rechnungen. *Zeitschrift Fur Kristallographie* 205 (1993), 99–113.
- [2] ALLMANN, R. Refinement of the hybrid layer structure $[\text{Ca}_2\text{Al}(\text{OH})_6]^+ \cdot [\frac{1}{2}\text{SO}_4 \cdot 3\text{H}_2]^-$. *Neues Jahrbuch für Mineralogie Monatshefte* (1977), 1365–144.
- [3] BARKER, A., AND CORY, H. P. The early hydration of limestone-filled cements. In *Blended Cements in Construction. Papers presented at the international conference, University of Sheffield, UK, 9–12 September 1991* (Sheffield, 1991), Elsevier Science Publisher Limited, pp. 107–124.
- [4] BARNETT, S. J., MACPHEE, D. E., AND CRAMMOND, N. J. Extent of immiscibility in the ettringite – thaumasite system. *Cement and Concrete Composites* 25 (2003), 851–855.
- [5] BENSTED, J. Thaumasite-background and nature in deterioration of cements, mortars and concretes. *Cement and Concrete Composites* 21 (1999), 117–121.
- [6] BENTUR, A. Effect of gypsum on the hydration and strength of C_3S pastes. *Journal of the American Ceramic Society* 59 (1976), 210–213.
- [7] BLANCO-VALERA, M. T., AGUILERA, J., AND MARTINEZ-RAMIREZ, S. Effect of cement C_3A content, temperature and storage medium on thaumasite formation in carbonated mortars. *Cement and Concrete Research* 36 (2006), 707–715.
- [8] BONAVETTI, V., DONZA, H., MENDEZ, G., CARBERA, O., AND IRASSAR, E. Limestone filler cement in low w/c concrete: A rational use of energy. *Cement and Concrete Research* 33 (2003), 865–871.
- [9] BONAVETTI, V., RAHHAL, V., AND IRASSAR, E. Studies on the carboaluminate formation in limestone filler-blended cements. *Cement and Concrete Research* 31 (2001), 853–859.
- [10] BOUASKER, M., MOUNANGA, P., TURCRUY, P., AND KHELIDJ, A. L. A. Chemical shrinkage of cement pastes and mortars at very early age: Effect of lime-

- stone filler and granular inclusions. *Cement and Concrete Composites* 30 (2008), 13–22.
- [11] BROWN, P. W. Thaumasite formation and other forms of sulfate attack. *Cement and Concrete Composites* 24 (2002), 301–303.
- [12] BROWN, P. W., AND TAYLOR, H. F. W. The role of ettringite in external sulfate attack. *Materials of Science of Concrete: Sulfate Attack Mechanism, Special volume The American Ceramic Society* (1998), 73–97.
- [13] CAMPITELI, V., AND FLORINDO, M. The influence of limestone additions on optimum sulfur trioxide content in Portland Cement. *Carbonate Additions to Cement ASTM STO 1064* (1990), 30–40.
- [14] CANTRILL, E. R., STEVENS, M. G., RAY, A., AND ALDRIDGE, L. The use of DTA to determine the effects of mineralizers on the cement–quartz autoclave reactions Part1. Gibbsite addition. *Thermochimica Acta* 224 (1993), 241–246.
- [15] COHEN, M. D. Theories of expansion in sulfoaluminate – type expansive cements: Schools of thought. *Cement and Concrete Research* 13 (1983), 809–818.
- [16] COLE, W. F., AND LANCUCKI, C. J. A refinemenr of the crystal structure of gypsum $\text{CaSO}_4(\text{H}_2\text{O})_2$. *Acta Crystallographica* 30 (1974), 921–929.
- [17] COLEVILLE, A. A., AND GELLER, S. The crystal structure of Brownmillerite, $\text{Ca}_2\text{FeAlO}_5$. *Acta Crystallographica B27* (1971), 2311–2315.
- [18] CRAMMOND, N. J. The thaumasite form of sulphate attack in the UK. *Cement and Concrete Composites* 25 (2003), 809–818.
- [19] DE LA TORRE, A. G., BRUQUE, S., CAMPO, J., AND ARANDA, M. A. G. The superstructure of C_3S from synchrotron and neutron powder diffraction and its role in quantitative phase analyses. *Cement and Concrete Research* 32 (2002), 1347–1356.
- [20] DE NOIRFONTAINE, M.-N., DUNSTETTER, F., COURTIAL, M., GASECKI, G., AND SIGNES-FERHEL, M. Polymorphism of tricalcium silicate, the major compound of Portland cement clinker 2. Modelling alite for Rietveld analysis, and industrial challenge. *Cement and Concrete Research* 36 (2006), 54–64.
- [21] DOLLASE, W. A. Correction of Intensities for preferred orientation in powder diffractometry–application of the March Model. *Journal of Applied Crystallography* 19 (1986), 267–272.
- [22] EL-DIDAMONY, H., AND EL-ALFI, E.-S. Addition of limestone in the low heat Portland Cement Part 1. *Ceramics – Silikaty* 44 (1999), 109–113.

-
- [23] EL-DIDAMONY, H., AND EL-ALFI, E.-S. Addition of limestone in the low heat Portland Cement Part 2. *Ceramics – Silikaty* 44 (2000), 146–150.
- [24] ESCALANTE-GARCIA, J. I., AND SHARP, J. H. Effect of temperature on the hydration of the main clinker phases in Portland cements: part I, neat cements. *Cement and Concrete Research* 28 (1998), 1245–1257.
- [25] ESCALANTE-GARCIA, J. I., AND SHARP, J. H. The microstructure and mechanical properties of blended cements hydrated at various temperatures. *Cement and Concrete Research* 31 (2001), 695–702.
- [26] FERNANDEZ, R. *Calcined clayey soils as a potential replacement for cement in developing countries*. EPFL Thesis, no 4302, 2009.
- [27] FORDHAM, C. J., AND SMALLEY, I. J. A simple thermogravimetric study of hydrated cement. *Cement and Concrete Research* 15 (1985), 141–144.
- [28] FRANCOIS, M., RENAUDIN, G., AND EVRARD, O. *A cementitious compound with composition $3\text{CaO} \cdot \text{Al}_2\text{O}_3 \cdot \text{CaCO}_3 \cdot 11\text{H}_2\text{O}$* . Acta Crystallographica – Section C, 1998.
- [29] GALLUCCI, E., MATHUR, P., AND SCRIVENER, K. L. Microstructural development of early age hydration shells around cement grains. *Cement and Concrete Research* 40 (2010), 4–13.
- [30] GOETZ-NEUNHOEFFER, F., AND NEUBAUER, J. Refined ettringite ($\text{Ca}_6\text{Al}_2(\text{SO}_4)_3(\text{OH})_{12} \cdot 26(\text{H}_2\text{O})$). Structure for quantitative X-ray diffraction analysis. *Powder Diffraction* 21 (2006), 4–11.
- [31] GONZÁLEZ, M., AND IRASSAR, E. Effect of limestone filler on the sulfate resistance of low C_3A portland cement. *Cement and Concrete Research* 28 (1998), 1655–1667.
- [32] HAWKINS, P., TENNIS, P., AND DETWILER, R. *The Use of Limestone in Portland Cement: A State-of-Art Review*. Portland Cement Association, 5420 Old Orchard Road, Skokie, Illinois 60077-1083, 2003.
- [33] HAWTHORNE, F. C., AND FERGUSON, R. B. Anhydrous Sulfates II. Refinement of the crystal structure of anhydrite. *Canadian Mineralogist* 13 (1975), 289–292.
- [34] HEWLETT, P. C. *Lea’s Chemistry of Cement and Concrete*. Arnold, 1998.
- [35] HUANG, Q., CHMAISSEM, O., CAPPONI, J. J., CHAILLOUT, C., MAREZIO, M., THOLENCE, J. L., AND SANTORO, A. Neutron powder diffraction study of the crystal structure of $\text{HgBa}_2\text{Ca}_4\text{Cu}_5\text{O}_{12+\delta}$ at room temperature and at 10 K. *Physica C: Superconductivity* 227 (1–2) (1994), 1–9.

- [36] ITIM, A., EZZIANE, K., AND KADRI, E.-H. Effect of gypsum on the strength development of Portland Cement by Mössbauer spectrometry. *Hyperfine Interactions* 42 (1988), 1199–1202.
- [37] JELENIC, I., PANOVIC, A., HALLE, R., AND GACESA, T. Effect of gypsum on the hydration and strength development of commercial Portland Cements containing alkali sulfates. *Cement and Concrete Research* 7 (1977), 239–246.
- [38] KAKALI, G., TSIVILIS, S., AGGELI, E., AND BATI, M. Hydration products of C_3A , C_3S and Portland cement in the presence of $CaCO_3$. *Cement and Concrete Research* 30 (2000), 1073–1077.
- [39] KALOUSEK, G. Approach to fundamentals of concrete strength. *Cement and Concrete Research* 1 (1971), 63–73.
- [40] KASSELOURI, V., FTIKOS, C., AND PARISSAKIS, G. DTA–TG study on the $Ca(OH)_2$ – pozzolan reaction in cement pastes hydrated up to three years. *Cement and Concrete Research* 13 (1983), 649–654.
- [41] KENAI, S., SOBOYEJO, W., AND SOBOYEJO, A. Some Engineering Properties of Limestone Concrete. *Materials and Manufacturing Processes* 19 (2004), 949–961.
- [42] KJELSEN, K. O., AND DETWILER, R. J. Reaction kinetics of portland cement mortars hydrated at different temperatures. *Cement and Concrete Research* 22 (1992), 112–120.
- [43] KLEBER, W. *An introduction to crystallography*. Verlag Technik, VEB, 1970.
- [44] KLIEGER, P., AND HOOTON, D. *Carbonate Additions to Cement*. ASTM International, 1990.
- [45] KLIMESCH, D. S., AND RAY, A. The use of DTA/TGA to study the effects of ground quartz with different surface areas in autoclaved cement: quartz pastes Part 1: A method for evaluating DTA/TGA results. *Thermochimica Acta* 289 (1996), 41–54.
- [46] LAMOND, J. F., AND PIELERT, J. H. *Significance of Tests and Properties of Concrete and Concrete-Making Materials*. ASTM International, 2006.
- [47] LERCH, W. *The influence of gypsum on the hydration and properties of Portland Cement Pastes*. American Society for Testing Materials, 1946.
- [48] LIVESY, P. Strength Characteristics of Portland-limestone cements. *Construction and Building Materials* 5 (1991), 147–150.
- [49] LOTHENBACH, B., SAOUT, G. L., GALLUCCI, E., AND SCRIVENER, K. L. Influence of limestone on the hydration of Portland cements. *Cement and Concrete Research* 38 (2008), 848–860.

-
- [50] MARTINEZ-RAMIREZ, S., BLANCO-VARELA, M. T., AND RAPAZOTE, J. Thaumassite formation in sugary solutions: Effect of temperature and sucrose concentration. *Cement and Building Materials* 25 (2011), 21–29.
- [51] MATSCHEI, T., LOTHENBACH, B., AND GLASSER, F. The role of calcium carbonate in cement hydration. *Cement and Concrete Research* 37 (2007), 551–558.
- [52] MCGINNETY, J. A. Redetermination of the structures of potassium sulphate and potassium chromate: the effect of electrostatic crystal forces upon observed bond lengths. *Acta Crystallographica* 28 (1972), 2845–2852.
- [53] MEHTA, P. K. Mechanism of expansion associated with ettringite formation. *Cement and Concrete Research* 3 (1973), 1–6.
- [54] MEHTA, P. K., PIRTZ, D., AND POLIVKA, M. Properties of alite cements. *Cement and Concrete Research* 9 (1979), 439–450.
- [55] MOHAN, K., AND TAYLOR, H. F. W. *University of Aberdeen, Old Aberdeen, Scotland*. Grant-in-Aid, 1980.
- [56] MONDAY, P., AND JEFFERY, J. W. The crystal structure of tricalcium aluminate, $\text{Ca}_3\text{Al}_2\text{O}_6$. *Acta Crystallographica B31* (1975), 689–697.
- [57] NISHI, F., AND TAKÉUCHI, Y. The Al_2O_{18} rings of tetrahedra in the structure of $\text{Ca}_8 \cdot 5\text{NaAl}_6\text{O}_{18}$. *Acta Crystallographica B31* (1975), 1169–1173.
- [58] ODLER, I., AND ABDUL-MAULA, S. Investigation on the relationship between porosity structure and strength of hydrated portland cement pastes III. Effect of clinker composition and gypsum addition. *Cement and Concrete Research* 17, 2 (1987), 22–30.
- [59] PERRA, J., HUSSON, S., AND GUILHOT, B. Influence of finely ground limestone on cement hydration. *Cement and Concrete Composites* 21, 2 (1999), 99–105.
- [60] PETCH, H. E. The hydrogen positions in portlandite, $\text{Ca}(\text{OH})_2$, as indicated by the electron distribution. *Acta Crystallographica* 14 (1961), 950–957.
- [61] PETERSON, V. K., RAY, A. S., AND HUNTER, B. A. A comparative study of Rietveld phase analysis of cement clinker using neutron, laboratory X-ray, and synchrotron data. *Powder Diffraction* 21 (2006), 12–18.
- [62] PIPILIKAKI, P., PAPAGEORGIOU, D., TEAS, C., CHANIOTAKIS, E., AND KATSIOTI, M. The effect of temperature on thaumasite formation. *Cement and Concrete Composites* 30 (2008), 964–969.
- [63] PÖLLMANN, H., KUZEL, H. J., AND WENDA, R. Compounds with ettringite structure. *Neues Jahrbuch für Mineralogie Abhandlungen*–160 (1989), 133–158.

- [64] POOLE, J. L., RIDING, K., FOLLIARD, K. J., JUENGER, M. C. G., AND SCHINDLER, A. K. Methods for Calculating Activation Energy for Portland Cement. *ACI Materials Journal* 101 (2007), 303–311.
- [65] POPILIKAKI, P., KATSIOTI, M., AND GALLIAS, J. L. Performance of limestone cement mortars in a high sulfates environment. *Cement and Building Materials* 23, 2 (2009), 1042–1049.
- [66] PRITULA, O., SMRCOK, L., TÖBBENS, D. M., AND LANGER, V. X-ray and neutron Rietveld quantitative phase analysis of industrial Portland cement clinkers. *Powder Diffraction* 19 (2004), 232–239.
- [67] PURNELL, P., FRANCIS, O. J., AND PAGE, C. L. Formation of thaumasite in synthetic cement mineral slurries. *Cement and Concrete Composites* 25 (2003), 857–860.
- [68] QUENNOZ, A. *Hydration of C_3A with calcium sulfate alone and in the presence of calcium silicate*. EPFL Thesis 5035, 2011.
- [69] RAMACHANDRAN, V. Thermal analysis of cement components hydrated in the presence of calcium carbonate. *Thermochimica Acta* 127 (1988), 385–394.
- [70] RAMACHANDRAN, V., FELDMAN, R., AND BEAUDOIN, J. J. Influence of sear eater solution on mortar containing calcium carbonate. *Materials and Structures* 23 (1990), 412–417.
- [71] RAMACHANDRAN, V., AND ZHANG, C. Hydration kinetics and microstructural development in the $3\text{CaO} \cdot \text{Al}_2\text{O}_3 - \text{CaSO}_4 \cdot 2\text{H}_2\text{O} - \text{CaCO}_3 - \text{H}_2\text{O}$ system. *Materiaux et constructions. Materials and Structures* 19 (1986), 437–444.
- [72] RAY, A., CANTRILL, E. R., STEVENS, M. G., AND ALDRIDGE, L. Use of DTA to determine the effect of mineralizers on the cement – quartz hydrothermal reactions. Part 2. Clay addition. *Thermochimica Acta* 250 (1995), 189–195.
- [73] SANTHANAM, M., COHEN, M. D., AND OLEK, J. Effect of gypsum formation on the performance of cement mortars during external sulfate attack. *Cement and Concrete Research* 33 (2003), 325–332.
- [74] SCARLETT, N. V. Y., MADSEN, I. C., MANIAS, C., AND RETALLACK, D. On-line X-ray diffraction for quantitative phase analysis: Application in the Portland cement industry. *Powder Diffraction* 16 (2001), 71–80.
- [75] SCHERER, G. W. Stress from crystallisation of salt. *Cement and Concrete Research* 34 (2004), 1613–1624.
- [76] SCHILLER, B., AND ELLERBROCK, H.-G. The Grinding and Properties of Cement with Several Main Constituents. *Zement-Kalk-Gips* 45 (1992), 325–334.

-
- [77] SCHMIDT, M. Cement with Interground Additives-Capabilities and Environmental Relief. *Zement-Kalk-Gips* 45 (1992), 296–301.
- [78] SCHMIDT, T. *Sulfate attack and the role of internal carbonate on the formation of thaumasite*. EPFL Thesis 3853, 2007.
- [79] SCRIVENER, K. L., FÜLLMANN, T., GALLUCCI, E., WALENTA, G., AND BERMEJO, E. Quantitative study of Portland cement hydration by X-ray diffraction/Rietveld analysis and independent methods. *Cement and Concrete Research* 34 (2004), 1541–1547.
- [80] SERSALE, R., AND CIOFFI, R. Effect of SO_3 on the physical microstructure of Portland Cement mortars. *Cement and Concrete Research* 21, 2 (1991), 120–126.
- [81] SHARMA, R., AND PANDEY, S. Influence of mineral additives on the hydration characteristics of ordinary Portland cement. *Cement and Concrete Research* 29 (1999), 1525–1529.
- [82] SOROKA, I., AND ABAYNEH, M. Effect of gypsum on properies and internal structure of PC paste. *Construction and Building Materials* 16 (1986), 495–504.
- [83] SOROKA, I., AND RELIS, M. Effect of added gypsum on compressive strength of Portland Cement clinker. *Ceramik Bulletin* 62, 6 (1983), 695–703.
- [84] SOROKA, I., AND SETTER, N. The effect of fillers on strength of cement mortars. *Cement and Concrete Research* 7 (1977), 449–456.
- [85] SOROKA, I., AND STERN, N. Calcareous fillers and the compressive strength of Portland Cement. *Cement and Concrete Research* 6 (1976), 367–376.
- [86] SPRUNG, S., AND SIEBEL, E. Assessment of the Suitability of Limestone for producing Portland Limestone Cement. *Zement-Kalk-Gips* 44 (1991), 1–11.
- [87] TAE LEE, S., HOOTON, R. D., JUNG, H.-S., PARK, D.-H., AND CHOI, C. S. Effect of limestone filler on the deterioration of mortars and pastes exposed to sulfate solution at ambient temenrature. *Cement and Concrete Research* 38 (2008), 68–76.
- [88] TAYLOR, D. Thermal expansion data I. Biary oxides with the sodium chloride and wurtzite structure. *Transactions and Journal of the British Ceramic Society* 83 (1984), 5–9.
- [89] TEZUKA, Y., GOMES, D., MARTINS, D., AND DJANIKIN, J. Durability aspects of cement with high limestone filler content. In *Proceedings of the 9th International Congress of the Chemistry of Cement* (New Delhi, 1992), 9th International Congress of the Chemistry of Cement, pp. 53–59.

- [90] TIAN, B., AND COHEN, M. D. Does gypsum formation during sulfate attack on concrete lead to expansion? *Cement and Concrete Research* 30 (2000), 117–123.
- [91] TOSUN, K., FELEKOGLU, B., BARADAN, B., AND ALTUN, A. Effect of limestone replacement ration on the sulfate resistance of Portland limestone cement mortars exposed to extraordinary high sulfate concentrations. *Construction and Building Materials* 23 (2009), 2534–2544.
- [92] TSIVILIS, S., SOTIRIADIS, K., AND SKAROPOULOU, A. Thaumasite form of sulfate attack (TSA) in limestone cement pastes. *Journal of the European Ceramic Society* 27 (2007), 1711–1714.
- [93] TSURUMI, T., HIRANO, Y., KATO, H., KAMIYA, T., AND DIAMON, M. Crystal structure and hydration of belite. *Ceramic Transactions* 40 (1994), 19–25.
- [94] VUK, T., GABROVSEK, R., AND KAUCIC, V. The influence of mineral admxtures on sulfate resistance of limestone cement pastes aged in cold MgSO_4 solution. *Cement and Concrete Research* 32 (2002), 943–948.
- [95] WALENTA, G., AND FÜLLMANN, T. Advences in quantitative XRD analysis for clinker, cements, and cementitious additions. *Powder Diffraction* 19 (2004), 40–44.
- [96] WARTCHOW, R. Datensammlung nach der "Learnt profile"–Methode (LP) für Calcit und Vergleich mit der "Background peak background"–Methode (BPB). *Zeitschrift Fur Kristallographie* 186 (1989), 300–302.
- [97] ZHANG, X. *Quantitative microstructural characterisation of concrete cured under realistic temperature conditions*. EPFL Thesis 3725, 2007.
- [98] ZHOU, Q., HILL, J., BYARS, E. A., CRIPPS, J. C., LYNSDALE, C. J., AND SHARP, J. H. The role of pH in thaumasite sulfate attack. *Cement and Concrete Research* 36 (2006), 160–170.

Olga Chowaniec

24th September 1983, Polish

Place Chauderon 20
1003 Lausanne
Switzerland

Tel.: +41 78 7075761
olga.chowaniec@gmail.com



WORKING EXPERIENCE

2007 – ... **Doctoral research assistant, Laboratory of Construction Materials, École Polytechnique Fédérale de Lausanne.** Collaboration with Swiss Cement Industry – Holcim

Project “Limestone Addition in Cement” – to understand mechanism by which limestone addition affects the properties of the cementitious materials. Influence of limestone on the cement with different amount of C₃A in the clinker and different gypsum amount.

2007 – ... **Teaching Assistant, Laboratory of Construction Materials, École Polytechnique Fédérale de Lausanne**

Responsibilities : - Teaching small groups (6 people), subject : methods used in the cement research and materials testing
- Semester projects supervision

2005 – 2007 **Consultant and Sales Representative, Polish Cement Association, Publishing House**

Responsibilities: products promotion, improvement in the collaborator between members and in efficiency of the Polish Cement and Lime Industry

2005 – 2005
(3 months) **Stagier in the Concrete Quality Laboratory, Cemex Concrete Plant in Krakow, Poland**

Responsibilities: quality control in the construction of the national road “Zakopianka” in Poland

EDUCATION

- 2007 – ... Ph.D. in Material Science, École Polytechnique Fédérale de Lausanne,
sponsored by Holcim
Subject : “Limestone addition in Cement”
- 2002 – 2007 M.Sc. (Materials Science and Ceramics) AGH University of Science and
Technology
Major field of study: Construction Materials
Specification: Binding Materials

SKILLS

Ability to perform both individual and teamwork

Computer skills: LaTeX, Ms PowerPoint; Ms Office – Ms Word, Ms Excel – good knowledge of all

LABORATORY SKILLS

Good knowledge in techniques: SEM-EDX, XRD, TGA, MIP, Isothermal Calorimetry, NMR (modest), Chemical Shrinkage, Autogenous Shrinkage,

Good knowledge in durability test: flexural and compressive strength, elastic modulus, sulfate attack, chloride attack, sorptivity,

LANGUAGE SKILLS

English: spoken, written (very good)
German: spoken, written (basic)
French: spoken, written (intermediate)
Polish: native

INTERESTS

I have been always fascinated by unknown, science new technologies. My second passion is music, I used to play violin and piano, and hope to restart it after my PhD. After working day I like to relax by going swimming or to the gym. My favorite season is winter when every weekend I can enjoy and improve skiing which is my favorite sport. If there is time left I like to handcraft birthday gifts for my friends, clothes and small useful things for myself.